

**Development and Application of Novel Methodologies
to Interrogate X-chromosome Inactivation**

by

Emily T. Maclary

A dissertation submitted in partial fulfillment
of the requirements for the degree of
Doctor of Philosophy
(Human Genetics)
in the University of Michigan
2016

Doctoral Committee:

Assistant Professor Sundeep Kalantry, Chair
Professor David T. Burke
Professor Sally A. Camper
Professor Miriam H. Meisler
Professor Trisha Wittkopp

Acknowledgements

This work was made possible with the help and support of many people, both professionally and personally. I would first like to thank Dr. Sundeep Kalantry for his mentorship and support. Sundeep is dedicated to encouraging his student's growth and independence, and has pushed me to become a better scientist and, more importantly, a critical thinker. I would also like to thank the members of my dissertation committee, Dr. David Burke, Dr. Sally Camper, Dr. Miriam Meisler, and Dr. Trisha Wittkopp for their encouragement and constructive advice during the duration of my dissertation. Thank you as well to Dr. Jake Mueller and Dr. Sue Hammoud, as well as members of the Mueller and Hammoud labs, for the thought-provoking questions and helpful suggestions during lab meetings. I am grateful for the scientific and technical contributions of numerous friends and colleagues, including all past and present members of the Kalantry lab. Specifically, many thanks are due to Srimonta Gayen, Clair Harris, and Michael Hinten for derivation, maintenance, and characterization of numerous cell lines used in these projects; Emily Buttigieg and Archana Kumari for developing and optimizing strand-specific RNA FISH techniques; and Weisheng Wu, Kraig Stevenson, and Matt Iyer for advice and technical support in establishing an allele-specific RNA-sequencing analysis pipeline. Finally, I would like to thank my family and friends for their love and support over the past five and a half years.

Table of Contents

Acknowledgements	ii
List of Figures	vi
List of Tables	x
Abstract	xi
Chapter 1: Introduction	1
1-1: Introduction to Epigenetic Regulation and X-chromosome Inactivation.....	1
1-2: Identification and Mapping of the X-inactivation Center	4
1-3: The Xist Long Non-Coding RNA	6
1-4: Tsix RNA: an Antisense Regulator of Xist Expression	10
1-5: Beyond Xist and Tsix: Other lncRNAs at the X-inactivation Center	13
1-6: <i>Trans</i> -acting Regulators of X-inactivation.....	16
1-7: Concluding Remarks	19
Chapter 2: Differentiation-dependent requirement of Tsix long non-coding RNA in imprinted X-chromosome inactivation	26
2-1: Introduction	26
2-2: Role of Tsix During Initiation of Imprinted X-inactivation.....	30
2-3: Post-implantation Role of Tsix in Suppressing Xist	33
2-4: Differentiation-dependent Function of Tsix in TS Cells.....	37
2-5: Disassociation of H3-K27me3 Enrichment and X-inactivation.....	43
2-6: Tsix is Dispensable in X-chromosome Reactivation	46
2-6: Concluding Remarks	49
2-7: Materials and Methods	53
Movies	63

Chapter 3: A Primary Role for the Tsix lncRNA in Maintaining Random X-chromosome Inactivation	67
3-1: Introduction	67
3-2: Tsix Absence Results in Ectopic Xist RNA Expression and Coating in Male Embryonic Epiblasts	69
3-3: Ectopic Xist Induction in Differentiating But Not Undifferentiated $X^{\Delta Tsix}Y$ Epiblast Stem Cells	72
3-4: Ectopic Xist Induction in Differentiating $X^{\Delta Tsix}Y$ ESCs	76
3-5: Absence of Biased X-chromosome Choice in Tsix-heterozygous Female Epiblasts	78
3-6: Tsix-heterozygous EpiSCs Undergo Ectopic X-inactivation Only Upon Differentiation	83
3-7: Reduced Proliferation and Induced Cell Death Upon Ectopic X-inactivation in Tsix-heterozygous EpiSCs	92
3-8: Ectopic Xist Induction in Differentiating Tsix-heterozygous Female ESCs	97
3-9: Concluding Remarks	100
3-10: Materials and Methods	105
 Chapter 4: A Strand-Specific and Allele-Specific RNA-Seq Pipeline to Identify Novel Regulators of X-inactivation	 113
4-1: Introduction	113
4-2: Sample Derivation, Library Preparation, and Sequencing	116
4-3: Reference Genome Assembly and Allele-specific Mapping	118
4-4: Transcriptome Annotation and Novel Transcript Discovery	120
4-5: Allele-specific Transcriptome Analysis	123
4-6: Strategies for Follow-up Characterization of Gene Expression	125
4-7: Applications for Allele-Specific RNA-Seq Analysis and Future Goals	127
 Chapter 5: Repression of Basally Transcribed Inactive X-linked genes	 129
by PRC2 and Xist RNA	129
5-1: Introduction	129

5-2: Loss of H3-K27me3 Enrichment and Xist RNA Coating on the Inactive X-chromosome in <i>Eed</i> ^{-/-} TSCs.....	132
5-3: RNA FISH in <i>Eed</i> ^{-/-} TSCs Reveals Limited Derepression of X-linked genes	134
5-4: X-chromosome-wide Identification of Derepressed Genes in <i>Eed</i> ^{-/-} TSCs.....	136
5-5: Characterization of Derepressed Genes	151
5-6: Discussion	163
5-7: Materials and Methods	168
Chapter 6: Concluding Thoughts and Future Directions	206
6-1: Summary of Findings and Recent Advances	206
6-2: Current Work and Future Directions.....	213
References.....	216

List of Figures

Figure 1.1: Two types of X-inactivation in the mouse embryo.	3
Figure 1.2: Schematic of Searle’s Translocation, Used to Map the X-inactivation Center.	5
Figure 1.3: The X-inactivation Center.....	6
Figure 2.1: Absence of ectopic Xist induction from the $X^{\Delta Tsix}$ maternal X-chromosome in embryonic day (E) 3.5 blastocyst embryos.....	32
Figure 2.2: Limited Xist induction from the $X^{\Delta Tsix}$ maternal X-chromosome in embryonic day (E) 4.0 embryos.....	34
Figure 2.3: RNA FISH analysis of X-linked gene expression in intact wild-type and maternal $X^{\Delta Tsix}$ mutant E6.5 embryos.	35
Figure 2.4: Xist induction from the $X^{\Delta Tsix}$ maternal X-chromosome in E6.5 extra- embryonic cells.	36
Figure 2.5: The $X^{\Delta Tsix}$ maternal X-chromosome displays ectopic Xist induction only upon differentiation in trophoblast stem (TS) cells.	38
Figure 2.6: Characterization of differentiation-dependent Xist RNA induction from the $X^{\Delta Tsix}$ maternal X-chromosome.	40
Figure 2.7: Lack of Xist induction from the $X^{\Delta Tsix}$ maternal X-chromosome in cultured extra-embryonic endoderm (XEN) cells.	42

Figure 2.8: X-linked genes show concordance of allelic expression in $X^{\Delta Tsix}X$ and $X^{\Delta Tsix}Y$ E6.5 extra-embryonic tissues.	44
Figure 2.9: Disassociation of Xist induction, H3-K27me3 enrichment, and inactivation of the $X^{\Delta Tsix}$ maternal X-chromosome in E6.5 extra-embryonic cells.	46
Figure 2.10: Reactivation of the inactive $X^{\Delta Tsix}$ paternal X-chromosome in the inner cell mass (ICM).	48
Figure 2.11: A model for the role of Tsix in imprinted X-Inactivation.	52
Figure 3.1: Xist is induced from the $X^{\Delta Tsix}$ in E5.25 male epiblast cells.	71
Figure 3.2: Characterization of EpiSCs and ESCs	74
Figure 3.3: Ectopic Xist RNA induction in differentiated but not undifferentiated $X^{\Delta Tsix}Y$ EpiSCs and ESCs.	75
Figure 3.4: Characterization of male ESC-derived EpiLCs.	77
Figure 3.5: Xist expression in E6.5 and E5.25 WT and Tsix-heterozygous female epiblast cells.	80
Figure 3.6: Characterization of X-inactivation, allelic Xist expression, and proliferation in E5.25 female epiblasts.	81
Figure 3.7: Lack of uniformly biased X-inactivation in undifferentiated Tsix-heterozygous EpiSC lines.	85
Figure 3.8: Characterization of differentiating female EpiSC lines.....	86
Figure 3.9: Change in allelic Xist expression in differentiating Tsix heterozygous EpiSC lines.	88

Figure 3.10: Quantification of allelic expression of Rnf12 and Atrx during differentiation of EpiSCs.....	89
Figure 3.11: Characterization of allelic Xist expression in female EpiSCs, cell proliferation and cell viability in male EpiSCs, and analysis of Tsix-heterozygous ESCs.....	91
Figure 3.12: Ectopic Xist RNA coating in differentiated Tsix-heterozygous EpiSC lines.	94
Figure 3.13: Characterization of female ESC-derived EpiLCs.....	99
Figure 3.14: A model of <i>Tsix</i> function in X-inactivation.	104
Figure 5.1: Absence of H3-K27me3 enrichment and Xist RNA coating on the inactive X-chromosome in <i>Eed</i> ^{-/-} TSCs.....	133
Figure 5.2: RNA FISH analysis of X-linked gene expression in <i>Eed</i> ^{-/-} TSCs.....	135
Figure 5.3: RNA-Seq profiling of X-linked gene expression in <i>Eed</i> ^{+/+} , <i>Eed</i> ^{fl/fl} , and <i>Eed</i> ^{-/-} TSCs.....	137
Figure 5.4: Allelic Read Mapping with STAR.....	138
Figure 5.5: Identification and characterization paternal-X expression in in <i>Eed</i> ^{+/+} , <i>Eed</i> ^{fl/fl} , and <i>Eed</i> ^{-/-} TSCs.....	141
Figure 5.6: Distribution of Allelic Expression Profiles for X-linked Genes in Individual Cell Lines.	143
Figure 5.7: Differential Expression Analysis of X-linked Genes.	145
Figure 5.8: Identification and characterization paternal-X expression in in <i>Eed</i> ^{+/+} , <i>Eed</i> ^{fl/fl} , and <i>Eed</i> ^{-/-} TSCs at a 5X read coverage threshold.....	148
Figure 5.9: Validation of RNA-Seq results by RT-PCR and Sanger sequencing.....	150

Figure 5.10: Genomic PCR for selected X-linked genes validates the presence of both alleles in DNA samples from WT and *Eed*^{-/-} TSCs.....151

Figure 5.11: Chromatin context and genomic location of derepressed X-linked genes.153

Figure 5.12. Locations of X-chromosome Topologically Associated Domains compared to derepressed genes.....154

Figure 5.13: Xist RNA binding pattern is not predictive of derepression of paternal X-linked genes in *Eed*^{-/-} TSCs.....156

Figure 5.14: Assessment of Basal Transcription at Derepressed X-chromosome Genes.162

List of Tables

Table 3.1: Embryonic stage of cell line derivation for all wild-type and Tsix-mutant EpiSC lines.	84
Table 3.2: Comparisons of cell numbers and viability between individual wild-type (WT) and Tsix-heterozygous female EpiSCs at day 20 of differentiation.....	96
Table 5.1: Allelic Expression of X-linked Genes: 10X Read Coverage Threshold.....	179
Table 5.2: Differential Expression Analysis of X-chromosome Genes.....	186
Table 5.3: Allelic Expression of X-linked Genes: 5X Read Coverage Threshold	197
Table 5.4: SNP Locations and Primer Sequences for RT-PCR and Genomic PCR Amplicons.....	205

Abstract

X-chromosome inactivation equalizes X-linked gene expression between the mammalian sexes by epigenetically silencing genes of one of the two X-chromosomes in females. Once established, the transcriptional states of the inactive and active X-chromosomes are faithfully transmitted across many cell division cycles, making X-inactivation a paradigm of epigenetic inheritance. In mice, the transcriptional fates of the two X-chromosomes are thought to be established by opposing long non-protein-coding (lnc) RNAs, Xist and Tsix. Xist is exclusively expressed from the inactive X-chromosome and is postulated to trigger X-inactivation. Tsix RNA is expressed solely from the active-X-chromosome and is believed to prevent X-inactivation by repressing Xist.

Prior work by our group has shown that X-linked gene silencing is able to initiate in the absence of Xist RNA, calling into question current models of X-inactivation, including the role of the Tsix RNA. Here, I examined the spatial and temporal requirement of the Tsix RNA in X-inactivation. By developing a protocol to image nascent RNA expression in intact mouse embryos, I discovered that Tsix is dispensable during the initiation phase of X-inactivation. Instead, Tsix is required to prevent Xist expression and X-inactivation once X-inactivation has occurred normally.

Through these data, I hypothesized that novel X-linked lncRNAs and proteins contribute to X-inactivation. I therefore developed an allele-specific RNA-Seq pipeline to

catalog lncRNAs and proteins that are expressed from the inactive X-chromosome, which my data predict are candidate regulators of X-inactivation. I also leveraged this RNA-Seq pipeline to profile X-inactivation defects in mouse trophoblast stem cells (TSCs) lacking EED, a core subunit of Polycomb Repressive Complex 2 (PRC2) that is thought to silence X-linked genes. Unexpectedly, I found that only a small subset of genes is derepressed from the inactive X-chromosome in *Eed*^{-/-} TSCs. In wild-type TSCs, these genes are characterized by low-level transcription and open chromatin. Thus, PRC2 prevents induction of basally transcribed X-linked genes but is dispensable in the repression of stringently silenced X-linked genes, providing a novel mode of epigenetic transcriptional repression by PRC2. Future work will characterize novel regulators of X-inactivation discovered through my RNA-Seq pipeline.

Chapter 1: Introduction

Portions of this chapter have been previously published as part of a review in *Chromosome Research* as “Long non-coding RNAs at the X-inactivation Center”, by Emily Maclary, Michael Hinten, Clair Harris, and Sundeep Kalantry (*Chromosome Research*. 21, 601–614 (2013)).

1-1: Introduction to Epigenetic Regulation and X-chromosome Inactivation

Inside the nucleus, DNA is wrapped around octamers of histone proteins and packaged into chromatin. Both the DNA itself and the histones it wraps around can be covalently modified without altering DNA sequence; DNA can be methylated at CpG dinucleotides, whereas histone tails can be modified with a wide variety of covalent modifications, including methylation, acetylation, phosphorylation, ubiquitylation, and sumoylation (Kouzarides, 2007). These histone modifications can influence gene expression patterns by altering DNA accessibility to transcriptional machinery. Some histone modifications can be heritably propagate transcriptional patterns through multiple mitotic cell divisions, or even through meiosis, i.e., transgenerationally (Campos et al., 2014). These mitotically or meiotically heritable gene expression changes are considered “epigenetic”, in that they alter gene expression in a transmissible manner without changing the underlying DNA sequence. Although many of the enzymes that catalyze covalent modifications of DNA and histones have been identified, the cellular factors that trigger and maintain epigenetic transcriptional states remain largely unknown (Bonasio et al., 2010).

Understanding how epigenetic regulation is established and inherited is essential, as epigenetic regulation plays a critical role in a wide variety of biological processes, including embryonic development, aging, and disease (Sauvageau and Sauvageau, 2010).

X-chromosome inactivation is a paradigm of epigenetic regulation that offers a window into the mechanisms that establish and maintain epigenetic gene expression profiles in cells and their descendants (Lee, 2010; LYON, 1961). During X-inactivation, genes on one of the two X-chromosomes in XX female mammals are transcriptionally silenced in order to equalize the dosage of X-linked genes to that expressed in XY males (Payer and Lee, 2008). Thus, X-inactivation results in one of the two X-chromosomes within a shared nucleus becoming inactivated, while the other X-chromosome remains active. Once established, with a few notable exceptions, the transcriptional profiles of the two X-chromosomes are maintained through numerous rounds of cell division, essentially for the life of the organism. X-inactivation is an epigenetic process that occurs in all female mammalian cells, and the kinetics of X-inactivation are well-defined in the developing embryo, making X-inactivation an experimentally tractable model system for studying the factors involved in epigenetic regulation (Lee, 2010).

The study of X-chromosome inactivation originated with the observation in 1949 that female, but not male, feline cells harbored a dark structure near the nucleolus (Barr and Bertram, 1949). This structure, called a “Barr body”, was later demonstrated to be one of the X-chromosomes within a female cell (OHNO et al., 1959). In 1961, Mary Lyon then proposed, based on observation of coat color patterns in mice, that this Barr body was not just condensed, but was a genetically inactivated X-chromosome (LYON, 1961). Lyon’s hypothesis was borne out by early studies of human females bearing mutations in the X-linked gene *G6pdx* (Deys et al., 1972; Kattamis, 1967).

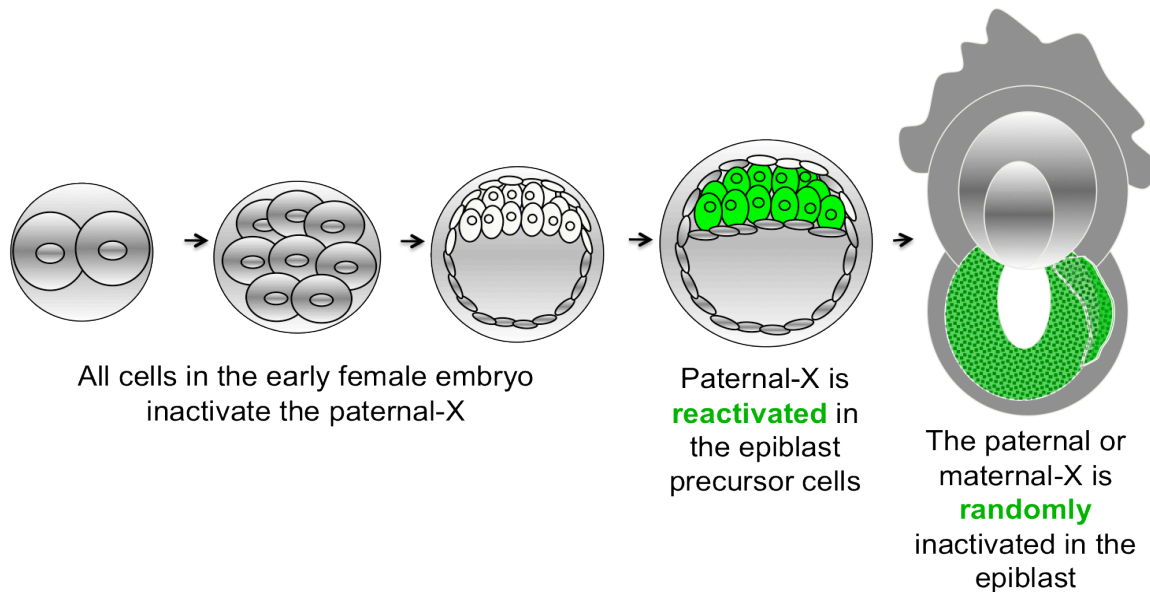


Figure 1.1: Two types of X-inactivation in the mouse embryo. Initially, beginning around the 2-4 cell stage, all cells in the developing mouse embryo inactivate the paternally-inherited X-chromosome. Epiblast precursor cells (green) later reactivate the paternal-X in the peri-implantation embryo; these cells then undergo random inactivation. Extra-embryonic cells (gray) maintain imprinted inactivation of the paternal X-chromosome.

Since the identification of the inactive X-chromosome in mammalian cells, mice have become the pre-eminent model system for the study of X-chromosome inactivation. Interestingly, over the course of embryonic development, mice undergo two distinct forms of X-chromosome inactivation: imprinted and random (See Fig. 1.1). Imprinted X-inactivation initiates at the 4-8 cell stage of embryonic development, and leads to the preferential inactivation of the paternal X-chromosome (Kalantry et al., 2009; Namekawa et al., 2010; Okamoto et al., 2004; Patrat et al., 2009; Takagi and Sasaki, 1975). Later, at the peri-implantation stage of development (128-256 cells), the paternal X-chromosome is reactivated in cells of the epiblast lineage, which will become the embryo proper (Mak et al., 2004; Sheardown et al., 1997). These cells subsequently undergo random X-inactivation, stochastically selecting either the maternal or paternally-inherited chromosome for silencing (McMahon et al., 1983; Rastan, 1982). The extra-embryonic tissues, which will give rise to the placenta and the yolk sac of the developing embryo, maintain imprinted

inactivation of the paternally-inherited X-chromosome (Takagi, 1978; Takagi and Sasaki, 1975; West et al., 1977). Since X-inactivation was first described, research has sought to identify the factors that trigger both imprinted and random X-chromosome inactivation in female mammalian cells.

1-2: Identification and Mapping of the X-inactivation Center

A key set of insights in X-inactivation came through chromosomal translocations and truncations involving the X-chromosome (Fig. 1.2). Through the study of these aberrant X-chromosomes in mice and mouse embryonic stem cells (ESCs), as well as in human disorders, a region on the X-chromosome was pinpointed as being both necessary and sufficient to bring about inactivation. One of the most well-studied translocations is the mouse T16H Searle's translocation, a reciprocal translocation between the X-chromosome and chromosome 16 (Eicher et al., 1972). Cytological assessments suggested that only one of the translocation products, 16X, but not the other, X16, can undergo inactivation (Rastan, 1983; Takagi, 1980). Based on these observations, a region required for X-inactivation – the X-inactivation center - was predicted to reside distal to the T16H breakpoint (Rastan, 1983).

A second mutation, termed HD3, in mouse ESCs truncated the X-chromosome but did not impede X-inactivation (Rastan and Robertson, 1985). Thus, the X-inactivation center was delimited to the interval between the T16H and HD3 breakpoints. Initial banding studies of these chromosomes followed by comparative genetic analyses of multiple rearranged X-chromosomes in mice, including the T16H translocation, narrowed the X-inactivation center to roughly 8 centimorgan (Brown, 1991; Keer et al., 1990; Rastan and Brown, 1990). These mapping experiments pinpointed the mouse T16H breakpoint to lie just proximal to the *Zfx* locus (Keer et al., 1990). Mapping the HD3 breakpoint would have similarly delineated the distal end of the X-

inactivation center, but the instability of this particular ESC line seems to have precluded molecular mapping (Brown, 1991).

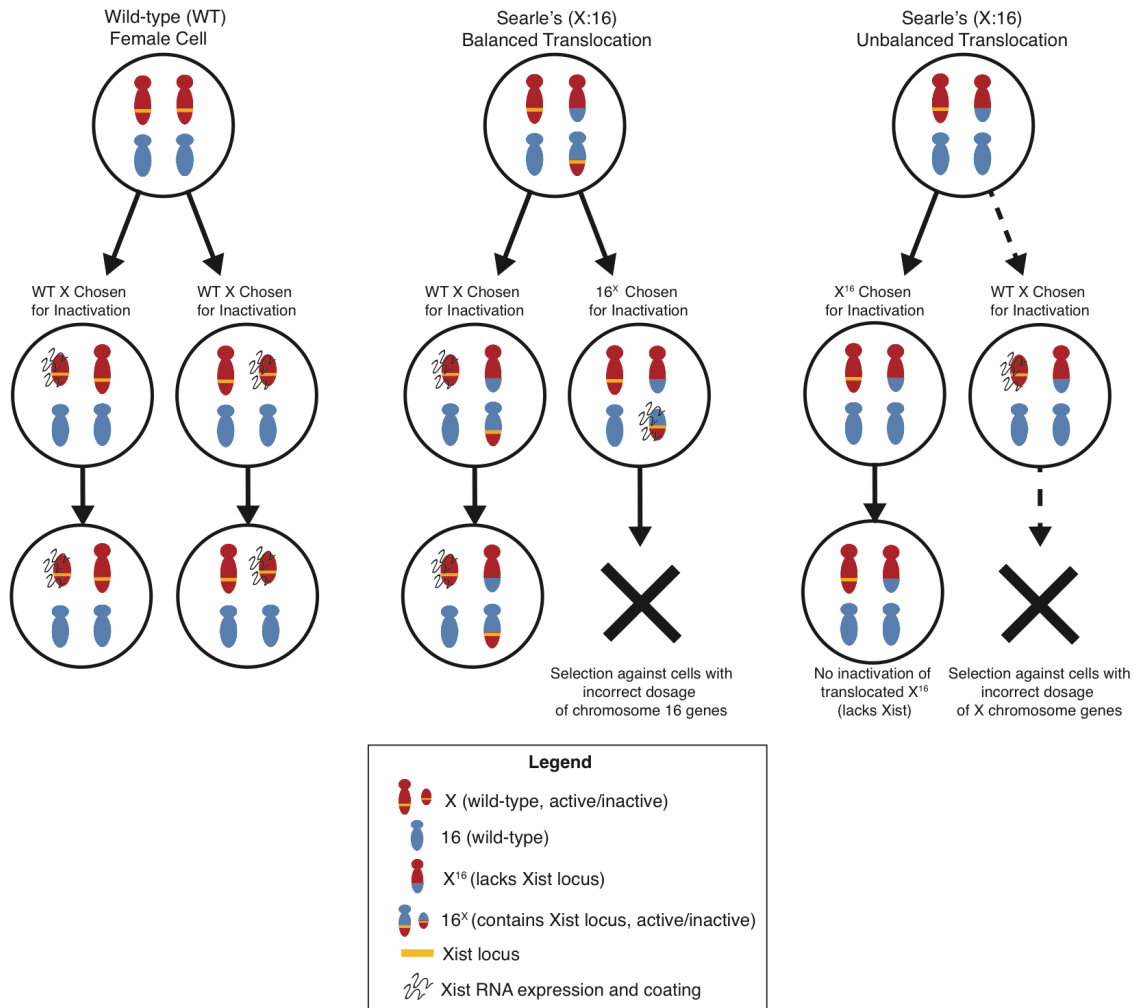


Figure 1.2: Schematic of Searle's Translocation, Used to Map the X-inactivation Center. Searle's translocation, a reciprocal translocation between the X-chromosome and chromosome 16, allowed for mapping of the minimal region required for a chromosome to undergo X-inactivation.

The human X-inactivation center was also defined by X-chromosomal abnormalities. In humans, the X-inactivation center was mapped distal to the *AR*, *CCG-1*, *RPS4X*, and *PHKA* loci and proximal to *PGK1* (Brown et al., 1991a; 1991b). A comparison of the X-inactivation center regions of mice and humans demonstrated that they both belonged to a conserved linkage group (Brown, 1991).

The X-inactivation center is now known to contain numerous genes, including a number of long non-protein coding RNAs (Fig. 1.3) (Augui et al., 2011; Maclary et al., 2013). The most prominently studied gene within the X-inactivation center is the *X-inactive specific transcript*, or *Xist*, and the antisense partner of *Xist*, *Tsix*.



Figure 1.3: The X-inactivation Center. The X-inactivation center spans a 700 kb (~8 centimorgan) region, and is home to numerous protein coding genes (gray) and long non-coding RNAs (colored)

1-3: The *Xist* Long Non-Coding RNA

XIST was first identified based on hybridization of a human cDNA probe to female but not male samples (Brown et al., 1991a). This cDNA clone intriguingly mapped to the human X-inactivation center (Brown et al., 1991a; 1991b). The sex-specific expression and the location of the transcript within the X-inactivation center made *XIST* a compelling candidate regulator of X-inactivation. The mouse homolog, *Xist*, was identified shortly thereafter, and was similarly expressed from the inactive X-chromosome (Borsani et al., 1991; Brockdorff et al., 1991). *Xist* RNA was subsequently found to physically coat the inactive-X chromosome, and studies in mice demonstrated that *Xist* RNA remains associated with the inactive-X during mitosis (Figure 2) (Brown et al., 1992; Clemson et al., 1996; Jonkers et al., 2008). The presence of *Xist* on the mitotic inactive-X supports its role as a transmitter of the epigenetic state of the inactive-X from one cell division cycle to the next. In human cells, however, *Xist* RNA appears to dissociate from the X-chromosome during mitosis (Clemson et al., 1996; Hall and Lawrence, 2003).

Xist has been shown to be instrumental in both the imprinted and random forms of X-inactivation in mice. At the onset of both imprinted and random X-inactivation, *Xist* RNA is induced from and coats the X-chromosome that will become inactivated, thus suggesting a causal

role in inactivation itself. In agreement, mutational studies have shown that Xist is essential for both imprinted and random X-inactivation in mice. Embryos that inherit a paternally transmitted Xist mutation die due to compromised extra-embryonic development, consistent with a defect in imprinted X-inactivation (Kalantry et al., 2009; Marahrens et al., 1997). Analysis of the epiblast-derived tissues, which have earlier undergone random X-inactivation, indicates that all fetal cells harboring a heterozygous Xist mutation will preferentially inactivate the wild-type X-chromosome (Kalantry et al., 2009; Marahrens et al., 1998). In differentiating female ESCs, which are derived from the epiblast lineage and are the favored in vitro random X-inactivation model system, X-inactivation is also biased in cells heterozygous for a null Xist mutation (Penny et al., 1996). These biases in random X-inactivation suggest that Xist may be required in *cis* to bring about silencing of the chromosome from which it is expressed. However, Xist-heterozygosity biases the choice of which X-chromosome becomes inactivated, such that the wild-type X is preferentially selected to become inactivated; the mutant-X therefore never has the option of being inactivated. Thus, strictly speaking, the biased choice step, which necessarily precedes random X-inactivation, precludes knowing if Xist is required for inactivation itself.

The most convincing evidence supporting a role for Xist in triggering silencing is via transgenes that ectopically express Xist (Plath et al., 2002; Wutz and Jaenisch, 2000; Wutz et al., 2002). In cultured ESCs, Xist transgenes can variably induce silencing of reporter constructs or endogenous genes surrounding the insertion site. Silencing is dependent on the genomic site of integration, the expression level, copy number of the transgene, as well as the inclusion of Xist regulatory regions present in the transgene. For example, a multi-copy 450 kb mouse transgene has been shown to induce Xist RNA expression and coating, as well as silencing of a LacZ reporter within the transgene in male ESCs (Lee et al., 1996). Additionally, fibroblast cells that

were derived from adult chimeric mice generated by injecting the transgenic ESCs into wild-type embryos displayed silencing of four endogenous autosomal genes spread across the length of the transgenic chromosome (Lee and Jaenisch, 1997; Lee et al., 1996). The conclusion in these studies was that the entire X-inactivation center function could be recapitulated by the 450 kb transgene sequence. Of note, however, is that haploinsufficiency for large regions of autosomes, which would occur in these cells if the Xist transgene resulted in extensive silencing of endogenous autosomal genes, typically results in early embryonic lethality, as suggested by studies of monosomic embryos and embryos harboring large chromosomal deletions (Baranov, 1983; Magnuson et al., 1985). The extensive contribution of transgenic ESCs to adult chimeric mice, which were estimated to show up to 90% chimerism, suggests that silencing of endogenous genes by this transgene may be weak (Lee and Jaenisch, 1997; Lee et al., 1996). Whereas multi-copy transgenes can bring about Xist induction and potentially gene silencing, single copies of similarly large transgenes are unable to induce silencing in ESCs. A single-copy 460 kb X-inactivation center transgene including Xist showed negligible Xist induction in a number of adult cell types and was insufficient to silence a linked LacZ reporter cassette in mice, leading to the conclusion that the transgene does not contain sequences within it to induce Xist expression (Heard et al., 1996; 1999). The same animals, however, display imprinted Xist expression in early mouse embryos; Xist is only induced when the transgene is paternally-inherited (Okamoto et al., 2005). Ectopic Xist RNA expression and coating in this study correlates with transcriptional silencing of a gene within the transgene construct; whether endogenous genes near the insertion site are also silenced, though, is not known. The fact that the development of these animals is not defective argues against large-scale inactivation of endogenous loci that reside at or near the transgene integration site. Moreover, given the failure of transgenic Xist

expression in cells that undergo random X-inactivation, the ability of the same transgene to express Xist and silence during imprinted X-inactivation is paradoxical. This differential silencing ability may suggest divergent mechanisms that influence both the expression and function of Xist RNA during imprinted versus random X-inactivation. Though large transgenes that harbor the Xist locus as well as other elements of the X-inactivation center are not always sufficient to induce silencing, single-copy inducible Xist transgenes often are. For example, inducible Xist cDNA transgenes targeted to the *Hprt* locus on the X-chromosome or on autosomes are able to trigger silencing of endogenous genes (Jiang et al., 2013; Wutz and Jaenisch, 2000; Wutz et al., 2002). This silencing function may, however, be due to the artificially high levels of Xist expression from these inducible transgenes. Some evidence also suggests that ectopic Xist induction is able to silence genes in some cell types in vivo, not just in cultured cells. In transgenic mice harboring an inducible Xist transgene, Xist induction is able to lead to ectopic X-inactivation in immature hematopoietic precursor cells, but not hematopoietic stem cells or mature cells (Savarese et al., 2006). Similar to studies of Xist transgenes in ESCs, this work suggests that there is a window of opportunity during development when Xist RNA is able to silence; this silencing function is closely linked to the differentiation state of cells as well as, importantly, to the level of Xist expression (Savarese et al., 2006; Wutz and Jaenisch, 2000).

Xist is thought to function by recruiting proteins to the prospective inactive-X that modify chromatin structure and alter gene expression. Xist RNA expression is followed by the formation of a repressive chromatin state that excludes transcriptional machinery from the inactive-X, potentially by recruiting chromatin-modifying proteins (Chaumeil et al., 2006). These proteins are thought to help establish the heterochromatic and transcriptionally inert chromatin state characteristic of the inactive X-chromosome.

1-4: Tsix RNA: an Antisense Regulator of Xist Expression

Following identification of Xist, an anti-sense transcript to Xist, called Tsix, was identified in the mouse model system. This antisense RNA was discovered following the observation that the region 3' to Xist influences X-chromosome counting, a process during which the cell senses the number of X-chromosomes present and determines how many, if any, to inactivate (Clerc and Avner, 1998). In the seminal study by Clerc and Avner, XX female cells inactivate a single X-chromosome, as expected. However, XO female cells that have lost the wild-type X chromosome and which also harbor a 65 kb deletion 3' of Xist on their intact X-chromosome induce Xist RNA and initiate silencing of their single X-chromosome. The expectation is that cells with a single X-chromosome should not activate Xist expression or undergo X-inactivation. Thus, in the absence of the Xist 3' region, the cells failed to correctly identify the number of X-chromosomes present (Clerc and Avner, 1998). The 65 kb deleted segment, therefore, normally controls X-chromosome counting by suppressing Xist.

Analysis of the Xist 3' region using RNA fluorescence *in situ* hybridization detected an RNA anti-sense to Xist in both male and female ESCs (Lee et al., 1999a). The transcript, termed Tsix (Xist spelled backwards) is expressed in females from both X-chromosomes prior to X-inactivation; however, upon differentiation of female ESCs that triggers X-inactivation, Tsix is downregulated from the Xist-expressing inactive-X and is expressed only from the active X-chromosome. Following the onset of X-inactivation, Xist and Tsix thus show mutually exclusive expression from the inactive and active X-chromosomes, respectively. Unlike Xist, however, Tsix RNA is expressed at relatively low levels and does not coat the active X-chromosome. Tsix transcription has been proposed to repress Xist at multiple key developmental time points. First, due to the early expression of Tsix, the Tsix RNA has been nominated as the instrument of the

oocyte-derived imprint that inhibits Xist expression from the maternally- inherited X chromosome during the onset of imprinted X-inactivation (Lee, 2000; Sado et al., 2001). Continued expression of Tsix is then posited to keep the maternal-X from undergoing X-inactivation in the extra-embryonic tissues of the developing embryo that maintain imprinted X-inactivation. This function of Tsix is clearly illustrated by the death of embryos harboring maternally-inherited Tsix mutations due to failed development of the extra-embryonic tissues (Lee, 2000; Sado et al., 2001).

Tsix also plays a prominent role in random X-inactivation. As part of its role as a repressor of Xist, Tsix has been proposed to function in the counting and choice processes of random X-inactivation. Random X-inactivation is thought to be a linear three-step process. In the first step, counting, the cell senses how many X-chromosomes it has (Grumbach et al., 1963; LYON, 1962). If and only if there are two or more X-chromosomes does the choice step ensue. During the choice step, the cell selects which X chromosome will remain active, and which will be inactivated. Following the choice step, X-inactivation initiates (Rastan, 1983). Evidence for a counting step in X-inactivation is supported by observations of cells harboring abnormal complements of sex chromosomes. Whereas normal XY male cells do not undergo X-inactivation, XXY nuclei inactivate one of their two X-chromosomes. Furthermore, in females, diploid cells with more than two X-chromosomes will inactivate all but one X, but XO cells do not undergo X-inactivation. This suggests that inactivation occurs, in part, as a function of the number of X-chromosomes in the cell. The autosomal complement also plays a critical role in X-chromosome counting. Whereas diploid XX cells always have a single active and single inactive X-chromosome, tetraploid cells maintain two active- and two inactive-Xs (Monkhorst et al., 2008; Webb et al., 1992). Tetraploid cells can therefore tolerate two active Xs. This suggests that

both X-linked and autosomal factors contribute to X-chromosome counting, and mediate the decision as to whether to undergo X-inactivation or not.

Tsix was initially implicated as a counting factor based on a series of deletions adjacent to, and upstream of, the Tsix locus. These mutations can lead to aberrant Xist induction in differentiating XO female and XY male ESCs, a phenotype that is considered indicative of a counting defect (Clerc and Avner, 1998; Cohen et al., 2007; Vigneau et al., 2006). The DXPas34 repetitive sequence, located adjacent to Tsix exon 3, has been identified as a regulator of counting based on these genetic studies. DXPas34 functions to enhance Tsix expression, thereby influencing X-chromosome counting (Cohen et al., 2007; Navarro et al., 2010).

Tsix is also suggested to control the choice of which X-chromosome will be inactivated. In Tsix-heterozygous female embryos and ESCs, the Tsix-mutant X-chromosome is observed to always be the inactive-X (Lee and Lu, 1999; Sado et al., 2001). There are two models that could explain this bias. The first and most popular model is a primary non-random X-chromosome choice model, where the Tsix-mutant X is always chosen for inactivation due to ectopic Xist induction from the mutant-X at the onset of inactivation (Lee, 2000; Sado et al., 2001). A second possibility that could give rise to the observed bias is that random X-inactivation occurs normally, with both the wild type and the mutant X-chromosome equally likely to undergo inactivation. Subsequently, Xist is ectopically expressed from the Tsix mutant X-chromosome if the wild-type X is initially chosen for inactivation. These cells would then rapidly be selected away due to two inactive Xs. Since inactivation of the wildtype X-chromosome is not observed at significant rates in differentiating Tsix-mutant ESCs and embryos, the model of primary non-random choice is favored. Incidentally, a secondary cell-selection effect has been invoked to explain X-inactivation patterns in Xist-heterozygous ESCs (Penny et al., 1996).

1-5: Beyond Xist and Tsix: Other lncRNAs at the X-inactivation Center

In addition to the Xist and Tsix lncRNAs, the X-inactivation center is home to five additional lncRNAs: RepA, XistAR, Ftx, Jpx/Enox, and Tsx. The roles of these lncRNAs are less well studied than the Xist and Tsix RNAs; however, all have ties to regulation of X-chromosome inactivation. Two of these lncRNAs, RepA and XistAR, reside completely within the exonic sequence of the *Xist* gene itself (Sarkar et al., 2015; Zhao et al., 2008). The remaining three RNAs flank the *Xist/Tsix* genomic locus.

Within Xist RNA, there are a number of small repeat units. One of these repeats, the “A” repeat, is located at the 5’ end of Xist and has been found to be expressed as a distinct transcriptional unit (Zhao et al., 2008). This RNA, termed RepA, spans from basepair 300 to basepair 1,948 of Xist exon 1, and is transcribed in the same direction as Xist. RepA RNA interacts with chromatin modifying proteins recruited by Xist RNA such as PRC2, and shRNA knockdown of RepA leads to reductions of both Xist RNA expression and enrichment of repressive histone modifications on the inactive-X (Zhao et al., 2008). Thus, the RepA transcriptional unit may play a role in recruitment of chromatin modifiers and establishment of silencing marks, however, polycomb group proteins can be recruited to Xist in the absence of RepA (Plath et al., 2003), suggesting that RepA is not the only sequence involved in recruitment of chromatin modifiers.

The XistAR RNA, like RepA, is a distinct transcriptional unit wholly contained within *Xist* exon 1; unlike RepA, XistAR is transcribed in the antisense direction from Xist (Sarkar et al., 2015). Targeted disruption of XistAR leads to disruption of Xist RNA expression *in cis* during the initiation of X-inactivation, suggesting that XistAR transcription is required to drive Xist RNA expression, perhaps functioning as an enhancer RNA (Sarkar et al., 2015).

Upstream of the *Xist* locus is the 63kb *Ftx* RNA, which is thought to play a role in activating *Xist* transcription (Chureau et al., 2011). *Ftx* escapes X-chromosome inactivation, and thus is expressed from both the active and inactive X-chromosomes, though expression levels from the inactive-X are lower (Chureau et al., 2011; Kunath et al., 2005; Mak et al., 2002). Genetic deletion of *Ftx* in male ES cells disrupts the expression of nearby genes, and intriguingly, appears to preferentially effect adjacent genes that are transcribed in the same orientation, including *Xist* (Chureau et al., 2011). This ablation of *Ftx* also leads to changes in DNA methylation and Histone H3 at lysine 4 dimethylation at the *Xist* promoter, suggesting that *Ftx* plays a role in regulating the chromatin environment at the *Xist* promoter (Chureau et al., 2011). The precise role of *Ftx* in X-inactivation currently remains unclear, as disruption of *Ftx* in female cells has not been assessed, and prior genetic studies have relied on deletions of a large genomic segment, which could itself affect chromatin structure and local gene expression, regardless of the role of *Ftx* RNA expression.

Approximately 40kb from the 3' end of *Xist* is *Tsx*, or testes-specific X-linked, ncRNA (Simmler et al., 1996). *Tsx* is highly expressed in the testes, but is also expressed at lower levels in both male and female brain (Anguera et al., 2011). Genetic deletion of *Tsx* leads to decreased female fertility and sex ratio distortion, with female offspring underrepresented among litters ((Anguera et al., 2011). In undifferentiated ES cells, *Tsx* is expressed in both male and female cells. *Tsx* expression is downregulated in differentiating female ES cells, coincident with *Xist* induction. In *Tsx* mutant ES cells, both female and male cells show a slight increase in the number of cells with *Xist* RNA coating on the active X. *Tsix* RNA, a repressor of *Xist*, is also downregulated in these mutants (Anguera et al., 2011). These data suggest that *Tsx* may function as a repressor of *Xist* RNA, perhaps via positive regulation of *Tsix* expression (Anguera et al.,

2011).

Jpx, also known as expressed neighbor of Xist, or Enox, lies 10kb upstream of Xist RNA and is transcribed in the antisense orientation to Xist (Johnston et al., 2002). Jpx was initially proposed to serve as a regulator of Xist after an 80kb transgene containing numerous components of the X-inactivation center, including Xist, Tsix, and the Tsix regulator Xite, was found to be unable to induce Xist RNA (Lee et al., 1999b). Deletion of Jpx in ES cells does not appear to have any phenotypic consequences in males, however, female ES cells heterozygous for Jpx mutations show growth defects, a decrease in Xist RNA coating, and increased cell death upon differentiation (Tian et al., 2010). These defects can be rescued by exogenous expression of Jpx from a transgene, suggesting that this lncRNA can, unusually, act in *trans* to activate Xist (Tian et al., 2010). The presence of a Jpx transgene in wild-type ES cells has been shown by one study to trigger low levels of ectopic Xist induction in male and female ES cells (Sun et al., 2013), though prior work did not detect Xist induction in male ES cells harboring a Jpx transgene (Jonkers et al., 2009). Overall, Jpx may have a modest activating effect on Xist RNA, though a conclusive role for Jpx in X-inactivation has yet to be confirmed by genetic studies in mice.

Whereas RepA, XistAR, Ftx, Jpx/Enox, and Tsx reside within the X-inactivation center and evidence suggests roles for some or all of these factors in X-inactivation, the Xist and Tsix RNAs remain the primary focus of many studies to elucidate the mechanisms of epigenetic silencing. The functions these two lncRNAs have been extensively studied both *in vitro* and *in vivo*, however, questions remain regarding their mechanisms of action and their precise roles in the cascade of events that trigger epigenetic silencing.

1-6: *Trans*-acting Regulators of X-inactivation

Xist and Tsix are postulated to function as the master regulators that orchestrate X-inactivation in *cis*, perhaps aided by the regulatory functions of other long non-coding RNAs at the X-inactivation center. In addition to these *cis*-acting RNAs, a number of *trans*-acting factors have also been identified as players in X-inactivation. Notable *trans*-acting factors postulated to be involved in X-chromosome inactivation include the Polycomb group proteins, which form Polycomb Repressive Complex 1 (PRC1) and Polycomb Repressive Complex 2 (PRC2), ASH2L, a member of the Trithorax group of chromatin modifying proteins, the X-linked RNF12 ubiquitin ligase, and a variety of proteins recently identified as Xist RNA interactors.

Xist RNA is known to recruit Polycomb group proteins, a process in which the RepA non-coding RNA that is encoded within Xist may play a role (Kohlmaier et al., 2004; Plath et al., 2003; Silva et al., 2003; Zhao et al., 2008). These complexes catalyze repressive histone modifications that are enriched on the inactive-X, with PRC1 catalyzing ubiquitination of lysine 119 in histone H2A (H2A-K119ub) and PRC2 catalyzing trimethylation of histone H3 lysine 27 (H3-K27me3) (Gieni and Hendzel, 2009; Margueron and Reinberg, 2010; Sauvageau and Sauvageau, 2010; Surface et al., 2010). PRC2, specifically, has a well-characterized role in X-chromosome inactivation.

At the onset of both random and imprinted X-inactivation, PRC2 proteins and H3-K27me3 are enriched on the inactive X-chromosome (Erhardt et al., 2003; Okamoto et al., 2004; Plath et al., 2003; Silva et al., 2003). PRC2 is a large evolutionarily conserved multimeric protein complex, which catalyzes H3K27me3 at target loci (Cao et al., 2002; Czermin et al., 2002; Kuzmichev et al., 2002; Müller et al., 2002; Tie et al., 2001). These post-translational modifications of histones within chromatin are thought to propagate epigenetic transcriptional

states across cell division (Margueron and Reinberg, 2011; Zhang et al., 2015). Mammalian PRC2 consists of the core components EZH2, EED, and SUZ12 (Cao et al., 2002; Kuzmichev et al., 2002). EZH2 is the enzymatic subunit of PRC2 that catalyzes H3-K27me₃, a mark that correlates with gene silencing (Cao et al., 2002; Zhang et al., 2015). PRC2 is proposed to be recruited to the inactive X-chromosome by long non-coding RNAs, including both Xist and RepA RNAs. By virtue of its early enrichment on the inactive-X and its gene silencing function, PRC2 is thought to be critical for the stable silencing of X-linked genes (Plath et al., 2003; Silva et al., 2003). In agreement with this idea, loss-of-function studies suggest that PRC2 is required in imprinted mouse X-inactivation (Silva et al., 2003; Wang et al., 2001).

Whereas Polycomb group proteins are perhaps the best known of the Xist recruits, a number of other proteins are also localized to the inactive-X, potentially via Xist RNA. ASH2L, a member of the Trithorax group of chromatin modifying proteins, is recruited to the inactive- X following the onset of X-inactivation (Pullirsch et al., 2010). Paradoxically, the trithorax group proteins catalyze H3K4 trimethylation, a chromatin modification typically associated with active transcription (Steward et al., 2006). The recruitment of ASH2L coincides with the recruitment of SAF-A, a nuclear scaffolding factor (Pullirsch et al., 2010). The histone variant macroH2A, a variant associated with transcriptional repression, is enriched on the inactive-X as well (Costanzi and Pehrson, 1998; Perche et al., 2000; Rasmussen et al., 2000).

In addition to these chromatin modifiers, one protein-coding gene within the X-inactivation center, *Rnf12*, has also been postulated to play a role in X-chromosome inactivation. A transgene-based screen found that overexpression of this E3 ubiquitin ligase led to ectopic Xist induction from the single X-chromosome in differentiating male and from both X-chromosomes female ES cells, suggesting a role for RNF12 as an activator of Xist (Jonkers et al., 2009).

Further work has not shown a conclusive role for RNF12 in initiation of X-inactivation, however. Female embryos harboring maternally-inherited mutations in the *Rnf12* gene show that Xist induction is reduced, but not entirely absent, in cells that have undergone imprinted X-inactivation, and that these embryos die post-implantation (Shin et al., 2010). Notably, this time point is far after the initiation of imprinted X-inactivation, which begins around the 4-cell stage of embryonic development. Through studies of paternally-inherited mutations, RNF12 was subsequently shown to be dispensable for random X-inactivation (Shin et al., 2014). Though RNF12 is, directly or indirectly, able to activate Xist expression and may be required during imprinted X-inactivation, it does not appear to be fundamentally required for the initiation of random X-inactivation.

Proteomic and genetic screens have recently identified a number of Xist interacting factors that may function as *trans*-acting regulators of X-inactivation. One protein identified by multiple high-throughput screens is SPEN, a transcriptional repressor that interacts with nuclear receptor co-repressor 2 (NCOR2) and histone deacetylases (Chu et al., 2015; McHugh et al., 2015; Minajigi et al., 2015; Moindrot et al., 2015; Monfort et al., 2015). Both NCOR2 and histone deacetylases are associated with transcriptional silencing. Knockdown of SPEN in differentiating ES cells results in defects in X-linked gene silencing (McHugh et al., 2015), whereas CRISPR/Cas9-mediated deletion of SPEN in male ES cells with an inducible Xist transgene similarly impairs silencing upon Xist induction (Monfort et al., 2015). SPEN loss additionally impairs both Polymerase II exclusion from the Xist RNA coated inactive-X and recruitment of PRC2 (McHugh et al., 2015; Monfort et al., 2015). SPEN was the only factor identified by all screening approaches, proteomic analysis consistently identified SAF-A, hnRNPM, RALY, RBM15, and MYEF2 as additional Xist-interacting factors (Chu et al., 2015;

McHugh et al., 2015; Minajigi et al., 2015). Knockdown of Myef2 and hnRNPM RNAs did not alter X-linked gene silencing, whereas hnRNPU knockdown leads to loss of Xist RNA localization and defects in X-linked gene silencing (McHugh et al. 2015). Knockdown of Rbm15 in ES cells had mixed results, with one study reporting impaired silencing and another reporting no effect (McHugh et al., 2015; Moindrot et al., 2015). Individual studies also identified, and validated via shRNA screens, putative roles for LBR, WTAP, and hnRNPK as regulators of Xist localization or X-linked gene silencing (Chu et al., 2015; McHugh et al., 2015; Moindrot et al., 2015), and numerous other Xist interactors have been identified, but have yet to be further investigated or validated.

Genetic studies and high-throughput screens have begun to characterize roles for numerous *trans*-acting factors in X-inactivation; taken together, these data begin to illustrate the complexity of the regulatory network that initiates and maintains X-chromosome inactivation. Many of these *trans*-acting factors, however, thus far appear to function downstream of Xist RNA, playing roles in mediating X-linked gene silencing after Xist RNA coating is established, or tethering Xist RNA to the inactive-X chromosome.

1-7: Concluding Remarks

Current models of X-inactivation center on the role of the Xist and Tsix RNAs; additional *cis*-acting factors, such as other lncRNAs expressed from the X-inactivation center, function as regulators of these primary effectors of X-inactivation. The Xist RNA then recruits a set of *trans*-acting factors that are then thought to silence gene expression on the inactive X-chromosome. Numerous studies have provided important insights into the expression and function of Xist and Tsix RNAs, however, crucial gaps remain in our knowledge of the mechanisms underlying Xist and Tsix function in X-inactivation.

Critically, the temporal and lineage-specific function of Xist in X-linked gene silencing remains unclear. Xist RNA appears to be required during precise developmental windows in both imprinted and random X-inactivation. Evidence shows that Xist is dispensable during the early initiation phase of imprinted X-inactivation for many X-linked genes assayed (Kalantry et al., 2009). Conversely, Xist is also not required to maintain random X-inactivation in differentiated cells, despite the persistence of Xist RNA coating in somatic cells (Brown and Willard, 1994; Csankovszki et al., 1999; Wutz and Jaenisch, 2000). The data therefore suggest that Xist plays a tightly regulated, temporally specific role in controlling X-inactivation. Additionally, in both imprinted and random X-inactivation, gene expression in the absence of Xist varies from gene to gene. Some genes are dependent more on Xist for silencing, but others are less so (Csankovszki et al., 1999; Kalantry et al., 2009).

In addition to questions regarding the context-dependent requirement for Xist RNA in transcriptional silencing, how precisely Xist RNA acts as a catalyst for inactivation – i.e., through which of its recruited proteins – remains largely unknown. Both PRC1 and PRC2 that are recruited to the inactive-X by Xist are dispensable for random X-inactivation (Kalantry and Magnuson, 2006; Leeb and Wutz, 2007; Schoeftner et al., 2006). Mutations in SAF-A, another recruit of Xist, disrupt both Xist localization and X-linked gene silencing in ESCs, though not absolutely (Hasegawa et al., 2010). Both SAF-A and ASH2L, which are recruited to the inactive-X after the onset of X-inactivation, are able to be recruited to the X-chromosome by mutant Xist transcripts that are unable to induce X-linked gene silencing (Pullirsch et al., 2010). Furthermore, a null mutation in macroH2A1 does not result in defective X-inactivation (Changolkar et al., 2007). A paralog of MacroH2A1, macroH2A2, can potentially substitute for macroH2A1. In studies in which both macroH2A genes are knocked-down, X-inactivation is again normal

(Tanasijevic and Rasmussen, 2011). These data suggest that additional *trans*-acting factors contribute to X-linked gene silencing. These may include additional proteins recruited by Xist RNA, such as those recently identified in high-throughput screens, as well as via Xist-independent mechanisms. Analysis of dosage compensation in marsupials suggests that the ancestral form of X-inactivation occurs independently of Xist, making the possibility of Xist-independent mechanisms of X-inactivation particularly intriguing (Davidow et al., 2007; Hore et al., 2007; Shevchenko et al., 2007).

Beyond remaining questions about Xist itself, numerous questions remain regarding the precise role of Tsix in X-inactivation, including the mechanisms underlying Tsix-mediated regulation of Xist. DNA methylation and chromatin modifications of the Xist promoter region have been proposed as mechanisms through which Tsix may influence Xist expression. Tsix transcription across the Xist promoter indeed leads to DNA methylation and accumulation of repressive histone modifications at Xist promoter (Navarro et al., 2006; Sado et al., 2005). DNA methylation changes induced by Tsix, however, may not be a primary mechanism for regulation of Xist, as loss of both Dnmt3a and Dnmt3b, the de novo methyltransferases shown to associate with Tsix, does not lead to defects in X-inactivation (Sado et al., 2004). Understanding the regulation of Tsix expression itself is also a work in progress. Induction of Tsix is dependent on the recruitment of REX1, a pluripotency factor, to the Tsix locus (Navarro et al., 2010). Interestingly, *Rex1*^{-/-} female and male mice are born at the same rate, and show no defects in survival, suggesting that though REX1 may contribute to Tsix regulation it is not required for the establishment or maintenance of X-inactivation (Masui et al., 2008). Tsix regulation is also mediated by Xite, a non-coding RNA lying upstream of Tsix that promotes Tsix expression (Ogawa and Lee, 2003b). The DXPas34 repetitive element within the Tsix locus is believed to

serve a dual role as both an enhancer and repressor of Tsix (Cohen et al., 2007). Whereas these regulators of Tsix have been identified, the temporal requirement of these elements in regulating Tsix, Xist, and X-inactivation at the onset of both imprinted and random X-inactivation needs more scrutiny.

The role of Tsix in X-chromosome counting is also highly contested. Mutations that abrogate Tsix RNA expression sometimes, but not always, lead to aberrant Xist induction (Lee, 2000; Luikenhuis et al., 2001; Morey et al., 2001; Ohhata et al., 2006; Sado et al., 2001; Vigneau et al., 2006). Since Xist is not always induced in cells lacking Tsix, Tsix RNA itself may not be directly involved in counting. The DXPas34 enhancer of Tsix has also been implicated in X-chromosome counting, and was initially presumed to act through Tsix RNA (Cohen et al., 2007; Navarro et al., 2008). Whereas deletion of DXPas34 results in ectopic Xist induction that is consistent with a counting defect, an overdose of the DXPas34 genomic segment unexpectedly leads to failure of Xist induction (Lee, 2005). This genomic segment is proposed to function in counting by sequestering proteins that would normally activate Xist, i.e., by repressing Tsix.

Finally, questions remain about The Tsix RNA is also thought to be involved in the reactivation of the inactive paternal X-chromosome prior to random X-inactivation. The reactivation of the paternal-X is characterized by loss of Xist RNA coating in epiblast precursor cells, a process posited to be mediated by Tsix, though again no direct genetic evidence supports this assertion (Mak et al., 2004; Nesterova et al., 2011; Sheardown et al., 1997). In contrast, reactivation is not disrupted in the epiblast lineage of embryos harboring paternally-inherited Tsix mutations, suggesting that Tsix may in fact be dispensable during reactivation of the inactive-X (Kalantry and Magnuson, 2006). Moreover, surprisingly, X-linked gene reactivation appears to occur prior to the loss of Xist coating during reactivation (Williams et al., 2011). If

Tsix is involved in Xist repression and X-reactivation, how Tsix is induced from the inactive paternal-X is also unclear. Careful analysis of the expression and function of Tsix in these early embryonic stages in future studies may help elucidate the precise role of the Tsix long non-coding RNA in these processes.

I first define a spatially and temporally specific role for Tsix RNA during the initiation and maintenance of imprinted and random X-chromosome inactivation by assessing the effects of a Tsix null mutation in developing mouse embryos and in stem cell models of X-inactivation. I found that, during initiation of imprinted inactivation, Tsix is not required to forestall Xist induction from the active X-chromosome. Tsix is instead required for the continued repression of Xist RNA in differentiating cells. I additionally find that Tsix is not required for X-chromosome reactivation at the peri-implantation stage of embryogenesis. During random X-inactivation, I find that Tsix RNA does not influence X-chromosome choice, and is again not required for the initiation of X-chromosome inactivation. Instead, as with imprinted X-inactivation, Tsix RNA is required for the continued repression of Xist RNA in differentiating cells.

These analyses, coupled with prior data indicating that X-inactivation is able to initiate in the absence of Xist RNA, indicate that current models are insufficient to explain initiation of epigenetic silencing during X-chromosome inactivation. I hypothesize, based on my current work as well as evolutionary analysis of the X-chromosome, that X-inactivation is triggered regionally, by novel lncRNAs; Studies of the evolutionary history of the X and Y chromosomes in mammals indicate that X-inactivation likely arose in a piecemeal fashion, with discrete regions of the evolving X-chromosome becoming silenced as homologous genes were lost from the evolving Y-chromosome, suggesting regional control of dosage compensation (Bellott et al., 2014; Jegalian and Page, 1998; Lahn and Page, 1999). My analysis of Tsix mutant embryos and

stem cells has also implicated *trans*-acting products of X-linked genes that escape from X-inactivation as potential dosage-dependent regulators of X-inactivation in female cells. To identify potential novel lncRNAs and escapers of X-inactivation that may play a role in the regulation of imprinted and random X-inactivation, I have developed a strand-specific and allele-specific RNA-sequencing pipeline to comprehensively evaluate the transcriptomes of stem cell models of both imprinted and random X-inactivation. Through this transcriptomic analysis, I identify numerous novel RNAs, including putative inactive-X specific transcripts, and delineate escapers of X-inactivation in both imprinted and randomly inactivated populations of cells.

I have further applied this RNA-seq analysis pipeline to characterize X-chromosome inactivation defects in mutant mouse stem cells. Allele-specific RNA-seq allows for high-throughput screening for defective X-linked gene silencing. I analyzed trophoblast stem cells (TSCs) lacking the EED protein, a core subunit of PRC2. I found that loss of EED leads to loss of H3K27me3 enrichment as well as of Xist RNA from the inactive-X. Surprisingly, only a subset of genes on the X-chromosome show defects in silencing when EED, Xist RNA, and H3K27me3 are absent, implicating factors other than PRC2 and Xist RNA in maintaining X-linked gene silencing.

Through these studies, I have defined the precise role of the Tsix lncRNA in mouse imprinted and random X-inactivation. Contrary to the broadly hypothesized function of lncRNAs as initiators of epigenetic transcriptional regulation, I show that the Tsix lncRNA serves instead as a factor that maintains epigenetic silencing in a differentiation-dependent manner. These observations establish a new model for lncRNA function, which may apply to other epigenetic regulatory processes in the genome, such as clusters of genes subject to genomic imprinting. I further establish an experimental pipeline for allele-specific analysis of X-linked gene expression

in mouse embryos and stem cells. Characterization of the transcriptomes of extra-embryonic and embryonic cell lineages identifies numerous escapers of X-inactivation, which may play a role in X-linked gene silencing (Gayen et al., 2015), as well as inactive-X specific transcription. Using this pipeline, I have characterized the role of PRC2 in X-inactivation. Together, these data demonstrate that current models of X-inactivation paint an incomplete picture of the processes that initiate epigenetic silencing in the developing embryo. Future work will characterize escapers of X-inactivation and novel transcripts identified by RNA-sequencing, and will continue to characterize the precise role of PRC2 in initiation and maintenance of X-chromosome inactivation.

Chapter 2: Differentiation-dependent requirement of Tsix long non-coding RNA in imprinted X-chromosome inactivation

This chapter was previously published in *Nature Communications* as Maclary, E. Buttigieg E., Hinten M., Gayen S., Harris C., Sarkar M.K., Purushothaman S., and Kalantry S.

“Differentiation-dependent requirement of Tsix long non-coding RNA in imprinted X-chromosome inactivation”. (*Nature Communications* 5, 4209 (2014)). Data was predominantly generated by E.M., and all final images and figures were generated by E.M., E.B., and S.K. wrote the manuscript. M.H., E.B., and S.P. assisted with initial analysis of E3.5 embryos. C.H., S.G., and M.K.S derived and cultured TS and XEN cell lines. E.B. generated and optimized strand-specific RNA FISH probes.

2-1: Introduction

X-chromosome inactivation results in the mitotically-stable epigenetic transcriptional silencing of genes along one of the two X-chromosomes in female mammals, thereby equalizing X-linked gene expression between males and females (Morey and Avner, 2011). X-inactivation is thought to be separable into three phases: initiation, establishment, and maintenance (Plath et al., 2002). During the initiation phase, cell autonomous epigenetic mechanisms identify the future inactive X-chromosome and trigger the formation of transcriptionally inert heterochromatin on that X. This heterochromatic configuration is then proposed to spread during

the establishment phase to envelop genes across most of the inactive X-elect. Once inactivated, replicated copies of that X-chromosome are transmitted as inactive through multiple mitotic cell division cycles during the maintenance phase. While one X-chromosome is transmitted as inactive during mitosis, the other X within the same nucleus is maintained in a transcriptionally active state.

The epigenetic transcriptional states of both the inactive and active X-chromosomes are controlled in *cis* by a segment on the X-chromosome that encodes long non-coding RNAs (lncRNAs) which play key roles in both X-inactivation and in forestalling inactivation of the active-X (Lee, 2011; Rastan, 1983; Rastan and Robertson, 1985). The two most prominent lncRNAs are Xist and Tsix. Xist is induced exclusively from the inactive X-chromosome and is considered a primary determinant of X-inactivation (Marahrens et al., 1998; Penny et al., 1996). Current models posit that Xist RNA transcription initiates a cascade of events that ultimately leads to X-inactivation (Morey and Avner, 2011; Payer and Lee, 2008). Xist RNA physically coats the chromosome from which it is expressed, leading to the deposition of proteins that catalyze epigenetic transcriptional silencing along this X-chromosome (Kalantry, 2011; Plath et al., 2002). The most notable of the Xist RNA recruits are Polycomb group proteins. Distinct Polycomb group complexes are thought to contribute to the formation of the unique facultative heterochromatic structure of the inactive-X via post-translational modification of histones (Lee, 2011; Mak et al., 2002; Plath et al., 2003; 2004; Rastan, 1983; Rastan and Robertson, 1985; Silva et al., 2003). While expression of the Xist RNA is required in *cis* for X-inactivation, transcription of the Xist anti-sense RNA, Tsix, is necessary to prevent inactivation of the active-X (Lee, 2000; Lee and Lu, 1999; Marahrens et al., 1998; Penny et al., 1996; Sado et al., 2001). Tsix

transcription across the *Xist* gene is posited to inhibit *Xist* expression, potentially by influencing chromatin modifications at the *Xist* promoter (Sado et al., 2001; 2005).

In mice, all cells of the developing zygote initially undergo imprinted inactivation of the paternal X-chromosome, beginning at around the 4-8 cell stage of zygotic development (Kalantry et al., 2009; Namekawa et al., 2010; Okamoto et al., 2004; Patrat et al., 2009). The pre-programmed fate of the two Xs during imprinted X-inactivation implies that the X-chromosomes are differentially marked in the parental germlines. In the pre-implantation embryo, *Xist* is expressed exclusively from the paternal-X and *Tsix* only from the maternal-X (Lee, 2000; Sado et al., 2001). The mutually exclusive expression and divergent transcriptional impact of *Xist* and *Tsix* lncRNAs represent a paradigm of how parent-of-origin specific gene regulation is executed in the offspring (Lee, 2009). While the paternal-X undergoes imprinted X-inactivation, evidence indicates that the epigenetic imprint itself resides on the maternal-X (LYON and Rastan, 1984). This notion is supported by the observation that in early embryos that harbor two maternal X-chromosomes, neither X-chromosome undergoes X-inactivation (Goto and Takagi, 2000; Kay et al., 1994; Tada et al., 2000). Conversely, embryos with two paternal-Xs initially express *Xist* from both X-chromosomes, but then down-regulate *Xist* from one of the two Xs and appear to stably inactivate the other *Xist*-coated X-chromosome (Okamoto et al., 2000). Due to its expression exclusively from the maternal-X, its *Xist*-antagonistic function, and that embryos harboring a *Tsix*-mutant maternal X-chromosome die during gestation, *Tsix* RNA has been nominated as the factor via which the oocyte prevents inactivation of the maternal X-chromosome in the embryo (Lee, 2000; Sado et al., 2001). However, the temporal requirement of *Tsix* in imprinted X-inactivation, i.e., whether it functions during the initiation phase in the early

embryo, which would support an oogenic imprint role, or in the maintenance phase in the later embryo, remains unclear.

At the peri-implantation (~128-cell) stage of embryogenesis, the pluripotent epiblast precursor cells in the inner cell mass compartment reactivate the inactive paternal X-chromosome (Mak et al., 2002; Williams et al., 2011). The epiblast lineage is the sole contributor of cells that will form the fetus; the rest of the cells from the early embryo give rise to the trophoblast and the primitive endoderm lineages that will contribute to the extra-embryonic structures of the placenta and yolk-sac, respectively (Hogan et al., 1999). After the embryo implants, descendants of the epiblast precursor cells undergo transcriptional reactivation of the paternal X-chromosome, followed by random X-inactivation of either the maternal or paternal X-chromosome (Rastan, 1982).

The transcriptional reactivation of the inactive paternal X-chromosome in pluripotent epiblast progenitors is characterized by loss of Xist RNA coating (Mak et al., 2002; Sheardown et al., 1997; Williams et al., 2011). Xist RNA depletion is thought to contribute to the epigenetic remodeling of the inactive paternal X-chromosome, leading to the re-expression of paternal X-linked genes (Mak et al., 2002). Similarly, Xist repression and the absence of or reactivation of the inactive-X are considered epigenetic hallmarks of pluripotency; female mouse embryonic stem (ES) cells and induced pluripotent stem (iPSCs) both display two active-Xs (Minkovsky et al., 2012; Payer et al., 2011; Plath and Lowry, 2011). As a negative regulator of Xist, Tsix is proposed to facilitate the loss of Xist RNA coating and reactivation of the inactive-X (Navarro et al., 2010; 2009; Nesterova et al., 2011). To date, however, genetic evidence linking Tsix expression to Xist repression during X-chromosome reactivation is lacking.

Here, we comprehensively examine the role of Tsix RNA in imprinted X-inactivation and -reactivation *in vivo* and *in vitro*. We find that Tsix is dispensable in suppressing Xist and for preventing X-inactivation during the initiation as well as maintenance phases of imprinted X-inactivation through studies in the pre-implantation embryo and in stem cells of the trophectoderm and primitive endoderm lineages. Instead, Tsix is required to prevent Xist induction during the differentiation of trophoblast cells *in vivo* and *in vitro*. Despite the induction of intact Xist RNA and accumulation of Polycomb group-catalyzed histone methylation on the Tsix-mutant X-chromosome, a substantial number of trophoblast cells do not display ectopic X-inactivation. We further find that both the repression of Xist and the reversal of imprinted X-inactivation that occur in epiblast precursor cells prior to random X-inactivation do not require Tsix RNA.

2-2: Role of Tsix During Initiation of Imprinted X-inactivation

If Tsix expression serves to repress Xist during the initiation phase of imprinted X-inactivation, then a maternal-X devoid of Tsix transcription should ectopically express Xist in the pre-implantation embryo. We therefore generated embryonic day (E) 3.5 blastocyst-stage (~64-cell) embryos that inherit either a wild-type (WT) or a Tsix-mutant maternal-X from Tsix-heterozygous females. The Tsix mutation, $Tsix^{AA2\Delta 1.7}$, truncates the Tsix transcript in exon 2 and deletes the critical *DXPas34* repeat sequence that controls Tsix expression (herein referred to as $X^{\Delta Tsix}$) (Fig. 2.1 A)(Cohen et al., 2007; Sado et al., 2001; Stavropoulos et al., 2005; Vigneau et al., 2006). Since Tsix transcription across the Xist promoter region is required for Tsix RNA to inhibit Xist expression, $X^{\Delta Tsix}$ is functionally a null Tsix mutation (Navarro et al., 2005; Sado et al., 2001; Sado and Ferguson-Smith, 2005). We first assayed Tsix and Xist expression by RNA

fluorescence *in situ* hybridization (RNA FISH) with single-stranded riboprobes that uniquely detect Tsix or Xist. Tsix expression is detectable from the active (maternal) X-chromosome in most nuclei of approximately half of the embryos; in the remaining embryos, Tsix is undetectable in all nuclei (Fig. 2.1 B). The active-X is additionally marked by expression of the *Atrx* gene, which is subject to X-inactivation. We therefore classified embryos with Tsix RNA FISH signals as WT XX and XY and the ones without as mutant $X^{\Delta\text{Tsix}}X$ and $X^{\Delta\text{Tsix}}Y$. These embryos displayed Xist RNA coating in XX but not XY embryos, as expected (Fig. 2.1 B). To our surprise, $X^{\Delta\text{Tsix}}X$ blastocysts also showed Xist RNA coating of only one X-chromosome, and no inactivation of the $X^{\Delta\text{Tsix}}$ maternal X-chromosome (Fig. 2.1 B-C). As in $X^{\Delta\text{Tsix}}X$ females, $X^{\Delta\text{Tsix}}Y$ males also failed to display Xist induction or defective gene expression from their single, maternally-inherited X-chromosome (Fig. 2.1 B-C).

To independently validate the RNA FISH data, we performed allele-specific RT-PCR amplification of Xist RNA in individual hybrid blastocyst stage embryos harboring polymorphic X-chromosomes. While the maternal X-chromosome is transmitted by *M. domesticus*-derived laboratory and Tsix-mutant strains (WT X^{Lab} and mutant $X^{\Delta\text{Tsix}}$, respectively), the paternal X-chromosome is derived from the divergent *M. molossinus* JF1 (X^{JF1}) strain; these strains contain numerous single nucleotide polymorphisms (SNPs), which permits defining the allele-specific origin of RNAs. We again assigned genotypes to the embryos by assaying Tsix RNA expression (Fig. 2.1 D). As expected, in WT $X^{\text{Lab}}X^{\text{JF1}}$ and $X^{\text{Lab}}Y$ embryos Xist was expressed only in females and not in males (Fig. 2.1 D). We observed a similar pattern of Xist RNA expression in $X^{\Delta\text{Tsix}}X^{\text{JF1}}$ and $X^{\Delta\text{Tsix}}Y$ mutant blastocysts (Fig. 2.1 D). $X^{\Delta\text{Tsix}}Y$ mutant males did not exhibit Xist expression, consistent with the RNA FISH data. We exploited a SNP in the Xist RT-PCR amplicon to identify the chromosomal source of Xist RNA in $X^{\text{Lab}}X^{\text{JF1}}$ and $X^{\Delta\text{Tsix}}X^{\text{JF1}}$ embryos. Both genotypes

displayed Xist expression only from the paternal X-chromosome (Fig. 2.1 E). Taken together, the RNA FISH and RT-PCR results lead us to conclude that Tsix is dispensable in pre-implantation embryos during the initiation phase of imprinted X-inactivation, both to prevent Xist expression and to forestall inactivation of the maternally-inherited X-chromosome.

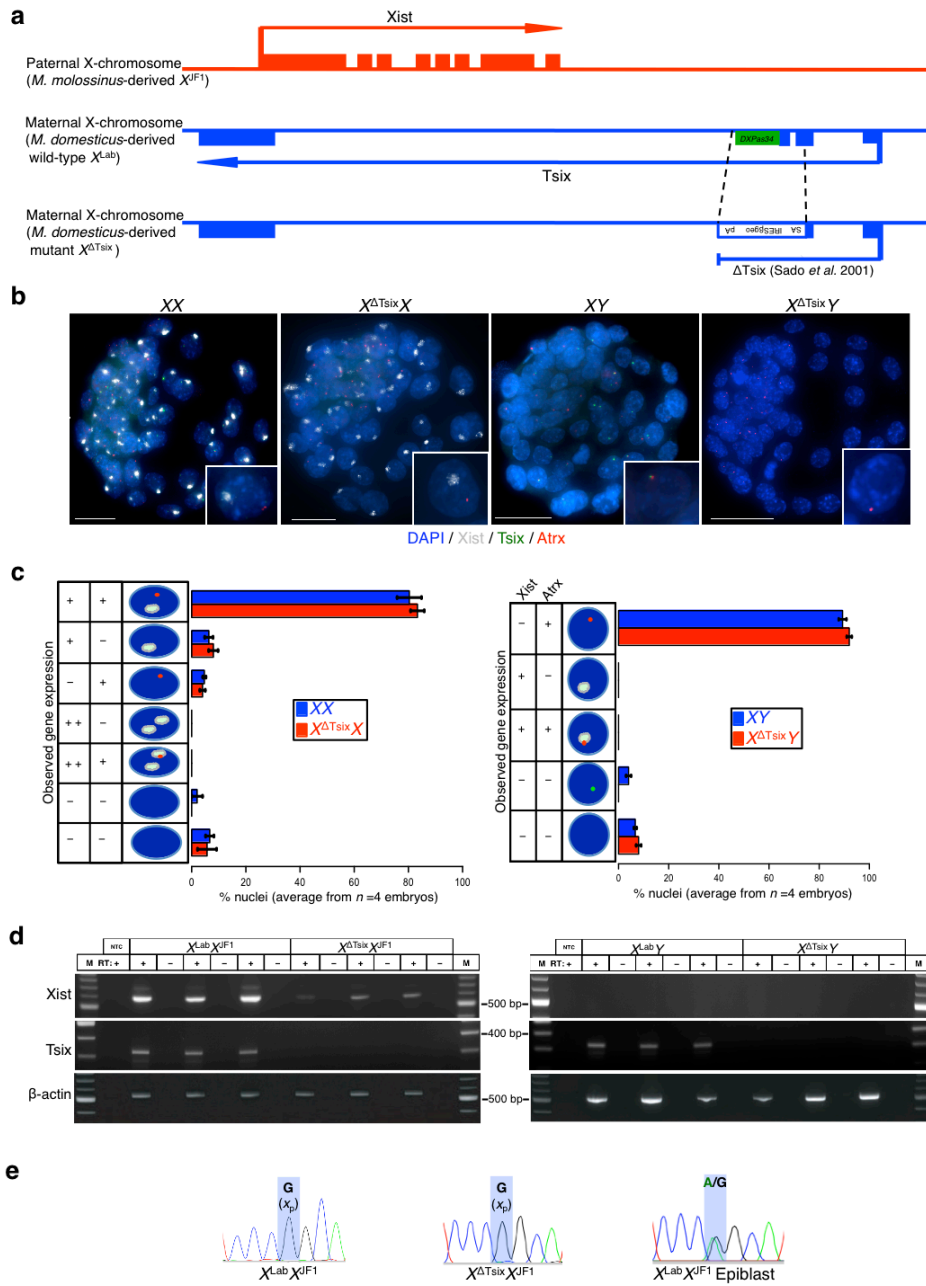


Figure 2.1: Absence of ectopic Xist induction from the $X^{\Delta Tsix}$ maternal X-chromosome in embryonic day (E) 3.5 blastocyst embryos. (a) Schematic representation of the genomic structure of *Xist*, *Tsix*, and the Tsix RNA

truncation mutant $X^{\Delta Tsix}$. (b) RNA FISH detection of Xist (white), Tsix (green) and Atrx (red) RNAs in representative E3.5 embryos. Nuclei are stained blue with DAPI. Insets show representative nuclei. Scale bar, 25 μm . (c) Quantification of Xist, Tsix, and Atrx RNA expression patterns in blastocyst nuclei. The X-axis of each graph represents the average % nuclei observed in each class for each genotype. $n=4$ embryos per genotype. Diagrams along the Y-axis depict all observed expression patterns. +, RNA expression detected from a single X-chromosome; ++, RNA expression detected from both X-chromosomes; -, absence of RNA detection. Gene expression pattern does not differ significantly between wild-type and Tsix mutant blastocysts (Fisher's exact test). Error bars, S.D. (d) RT-PCR detection of Xist, Tsix, and control β -actin RNAs. Three individual embryos are shown for each genotype. M, marker; NTC, no template control; +, reaction with reverse transcriptase (RT); -, no RT control lane. (e) Sanger sequencing chromatograms of representative Xist RT-PCR products. Highlights mark a single nucleotide polymorphism that differs between the maternal $X^{Lab} / X^{\Delta Tsix}$ alleles and the paternal X^{JF1} allele (see Methods). Both $X^{Lab}X^{JF1}$ and $X^{\Delta Tsix}X^{JF1}$ females express Xist only from the paternally-inherited X-chromosome (Xp). The $X^{Lab}X^{JF1}$ epiblast is a control sample displaying expression from both parental alleles.

2-3: Post-implantation Role of Tsix in Suppressing Xist

Maternally-inherited Tsix mutations are typically embryonic lethal, suggesting an essential requirement for Tsix during embryonic development (Lee, 2000; Sado et al., 2001). Since $X^{\Delta Tsix}X$ and $X^{\Delta Tsix}Y$ pre-implantation embryos displayed normal imprinted X-inactivation, we investigated imprinted X-inactivation in peri- and post-implantation embryos to pinpoint when Tsix is required. At the E4.0 peri-implantation stage, $X^{\Delta Tsix}X$ and $X^{\Delta Tsix}Y$ embryos begin to exhibit Xist induction from the $X^{\Delta Tsix}$ X-chromosome in a few nuclei, typically fewer than 3% (Fig. 2.2). We next examined Xist expression and X-inactivation in XX, $X^{\Delta Tsix}X$, XY, and $X^{\Delta Tsix}Y$ E6.5 post-implantation embryos. We initially assessed Xist RNA coating and expression of the X-linked gene *Pgkl*, which is subject to X-inactivation, in whole E6.5 embryos using double-stranded probes that detect Xist and Tsix simultaneously (Kalantry et al., 2009; 2006). At E6.5, the extra-embryonic cell types derived from the trophectoderm and the primitive endoderm of earlier embryos maintain imprinted X-inactivation, while the epiblast cells display random X-inactivation. We observed ectopic Xist expression from the mutant X-chromosome in both $X^{\Delta Tsix}X$ and $X^{\Delta Tsix}Y$ embryos but not in WT XX and XY counterparts (Fig. 2.3 A-D, Movies 1-4). Using single-stranded riboprobes, we next quantified Xist RNA coating and *Pgkl* expression in isolated extra-embryonic tissues and found that 15% of $X^{\Delta Tsix}X$ and 12% of $X^{\Delta Tsix}Y$ cells showed

ectopic Xist RNA coating and *Pgkl* silencing. These percentages represent a significant level of ectopic X-inactivation in extra-embryonic cells ($p=3.5 \times 10^{-5}$ and $p=0.0003$, respectively, Fisher's exact test; Fig. 2.4 A-B). We confirmed ectopic expression of Xist RNA from the maternal X-chromosome in mutant extra-embryonic cells and its absence in WT cells by allele-specific RT-PCR followed by Sanger sequencing to determine the allelic origin of the transcript (Fig. 2.4 C-D). Tsix deficiency, therefore, induces Xist expression and inactivation of the maternal X-chromosome in the extra-embryonic tissues of post-implantation embryos.

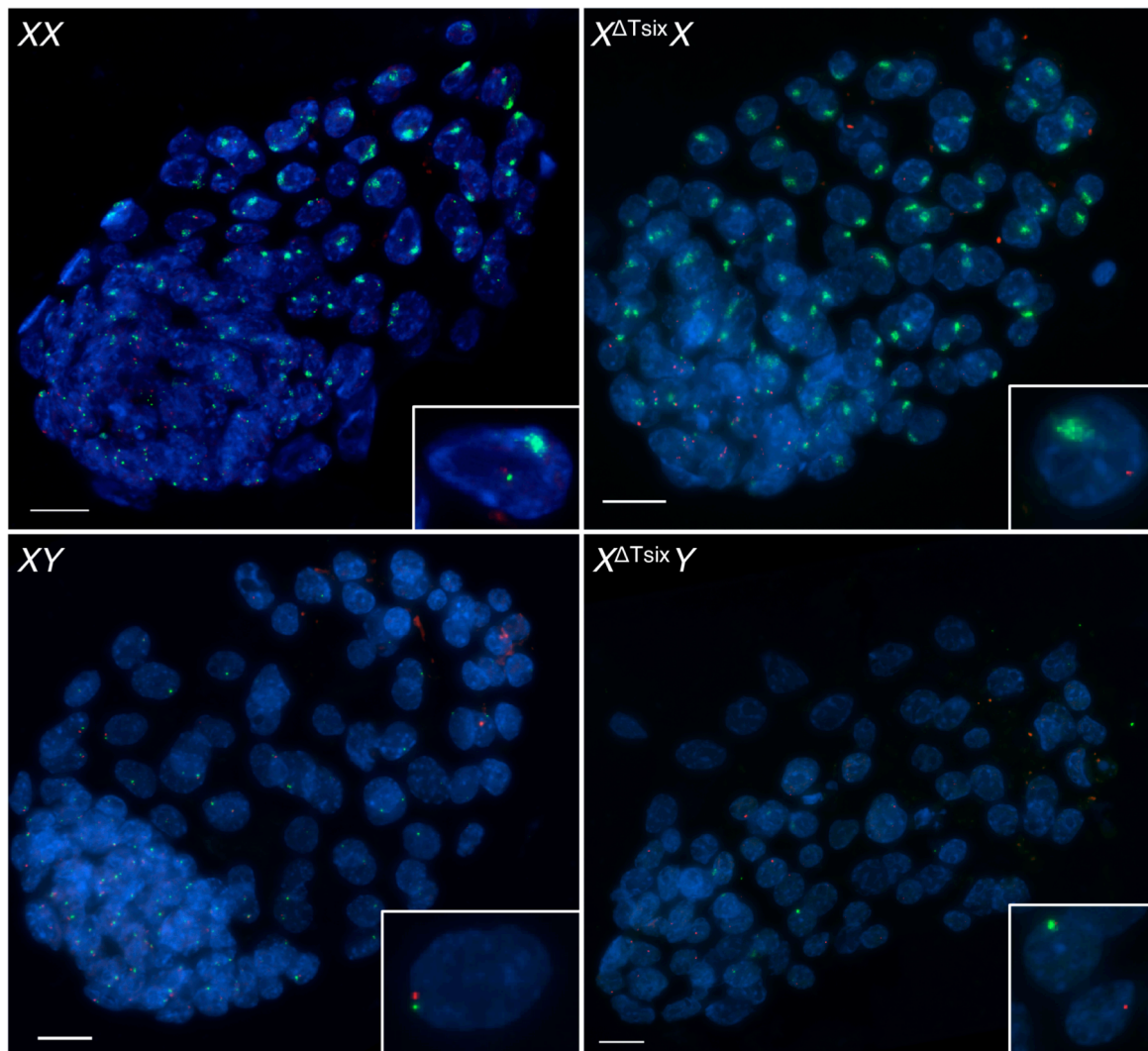


Figure 2.2: Limited Xist induction from the $X^{\Delta Tsix}$ maternal X-chromosome in embryonic day (E) 4.0 embryos. RNA FISH staining of whole E4.0 XX, $X^{\Delta Tsix}$ X, XY, and $X^{\Delta Tsix}$ Y embryos. Three embryos were examined per genotype. Xist RNA coating and Tsix RNA are simultaneously detected in green using a double-stranded probe.

RNA expressed from the X-linked gene *Atrx* is shown in red. Nuclei are stained blue with DAPI. Insets show representative nuclei. Faint *Xist* induction from the *X^{Tsix}* can be seen in fewer than three percent of the *XtsixX* and *XtsixY* nuclei. Scale bar, 20 μ m.

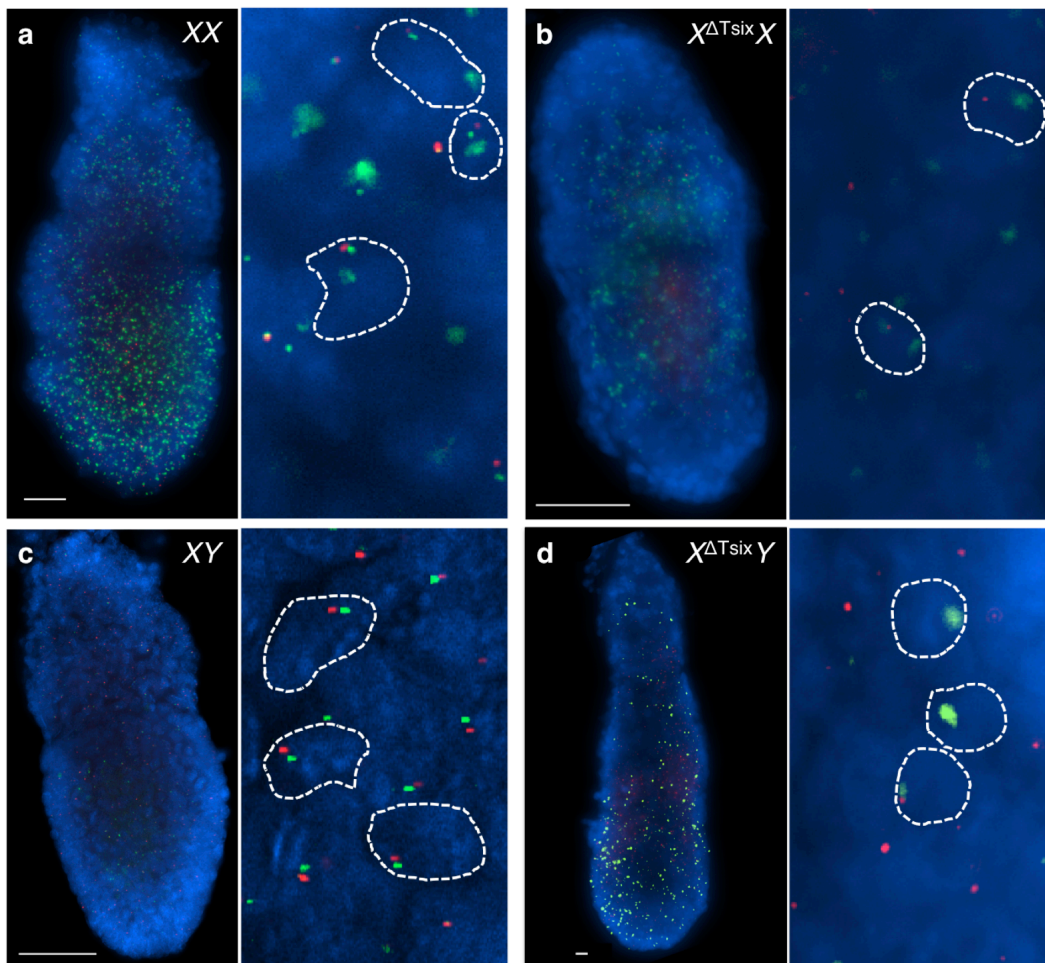


Figure 2.3: RNA FISH analysis of X-linked gene expression in intact wild-type and maternal $X^{\Delta Tsix}$ mutant E6.5 embryos. Maximum intensity projections (left) and representative extra-embryonic nuclei (right) from embryos depicted in movies 1-4. (a) XX; (b) $X^{\Delta Tsix}X$; (c) XY; (d) $X^{\Delta Tsix}Y$. *Xist* RNA coating and *Tsix* RNA pinpoints are detected in green with a double-stranded probe. RNA expressed from the X-linked gene *Pgl1* is detected in red. Nuclei are stained blue with DAPI. Scale bar, 50 μ m.

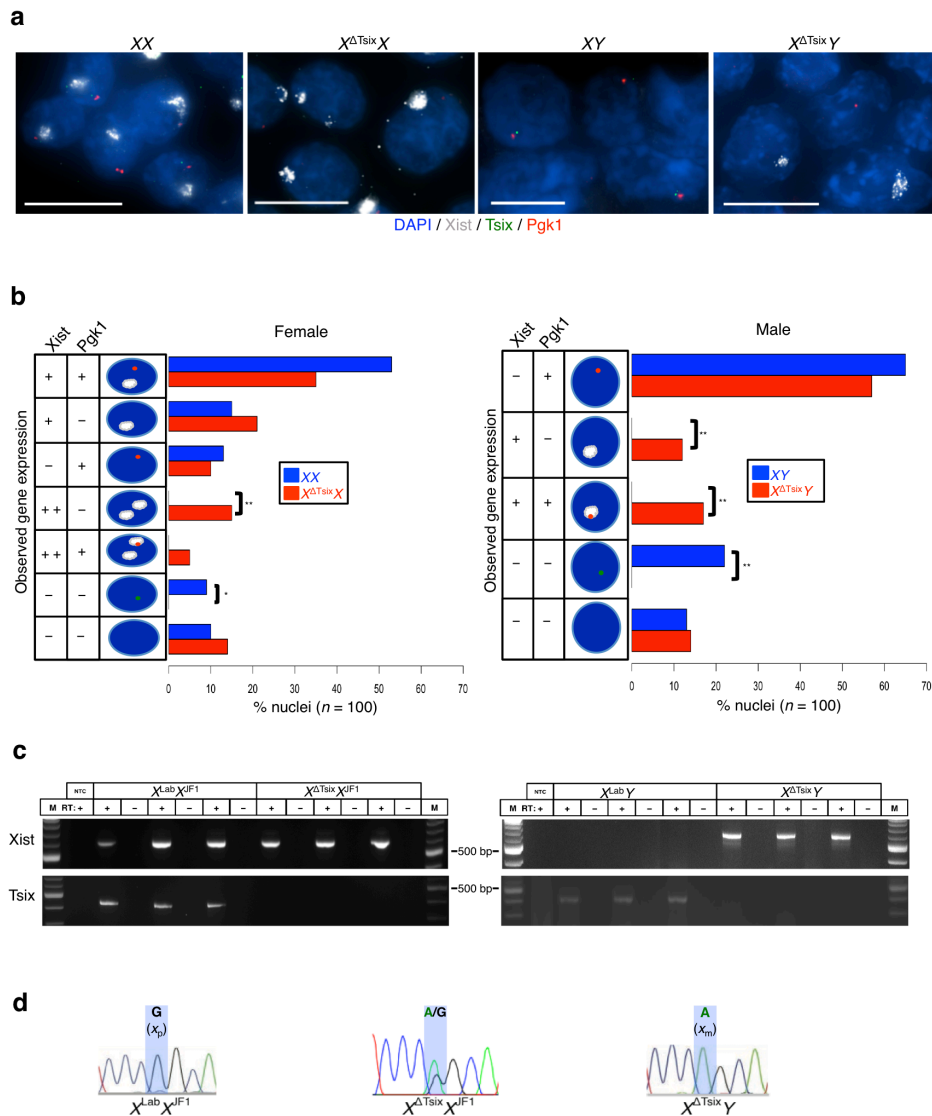


Figure 2.4: Xist induction from the $X^{\Delta Tsix}$ maternal X-chromosome in E6.5 extra-embryonic cells. (a) RNA FISH detection of Xist (white), Tsix (green), and Pgl1 (red) RNAs in E6.5 extra-embryonic cells. Nuclei are stained blue with DAPI. Dashed boxes mark representative nuclei. Scale bar, 10 μ m. (b) Quantification of Xist, Tsix, and Pgl1 RNA expression patterns. The X-axis of each graph represents the % nuclei in each class out of 100 total nuclei counted per genotype (from $n \geq 3$ embryos per genotype). Diagrams along the Y-axis depict all observed expression patterns. +, RNA expression detected from a single X-chromosome; ++, RNA expression detected from both X-chromosomes; -, absence of RNA detection. Pairwise comparisons of the frequency of individual gene expression patterns between wild-type and $X^{\Delta Tsix}$ mutant embryos were performed using Fisher's exact test. *, $0.001 < p < 0.01$; **, $p \leq 0.001$. Extra-embryonic cells show significantly increased level of inactivation of the $X^{\Delta Tsix}$ X-chromosome ($p=0.0003$ for males; $p=3.5 \times 10^{-5}$ for females). (c) RT-PCR detection of Xist and Tsix RNAs in extra-embryonic tissues from individual E6.5 embryos. Results from three individual embryos of each genotype are shown. M, marker; NTC, no template control; +, RT; -, no RT control lane. (d) Sanger sequencing chromatograms of Xist RT-PCR products. Highlights mark a single nucleotide polymorphism that differs between the maternal $X^{Lab} / X^{\Delta Tsix}$ alleles and the paternal X^{IF1} allele. $X^{Lab} X^{IF1}$ females express Xist only from the paternally-inherited X-chromosome, while $X^{\Delta Tsix} X^{IF1}$ females express Xist biallelically in extra-embryonic tissues. $X^{\Delta Tsix} Y$ embryos variably express Xist from the maternally-inherited X-chromosome.

2-4: Differentiation-dependent Function of Tsix in TS Cells

Whole-mount RNA FISH stains of Tsix-mutant E6.5 embryos suggested that ectopic Xist induction primarily characterized the trophoctoderm-derived extra-embryonic ectoderm or its differentiated derivatives (Fig. 2.3 A-D, Movies 1-4). To further examine the role of Tsix in imprinted X-inactivation, we generated $X^{Lab}X^{JF1}$, $X^{\Delta Tsix}X^{JF1}$, $X^{Lab}Y$, and $X^{\Delta Tsix}Y$ trophoblast stem (TS) cells. TS cells arise from trophoctoderm cells of the early embryo, and provide an *in vitro* model of early imprinted X-inactivation (Kalantry et al., 2006; Mak et al., 2002; Tanaka et al., 1998). Strand-specific RNA FISH analysis of the TS cells showed that Xist RNA is expressed from and coats a single X-chromosome in undifferentiated WT and $X^{\Delta Tsix}$ -mutant female TS cells, and is not expressed in male TS cells of either genotype (Fig. 2.5 A). We confirmed that Xist RNA is restricted to female cells despite the absence of Tsix by allele-specific RT-PCR (Fig. 2.5 B). These data not only reinforce the conclusion from embryos that X-inactivation is unperturbed in the absence of Tsix transcription from the maternal X-chromosome in trophoctoderm cells, but also demonstrate that Tsix is not required to stably maintain Xist repression in undifferentiated TS cells in culture.

To reconcile why the extra-embryonic ectoderm in $X^{\Delta Tsix}X^{JF1}$ and $X^{\Delta Tsix}Y$ post-implantation embryos but not TS cells displayed ectopic Xist expression and X-inactivation, we hypothesized that Tsix is required in a differentiation-dependent manner, rather than a temporally-specific manner, in the trophoctoderm lineage. We therefore tested if differentiation of $X^{\Delta Tsix}X^{JF1}$ and $X^{\Delta Tsix}Y$ TS cells would cause Xist induction from the Tsix-mutant X-chromosome. TS cell differentiation indeed led to ectopic Xist induction from the Tsix-mutant but not the WT maternal X-chromosome in both male and female cells by RNA FISH (Fig. 2.5 C-E). We

confirmed ectopic Xist induction from the maternal $X^{\Delta Tsix}$ in differentiated TS cells by allele-specific RT-PCR followed by Sanger sequencing (Fig. 2.5 F-G).

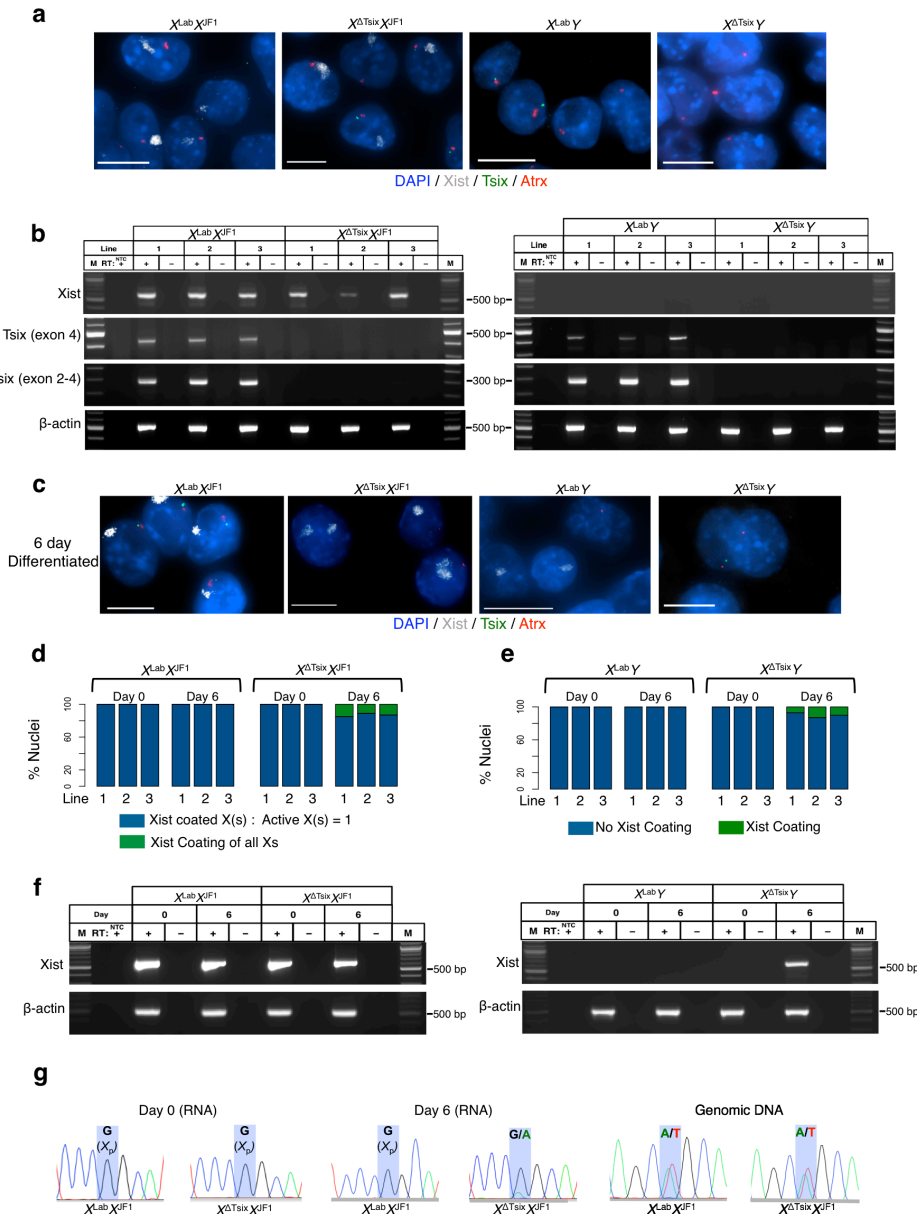


Figure 2.5: The $X^{\Delta Tsix}$ maternal X-chromosome displays ectopic Xist induction only upon differentiation in trophoblast stem (TS) cells. RNA FISH detection of Xist (white), Tsix (green), and Atrx (red) RNAs in representative TS cell lines. Nuclei are stained blue with DAPI. Scale bar, 10 μ m. Three cell lines of each genotype were analyzed. (b) RT-PCR detection of Xist, Tsix (two different amplicons), and control β -actin RNAs in wild-type (WT) and Tsix-mutant TS cells. Three TS cell lines of each genotype were analyzed. M, marker; NTC, no template control; +, RT; -, no RT control lane. (c) RNA FISH detection of Xist (white), Tsix (green), and Atrx

(red) RNAs in 6-day (d6) differentiated TS cell lines. Three cell lines of each genotype were analyzed. Scale bar, 10 μm . (d) Quantification of Xist induction from the $X^{\Delta\text{Tsix}}$ X-chromosome in females. Aberrant Xist RNA coating (defined as two Xist RNA coats in a diploid cell or Xist coating of all chromosomes in polyploid giant cells) is observed in mutant but not WT d6 differentiated TS cells. For giant cells, the number of X-chromosomes was identified based on distinct Xist and Atrx RNA FISH signals. $n=100$ nuclei counted for each cell line per day of differentiation. (e) Quantification of Xist induction from the $X^{\Delta\text{Tsix}}$ X-chromosome in males. Aberrant Xist RNA coating is observed in mutant but not WT d6 differentiated TS cells. $n=100$ nuclei counted for each cell line per day of differentiation. (f) RT-PCR detection of Xist and control β -actin RNA in undifferentiated (d0) and d6 differentiated wild-type (WT) and Tsix-mutant TS cells. A single representative TS cell line from each genotype is shown. M, marker; NTC, no template control; +, RT; -, no RT control lane. (g) Sanger sequencing chromatograms of representative $X^{\text{Lab}}X^{\text{JF1}}$ and $X^{\Delta\text{Tsix}}X^{\text{JF1}}$ Xist RT-PCR products (RNA), and an Xist genomic DNA amplicon (gDNA) within exon 1. Highlights mark a single nucleotide polymorphism that differs between the maternal $X^{\text{Lab}} / X^{\Delta\text{Tsix}}$ alleles and the paternal X^{JF1} Xist allele.

Next, we characterized when during differentiation TS cells induce Xist from the $X^{\Delta\text{Tsix}}$. Only cells devoid of CDX2, a marker of trophoblast progenitor cells, displayed ectopic Xist induction (Fig. 2.6 A-D). Moreover, Xist induction from the maternal $X^{\Delta\text{Tsix}}$ coincided with a failure of the mutant TS cells to differentiate to completion. Whereas WT TS cells of both sexes are able to terminally differentiate into trophoblast giant cells, $X^{\Delta\text{Tsix}}X^{\text{JF1}}$ and $X^{\Delta\text{Tsix}}Y$ TS cells displayed a significant reduction in the percentage of giant cells (Fig. 2.6 E-F). Together, these results demonstrate that Tsix prevents Xist induction from the maternal X-chromosome during the differentiation of trophectodermal progenitor cells. Ectopic Xist induction and the ensuing inactivation of both Xs in females or of a single X in males results in a paucity of X-linked gene expression, which in turn is expected to cause reduced or stalled cell proliferation and prevent terminal differentiation. A block in TS cell differentiation is also consistent with the variable ectopic Xist induction and X-inactivation in the trophectoderm lineage of $X^{\Delta\text{Tsix}}X^{\text{JF1}}$ and $X^{\Delta\text{Tsix}}Y$ post-implantation embryos (Fig. 2.4, Fig. 2.3 A-D, Movies 1-4).

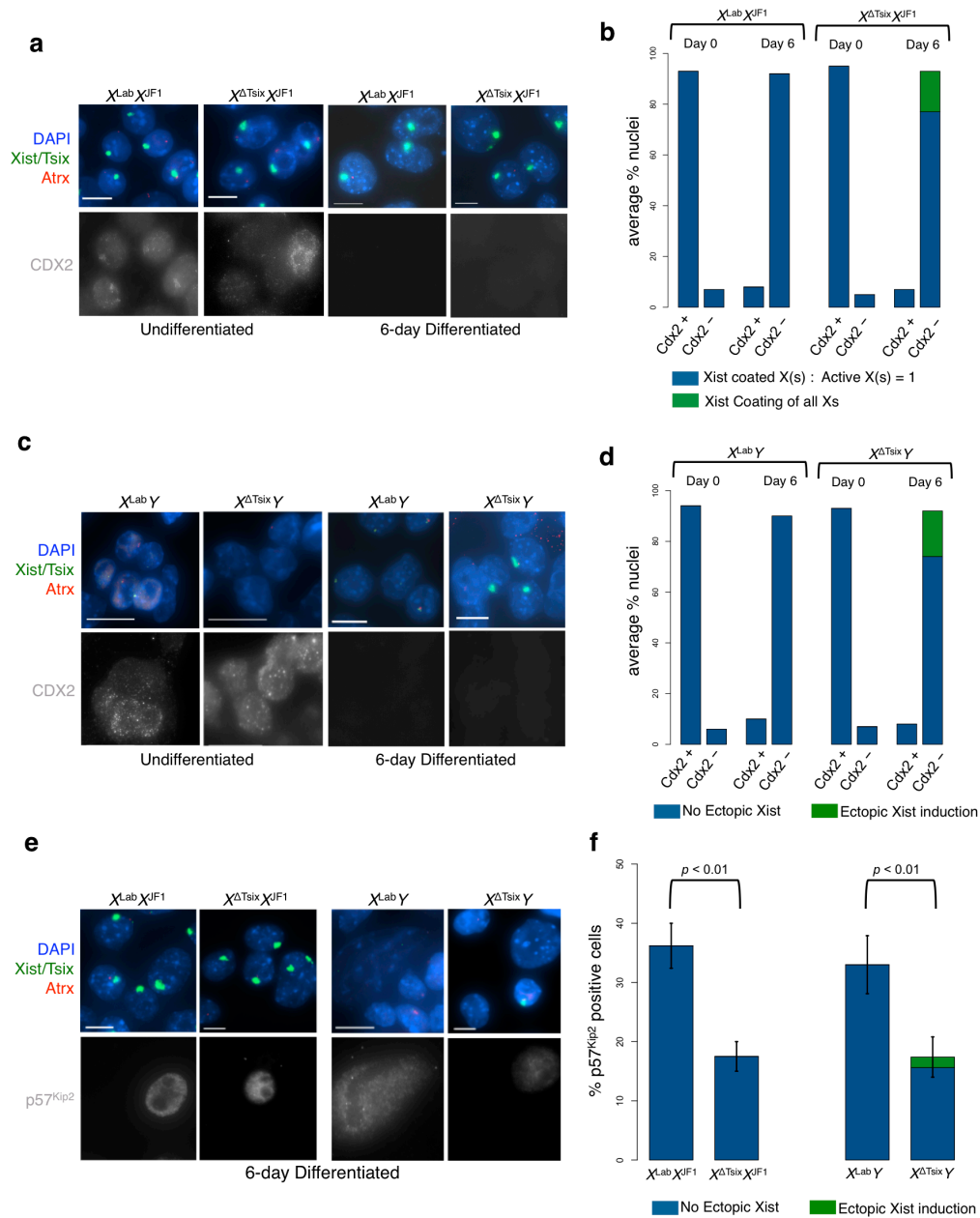


Figure 2.6: Characterization of differentiation-dependent Xist RNA induction from the $X^{\Delta Tsix}$ maternal X-chromosome. (a) RNA FISH detection of Xist, Tsix, and the X-linked gene Atrx in undifferentiated and 6-day (d6) differentiated trophoblast stem (TS) cells. Immunofluorescence (IF) staining of the same cells detects CDX2, a marker of undifferentiated trophoctodermal cells. Scale bar, 10 μ m. (b) Quantification of Xist induction in CDX2 positive and negative in undifferentiated and differentiated female TS cells. 100 nuclei were counted per cell line at each time point ($n = 3$ cell lines per genotype). No aberrant Xist induction is observed from the $X^{\Delta Tsix}$ in undifferentiated cells. In d6 differentiated $X^{\Delta Tsix}X^{IF1}$ TS cells, ectopic Xist induction is restricted to cells that lack CDX2 staining. A subset of differentiated nuclei show both multiple Xist-coated inactive X-chromosomes and multiple active X-chromosomes, due to endoreduplication. (c) IF/RNA FISH analysis of male TS cells, as in (a). Scale bar, 10 μ m. (d) Quantification of Xist induction in undifferentiated and d6 differentiated male TS cells. 100 nuclei were counted per cell line at each time point ($n = 3$ cell lines per genotype). (e) IF/RNA FISH detection of

Xist, Tsix, and the X-linked gene Atrx, in differentiated TS cells. p57^{Kip2}, a marker of trophoblast giant cells, is detected in the same cells by IF. Scale bar, 10 μ m. (f) Quantification p57^{Kip2} positive cells and aberrant Xist induction in the TS cells. 100 nuclei were counted per cell line ($n = 3$ cell lines per genotype). $X^{\Delta Tsix}X^{JF1}$ and $X^{\Delta Tsix}Y$ TS cells show significantly reduced levels of p57^{Kip2} staining, suggesting failure of these genotypes to terminally differentiate. Error bars, S.D.

In addition to TS cells, XEN cells undergo imprinted X-inactivation of the paternal X-chromosome (Kalantry et al., 2006; Kunath et al., 2005). XEN cells are derived from the primitive endoderm layer of blastocysts that generates the extra-embryonic yolk-sac in later-stage embryos. To test if Tsix-mutant XEN cells can stably undergo imprinted X-inactivation, we derived $X^{Lab}X^{JF1}$, $X^{\Delta Tsix}X^{JF1}$, $X^{Lab}Y$, and $X^{\Delta Tsix}Y$ XEN cells. By both RNA FISH and allele-specific RT-PCR, we found that, just like in TS cells, XEN cells can stably repress Xist from the maternal X-chromosome independently of Tsix (Fig. 2.7).

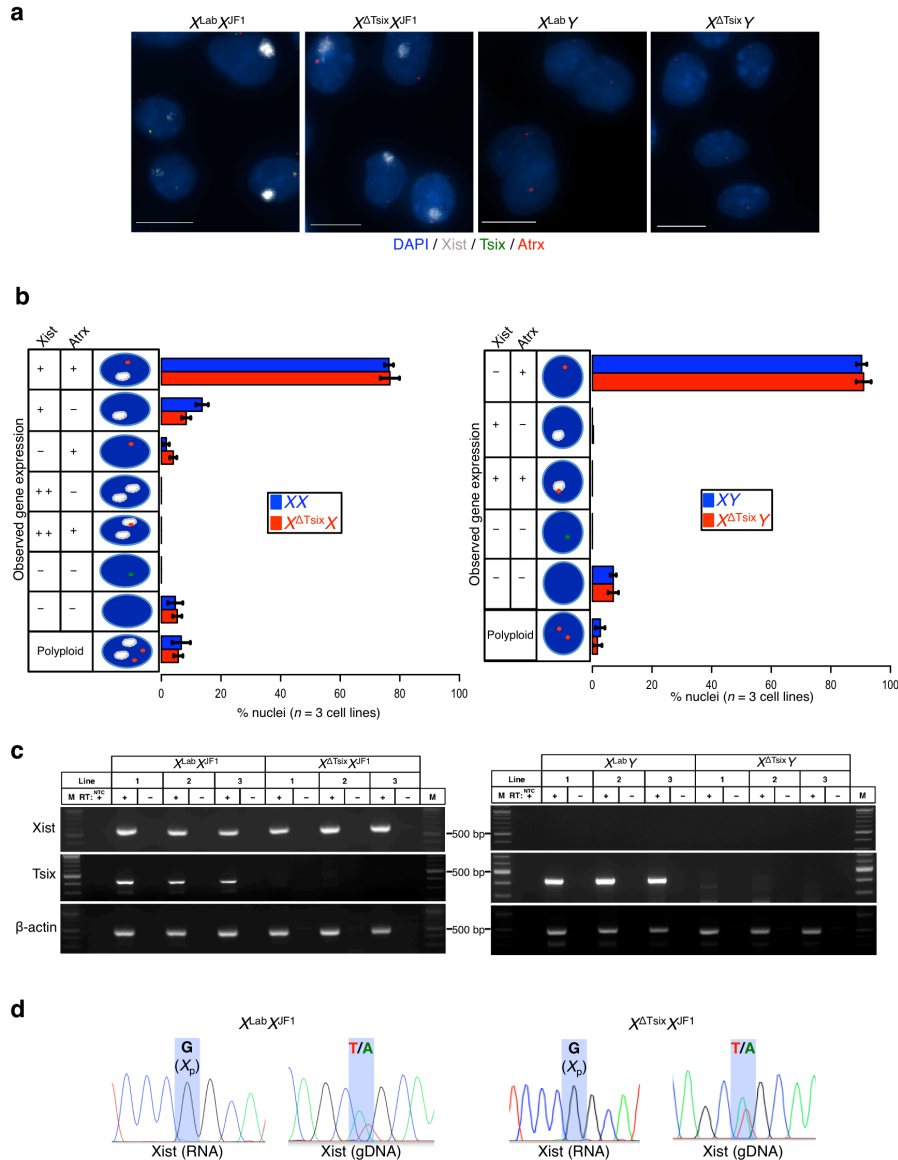


Figure 2.7: Lack of Xist induction from the $X^{\Delta Tsix}$ maternal X-chromosome in cultured extra-embryonic endoderm (XEN) cells. (a) RNA FISH detection of Xist (white), Tsix (green) and Atrx (red) RNAs in representative XEN cell lines. Nuclei are stained blue with DAPI. Three cell lines of each genotype were analyzed. Scale bar, 10 μ m. (b) Quantification of Xist RNA coating and X-linked gene expression in the XEN cells. The X-axis of each graph represents average % nuclei in each class from 100 cells counted per cell line ($n = 3$ cell lines per genotype). Diagrams along the Y-axis depict all observed expression patterns. +, RNA expression detected from a single X-chromosome; ++, RNA expression detected from both X-chromosomes; -, absence of RNA detection. A subset of tetraploid XEN nuclei show two Xist-coated inactive X-chromosomes and two active X-chromosomes, due to endoreduplication. Gene expression patterns do not differ significantly between wild-type and Tsix mutant XEN cells (Fisher's exact test). Error bars, S.D. (c) RT-PCR detection of Xist, Tsix, and control β -actin RNAs in three individual XEN cell lines of each genotype. M, marker; NTC, no template control; +, reaction with reverse transcriptase (RT); -, no RT control lane. (d) Sanger sequencing chromatograms of representative $X^{Lab}X^{JF1}$ and $X^{\Delta Tsix}X^{JF1}$ RT-PCR products spanning Xist exons 1-4 (RNA), and an Xist genomic DNA amplicon (gDNA) within exon 1. Highlights mark a single nucleotide polymorphism that differs between the maternal $X^{Lab} / X^{\Delta Tsix}$ alleles and the paternal X^{JF1} allele.

2-5: Disassociation of H3-K27me3 Enrichment and X-inactivation

Xist RNA coating is postulated to lead to X-inactivation in *cis* (Brockdorff, 2011; Payer and Lee, 2008; Schulz and Heard, 2013). We noticed, however, that in 5% of the E6.5 $X^{\Delta\text{tsix}}X$ extra-embryonic cells Xist RNA coated both X-chromosomes, but one Xist coated X-chromosome remained active, as indicated by expression of *Pgk1* from one of the two Xs in these cells (Fig. 2.4 A-B). In E6.5 $X^{\Delta\text{tsix}}Y$ extra-embryonic nuclei, 17% of cells displayed both ectopic Xist RNA coating and *Pgk1* expression from the single X-chromosome (Fig. 2.4 A-B). To determine if *Pgk1* expression from the ectopically Xist RNA-coated X-chromosome agreed with expression of other X-linked genes subject to X-inactivation, we performed pair-wise comparisons of expression of *Pgk1* with *Atrx* and *Atrx* with *Rnf12* (Fig. 2.8). We observed a high level of concordant expression of both sets of X-linked genes, leading to the conclusion that the ectopically Xist RNA-coated X-chromosome remained transcriptionally active in a subset of nuclei.

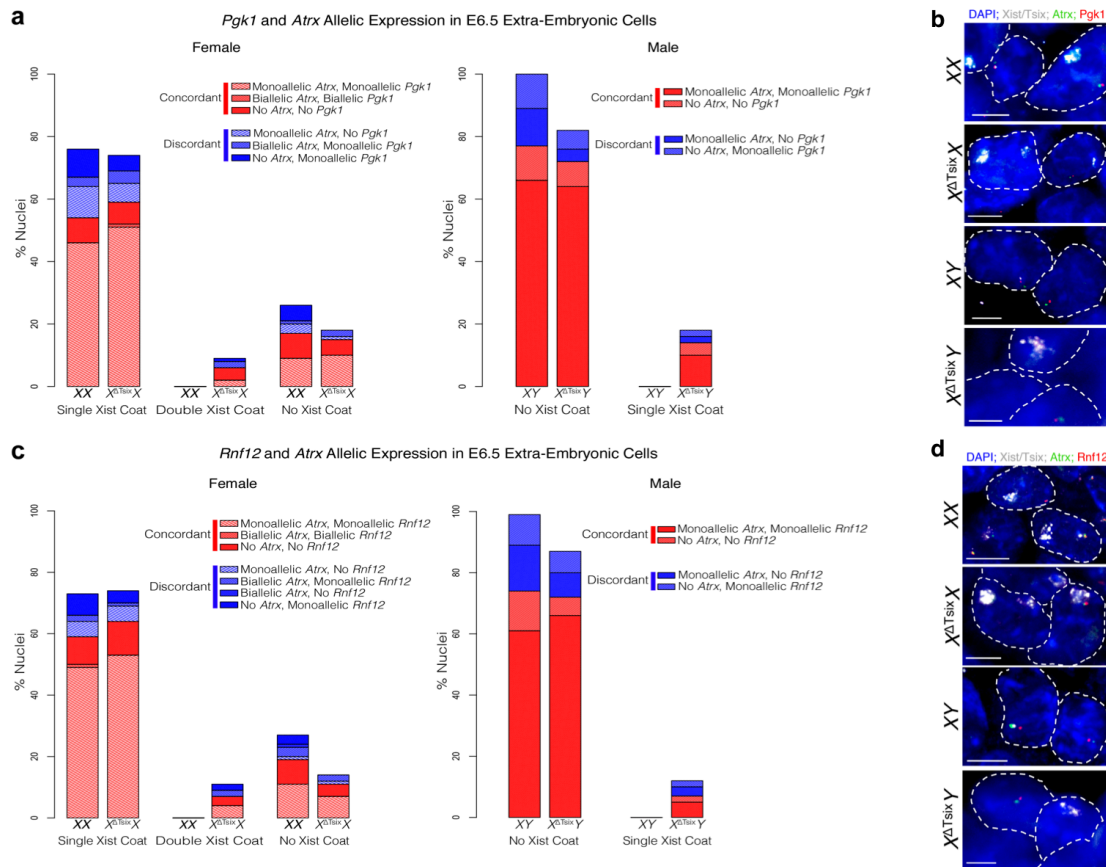


Figure 2.8: X-linked genes show concordance of allelic expression in $X^{\Delta Tsix}X$ and $X^{\Delta Tsix}Y$ E6.5 extra-embryonic tissues. (a) Bar plots quantifying allelic expression of the X-linked genes *Atrx* and *Pgk1* by RNA FISH in individual nuclei of XX, $X^{\Delta Tsix}X$, XY, and $X^{\Delta Tsix}Y$ E6.5 extra-embryonic cells. Nuclei are subdivided into classes based on observed Xist RNA expression and coating. Concordant expression of genes within a single nucleus is plotted in red. Discordant expression is plotted in blue. In females (left), expression of *Atrx* and *Pgk1* is 78% concordant in XX embryos and 79% concordant in $X^{\Delta Tsix}X$ embryos (100 total nuclei analyzed per genotype from $n = 3$ embryos). In males (right), expression of *Atrx* and *Pgk1* is 77% concordant in XY embryos and 87% concordant in $X^{\Delta Tsix}Y$ embryos (100 total nuclei analyzed per genotype from $n = 3$ embryos). (b) Representative RNA FISH-stained nuclei. Xist and Tsix RNAs are shown in white, Atrx RNA in green, and Pgl1 RNA in red. Nuclei are stained blue with DAPI. Scale bar, 5 μ m (c) Bar plots quantifying allelic expression of the X-linked genes *Atrx* and *Rnf12* in individual nuclei of E6.5 extra-embryonic cells. Analysis was carried out as described in (a). In females (left), *Atrx* and *Rnf12* expression is 78% concordant in XX embryos and 82% concordant in $X^{\Delta Tsix}X$ embryos (100 total nuclei analyzed per genotype from $n = 3$ embryos). In males (right), *Atrx* and *Rnf12* expression are 74% concordant in XY embryos and 79% concordant in $X^{\Delta Tsix}Y$ embryos (100 total nuclei analyzed per genotype from $n = 3$ embryos). (d) Representative RNA FISH-stained nuclei. Xist and Tsix RNAs are shown in white, Atrx RNA in green, and Rnf12 RNA in red. Nuclei are stained blue with DAPI. Scale bar, 5 μ m.

To investigate the uncoupling of Xist RNA coating and X-linked gene silencing, we tested whether ectopic Xist RNA expression and coating led to the functional enrichment of the Polycomb group proteins on that X-chromosome. Xist RNA is thought to induce X-inactivation

via the recruitment of protein complexes, most notably the Polycomb repressive complex 2 (PRC2), that inhibit transcription on the inactive-X (Plath et al., 2003; Schoeftner et al., 2006; Silva et al., 2003). PRC2 catalyzes methylation of lysine at amino acid position 27 in the tail of histone H3 (H3-K27me3), which is associated with transcriptional repression and is required for imprinted X-inactivation (Kalantry et al., 2006; Plath et al., 2003; Silva et al., 2003; Wang et al., 2001). Moreover, both PRC2 components and H3-K27me3 accumulate on the inactive-X early during X-inactivation, suggesting an intimate role for PRC2 and H3-K27me3 in the formation of the inactive-X heterochromatin (Plath et al., 2003; Silva et al., 2003). We therefore tested ectopic accumulation of PRC2-catalyzed H3-K27me3 in E6.5 XX, $X^{\Delta\text{Tsix}}X$, XY, and $X^{\Delta\text{Tsix}}Y$ extra-embryonic cells. We found discordance between Xist RNA coating and H3-K27me3 accumulation; nuclei with ectopic Xist RNA coating in the Tsix-mutant cells did not always display H3-K27me3 enrichment (Fig. 2.9 A-C). In cells with ectopic Xist RNA coating and concomitant H3-K27me3 accumulation, however, a substantial percentage (20% of female and 16% of male nuclei) harbored a transcriptionally-competent X-chromosome, as reflected by *Pgk1* expression (Fig. 2.9 B-C). Together, these data demonstrate that Xist RNA induction often, but not always, leads to H3-K27me3 accumulation on the $X^{\Delta\text{Tsix}}$ maternal X-chromosome, and that X-inactivation does not necessarily follow.

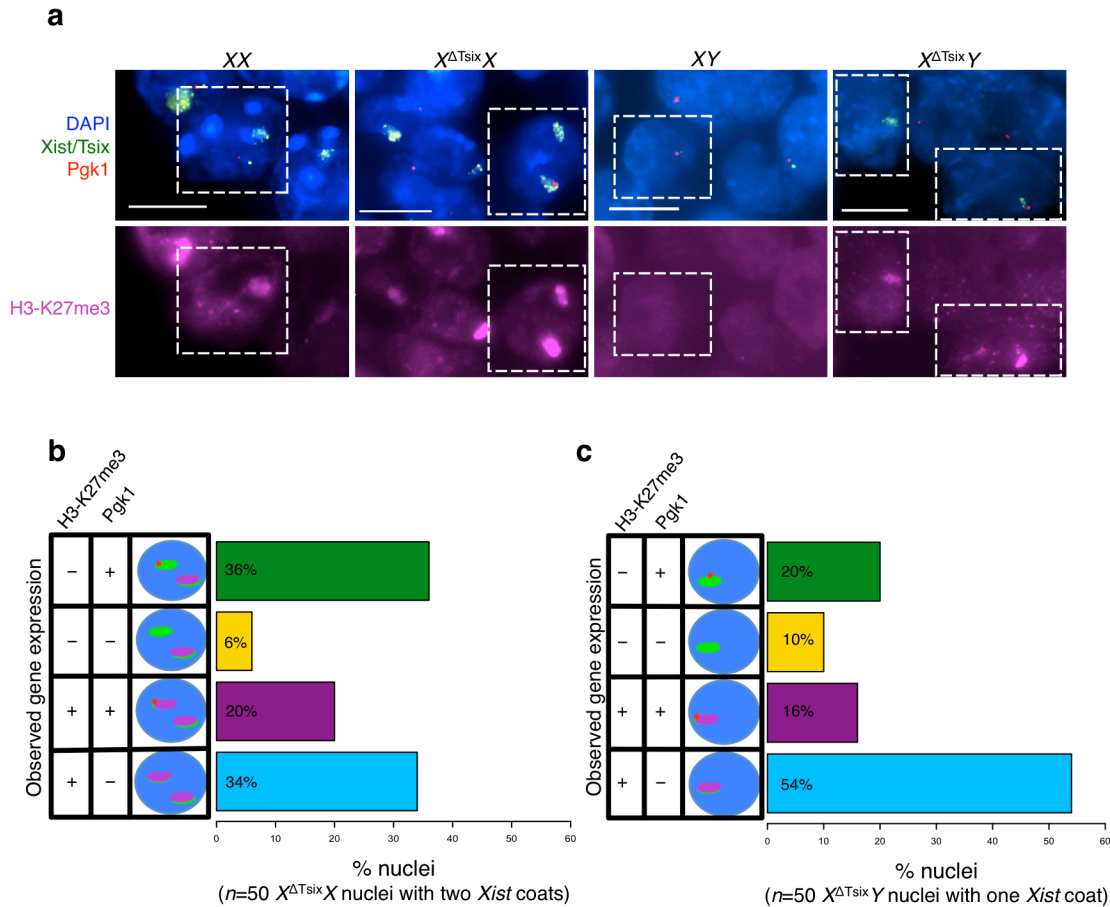


Figure 2.9: Disassociation of Xist induction, H3-K27me3 enrichment, and inactivation of the $X^{\Delta Tsix}$ maternal X-chromosome in E6.5 extra-embryonic cells. (a) RNA FISH detection of Xist, Tsix, and Pgf1 RNAs coupled with immunofluorescence (IF) detection of H3-K27me3 in extra-embryonic cells of E6.5 embryos. Dashed boxes mark representative nuclei. Scale bar, 10 μ m. (b) Quantification of H3-K27me3 enrichment and Pgf1 expression in nuclei displaying Xist RNA coating of both X-chromosomes in $X^{\Delta Tsix}X$ extra-embryonic cells (50 nuclei with Xist RNA coating of both X-chromosomes were analyzed [$n=5$ $X^{\Delta Tsix}X$ embryos]). Wild-type (WT) XX embryos show Xist RNA coating and enrichment of H3-K27me3 on a single X-chromosome ($n=5$ embryos). (c) Quantification of H3-K27me3 enrichment and Pgf1 expression in nuclei displaying Xist RNA coating of the X-chromosome in $X^{\Delta Tsix}Y$ extra-embryonic cells (50 nuclei with Xist RNA coating of the single X-chromosome [$n=4$ $X^{\Delta Tsix}Y$ embryos] were analyzed). WT XY cells show neither Xist RNA coating nor H3-K27me3 enrichment ($n=4$ embryos).

2-6: Tsix is Dispensable in X-chromosome Reactivation

In addition to preventing Xist RNA expression and X-inactivation, Tsix is also implicated in Xist repression in pluripotent embryonic stem (ES) cells, an *in vitro* analog of the pluripotent epiblast precursor cells within the inner cell mass (ICM) of hatched blastocysts (Navarro et al., 2009; 2010; Nesterova et al., 2011). Loss of Xist RNA coating is a hallmark of the chromosome-

wide epigenetic remodeling that accompanies reactivation of the inactive-X in epiblast precursors (Mak et al., 2004; Sheardown et al., 1997; Williams et al., 2011). To test whether *Tsix* is required to repress *Xist* in the epiblast precursors, we isolated ICMs from *XX* and *XX^{ΔTsix}* E4.0 embryos. In both *XX* and *XX^{ΔTsix}* ICMs, we observed loss of *Xist* RNA coating and biallelic expression of *Atrx*, a gene subject to X-inactivation, indicating that reactivation of the paternal-X had occurred in spite of its lacking functional *Tsix* (Fig. 2.10 A-C). We independently validated reactivation of the *X^{ΔTsix}* paternal X-chromosome by allele-specific RT-PCR amplification of the X-linked genes *Pdhal*, *Rnf12*, and *Utx* in E5.0 *X^{IF1}X^{Lab}* and *X^{IF1}X^{ΔTsix}* epiblasts (Fig. 2.10 D). Whereas *Pdhal* and *Rnf12* are subject to X-inactivation, *Utx* escapes X-inactivation and serves as a control for the assay to gauge biallelic X-linked gene expression. If the paternal X-chromosome is reactivated, then transcription of all three genes should be apparent from both X-chromosomes. In agreement, all three genes displayed biallelic expression in both genotypes in E5.0 epiblasts. Based on these data, we conclude that the paternal X-chromosome is reactivated in pluripotent stem cells independently of *Tsix*.

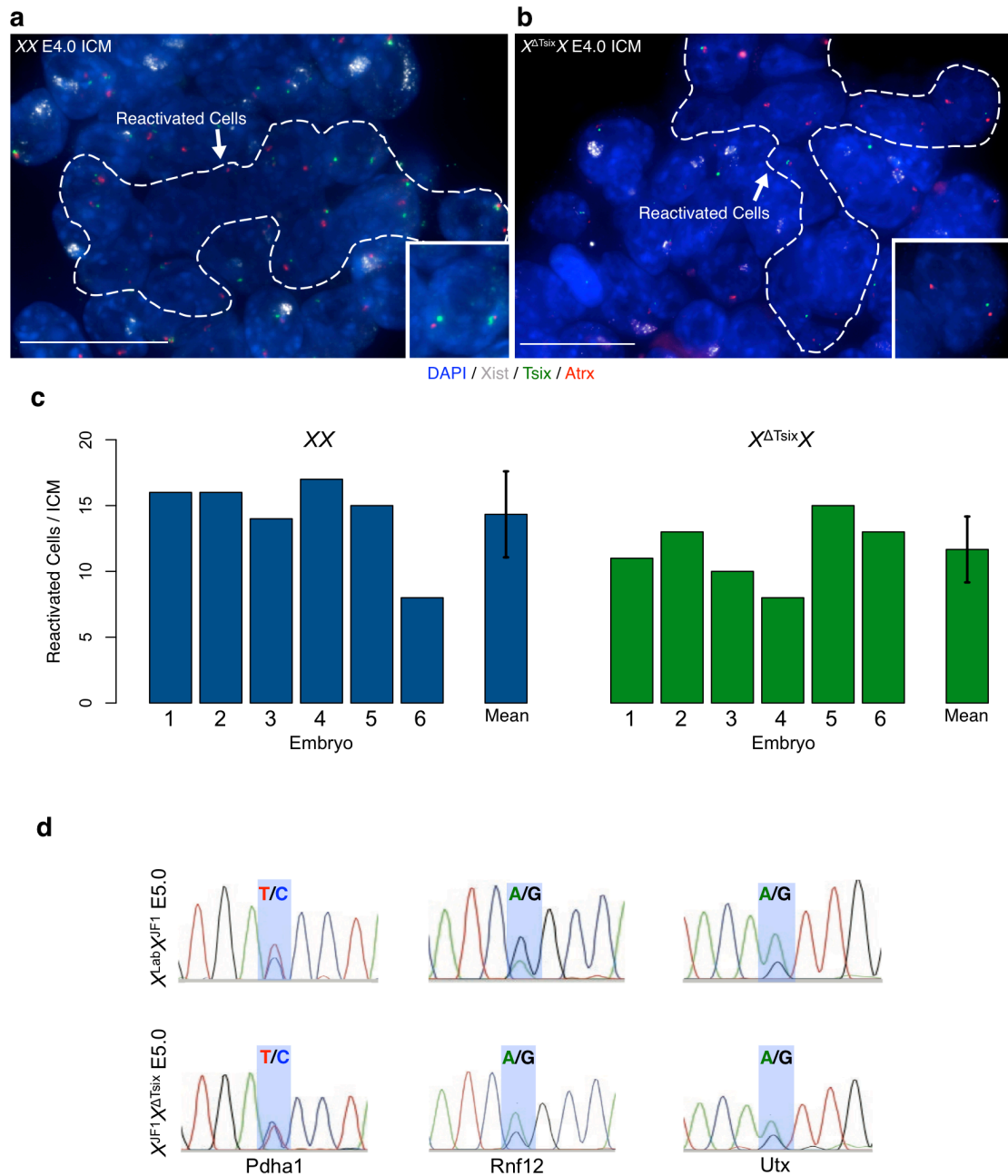


Figure 2.10: Reactivation of the inactive $X^{\Delta Tsix}$ paternal X-chromosome in the inner cell mass (ICM). RNA FISH detection of Xist (white), Tsix (green), and Atrx (red) RNAs in E4.0 ICMs. Nuclei are stained blue with DAPI. Insets show representative reactivated nuclei. Scale bar, 20 μ m. (c) Quantification of the number of reactivated nuclei, as characterized by loss of Xist RNA coating and biallelic Atrx expression, in individual ICMs ($n=6$ ICMs per genotype). The mean number of reactivated cells per ICM does not differ significantly between XX and $XX^{\Delta Tsix}$ ICMs ($p = 0.23$, two-tailed T -test). Error bars, S.D. (d) Allele-specific X-linked gene expression analysis in E5.0 epiblast cells. Representative chromatograms of sequenced cDNAs show biallelic expression of the X-linked genes *Pdha1*, *Rnf12*, and *Utx*, regardless of genotype.

2-6: Concluding Remarks

Tsix transcription across the Xist promoter is thought to inhibit Xist expression, and thereby prevent X-inactivation (Navarro et al., 2005; Sado et al., 2005). We show instead that Tsix is not required to repress Xist and prevent X-inactivation in the early embryo and in stem cells of the trophoctoderm and primitive endoderm lineages. Earlier studies implicating Tsix in imprinted X-inactivation did not profile the onset of X-inactivation in Tsix-mutant preimplantation embryos or in TS and XEN cells (Lee, 2000; Sado et al., 2001). We find that Tsix expression in *cis* is required to forestall inactivation of the maternal X-chromosome as the trophoctoderm cells differentiate. By the post-implantation stage, the Tsix-mutant maternal X-chromosome displayed ectopic Xist RNA coating in 25% and 20% of extra-embryonic cells isolated from E6.5 $X^{\Delta Tsix}X$ and $X^{\Delta Tsix}Y$ male and female embryos, respectively. The variable induction of Xist reflects a requirement for Tsix in differentiating but not undifferentiated trophoblast cells to prevent Xist induction and X-inactivation.

Xist expression from and coating of the $X^{\Delta Tsix}$ maternal X-chromosome coincided with enrichment of the histone modification H3-K27me3 on the mutant-X in many, but not all, $X^{\Delta Tsix}X$ (54%) and $X^{\Delta Tsix}Y$ (70%) extra-embryonic nuclei. Despite Xist RNA coating and H3-K27me3 accumulation, however, we unexpectedly found that 20% of the $X^{\Delta Tsix}$ maternal X-chromosomes in females and 16% in males did not undergo inactivation. This finding is consistent with and extends previous work showing that the recruitment of PRC2 and the catalysis of H3-K27me3 are insufficient to trigger gene silencing by ectopically integrated Xist transgenes or by a mutant Xist RNA expressed from the endogenous locus (Plath et al., 2003; Silva et al., 2003; Wutz et al.,

2002). In these studies, however, the site of integration of the Xist transgene or the specific mutation in Xist cannot be excluded as the cause of defective silencing. We find that ectopic coating of the X-chromosome by an unmodified and endogenous Xist RNA followed by robust H3-K27me3 enrichment nevertheless results in active transcription of endogenous X-linked genes.

Our work shows that the oocyte-derived imprint that prevents inactivation of the maternal X-chromosome in the early embryo does not act through Tsix RNA. We instead propose a model where the oocyte marks the maternal-X with chromosome-wide histone modifications, ensuring that genes along the maternal X-chromosome remain transcriptionally competent during early embryogenesis (Fig. 2.11). This chromatin profile is sufficient to repress Xist during the initiation of imprinted X-inactivation in the early embryo independently of Tsix RNA. Tsix RNA is also not needed to maintain Xist repression in undifferentiated trophoblast stem cells. During trophectodermal differentiation, by contrast, Tsix absence leads to Xist induction from and X-inactivation of the maternal-X. These data are consistent with previous findings that cellular differentiation can trigger X-inactivation defects, for example through large-scale chromatin changes that are inherent to differentiation (Corbel et al., 2013; Kalantry et al., 2006). The insufficiency of the germline-derived chromatin imprint to prevent inactivation of the maternal X-chromosome is also highlighted by the observations that the maternal-X in parthenogenetic embryos harboring two maternal-Xs is subject to inactivation in extra-embryonic tissues of post-implantation embryos but not in pre-implantation embryos (Goto and Takagi, 2000; Rastan et al., 1980). We further propose that Tsix expression from the maternal X-chromosome is not directly programmed by the oocyte, but is simply a byproduct of the absence of Xist transcription from that chromosome. Indeed, Tsix RNA is induced when Xist expression is absent (Hoki et al., 2009;

Rastan et al., 1980). Tsix transcription then contributes to the chromatin structure at the Xist promoter region, and these Tsix-induced modifications may assume the Xist-inhibitory role in differentiating trophectodermal cells (Navarro et al., 2005; Sado et al., 2005). This mode of lncRNA function in epigenetic transcriptional regulation may also apply to other loci subject to imprinted, parent-of-origin specific gene expression, where opposing sense-antisense lncRNA functions are invoked (Barlow, 2011). The reciprocal regulation by Tsix of Xist, in turn, is the cause of the Tsix-mutant maternal-Xs ectopically accumulating Xist RNA and H3-K27me3 in trophoblast cells. But, despite the enrichment of both Xist RNA and H3-K27me3 a significant percentage of $X^{\Delta\text{Tsix}}$ maternal X-chromosomes do not undergo inactivation. These findings are consistent with the hypothesis that factors in addition to or other than Xist RNA and H3-K27me3 contribute to the initiation of X-inactivation (Kalantry and Magnuson, 2006; Kalantry et al., 2006; 2009).

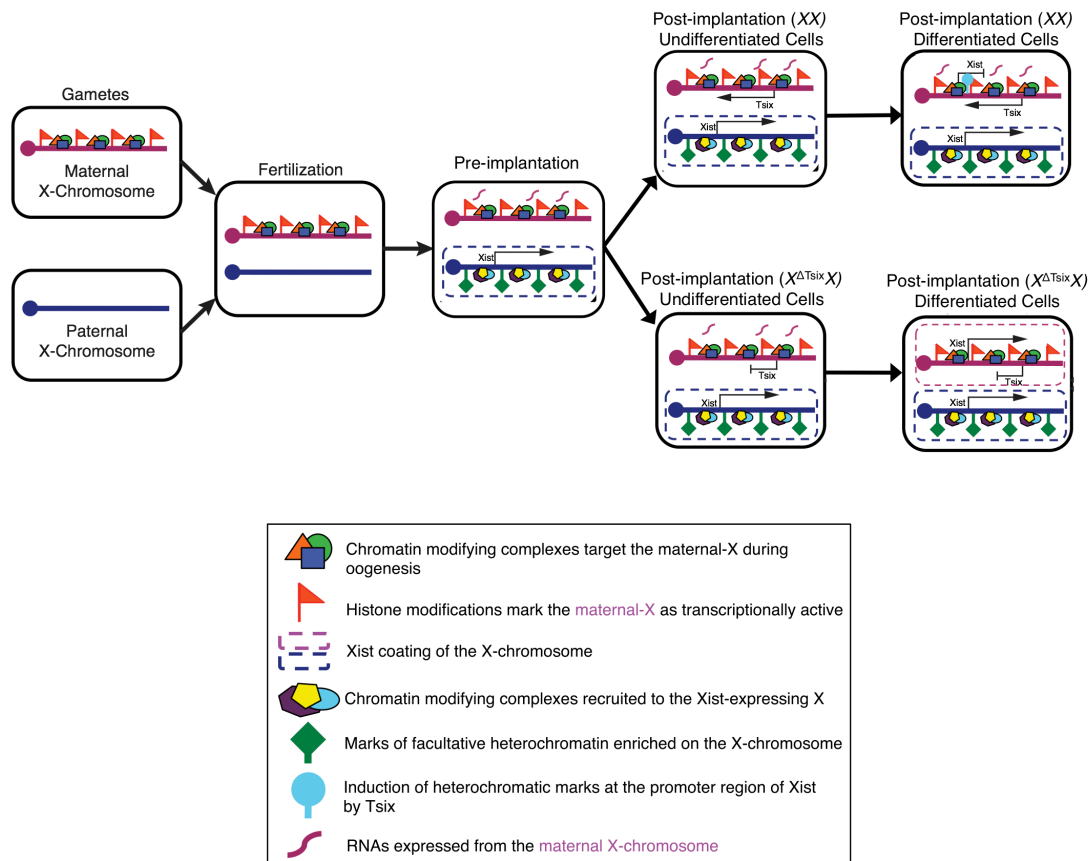


Figure 2.11: A model for the role of Tsix in imprinted X-Inactivation. The maternal X-chromosome, but not the paternal-X, is marked by histone modifications during gametogenesis that are transmitted to the offspring upon fertilization. In the pre-implantation embryo, these histone modifications prevent inactivation of the maternal-X, while the paternal X-chromosome is subject to inactivation. Xist is induced from the paternally-derived X-chromosome in the pre-implantation embryo, and helps recruit protein complexes that catalyze histone marks characteristic of facultative heterochromatin on the paternal-X. The oocyte-configured chromatin of the maternal-X, conversely, prevents Xist induction from the maternal X-chromosome during the initiation phase of X-inactivation (pre-implantation) and does not require Tsix. The maternal-X then remains active during the maintenance phase of imprinted X-inactivation in undifferentiated extra-embryonic nuclei (post-implantation, undifferentiated cells), independently of Tsix expression. Tsix is induced from the maternal-X due to the absence of Xist expression from this X-chromosome. Upon differentiation, Tsix transcription across the Xist promoter region is required to induce heterochromatinization of the Xist promoter to keep Xist silenced in the extra-embryonic trophectodermal lineage. In XX differentiated extra-embryonic cells, the wild-type maternal-X remains transcriptionally competent while the paternal-X is maintained as transcriptionally inactive in imprinted X-inactivated cells. Upon differentiation of $X^{\Delta Tsix}X$ trophectoderm cells, the Tsix-mutant maternal X-chromosome induces Xist.

Our analysis additionally uncouples Tsix expression from the reactivation of the inactive paternal X-chromosome, a process that characterizes pluripotent epiblast precursor cells in the developing embryo (Mak et al., 2004; Williams et al., 2011). X-reactivation is also a prominent

epigenetic feature of pluripotent ES and iPSC cells(Minkovsky et al., 2012; Navarro et al., 2010; Plath and Lowry, 2011). Tsix induction from the inactive-X is posited to contribute to Xist repression and to the transcriptional equality of the two Xs in pluripotent cells(Navarro et al., 2009; 2010; Nesterova et al., 2011). We find, however, that despite Tsix-absence, Xist RNA is repressed and the paternal X-chromosome is efficiently reactivated in epiblast precursor cells. In addition to by Tsix, Xist repression is postulated to occur via the pluripotency factors NANOG, OCT4, and SOX2, which are expressed in pluripotent epiblast progenitors and have been shown to bind within intron 1 of *Xist* in undifferentiated ES cells (Donohoe et al., 2009; Navarro et al., 2008; 2010; Nesterova et al., 2011). Thus, it is conceivable that these pluripotency factors may function to repress Xist and induce reactivation of the X^{ATsix} paternal X-chromosome in the embryo. Countering this argument, however, Xist RNA upregulation and coating during random X-inactivation in the epiblast occurs despite high levels of NANOG, OCT4, and SOX2 expression, suggesting the involvement of additional factors in both Xist repression and X- reactivation(Pfister et al., 2007).

2-7: Materials and Methods

Ethics Statement.

This study was performed in strict accordance with the recommendations in the Guide for the Care and Use of Laboratory Animals of the National Institutes of Health. All animals were handled according to protocols approved by the University Committee on Use and Care of Animals (UCUCA) at the University of Michigan (Protocol #PRO00004007).

Mice.

Mice harboring the *Tsix*^{AA2Δ1.7} mutation were generated from targeted ES cells that were a kind gift of Takashi Sado and have been described elsewhere (Kalantry and Magnuson, 2006; Sado et al., 2001). *Tsix* mutant mice were maintained on a CD1 strain background. The mice recapitulate the published transmission frequency and phenotype (Sado et al., 2001). The X-linked *GFP* transgenic (*X-GFP*) strain is available via Jackson Labs [Tg (CAG-EGFP)D4Nagy/J] and have been described previously (Hadjantonakis et al., 2001; Kalantry and Magnuson, 2006; Kalantry et al., 2006; 2009). The *M. molossinus* JF1 strain was sourced from Jackson Laboratories (JF1/ms).

Embryo Dissections and Processing.

E3.5-E4.0 embryos were flushed from the uterine limbs in 1X PBS (Invitrogen, #14200075) containing 6% bovine serum albumin (BSA; Invitrogen, #15260037). Zona pellucidas surrounding E3.5 embryos were removed through incubation in cold acidic Tyrode's Solution (Sigma, #T1788), immediately followed by neutralization through several transfers of cold M2 medium (Sigma, #M7167). GFP fluorescence conferred by the paternal transmission of the *X-GFP* transgene was used to distinguish female from male embryos, since only females inherit the paternal-X. Embryos were rinsed in 1X PBS with 6 mg/ml BSA, plated on gelatin-coated glass coverslips, excess solution was aspirated, and the embryos air-dried for 15 min. After drying, embryos were permeabilized and fixed with 50 μL of 1X PBS containing 0.05% Tergitol (Sigma, #NP407) together with 1% paraformaldehyde for 10 min. Excess solution was

tapped off, and coverslips were rinsed 3X with 70% ethanol and stored in 70% ethanol at -20°C prior to RNA fluorescence *in situ* hybridization (RNA FISH) staining.

For isolation of E5.0-E6.5 embryos, dissections were carried out in 1X PBS containing 6% BSA. Individual implantation sites were cut from the uterine limbs, and decidua were removed with forceps. Embryos were dissected from the decidua, and the Reichert's membranes surrounding post-implantation embryos were removed using fine forceps. For separation of extra-embryonic and epiblast portions of E6.5 embryos, fine forceps were used to physically bisect the embryos at the junction of the extra-embryonic ectoderm and epiblast.

Immunofluorescence (IF) and/or RNA FISH staining were performed as described below.

Trophoblast Stem Cells.

E3.5 embryos were flushed out from the uterus with MEM α (Invitrogen, #12561) with 10% fetal bovine serum (FBS; Invitrogen, #10439-024) and plated on mouse embryonic fibroblast (MEF) cells in medium consisting of RPMI (Invitrogen, #21870076) with 20% FBS, 1 mM sodium pyruvate (Invitrogen, #11360-070), 100 μ M β -mercaptoethanol (Sigma, #M7522), 2 mM L-glutamine (Invitrogen, #25030), 37.5 ng/mL FGF4 (R&D Systems, #235-F4-025), and 1.5 μ g/mL heparin (Sigma, #H3149-10KU). Following five days of growth at 37°C with 5% CO₂ blastocyst outgrowths were dissociated with 0.05% trypsin (Invitrogen, #25300-054).

Dissociated cells were plated on MEFs and cultured at 37°C with 5% CO₂. RNA was harvested from TS cells using Trizol (Invitrogen, #15596-018) and RT-PCR was performed as described below. For RNA FISH and/or IF, TS cells were split onto gelatin-coated glass coverslips and allowed to grow for 3-6 days. The cells were then permeabilized through sequential treatment with ice-cold cytoskeletal extraction buffer (CSK; 100 mM NaCl, 300 mM sucrose, 3 mM

MgCl₂, and 10 mM PIPES buffer, pH 6.8) for 30 sec, ice-cold CSK buffer containing 0.4% Triton X-100 (Fisher Scientific, #EP151) for 30 sec, followed twice with ice-cold CSK for 30 sec each. After permeabilization, cells were fixed by incubation in 4% paraformaldehyde for 10 min. Cells were then rinsed 3X in 70% ethanol and stored in 70% ethanol at -20°C prior to IF and/or RNA FISH. For differentiation of TS cells, cells were split onto gelatinized dishes or coverslips and cultured for 6 days (d6) in media without FGF4 or heparin. On d6 of differentiation, RNA was harvested or cells were processed as described above for IF and RNA FISH.

RNA Fluorescence in situ Hybridization (RNA FISH).

Double-stranded RNA FISH (dsRNA FISH) probes were created by randomly priming DNA templates using BioPrime DNA Labeling System (Invitrogen, #18094011). Probes were labeled with Fluorescein-12-dUTP (Invitrogen), Cy3-dCTP (GE Healthcare, #PA53021), or Cy5-dCTP (GE Healthcare, #PA55031). Labeled probes for multiple genes were precipitated in a 3M sodium acetate (Teknova, #S0298) solution along with 300 µg of yeast tRNA (Invitrogen, #15401-029), 15 µg of mouse COT-1 DNA (Invitrogen, #18440-016) and 150 µg of sheared, boiled salmon sperm DNA (Invitrogen, #15632-011). The solution was then spun at 15,000 rpm for 20 min at 4°C. The resulting pellet was washed in 70% ethanol, then washed in 100% ethanol, dried, and re-suspended in deionized formamide (ISC Bioexpress, #0606-500ML). The re-suspended probe was denatured via incubation at 90°C for 10 min followed by an immediate 5 min incubation on ice. A 2X hybridization solution consisting of 4X SSC, 20% Dextran sulfate (Millipore, #S4030), and 2.5 mg/ml purified BSA (New England Biolabs, #B9001S) was added to the denatured solution. The probe was then pre-annealed by incubation at 37°C for 1 hr to

minimize probe hybridization to repetitive sequences. Probes were stored at -20°C until use. Strand-specific RNA FISH (ssRNA FISH) probes were labeled with Fluorescein-12-UTP (Roche, #11427857910) or Cy3 CTP (GE Healthcare, # 25801086) using the Invitrogen MAXIscript Kit (Invitrogen, #AM-1324). Labeled probes were column purified (Roche, #11814427001). The labeled probes were then precipitated in an 0.25M ammonium acetate solution essentially as described above for dsRNA FISH probes, but without the addition of COT-1 DNA. Probes were resuspended as described for dsRNA FISH probes and stored at -20 without preannealing. Embryos, embryo fragments, or TS cells mounted on coverslips were dehydrated through 2 min incubations in 70%, 85%, 95%, and 100% ethanol solutions and subsequently air-dried. The coverslips were then hybridized to the probe overnight in a humid chamber at 37°C. The samples were then washed 3X for 7 min each while shaking at 39°C with 2XSSC/50% formamide, 2X with 2X SSC, and 2X with 1X SSC. A 1:250,000 dilution of DAPI (Invitrogen, #D21490) was added to the third 2X SSC wash. The embryos were then mounted in Vectashield (Vector Labs, #H-1200). A total of 64 E3.5 embryos (18 XX, 16 X^{ΔTsix}X, 17 XY, and 13 X^{ΔTsix}Y) from eight litters were analyzed by RNA FISH. For assessment of E4.0 embryos, 13 embryos from 2 litters were analyzed by RNA FISH.

Whole-mount RNA FISH.

E6.5 embryos were permeabilized through sequential transfers into ice-cold cytoskeletal extraction buffer (CSK; 100 mM NaCl, 300 mM sucrose, 3 mM MgCl₂, and 10 mM PIPES buffer, pH 6.8) for 1 min, ice-cold CSK buffer containing 0.4% Triton X-100 (Fisher Scientific, #EP151) for 10 min, followed twice with ice-cold CSK for 1 min each. After permeabilization, the embryos were rinsed 3X in 70% ethanol and stored in 70% ethanol at -20°C prior to RNA

FISH. Embryos were rehydrated by incubating in decreasing concentrations of ethanol diluted in 2X SSC for 3 min each. Embryos were then placed in a droplet of 2X SSC in a depression well slide (Fisher Scientific, #S175201). Embryos were incubated in 10 μ L of probe (probe generation described in Experimental Procedures) overnight in a depression-well slide (Fisher Scientific, #S175201) sealed with a glass coverslip in a humid chamber at 37°C. Embryos were then rinsed with pre-warmed (50°C) 2X SSC/50% deionized formamide (Amresco, #NC9473844) and washed with 50% formamide/2X SSC solution 3X for 15 min each at 50°C, with periodic agitation via pipetting. Embryos were next washed with pre-warmed 2X SSC (50°C) 3X for 15 min each. In the first two 2X SSC washes, 4',6-diamidino-2-phenylindole dichloride (DAPI; Invitrogen, #D21490) was included at a dilution of 1:200,000. Embryos were next washed in pre-warmed 1X SSC solution (50°C) 2X for 15 min each. After washing, embryos were processed through sequential incubations in PBS with 25%, 50%, 75%, and 100% Vectashield (Vector Labs, #H-1000) and mounted in depression-well slides with Vectashield.

PCR and Allele-specific Reverse Transcriptase Polymerase Chain Reaction (RT-PCR).

Embryos and embryo fragments were lysed in 100 μ L of lysis/binding buffer (Dynabeads mRNA DIRECT Micro Kit; Invitrogen, #610.21). Messenger RNA was isolated by following manufacturer's instructions. SuperScript III One-Step RT-PCR Platinum *Taq* enzyme mixture (Invitrogen, #12574-035) was used to prepare and amplify the complementary DNA (cDNA). Strand-specific reverse transcription of *Xist* was performed using the XR-9816 primer, which spans bp 9815-9775 of *Xist* (CTCCACCTAGGGATCGTCAA). For PCR amplification, the forward primer XF-9229, which spans bp 9229-9248 of *Xist* (GACAACAATGGGAGCTGGTT)

was added upon completion of the RT reaction and prior to the PCR step. The *Xist* amplicon spans two introns, thus permits distinguishing genomic DNA sequence amplification by size. Genomic PCR for the *Xist* locus was performed the XR-271 primer, which spans 721-740 of *Xist* (CGGGGCTTGGTGGATGGAAAT), and XF-1083, which spans 1083-1064 of *Xist* (GCACAACCCCGCAAATGCTA). RT-PCR amplification of *Tsix* exon 4 in TS cells and E3.5 embryos was performed using the RT primer TR-4224, which spans base pairs 4224-4205 of *Tsix* (TCGGATCCCCTACAGATGA), and the forward PCR primer TF-3796, which spans base pairs 3796-3815 of *Tsix* (CTAAGAGCACCTGGCTCCAC). For E3.5 blastocysts, an additional round of nested PCR was performed to detect *Tsix* using TR-4224 and TF-3987, which spans base pairs 3987- 4006 of *Tsix* (TCCCAATTCTTGCAAACCTC). RT-PCR for the *Tsix* amplicon spanning exons 2-4 was performed using the RT primer TR-732, which spans base pairs 732-713 of *Tsix* (GGAGAGCGCATGCTTGCAAT) and the forward PCR primer TF-350, which spans base pairs 350-369 of *Tsix* (CCTGCAAGCGCTACACACTT). RT-PCR for β -Actin was performed using the RT primer β A-R, which spans base pairs 673-655 of *Actb* (GTAGCCACGCTCGGTCAGG), and the forward primer β A-F, which spans base pairs 142-159 of *Actb* (CGCGGGCGACGATGCTCC). Amplified cDNAs were run on agarose gels and purified using the Clontech NucleoSpin Kit (Clontech, #740609). The purified cDNAs were then sequenced and sequencing traces were examined for single nucleotide polymorphisms (SNPs) characteristic of the *M. musculus*-derived X^{JF1} chromosome and the *M. domesticus*-derived wild-type X^{Lab} and mutant $X^{\Delta Tsix}$ chromosomes. The SNP within the *Xist* amplicon localizes to bp 9399 of *Xist*. The *M. domesticus*-derived wild-type X^{Lab} and mutant $X^{\Delta Tsix}$ SNP is an adenosine while the *M. musculus* derived X^{JF1} SNP is a guanosine. The SNP within the *Xist* genomic PCR amplicon localizes to bp 804 of *Xist*. The *M. domesticus*-derived wild-type X^{Lab} and mutant $X^{\Delta Tsix}$

SNP is a thymidine while the *M. musculus* derived X^{JF1} SNP is an adenosine. SNPs within X-linked genes *Rnf12* (bp 860, NM_011276), *Pdhal* (bp 969, NM_008810.2), and *Utx* (bp 1383, NM_009483.1) have been described previously (Kalantry et al., 2009). RT and PCR primers for these genes have also been described previously (Kalantry et al., 2009; Sado et al., 2001).

Immunofluorescence.

Embryo fragments mounted on glass coverslips were washed 3X in PBS for 3 min each while shaking. The fragments were then incubated in blocking buffer (0.5 mg/mL BSA (New England Biolabs, #B9001S), 50 ug/mL yeast tRNA, 80 units/mL RNaseOUT (Invitrogen, #10777-019), and 0.2% Tween 20, in PBS) in a humid chamber for 30 min at 37°C. The samples were next incubated with primary antibody, diluted in blocking buffer, for 1 hr in the humid chamber at 37°C. The H3-K27me3 (EMD Millipore, #ABE44) was used at 1:2500 dilution in blocking buffer. The CDX2 antibody (BioGenex, #MU328A-UC) was used at a 1:75 dilution in blocking buffer. The p57^{Kip2} antibody (Thermo Scientific, #RB-1637) was used at a 1:150 dilution in blocking buffer. Following three washes in PBS/0.2% Tween-20 for 3 min each while shaking, the embryos were incubated in blocking buffer for 5 min at 37°C in the humid chamber. The embryos were then incubated in blocking buffer containing a 1:300 dilution of fluorescently-conjugated secondary antibody (Alexa Fluor, Invitrogen) for 30 min in a humid chamber, followed by three washes in PBS/0.2% Tween-20 while shaking for 3 min each. The samples were then processed for RNA FISH as described above.

Immunosurgery.

To isolate the inner cell mass (ICM) of E4.0 embryos, embryos were incubated in pre-warmed rabbit anti-mouse serum (Rockland Immunochemicals, #110-4101) at a 1:5 dilution in M2 medium for 1 hr in a humid chamber at 37°C. After briefly rinsing in M2 medium, embryos were incubated in pre-warmed guinea pig complement (Sigma, cat No. S1639) at a 1:5 dilution in M2 medium for 45 min to 1 hr in a humid chamber at 37°C. The embryos were then repeatedly pipetted using a finely-pulled glass Pasteur pipette to remove trophoctoderm cells. Isolated ICMs were treated with 0.05% trypsin for 10 min for mild dissociation, then incubated in M2 media with 10% fetal bovine serum (FBS) for 10 min to neutralize the trypsin. ICMs were then rinsed in 1X PBS and permeabilized through sequential transfers into ice-cold CSK for 1 min, ice-cold CSK containing 0.4% Triton X-100 buffer for 5 min, followed twice with ice-cold CSK for 1 min each. ICMs were mounted on a glass coverslip coated with 1X Denhardt's solution in a small drop of ice-cold solution of 1X PBS containing 1% paraformaldehyde and 20% CSK buffer. Excess solution was aspirated off and the coverslip air-dried for 15 min. The ICMs were then fixed in cold 3% paraformaldehyde for 10 min. After fixation, the coverslips were rinsed 3X in 70% ethanol and stored in 70% ethanol at -20°C prior to use.

Microscopy.

Stained samples were imaged using a Nikon Eclipse TiE inverted microscope with a Photometrics CCD camera. The images were deconvolved and uniformly processed using NIS-Elements software.

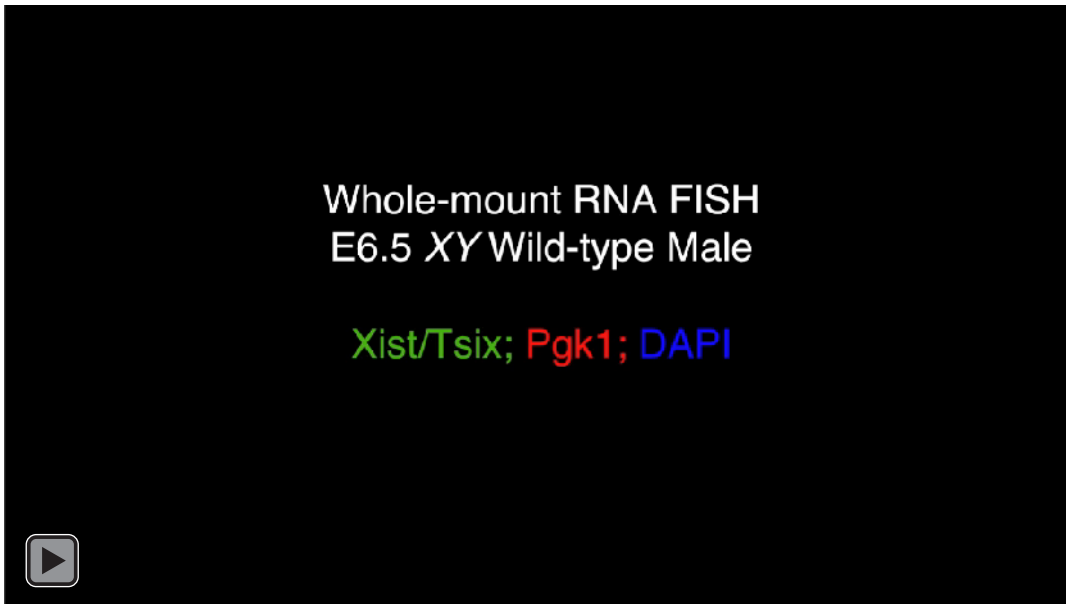
Statistics.

Comparisons between gene expression patterns were performed using a two-tailed Fisher's exact test. $p=0.01$ was used as the cutoff for statistical significance.

Movies



Movie 1: 3D imaging of X-linked gene expression in intact XX Embryonic day (E) 6.5 Embryos. Whole-mount RNA FISH of a representative wild-type (WT) XX E6.5 embryo. Xist RNA coating and Tsix RNA are detected in green. RNA expressed from the X-linked gene *Pgk1* is detected in red. Nuclei are stained blue with DAPI.



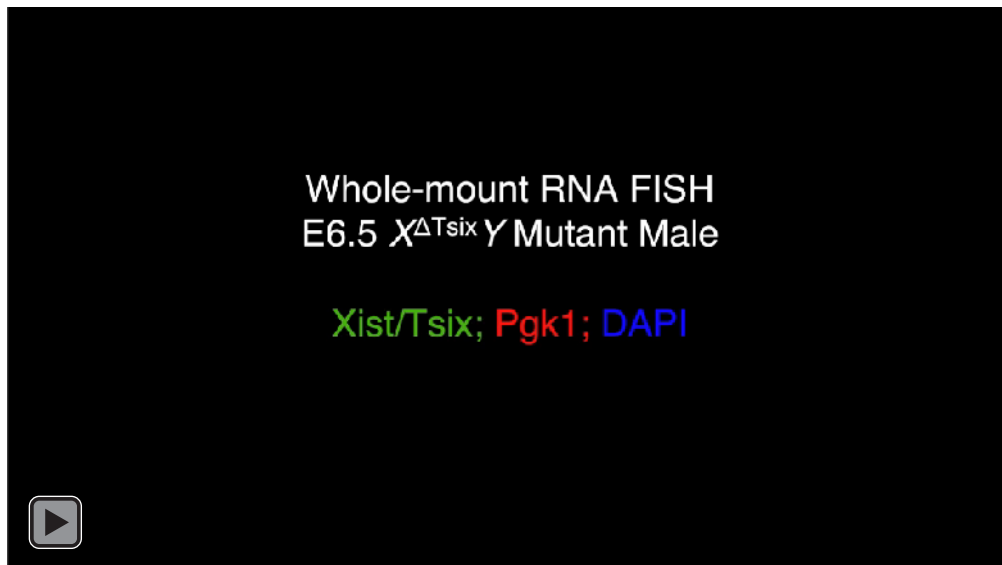
Movie 2: 3D imaging of X-linked gene expression in intact XY E6.5 Embryos. Whole-mount RNA FISH of a representative WT XY E6.5 embryo. Tsix expression is detected in green. RNA expressed from the X-linked gene *Pgk1* is detected in red. Nuclei are stained blue with DAPI.

Whole-mount RNA FISH
E6.5 $X^{\Delta Tsix}X$ Mutant Female

Xist/Tsix; Pgk1; DAPI



Movie 3: 3D imaging of X-linked gene expression in intact E6.5 $X^{\Delta Tsix}X$ Embryos. Whole-mount RNA FISH of a representative $X^{\Delta Tsix}X$ mutant E6.5 embryo. Xist RNA coating and Tsix expression are detected in green. RNA expressed from the X-linked gene *Pgk1* is detected in red. Nuclei are stained blue with DAPI. Ectopic Xist RNA expression and coating is observed in some cells.



Movie 4: 3D imaging of X-linked gene expression in intact $X^{\Delta Tsix} Y$ Embryos. Whole-mount RNA FISH of a representative $X^{\Delta Tsix} Y$ mutant E6.5 embryo. Xist RNA coating and Tsix expression are detected in green. RNA expressed from the X-linked gene *Pgf1* is detected in red. Nuclei are stained blue with DAPI. Ectopic Xist RNA induction is observed in some cells.

Chapter 3: A Primary Role for the Tsix lncRNA in Maintaining Random X-chromosome Inactivation

This chapter was originally published in *Cell Reports* as 1. Gayen, S*, Maclary, E*, Buttigieg, E., Hinten, M. & Kalantry, S. “A Primary Role for the Tsix lncRNA in Maintaining Random X-Chromosome Inactivation”. (*Cell Reports* 11, 1251–1265 (2015)). *, equal contribution. Data and figures were primarily generated by S.G. and E.M., E.M. is responsible for the data presented in figures 3.1, 3.5, 3.6, and 3.14. S.G. is responsible for the data presented in figures 3.2, 3.3, 3.4, 3.7, 3.8, 3.9, 3.10, 3.11, 3.12, and 3.13. E.M. performed all statistical analysis. E.B. assisted with development and optimization of strand-specific riboprobes. M.H. developed the allelic pyrosequencing assays utilized throughout the manuscript. E.M., S.G., and S.K. wrote the manuscript.

3-1: Introduction

X-chromosome inactivation results in the mitotically-stable transcriptional silencing of genes along one of the two X-chromosomes in female mammals (LYON, 1961). In the pluripotential mouse epiblast cells, which will form the embryo proper, the selection of which X to inactivate is random. Molecularly, random X-inactivation is posited to be controlled in *cis* by a pair of oppositely-transcribed X-linked long non-coding (lnc) RNAs, Xist and Tsix (Barakat and Gribnau, 2012). Xist RNA is believed to initiate epigenetic silencing of genes in *cis* by

physically coating the X-chromosome from which it is transcribed and recruiting proteins that catalyze heterochromatin formation (Payer and Lee, 2008). *Tsix* transcription across the *Xist* promoter, conversely, is proposed to inhibit *Xist* expression (Lee, 2000; Lee and Lu, 1999; Luikenhuis et al., 2001; Navarro et al., 2005; Sado et al., 2001; 2005). Because of its ability to repress *Xist*, the *Tsix* locus is postulated to be the site where molecular signals converge to help ensure that one X-chromosome remains active in both males and females (Clerc and Avner, 1998; Cohen et al., 2007; Debrand et al., 1999; Gontan et al., 2012; Lee, 2005; Luikenhuis et al., 2001; Morey et al., 2004; Navarro et al., 2010; Stavropoulos et al., 2005; Vigneau et al., 2006).

Investigations of mutations that reduce or abrogate *Tsix* RNA expression, however, have resulted in disparate outcomes. In differentiating male embryonic stem cells (ESCs), a cell culture model of X-inactivation, some *Tsix* mutations display ectopic *Xist* induction, consistent with *Tsix* serving to inhibit *Xist* and thereby X-inactivation (Clerc and Avner, 1998; Debrand et al., 1999; Luikenhuis et al., 2001; Morey et al., 2004; Sado et al., 2002; Vigneau et al., 2006). Other *Tsix*-mutant male ESCs, though, do not exhibit *Xist* expression upon differentiation (Cohen et al., 2007; Lee, 2000; Lee and Lu, 1999; Minkovsky et al., 2013). The differences observed between the mutant ESC lines may reflect residual *Tsix* expression due to the incomplete ablation of *Tsix* or differences in the protocols employed to differentiate ESCs.

Whereas ectopic X-inactivation may or may not occur in *Tsix*-mutant males, the choice of which X to inactivate appears absolutely biased in *Tsix*-heterozygous females (Cohen et al., 2007; Kalantry and Magnuson, 2006; Lee, 2000; Sado et al., 2001). In these mice, the *Tsix*-mutant X-chromosome is inactive in all cells of the differentiating epiblast lineage, which would otherwise undergo random X-inactivation. This bias in choice has been explained by the

preferential induction of Xist from the Tsix-mutant X-chromosome prior to or at the onset of X-inactivation in the epiblast lineage.

Despite the proposed models of Tsix function, the significance of Tsix RNA remains unclear in both males and females. In the course of a previous study, we noticed that the epiblast in $X^{\Delta Tsix}Y$ post-implantation embryos appeared to ectopically express Xist in the absence of Tsix (Maclary et al., 2014). We therefore hypothesized that Tsix-heterozygous females might also aberrantly express Xist during development. Thus, an alternative explanation for the apparent lack of ectopic Xist expression and skewed X-inactivation in Tsix-heterozygotes is that a secondary cell-selection effect rapidly removes cells with two inactive-Xs from the population. Due to the tight coupling of X-inactivation with epiblast differentiation (Monk and Harper, 1979), ectopic silencing of the previously active $X^{\Delta Tsix}$ may occur concurrently with or shortly after the initiation of random X-inactivation. Inactivation of both Xs in females would render the cells effectively nullizygous for many X-linked genes, thus compromising proliferation and viability. Later-stage epiblast and ESC derivatives would therefore consist only of cells with an active WT X-chromosome. Here, we investigate Tsix function by profiling embryos harboring a Tsix-null allele at the onset of random X-inactivation; and, by deriving Tsix hemizygous male and heterozygous female EpiSC and ESC lines.

3-2: Tsix Absence Results in Ectopic Xist RNA Expression and Coating in Male Embryonic Epiblasts

Random X-inactivation initiates in epiblast cells between embryonic day (E) 4.5-6.5 in mice, just as the pluripotential epiblast cells begin to differentiate (Gardner and LYON, 1971; Kalantry and Magnuson, 2006; McMahon et al., 1983; Rastan, 1982). To examine the role of

Tsix RNA at the onset of X-inactivation, we generated embryonic day (E) 5.25 post-implantation stage embryos that inherit either a WT or a Tsix-null maternal X-chromosome from Tsix-heterozygous females. The previously described Tsix mutation, *Tsix*^{AA2Δ1.7} (herein referred to as *X^{ΔTsix}*) (Sado et al., 2001), terminates the Tsix transcript in exon 2 and also deletes the critical *DXPas34* repeat thought to serve as a platform to drive Tsix expression (Fig. 3.1 A) (Cohen et al., 2007; Maclary et al., 2014; Navarro et al., 2010; Stavropoulos et al., 2005; Vigneau et al., 2006). Since transcription across the Xist promoter region is required for the Tsix RNA to inhibit Xist expression (Navarro et al., 2005; Sado and Ferguson-Smith, 2005), *X^{ΔTsix}* is a *bona fide* null Tsix mutation (Fig. 3.1 B) (Maclary et al., 2014; Sado et al., 2001). We first tested if the absence of Tsix RNA led to Xist induction in male epiblasts by RT-PCR. Whereas WT E5.25 XY epiblasts exhibited Tsix but not Xist expression, *X^{ΔTsix}Y* epiblasts displayed the opposite pattern (Fig. 3.1 B). We next independently assessed Xist induction and X-inactivation in E5.25 XY and *X^{ΔTsix}Y* epiblast cells by immunofluorescence (IF) coupled with RNA fluorescence *in situ* hybridization (RNA FISH). We first marked epiblast cells via IF detection of NANOG, which distinguishes the epiblast from the extra-embryonic cells (Fig. 3.1 C). In the same samples, using strand-specific RNA FISH probes we also assayed expression of Tsix and Xist RNAs. In WT XY epiblasts, Tsix RNA signal but not Xist RNA coating was detectable from the sole X-chromosome (Fig. 3.1 C). In contrast, in *X^{ΔTsix}Y* mutant embryos ~34% of the nuclei displayed Xist RNA coating (Fig. 3.1 C). Moreover, Xist coating resulted in the accumulation of histone H3 lysine 27 trimethylation (H3-K27me3), a chromatin mark catalyzed by the Polycomb repressive complex 2 that is associated with the inactive-X heterochromatin (Fig. 3.1 D) (Plath et al., 2003; Silva et al., 2003), and accompanied silencing of the X-linked *Pgk1* gene (Fig. 3.1 E).

Thus, Tsix absence leads to Xist RNA induction, coating, and gene silencing on the single X-chromosome in male epiblast cells.

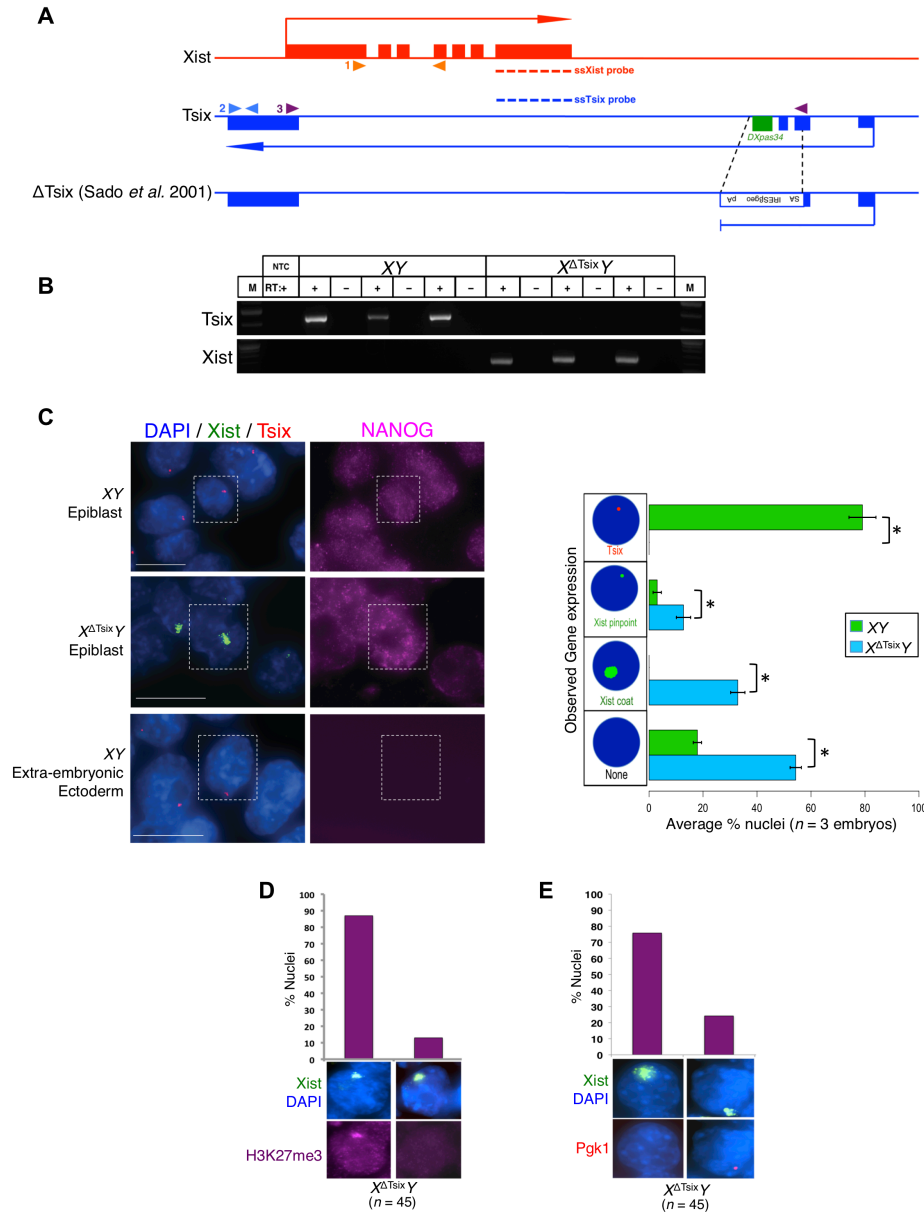


Figure 3.1: Xist is induced from the X^{ΔTsix} in E5.25 male epiblast cells. (A) Diagram illustrating WT Xist and Tsix loci and the Δ Tsix mutation. Dotted lines indicate the locations of strand-specific (ss) RNA FISH probes. Filled arrowheads mark the locations of RT-PCR primer pairs. 1 (orange arrowheads), Xist RT-PCR amplicon; 2 (blue arrowheads), Tsix exon 4 RT-PCR amplicon; 3 (purple arrowheads), Tsix RT-PCR amplicon spanning exons 2-4. (B) RT-PCR amplification of Tsix (exon 4) and Xist RNAs in E5.25 epiblasts. M, marker; NTC, no template control; +, reaction with reverse transcriptase (RT); -, no RT control lane. (C) Strand-specific RNA FISH detection of Xist RNA (green) and Tsix RNA (red) coupled with IF staining for NANOG (purple) in isolated epiblasts and extra-embryonic ectoderm, which serves as a negative control for NANOG expression. Nuclei are stained blue with DAPI. Scale bar, 10 μ m. Right, quantification of Xist and Tsix expression in NANOG-positive epiblast nuclei. The X-axis of each graph represents the average percentage of nuclei per embryo in each class ($n =$

3 embryos/genotype; 49-68 nuclei/embryo). Diagrams along the Y-axis depict all observed expression patterns. Error bars represent the standard deviation of data from 3 different embryos. *, $p \leq 0.001$ (Chi-square test). (D) Xist RNA coating (green) and H3-K27me3 enrichment (purple) in E5.25 $X^{\Delta Tsix}Y$ epiblast nuclei. (E) Silencing of the X-linked gene *Pgk1* (red) in E5.25 $X^{\Delta Tsix}Y$ epiblast nuclei upon ectopic Xist RNA coating (green).

3-3: Ectopic Xist Induction in Differentiating But Not Undifferentiated $X^{\Delta Tsix}Y$ Epiblast Stem Cells

To further explore the requirement of Tsix in the epiblast, we derived WT XY and mutant $X^{\Delta Tsix}Y$ epiblast stem cells (EpiSCs; Fig. 3.2 A-C; Table 3.1). EpiSCs are thought to represent an early phase of X-inactivation (Bernemann et al., 2011; Brons et al., 2007; Han et al., 2011; Pasque et al., 2011a; 2011b; Tesar et al., 2007). If Tsix negatively regulates Xist in undifferentiated epiblast cells, EpiSCs lacking Tsix are expected to display aberrant Xist activation. In assaying Xist expression by RT-PCR, we found that Xist RNA was undetectable in the WT XY EpiSC lines (Fig. 3.3 A). In $X^{\Delta Tsix}Y$ EpiSC lines, however, Xist RNA was expressed at minimally detectable levels (Fig. 3.3 A). This low level of Xist expression may reflect the induction of Xist in the small fraction of differentiated cells that are often found in stem cell cultures. This notion prompted us to test if Xist would be induced to high levels if we actively differentiated $X^{\Delta Tsix}Y$ EpiSCs (Fig. 3.2 D). Indeed, Xist expression in $X^{\Delta Tsix}Y$ but not XY cells increased markedly upon differentiation (Fig. 3.3 A).

To examine if the ectopic Xist expression coincided with coating of the X-chromosome, we performed Xist RNA FISH on undifferentiated and differentiated EpiSCs. As expected, neither undifferentiated nor differentiated XY EpiSC lines exhibited any Xist RNA coated X-chromosomes (Fig. 3.3 B). In all four of the $X^{\Delta Tsix}Y$ EpiSC lines, we observed a similar lack of Xist RNA coating in the undifferentiated cells (Fig. 3.3 B). However, upon differentiation a significant percentage of the mutant cells displayed Xist RNA coating (29-35%; Fig. 3.3 B-C). As in E5.25 mutant epiblast cells, many Xist RNA-coated $X^{\Delta Tsix}Y$ cells still expressed NANOG

(38-42%) (Fig. 3.2 E). Xist RNA coating also resulted in the accumulation of histone H3-K27me3 and silencing of *Pgk1* on the $X^{\Delta Tsix}$ in a vast majority of the mutant cells (84-94%) (Fig. 3.3 D-E). Together, the RT-PCR and RNA FISH data from $X^{\Delta Tsix}Y$ EpiSCs prompt the conclusion that Tsix RNA does not participate in repressing *Xist* in undifferentiated male EpiSCs. Instead, Tsix is required to prevent ectopic Xist induction and X-linked gene silencing during the differentiation of male epiblast progenitor cells.

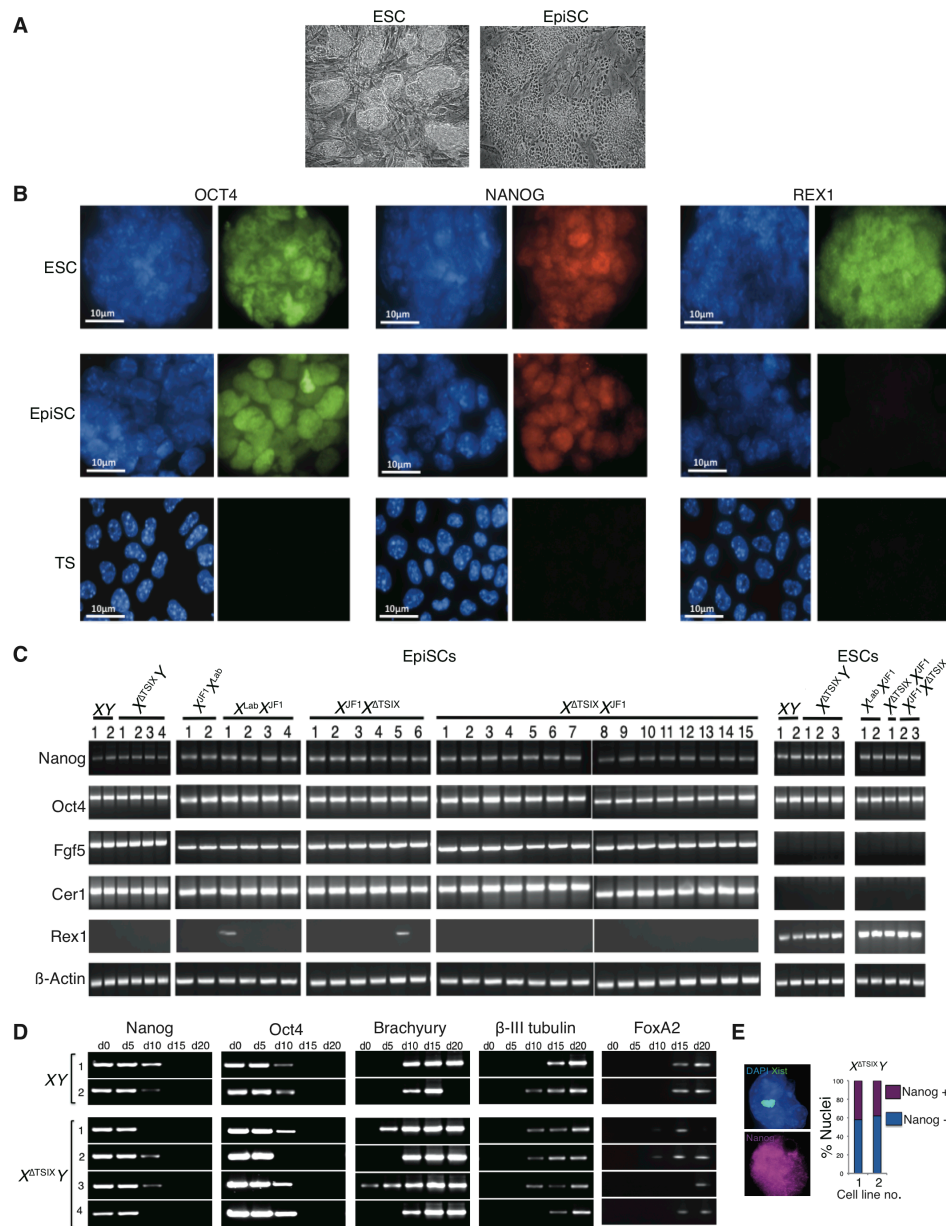


Figure 3.2: Characterization of EpiSCs and ESCs (A) Stereo micrographs of EpiSCs and ESCs highlighting differences in cellular morphology. (B) Comparison of ESC, EpiSC, and trophoblast stem cell (TSC) lines through IF detection of OCT4, NANOG, and REX1. A representative cell line is shown of each stain. Whereas ESCs express all three proteins, EpiSCs express OCT4 and NANOG but not REX1. TSCs serve as negative controls and lack expression of all three markers. Scale bars, 10 μ m. (C) Marker analysis by RT-PCR of all male and female EpiSC and ESC lines used in the study. Fgf5 and Cer1 are expressed only in EpiSCs while high Rex1 expression marks ESCs. (D) Characterization of differentiating male EpiSC lines. RT-PCR amplification of pluripotency markers Nanog and Oct4; mesodermal marker Brachyury; neuroectodermal marker β -III tubulin; hepatocyte marker FoxA2 at successive days of differentiation in WT and Tsix-hemizygous EpiSCs analyzed in Fig 2. d, days. Loss of expression of Oct4 and Nanog indicates that EpiSCs had lost pluripotency and differentiated. (E) Xist RNA coating in NANOG+ and NANOG- d5 differentiating $X^{\Delta Tsix}Y$ EpiSCs.

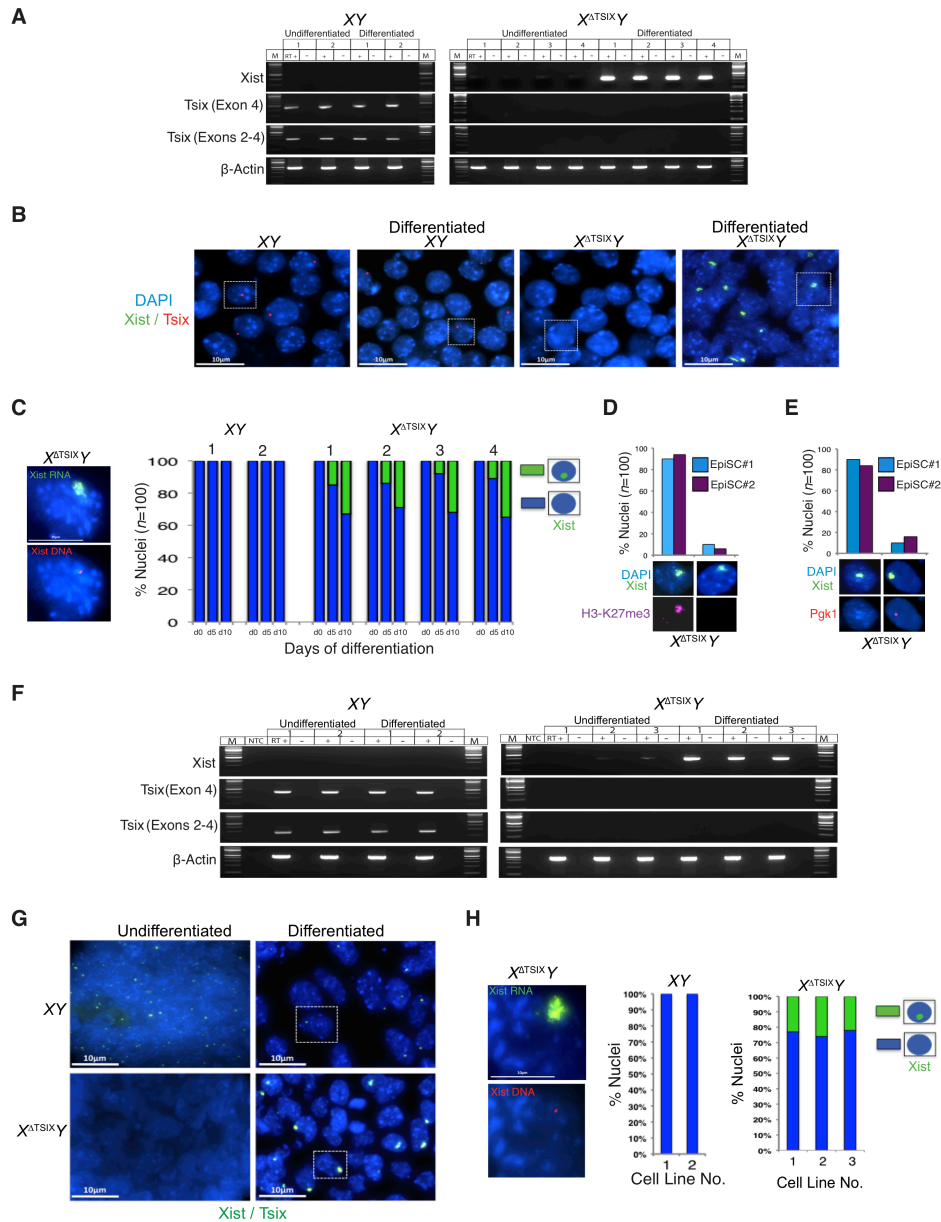


Figure 3.3: Ectopic Xist RNA induction in differentiated but not undifferentiated $X^{ATsix}Y$ EpiSCs and ESCs. (A) RT-PCR amplification of Xist and Tsix RNAs in undifferentiated and differentiated XY and $X^{ATsix}Y$ EpiSC lines (2 and 4 cell lines, respectively). β -actin amplification serves as control. M, marker; +, reaction with reverse transcriptase (RT); -, no RT control lane. (B) RNA FISH detection of Xist RNA (green) and Tsix RNA (red) in representative undifferentiated and day (d) 10 differentiated EpiSC lines (XY line number [no.] 1; $X^{ATsix}Y$ line no. 2). Nuclei are stained blue with DAPI. Scale bar, 10 μ m. (C) Quantification of Xist RNA coated nuclei in undifferentiated (d0) and d5 and d10 differentiated EpiSC lines. Scale bar, 10 μ m. Only cells with a single Xist locus detected by DNA FISH (left) following RNA FISH were counted; $n=100$ nuclei/cell line. (D) RNA FISH detection of Xist (green) combined with IF detection of H3-K27me3 (red) in d10 differentiated $X^{ATsix}Y$ EpiSCs. Data from two different lines are shown. (E) Silencing of *Pgl1* (red) upon Xist RNA (green) coating in representative d10 differentiated $X^{ATsix}Y$ EpiSCs. (F-G) RT-PCR (F) and RNA FISH (G) detection of Xist and Tsix RNAs in undifferentiated or embryoid body-differentiated XY and $X^{ATsix}Y$ ESC lines (2 and 3 lines, respectively). Scale bar, 10 μ m. (H) Quantification of Xist RNA coated nuclei in the differentiated ESC lines. Only cells with one Xist locus detected by DNA FISH (left) following RNA FISH were counted; $n=100$ nuclei/cell line. Scale bar, 10 μ m.

3-4: Ectopic Xist Induction in Differentiating $X^{\Delta Tsix}Y$ ESCs

That $X^{\Delta Tsix}Y$ EpiSCs displayed robust Xist induction only upon differentiation is incongruous with some previous studies with Tsix-mutant male ESCs. Tsix deficiency in male ESCs is suggested to either be innocuous in both undifferentiated and differentiated cells (Cohen et al., 2007; Lee, 2000; Lee and Lu, 1999; Minkovsky et al., 2013; Ohhata et al., 2006; Sado et al., 2001; 2002); or, conversely, result in ectopic Xist RNA coating of the Tsix-mutant X during differentiation (Debrand et al., 1999; Luikenhuis et al., 2001; Morey et al., 2004; Navarro and Avner, 2010; Vigneau et al., 2006). We therefore derived XY and $X^{\Delta Tsix}Y$ ESC lines (Fig. 3.2) and tested Xist induction in both undifferentiated and differentiated cells by RT-PCR and RNA FISH. As with EpiSCs, we found that *Xist* remained silenced in undifferentiated XY as well as in $X^{\Delta Tsix}Y$ ESCs (Fig. 3.3 F-G); however, upon differentiation Xist RNA was induced in $X^{\Delta Tsix}Y$ but not XY ESCs (Fig. 3.3 F-H).

To distinguish if Xist induction in $X^{\Delta Tsix}Y$ ESCs occurred at the onset of differentiation or later, we transiently differentiated the ESCs into epiblast-like cells (EpiLCs) (Hayashi et al., 2011). EpiLCs arise early during ESC differentiation and share key features with EpiSCs (Fig. 3.4 A-C) (Buecker et al., 2014). We found that the mutant EpiLCs displayed low-level Xist expression by RT-PCR, with only a few cells displaying Xist RNA coating (10%) (Fig. 3.4 C-E). The Xist RNA-coated cells appeared to have differentiated beyond the EpiLC state, as suggested by reduced NANOG expression (Fig. 3.4 E). When the EpiLCs were differentiated further, significantly more cells displayed Xist RNA coating (27-36%) (Fig. 3.4 F), consistent with the EpiSC data.

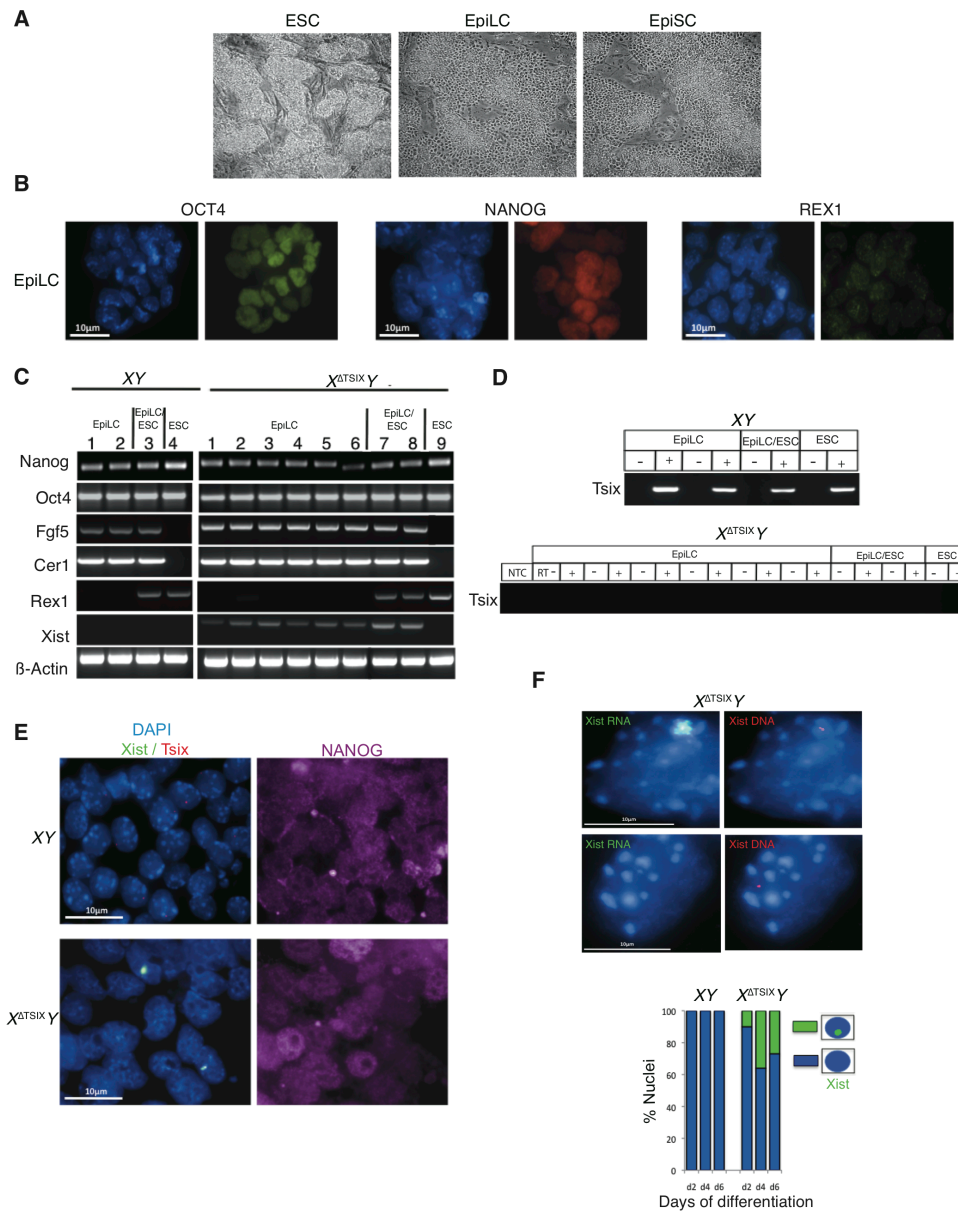


Figure 3.4: Characterization of male ESC-derived EpiLCs. (A) Stereo micrographs of ESCs, EpiLCs, and EpiSCs. (B) IF detection of OCT4, NANOG, and REX1 in EpiLCs. A representative image is shown of each stain. EpiLCs express OCT4 and NANOG but not REX1, similar to EpiSCs (see Fig. S1). Scale bars, 10 µm. (C) Analysis of male EpiLCs by RT-PCR. Fgf5 and Cer1 are expressed in EpiLCs, similarly to in EpiSCs, whereas high Rex1 expression exclusively marks ESCs. ‘EpiLC’ samples are individual fields in tissue culture wells containing largely if not exclusively cells morphologically resembling EpiLCs. ‘EpiLC/ESC’ samples are of entire tissue culture wells in which ESCs were being converted to EpiLCs. These samples display faint Rex1 expression, indicative of residual undifferentiated ESCs. ‘ESC’ samples are of unconverted ESC wells. Faint Xist expression is detected in $X^{ATsix}Y$ but not XY EpiLCs. (D) RT-PCR amplification of Tsix (exon 4) in XY and $X^{ATsix}Y$ EpiLCs. (E) Strand-specific RNA FISH detection of Xist (green) and Tsix (red) combined with IF detection of NANOG in EpiLCs. Scale bars, 10 µm. (F) Quantification of Xist RNA coated nuclei. d2, differentiation of ESCs into EpiLCs, d4 and d6 differentiation of the ESCs beyond the EpiLC stage. Scale bars, 10 µm. Only cells with one Xist locus detected by DNA FISH (left) following RNA FISH were counted; $n=100$ nuclei/cell line.

3-5: Absence of Biased X-chromosome Choice in Tsix-heterozygous Female Epiblasts

We next examined the impact of the $X^{\Delta Tsix}$ mutation in females. The two X-chromosomes in inbred XX epiblast cells are normally equally likely to undergo inactivation; in heterozygous Tsix-mutant epiblasts, however, previous work has concluded that only the $X^{\Delta Tsix}$ X-chromosome is chosen for inactivation (Lee, 2000; Sado et al., 2001). This model of biased inactivation in favor of the $X^{\Delta Tsix}$ is borne out by allele-specific Xist RT-PCR analyses of F1 hybrid WT and Tsix-heterozygous E6.5 epiblasts (Fig. 3.5 A-B). The X-chromosomes in these embryos are derived from two divergent mouse strains and are polymorphic, thereby allowing allele-specific expression analysis. Both Sanger sequencing (Fig. 3.5 A) and Pyrosequencing (Fig. 3.5 B), which quantifies allele-specific expression, of the cDNAs revealed that Xist is transcribed from either X in WT $X^{Lab}X^{JF1}$ and $X^{JF1}X^{Lab}$ embryos (by convention, the maternal allele precedes the paternal allele), whereas in $X^{\Delta Tsix}X^{JF1}$ and $X^{JF1}X^{\Delta Tsix}$ epiblasts Xist is expressed almost exclusively from the $X^{\Delta Tsix}$.

To evaluate the expression of Xist and Tsix in XX, $X^{\Delta Tsix}X$, and $XX^{\Delta Tsix}$ E6.5 epiblasts at the single cell resolution, we performed strand-specific RNA FISH. As with male embryos, we again confirmed the identity of epiblast cells by first assaying expression of NANOG by IF. We observed Xist RNA coating of both Xs by RNA FISH in a small fraction of $X^{\Delta Tsix}X$ and $XX^{\Delta Tsix}$ mutant (~2%), but not WT XX, E6.5 epiblast cells (Fig. 3.5 C). Based on this observation and the hypothesis that cells with ectopic inactivation of the $X^{\Delta Tsix}$ are eliminated, we reasoned that a higher percentage of cells in Tsix-heterozygotes may display Xist RNA coating of both X-chromosomes at an earlier stage of embryogenesis. We therefore assayed epiblast cells in E5.25 embryos by RNA FISH (Fig. 3.5 D). Although most nuclei displayed Xist RNA accumulation, a proportion lacked Xist RNA coating but displayed nascent Xist and Tsix RNAs, suggesting that

X-inactivation was just beginning in the epiblast. Of the Xist RNA coated nuclei, a small but significant percentage clearly displayed Xist RNA coating of both X-chromosomes in $X^{\Delta Tsix}X$ epiblasts (12%) compared to XX epiblasts (0%), although one of the two Xist coats in the mutants was often comparatively weaker (Fig. 3.5 D). To rule out a parent-of-origin effect, we also investigated E5.25 epiblasts with paternally-transmitted $X^{\Delta Tsix}$ mutation. A similar percentage of $XX^{\Delta Tsix}$ epiblast cells (11%) exhibited Xist RNA coating of both X-chromosomes (Fig. 3.5 D). Xist RNA coating of both Xs coincided with H3-K27me3 enrichment and silencing of *Pgk1* on both Xs in 80-90% of the nuclei, suggesting that both Xs were inactivated (Fig. 3.6 A-B).

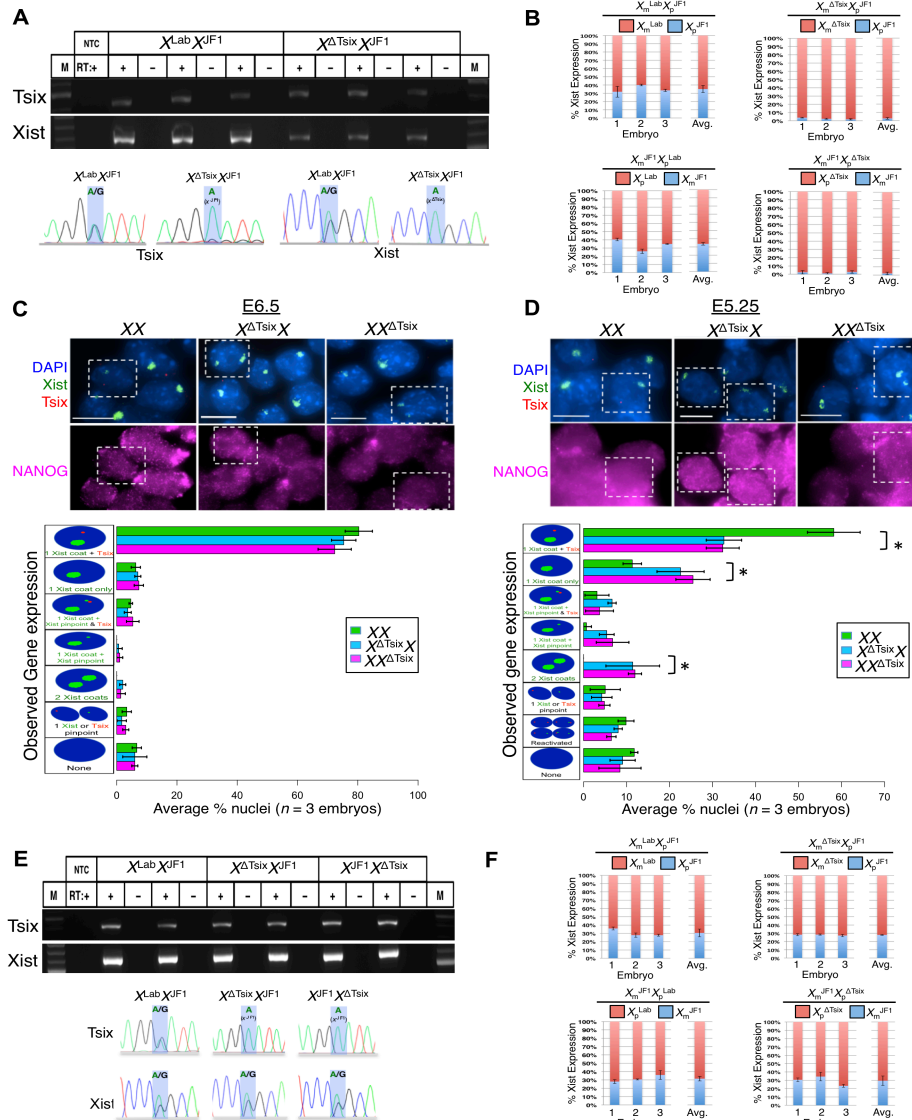


Figure 3.5: Xist expression in E6.5 and E5.25 WT and Tsix-heterozygous female epiblast cells. (A) Allele-specific RT-PCR detection of Tsix (exon 4) and Xist RNAs in epiblasts of three individual WT ($X^{Lab}X^{JF1}$) and Tsix-heterozygous ($X^{\Delta Tsix}X^{JF1}$) E6.5 embryos. M, marker; NTC, no template control; +, reaction with reverse transcriptase (RT); -, no RT control lane. Bottom, Sanger sequencing of the amplified cDNAs. Blue highlights mark a SNP that differs between the $X^{Lab} / X^{\Delta Tsix}$ and X^{JF1} mouse strains. (B) RT-PCR followed by Pyrosequencing-based quantification of allelic Xist expression in epiblasts of individual E6.5 embryos. Error bars represent the standard deviation of data from 3 different embryos. (C-D) RNA FISH detection of Xist and Tsix RNAs coupled with IF detection of NANOG in isolated E6.5 (C) and E5.25 (D) epiblasts. Nuclei are stained blue with DAPI. Scale bars, 10 μ m. Bottom, quantification of Xist and Tsix expression. The X-axis of each graph represents the average percentage of nuclei in each class ($n = 3$ embryos/genotype; 100 nuclei/E6.5 embryo and 45-71 nuclei/E5.25 embryo). Diagrams along the Y-axis depict all observed expression patterns. Error bars represent the standard deviation of data from 3 different embryos. *, $p \leq 0.01$ (Chi-square test). (E) RT-PCR amplification of Tsix (exon 4) and Xist RNAs in WT and Tsix-heterozygous epiblasts. Bottom, Sanger sequencing of the Tsix and Xist cDNAs. (F) RT-PCR followed by Pyrosequencing-based quantification of allelic Xist expression in epiblasts of individual E5.25 embryos. Error bars represent the standard deviation of data from 3 different embryos. No significant differences in allelic Xist expression were observed between WT and Tsix-mutant embryos ($p = 0.44$, E5.25 $X^{Lab}X^{JF1}$ vs. $X^{\Delta Tsix}X^{JF1}$; $p = 0.46$, E5.25 $X^{JF1}X^{Lab}$ vs. $X^{JF1}X^{\Delta Tsix}$; Welch's two-sample T-test.).

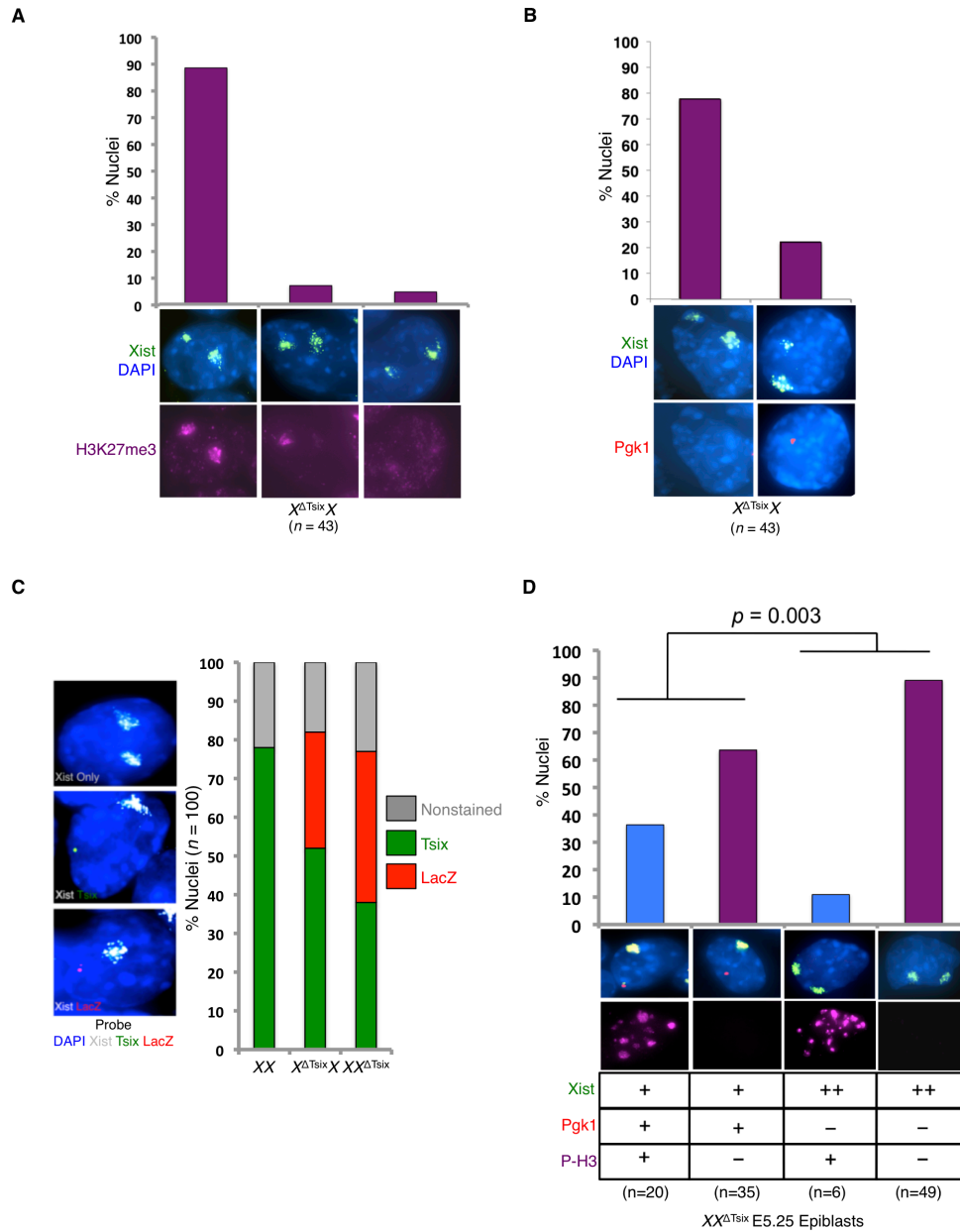


Figure 3.6: Characterization of X-inactivation, allelic Xist expression, and proliferation in E5.25 female epiblasts. (A) Combined IF and RNA FISH detects Xist RNA coating (green) and H3-K27me3 enrichment (purple) in E5.25 $X^{\Delta Tsix}X$ epiblast nuclei. Of the nuclei displaying ectopic Xist RNA coats, H3-K27me3 is enriched in >87% of the nuclei. (B) RNA FISH shows silencing of the X-linked gene *Pgk1* (red) in ~80% of nuclei upon ectopic Xist RNA coating (green). (C) RNA FISH detection of $X^{\Delta Tsix}$ as the active X-chromosome. Nuclei with two Xist RNA coats do not express LacZ or Tsix (top panel); both are subject to X-inactivation. Nuclei with an Xist RNA-coated inactive X-chromosome express either Tsix (green) from the WT X or LacZ (red) from the $X^{\Delta Tsix}$. n=100 nuclei/genotype. (D) Quantification of Xist RNA coating and phospho-histone H3 staining in $XX^{\Delta Tsix}$ E5.25 epiblast nuclei. A total of 55 nuclei with single inactive-X chromosomes and 55 nuclei with two inactive X-chromosomes (2 Xist RNA coats and no Pgk1 expression) were counted. Nuclei with two inactive X-chromosomes show a significant reduction in the proportion of phospho-H3 stained nuclei ($p=0.003$, Fisher's exact test).

In addition to nuclei with two Xist RNA coats, E5.25 Tsix-heterozygotes lacked Tsix RNA expression from the active-X in a significant percentage of nuclei (24%). We suspected that in these cells the $X^{\Delta Tsix}$ was chosen as the active-X, and, hence, the WT X as the inactive-X. Upon differentiation, this population of cells would ectopically induce Xist from and undergo inactivation of the $X^{\Delta Tsix}$. We therefore set out to test directly if the $X^{\Delta Tsix}$ can be chosen as the active-X in E5.25 epiblasts, by exploiting the expression of a β -galactosidase cassette integrated into the mutant Tsix locus (see Fig. 3.1 A); LacZ nascent transcripts uniquely mark the $X^{\Delta Tsix}$ (Sado et al., 2001). Both unmodified Tsix and the mutated Tsix locus expressing LacZ are subject to X-inactivation and therefore are only transcribed when they reside on the active-X (Fig. 3.6 C) (Maclary et al., 2014; Sado et al., 2001). Simultaneous probing of Xist, Tsix, and LacZ RNAs by FISH in WT XX E5.25 epiblasts, which do not carry the transgene, showed Tsix but not LacZ expression as expected (Fig. 3.6 C). In $X^{\Delta Tsix}X$ and $XX^{\Delta Tsix}$ epiblasts, by contrast, a significant percentage of nuclei (30-39%) expressed LacZ but not Tsix (Fig. 3.6 C). Thus, the $X^{\Delta Tsix}$ can indeed be chosen as the active-X at the onset of random X-inactivation.

To interrogate X-chromosomal choice further, we assayed Xist expression via allele-specific RT-PCR followed by Sanger sequencing and Pyrosequencing in individual F1 hybrid E5.25 WT and Tsix-heterozygous epiblasts. Both sets of epiblasts displayed biallelic Xist expression by Sanger sequencing and negligible differences in allelic Xist expression by Pyrosequencing (Fig. 3E-F). The similarly unequal expression of the two Xist alleles in WT and Tsix-mutant epiblasts is consistent with differences in the X-controlling element (*Xce*) on the polymorphic X-chromosomes in F1 hybrid embryos (Chadwick et al., 2006; Johnston and Cattanach, 1981; Ohhata et al., 2008).

We next tested the inference that the paucity of ectopic Xist RNA coated cells in Tsix-heterozygous E6.5 epiblasts compared to E5.25 epiblasts is due to a failure of mitotic division of E5.25 epiblast cells with two inactive X-chromosomes. We found that the mitotic index, as measured by the presence of phosphorylated-histone H3, is significantly reduced in E5.25 $X^{\Delta Tsix}X$ epiblast cells exhibiting Xist RNA coating and silencing of *Pgkl* on both Xs, compared to cells with Xist RNA coating and silencing of *Pgkl* on only one X ($p = 0.003$; Fig. 3.6 D). Thus, the proliferative potential of cells with two inactive-Xs is compromised.

3-6: Tsix-heterozygous EpiSCs Undergo Ectopic X-inactivation Only Upon Differentiation

We next wished to investigate if ectopic Xist RNA induction from the $X^{\Delta Tsix}$ in heterozygous females occurs at the onset of X-inactivation or is linked to epiblast differentiation as in $X^{\Delta Tsix}Y$ males. We therefore derived multiple WT $X^{Lab}X^{JF1}$ and $X^{JF1}X^{Lab}$ and mutant $X^{\Delta Tsix}X^{JF1}$ and $X^{JF1}X^{\Delta Tsix}$ EpiSC lines from F1 hybrid embryos (see Fig. 3.2 and Table 3.1). Although Tsix was expressed from both X-chromosomes in WT EpiSCs, in Tsix-heterozygotes only the WT X^{JF1} expressed Tsix (Fig. 3.7A-B). To quantify how often each of the two parental X-chromosomes were chosen for inactivation, we Pyrosequenced Xist cDNA and cDNAs from the X-inactivated genes *Rnfl2* and *Atrx*. The WT EpiSC lines displayed nearly equal levels of Xist expression from the two X-chromosomes, consistent with random choice (Fig. 3.7C). The Tsix-heterozygous EpiSC lines did not uniformly show Xist expression exclusively from the $X^{\Delta Tsix}$, nor were *Rnfl2* and *Atrx* expressed only from the WT X^{JF1} in all the mutant cell lines (Fig. 3.7C). The cell lines instead displayed a normal distribution of which of the two Xs was inactivated, demonstrating that X-inactivation is not skewed in favor of the $X^{\Delta Tsix}$. Although the variability was higher in the mutants, the mean as well as the median expression levels of *Xist*, *Rnfl2*, and

Atrx in parent-of-origin-matched WT and *Tsix*-mutant EpiSC lines were not significantly different ($p>0.1$ in all cases).

Embryonic Stage of EpiSC Derivation		
Genotype	EpiSC Line No.	Embryonic Stage
XY	1-2	E3.5
$X^{\Delta Tsix}Y$	1-2	E3.5
	3-4	E5.5
$X^{Lab}X^{JF1}$	1-3	E3.5
	4	E5.5
$X^{JF1}X^{Lab}$	1-2	E3.5
$X^{\Delta Tsix}X^{JF1}$	1,3,10-14	E3.5
	2,4-9,15	E5.5
$X^{JF1}X^{\Delta Tsix}$	5,6	E3.5
	2-4	E4.5
	1	E3.5

Table 3.1: Embryonic stage of cell line derivation for all wild-type and *Tsix*-mutant EpiSC lines.

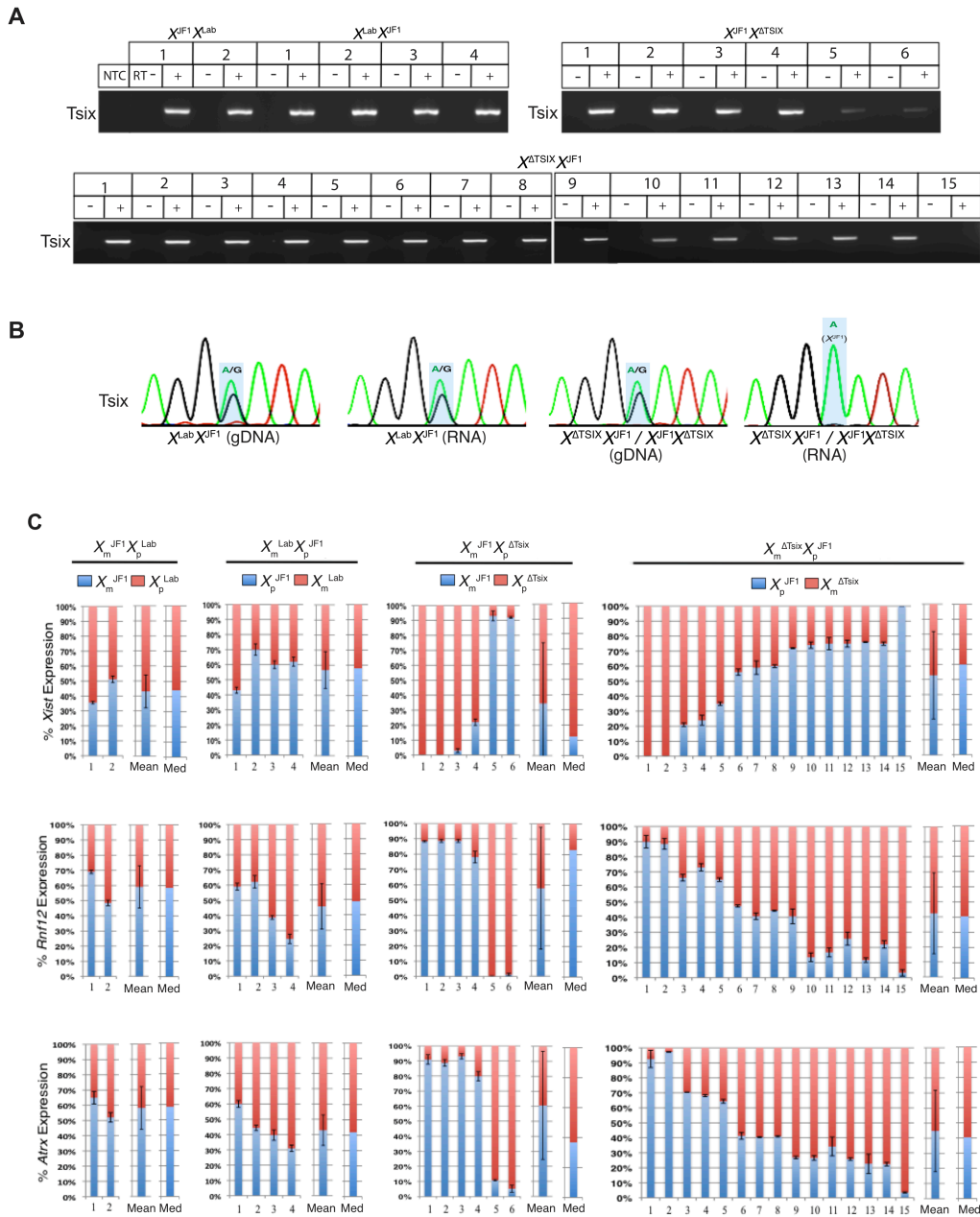


Figure 3.7: Lack of uniformly biased X-inactivation in undifferentiated Tsix-heterozygous EpiSC lines. (A) RT-PCR amplification of Tsix RNA from WT and Tsix-heterozygous EpiSC lines. M, marker; NTC, no template control; +, reaction with reverse transcriptase (RT); -, no RT control lane. (B) Representative Sanger sequencing chromatograms of Tsix cDNAs. (C) RT-PCR followed by Pyrosequencing-based quantification of allelic expression of Xist and the X-linked genes Rnf12 and Atrx. Each bar represents an individual EpiSC line. X_m , maternal X-chromosome; X_p , paternal X-chromosome. Error bars represent the standard deviation of ≥ 3 independent results. The mean and median of allelic expression of Xist, Rnf12, and Atrx lack significant difference ($p > 0.1$, Welch's two-sample T-test and Mood's Median test) between parent-of-origin matched WT and mutant EpiSCs.

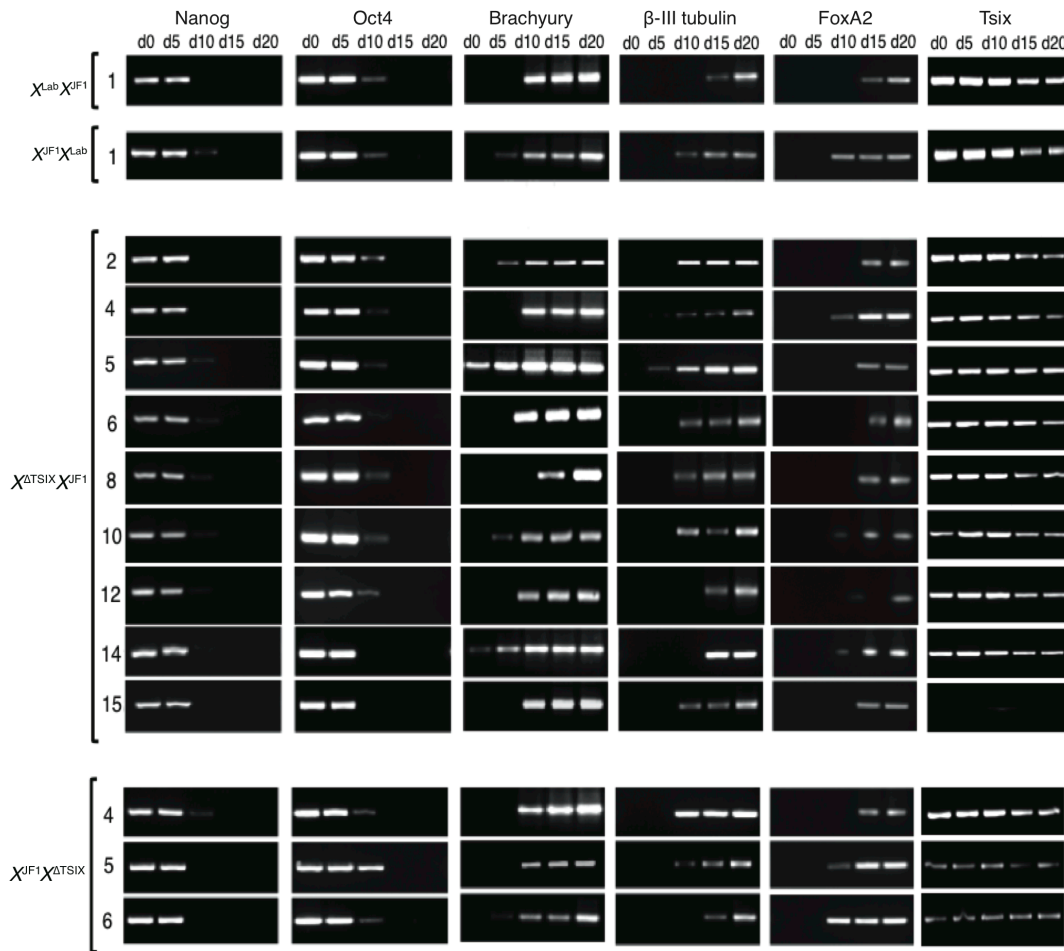


Figure 3.8: Characterization of differentiating female EpiSC lines. RT-PCR amplification of pluripotency markers Nanog and Oct4; mesodermal marker Brachyury; neuroectodermal marker β -III tubulin; hepatocyte marker FoxA2 at successive days of differentiation in WT and Tsix-heterozygous EpiSCs analyzed in Figs. 4-5. d, days. Loss of expression of Oct4 and Nanog indicates that EpiSCs had lost pluripotency and differentiated.

We next tested if the $X^{\Delta Tsix}$ induced Xist in female EpiSCs as a function of differentiation, as it does in $X^{\Delta Tsix}Y$ EpiSCs. We therefore differentiated a subset of the WT and Tsix-mutant female cell lines (Fig. 3.8). The selected $X^{\Delta Tsix}X^{JF1}$ and $X^{JF1}X^{\Delta Tsix}$ EpiSC lines encompassed different degrees of Xist mosaicism; the fraction of total Xist RNA transcribed from each of the two Xs varied between the cell lines, ranging from 0 – 100% of the total Xist expression in the undifferentiated EpiSCs (Fig. 3.9). Upon differentiation, the allelic ratio of Xist, Rnf12, and Atrx RNAs did not change in WT $X^{Lab}X^{JF1}$ and $X^{JF1}X^{Lab}$ EpiSC lines. In differentiating $X^{\Delta Tsix}X^{JF1}$ and

$X^{JF1}X^{\Delta Tsix}$ EpiSC lines, however, we found distinct alterations in allelic Xist expression (Fig. 3.9). In the eight mutant EpiSC lines most highly mosaic for Xist, where the WT X^{JF1} accounted for ~25 – 75% of total Xist RNA output ($X^{JF1}X^{\Delta Tsix}$ line 4; and, $X^{\Delta Tsix}X^{JF1}$ lines 4, 5, 6, 8, 10, 12, and 14), Xist expression became restricted to the $X^{\Delta Tsix}$ mutant X-chromosome by the end of 20 days (d20) of differentiation (Fig. 3.9). Conversely, we found that *Rnf12* and *Atrx* in these cell lines were increasingly expressed from the WT X^{JF1} over the course of differentiation (Fig. 3.10 B-C). In two mutant EpiSC lines in which >90% of Xist RNA was expressed from the WT X^{JF1} at d0 ($X^{JF1}X^{\Delta Tsix}$ lines 5 and 6), Xist expression from the mutant $X^{\Delta Tsix}$ increased only slightly by d20 of differentiation (Fig. 3.9). *Rnf12* and *Atrx* displayed a correspondingly minimal decrease in expression from the $X^{\Delta Tsix}$ in these cell lines (Fig. 3.10 B). In the mutant cell lines in which Xist was expressed almost exclusively from the WT X^{JF1} or from the $X^{\Delta Tsix}$ at d0 ($X^{\Delta Tsix}X^{JF1}$ lines 15 and 2, respectively), the allelic expression profile of *Xist*, *Rnf12*, and *Atrx* did not change upon differentiation (Figs. 3.9 and 3.10C).

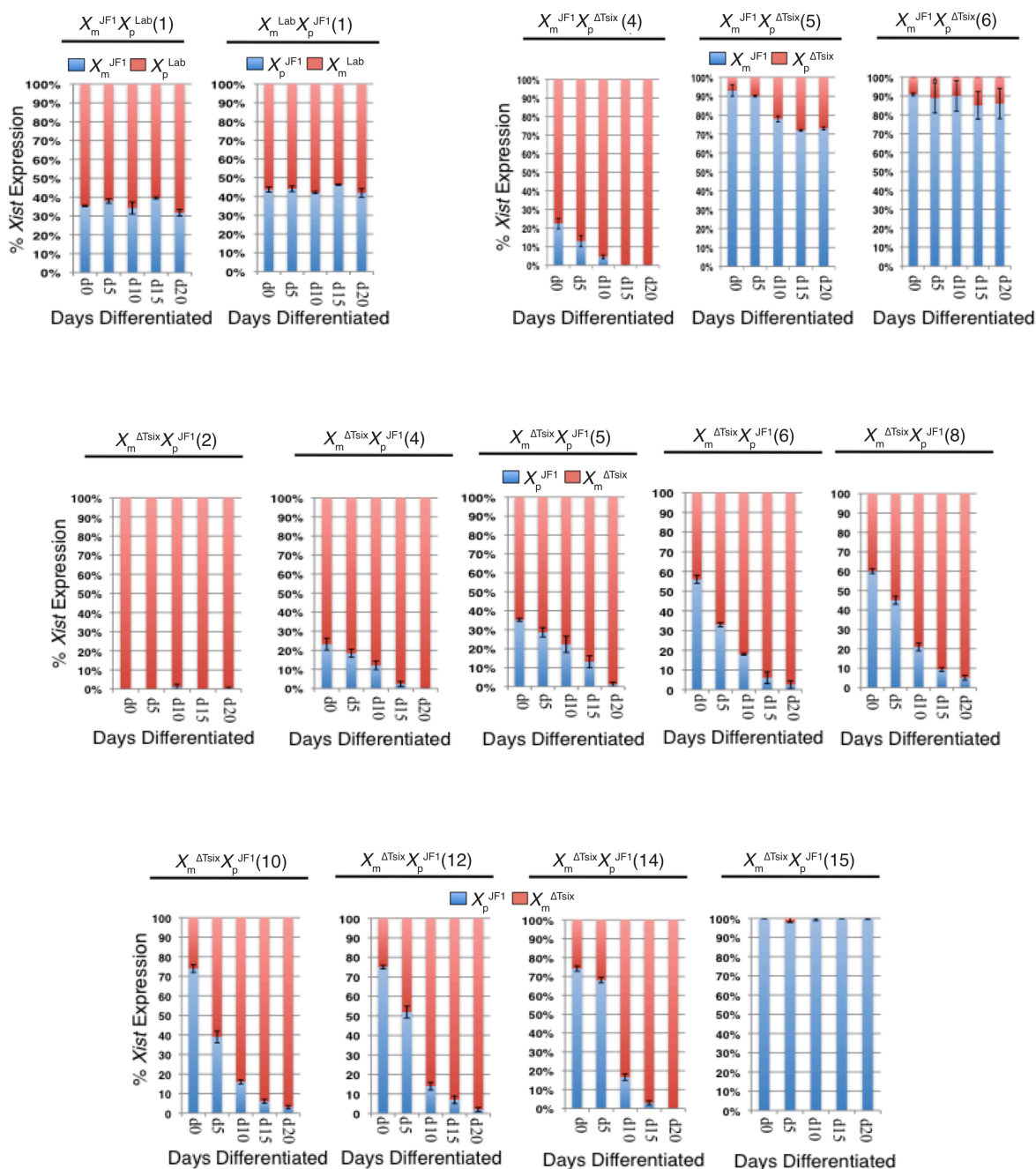


Figure 3.9: Change in allelic Xist expression in differentiating Tsix heterozygous EpiSC lines. (A) RT-PCR followed by Pyrosequencing-based quantification of Xist expression in EpiSC lines (cell line numbers in parentheses) differentiated for 0, 5, 10, 15, and 20 days (d). X_m , maternal X-chromosome; X_p , paternal X-chromosome. Each bar represents an individual EpiSC line. Error bars represent the standard deviation of ≥ 3 independent results.

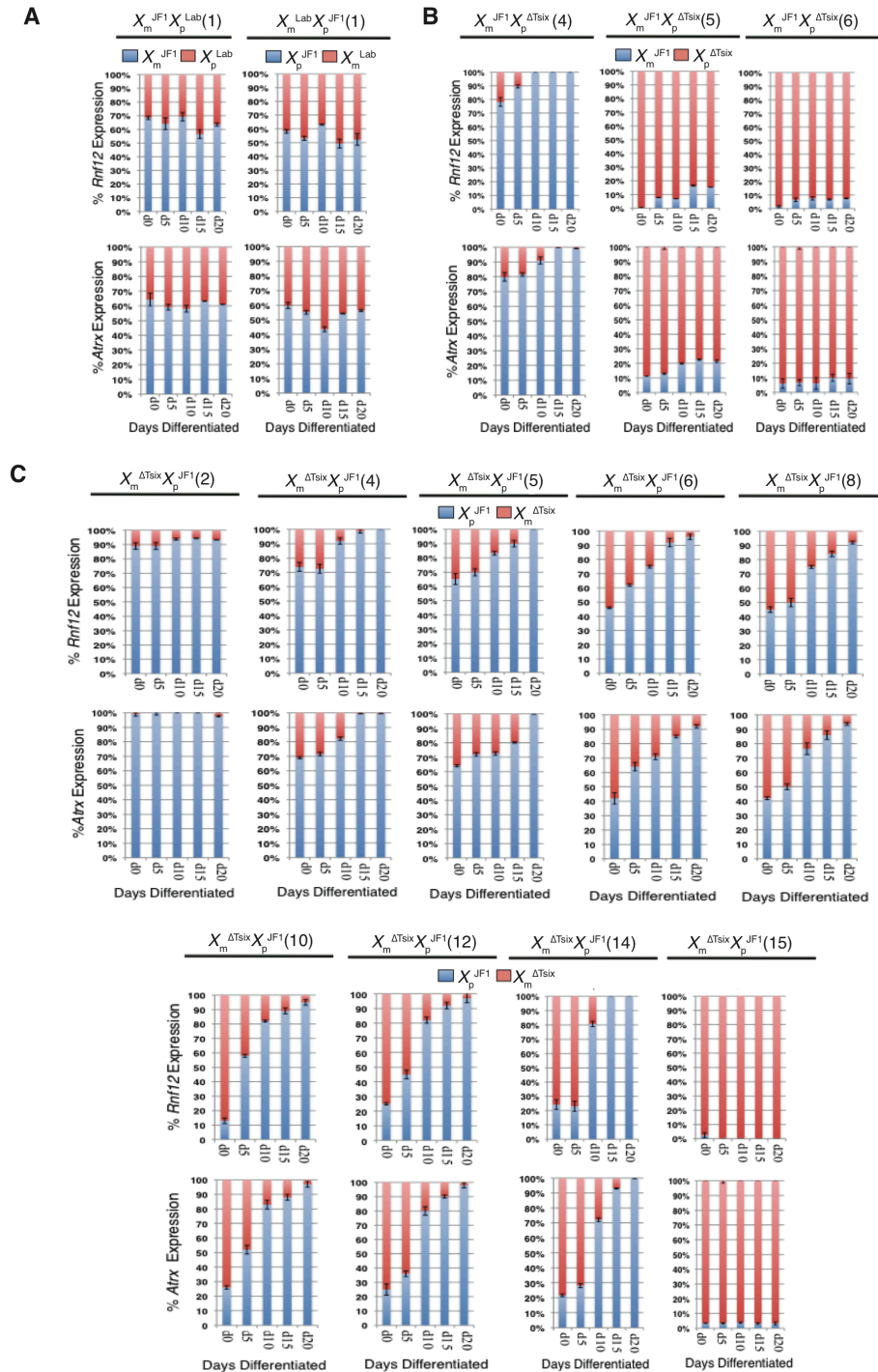


Figure 3.10: Quantification of allelic expression of Rnf12 and Atrx during differentiation of EpiSCs. RT-PCR followed by Pyrosequencing-based quantitation of allelic expression in (A) $X_m^{Lab} X_p^{JF1}$ and $X_m^{JF1} X_p^{Lab}$, (B) $X_m^{JF1} X_p^{\Delta Tsix}$, and, (C) $X_m^{\Delta Tsix} X_p^{JF1}$ female cell lines (cell line number in parentheses) from day (d) 0 to d20 of differentiation. X_m , maternal X-chromosome; X_p , paternal X-chromosome. Error bars represent the standard deviation of ≥ 3 independent Pyrosequencing results.

We observed a similar change in X-inactivation patterns by RNA FISH in the differentiating EpiSCs. As in E5.25 epiblasts, we exploited the mutually exclusive expression of Tsix and LacZ RNAs from the WT X^{Jf1} and mutant $X^{\Delta Tsix}$, respectively, to determine which of the two X-chromosomes is chosen as the active-X. We profiled three EpiSC lines that displayed distinct and varied patterns of inactivation suggested by allele-specific Xist expression ($X^{\Delta Tsix}X^{Jf1}$ lines 2, 6, and 15; see Fig. 3.7C). Consistent with the inactivation pattern inferred by allele-specific Xist RT-PCR, $X^{\Delta Tsix}X^{Jf1}$ EpiSC line 2 lacked LacZ RNA FISH signal in all cells examined throughout differentiation (Fig. 3.11 A). $X^{\Delta Tsix}X^{Jf1}$ EpiSC line 6 displayed nearly equal numbers of cells expressing LacZ and Tsix at d0, but during the course of differentiation this pattern gradually shifted to yield only cells with a Tsix RNA FISH signal by d20 (Fig. 3.11 A). By contrast, although EpiSC $X^{\Delta Tsix}X^{Jf1}$ line 15 only exhibited cells with a LacZ signal at d0, consistent with the entire population being eligible to undergo ectopic inactivation, this pattern did not change appreciably even by d20 of differentiation (Fig. 3.11 A).

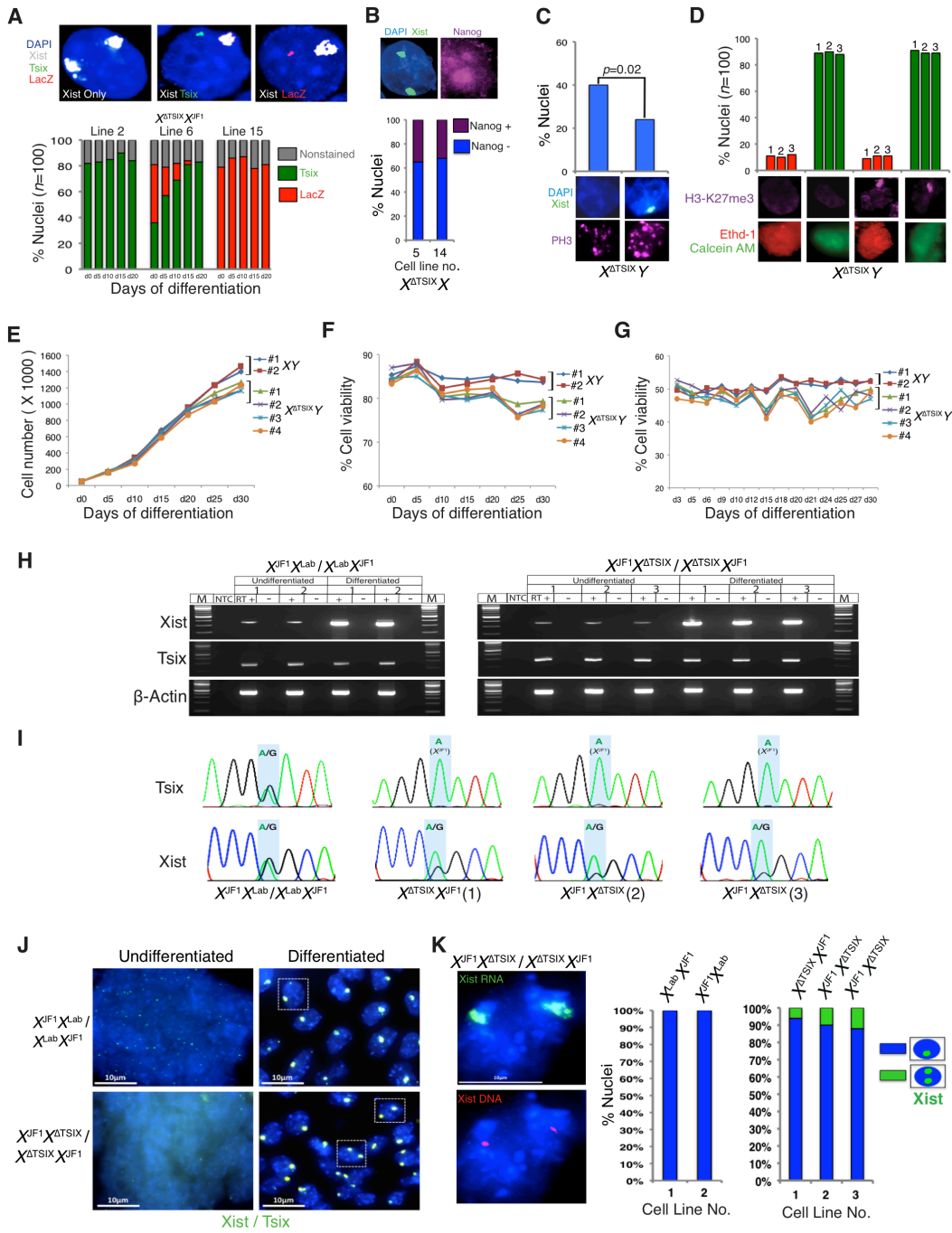


Figure 3.11: Characterization of allelic Xist expression in female EpiSCs, cell proliferation and cell viability in male EpiSCs, and analysis of Tsix-heterozygous ESCs. (A) RNA FISH detection of $X^{ΔTsix}$ as the active X-chromosome. Nuclei with two Xist RNA coats do not express LacZ or Tsix (top panel); both are subject to X-inactivation. Nuclei with an Xist RNA-coated inactive X-chromosome express either Tsix (green) from the WT X or LacZ (red) from the $X^{ΔTsix}$. $n=100$ nuclei from each of three Tsix-heterozygous EpiSC lines. The pattern of X-inactivation is subject to change during differentiation, depending on the number of cells eligible to ectopically inactivate the $X^{ΔTsix}$, ultimately only yielding cells with the LacZ-expressing $X^{ΔTsix}$ as the inactive-X. (B) Xist RNA coating in NANOG+ and NANOG- d5 differentiating $X^{ΔTsix}X^{JF1}$ EpiSCs (lines 1 and 2). (C) Phospho-H3 staining, a marker of cell proliferation, of a representative d10 differentiated $X^{ΔTsix}Y$ cell line (line 1). (D) Staining of live and dead d10 differentiated $X^{ΔTsix}Y$ EpiSCs. H3-K27me3 accumulation (purple) marks Xist RNA coated X-

chromosomes (see Fig. 2D). Ethd-1 (red) marks dead cells and Calcein AM (green) marks live cells. Data from 3 different mutant EpiSC lines are plotted (lines 1-3). (E) Cell counts during differentiation of XY and $X^{\Delta Tsix}Y$ EpiSCs. (F-G) Viability of adherent cells (F) and non-adherent cells in suspension (G) in differentiating XY and $X^{\Delta Tsix}Y$ EpiSCs. (H) RT-PCR amplification of Xist and Tsix RNAs in WT and Tsix-heterozygous undifferentiated and embryoid body-differentiated female ESC lines (2 and 3 cell lines, respectively). β -actin serves as control. M, marker; +, reaction with reverse transcriptase (RT); -, no RT control lane. (I) Sanger sequencing chromatograms of Tsix and Xist cDNAs amplified from differentiated cells in (H). Blue highlights mark a SNP that differs between the $X^{Lab} / X^{\Delta Tsix}$ and X^{Jf1} mouse strains. (J) RNA FISH detection of Xist and Tsix RNAs in representative undifferentiated and embryoid body-differentiated WT and Tsix-heterozygous female ESC lines. Scale bars, 10 μ m. (K) Quantification of Xist RNA coated nuclei in embryoid body-differentiated ESC lines. Only cells with two Xist loci detected by DNA FISH (left) following RNA FISH were counted; $n=100$ nuclei/cell line.

3-7: Reduced Proliferation and Induced Cell Death Upon Ectopic X-inactivation in Tsix-heterozygous EpiSCs

The changes in X-inactivation patterns in differentiating $X^{\Delta Tsix}$ mutant EpiSCs could arise from one of two possibilities. In the first, Xist expression switches from the WT X^{Jf1} in favor of the mutant $X^{\Delta Tsix}$ in individual cells. Alternatively, the ectopic induction of Xist from the $X^{\Delta Tsix}$ results in two inactive-Xs in differentiating EpiSCs that had originally activated Xist from the WT X^{Jf1} . In this latter scenario, the deficiency in X-linked gene expression due to both Xs being inactivated would drive selection against these cells. The remaining population of cells would then be descendants of cells that had initially chosen to inactivate the $X^{\Delta Tsix}$, which do not undergo ectopic Xist induction from the WT X^{Jf1} .

To further distinguish amongst the two possibilities, we performed single-cell analysis of differentiating EpiSCs. We found that whereas XX EpiSCs displayed Xist RNA coating of only a single X-chromosome in undifferentiated and in d5 and d10 differentiated cells, $X^{\Delta Tsix}X$ and $XX^{\Delta Tsix}$ EpiSC lines exhibited Xist RNA coating of a single X in undifferentiated cells but of both Xs upon differentiation (Fig. 3.12A-C). A substantial percentage of the double Xist RNA-coated cells early in differentiation (d5) were also NANOG+ (32-35%; Fig. 3.11 B), consistent with the data from embryos. Nearly all the nuclei with double Xist RNA coats also displayed enrichment

of H3-K27me3 and silencing of *Pgk1* on both Xs (both >90%; Fig. 3.12D-E). To examine if the cells with two inactive Xs are selected against, we compared the mitotic indices of cells with one inactive- vs. two inactive-Xs by staining for phosphorylated-histone H3. Differentiating EpiSCs with two Xist RNA coats appeared to divide significantly less often than with one Xist coat ($p<0.001$; Fig. 3.12F). We also evaluated cell death in differentiating EpiSCs, and found that cells with two Xist RNA coats were significantly more likely to be dead or dying compared to cells with one Xist coat ($p<0.001$; Fig. 3.12G).

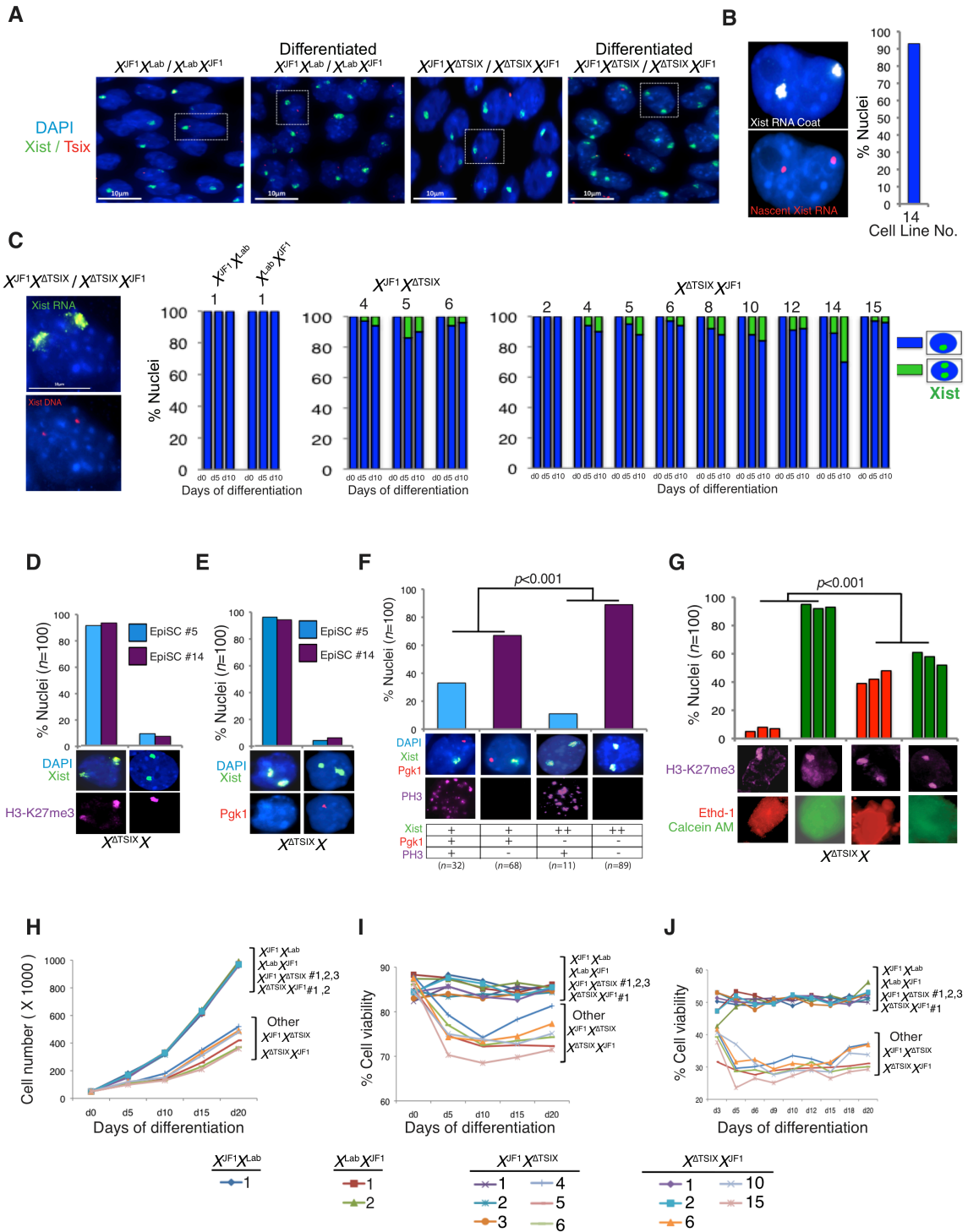


Figure 3.12: Ectopic Xist RNA coating in differentiated Tsix-heterozygous EpiSC lines. (A) RNA FISH detection of Xist RNA (green) and Tsix RNA (red) in representative undifferentiated and d10 differentiated WT and Tsix-heterozygous EpiSC lines ($X^{IF1}X^{Lab}$ cell line no. 1; $X^{\Delta TSIX}X^{IF1}$ cell line no. 14). Nuclei are stained blue with DAPI. Scale bars, 10 μ m. (B) RNA FISH detection of Xist RNA coat using an exonic probe (white) and nascent Xist RNA with an intronic probe (red), demonstrating that in cells with two Xist RNA coats both Xist alleles are

transcribed. (C) Quantification of EpiSC nuclei displaying single vs. double Xist RNA coats during differentiation. Scale bar, 10 μm . Only cells with two Xist loci detected by DNA FISH (left) following RNA FISH were counted; $n=100$ nuclei/cell line. (D) Enrichment of H3-K27me3 on Xist RNA coated X-chromosomes in d10 differentiated $X^{\Delta Tsix}X^{JF1}$ EpiSCs. Data from two different lines (nos. 5 and 14) are shown. (E) Silencing of *Pgkl* (red) upon ectopic Xist RNA coating (green) in d10 differentiated $X^{\Delta Tsix}X^{JF1}$ EpiSCs. (F) Reduced phospho-H3 staining, a marker of cell proliferation, in d10 differentiated $X^{\Delta Tsix}X^{JF1}$ EpiSCs (cell line 14) with two Xist RNA coats compared to nuclei with a single Xist coat ($p<0.001$, Fisher's exact test). (G) Increased death of cells with two inactive-Xs compared to cells with one inactive-X in d10 differentiated $X^{\Delta Tsix}X^{JF1}$ EpiSCs ($p<0.001$, Welch's two-sample T-test). The inactive-X is marked by H3-K27me3 accumulation (purple). Ethd-1 (red) marks dead cells and Calcein AM (green) marks live cells. (H) Reduced cell counts during differentiation of Tsix-heterozygous compared to WT EpiSCs. (I-J) Reduced viability of adherent (I) and non-adherent cells in suspension (J) during differentiation of Tsix-heterozygous compared to WT EpiSCs.

The reduced proliferation of cells with two inactive-Xs would predict decreased cell numbers during differentiation of some but not other Tsix-heterozygous EpiSCs. Tsix-mutant EpiSC lines with few cells eligible to undergo ectopic inactivation are expected to display comparable cell counts to WT EpiSCs. Consistent with this scenario, $X^{JF1}X^{\Delta Tsix}$ EpiSC lines 1-3 and $X^{\Delta Tsix}X^{JF1}$ EpiSC lines 1-2, which exhibit exclusive or almost exclusive inactivation of the $X^{\Delta Tsix}$ and therefore lack cells that can undergo ectopic inactivation (Fig. 3.7C), have the highest cell counts throughout differentiation and are indistinguishable from WT EpiSCs (Fig. 3.12H and Table 3.2). Conversely, EpiSC lines that have completely or almost completely inactivated the WT X^{JF1} X-chromosome, $X^{JF1}X^{\Delta Tsix}$ lines 5 and 6 and $X^{\Delta Tsix}X^{JF1}$ line 15 (see Fig. 3.7C), and thus harbor the highest percentage of cells that are able to undergo ectopic inactivation, have the lowest cell counts by d20 of differentiation (Fig. 3.12H and Table 3.2). Cell counts in $X^{JF1}X^{\Delta Tsix}$ line 4 and $X^{\Delta Tsix}X^{JF1}$ lines 6 and 10 with intermediate percentages of cells subject to ectopic inactivation (~20-75%) again correlate with the available pool of cells eligible to ectopically inactivate the $X^{\Delta Tsix}$ (Figs. 3.7C and 3.12H; Table 3.2). Thus, EpiSC lines with a higher percentage of cells that can ectopically induce Xist from the $X^{\Delta Tsix}$ and thereby inactivate the second X display lower cell counts during differentiation ($r = -0.94$).

We also quantified cell viability in populations of differentiating EpiSCs. Consistent with the higher rate of death of cells with two inactive-Xs (Fig. 3.12G), cell viability measurements

showed that the higher the percentage of EpiSCs subject to ectopic X-inactivation the lower their viability during differentiation (Fig. 3.12I-J and Table 3.2; $r = -0.95$ for adherent viable cells and -0.99 for viable cells in suspension). The phospho-histone H3 staining and cell death results together with the cell count and viability data lead to the conclusion that ectopic Xist induction from the $X^{\Delta Tsix}$ and the resultant inactivation of both Xs potently selects against cells via both reduced cell proliferation and induced cell death. Ultimately, the outcome is skewed X-inactivation in favor of cells that had chosen to initially inactivate the $X^{\Delta Tsix}$.

Comparisons of Cell Numbers and Viability Between Individual Wild-type and Tsix-heterozygous EpiSCs (Day 20 of Differentiation)

Cell Line	Xist Allelic Expression Ratio ($X^{JF1} : X^{\Delta Tsix}$)	Adherent Total Cell Count (x1000)		Adherent Viability		Suspension Viability	
		Average Count	P Value (T Test vs. $X^{Lab}X^{JF1}$ #1)	Average Percent	P Value (T Test vs. $X^{Lab}X^{JF1}$ #1)	Average Percent	P Value (T Test vs. $X^{Lab}X^{JF1}$ #1)
$X^{Lab}X^{JF1}$ #1	no $X^{\Delta Tsix}$	970	NA	86	NA	53	NA
$X^{Lab}X^{JF1}$ #2	no $X^{\Delta Tsix}$	973	0.7676	86	0.7521	51	0.1214
$X^{JF1}X^{Lab}$ #1	no $X^{\Delta Tsix}$	980	0.4353	85	0.3819	56	0.0115
$X^{\Delta Tsix}X^{JF1}$ #1	0 : 100	960	0.2879	85	0.5012	52	0.6695
$X^{\Delta Tsix}X^{JF1}$ #2	0 : 100	970	1	86	0.5763	53	0.7135
$X^{JF1}X^{\Delta Tsix}$ #1	0 : 100	973	0.6433	88	0.6503	50	0.0230
$X^{JF1}X^{\Delta Tsix}$ #2	0 : 100	967	0.6433	84	0.1037	51	0.0997
$X^{JF1}X^{\Delta Tsix}$ #3	3 : 97	977	0.5614	85	0.2182	53	0.8278
$X^{JF1}X^{\Delta Tsix}$ #4	22 : 78	530	2.83×10^{-6}	81	0.0043	37	4.48×10^{-5}
$X^{\Delta Tsix}X^{JF1}$ #6	56 : 44	490	5.01×10^{-7}	77	0.0006	37	0.0003
$X^{\Delta Tsix}X^{JF1}$ #10	75 : 26	480	1.84×10^{-6}	76	0.0011	34	0.0003
$X^{JF1}X^{\Delta Tsix}$ #5	93 : 7	420	2.90×10^{-7}	72	7.85×10^{-5}	31	1.10×10^{-5}
$X^{JF1}X^{\Delta Tsix}$ #6	92 : 8	370	2.05×10^{-7}	74	0.0003	30	1.21×10^{-5}
$X^{\Delta Tsix}X^{JF1}$ #15	100 : 0	363	1.39×10^{-6}	72	9.33×10^{-5}	29	5.10×10^{-6}

Table 3.2: Comparisons of cell numbers and viability between individual wild-type (WT) and Tsix-heterozygous female EpiSCs at day 20 of differentiation. NA, not applicable. The percentage of Xist expression from the WT X (X^{JF1}) is strongly negatively correlated with total cell count ($r = -0.94$), adherent cell viability ($r = -0.99$), and suspension cell viability ($r = -0.95$).

We also tested if ectopic Xist induction selects against $X^{\Delta Tsix}Y$ cells. Phospho-histone H3 staining suggested slightly if not significantly reduced proliferation of cells with an Xist RNA coated X-chromosome compared to those without ($p=0.02$; Fig. 3.11 C). The ratio of live:dead cells, however was indistinguishable between cells with Xist RNA coating and those without (Fig. 3.11 D). The cell numbers and viability through 30d of differentiation were reduced in the mutants, but mostly at d25 and d30 time points (Fig. 3.11 E-G), which contrasts with the striking reduction in both measurements by d20 of differentiation in Tsix-heterozygous female EpiSCs. This difference potentially reflects a reduced level of ectopic Xist induction and X-linked gene silencing in mutant males compared to females (see Discussion).

3-8: Ectopic Xist Induction in Differentiating Tsix-heterozygous Female ESCs

As with $X^{\Delta Tsix}Y$ EpiSCs, we sought to test if our observations of Tsix-heterozygous EpiSCs also apply to mutant ESCs. Although both WT $X^{Lab}X^{Jf1} / X^{Jf1}X^{Lab}$ and mutant $X^{\Delta Tsix}X^{Jf1} / X^{Jf1}X^{\Delta Tsix}$ undifferentiated ESCs displayed a low level of Xist RNA expression by RT-PCR, all four genotypes induced Xist from either allele upon differentiation (Fig. 3.11 H-I). In agreement with the RT-PCR results, both WT and mutant ESCs displayed Xist RNA coating only upon differentiation (Fig. 3.11 J). A subset of the differentiating mutant (but not WT) cells, though, exhibited Xist RNA coating of both Xs (Fig. 3.11 J-K).

We next differentiated the ESCs into EpiLCs to determine when during differentiation Tsix-heterozygous ESCs ectopically induced Xist (Fig. 3.13 A-C). The two Xs in WT EpiLCs were nearly equally likely to be chosen as the inactive-X, as evidenced by the allelic expression profiles of Xist (Fig. 3.13 D). Although the mutant EpiLC samples displayed a wide distribution of allelic Xist expression, the average expression ratios of the two Xist alleles matched closely

that of the WT EpiLCs (Fig. 3.13 D), recapitulating the pattern observed in EpiSCs (Fig. 3.7 C). RNA FISH demonstrated that a vast majority of the Tsix-heterozygous EpiLCs harbored only one Xist RNA coated X-chromosome (96%; Fig. 3.13 E-F). Upon further differentiation, the mutant cells displayed increasingly biased inactivation of the $X^{\Delta Tsix}$, consistent with selection favoring cells that had originally inactivated the $X^{\Delta Tsix}$ (Fig. 3.13 G).

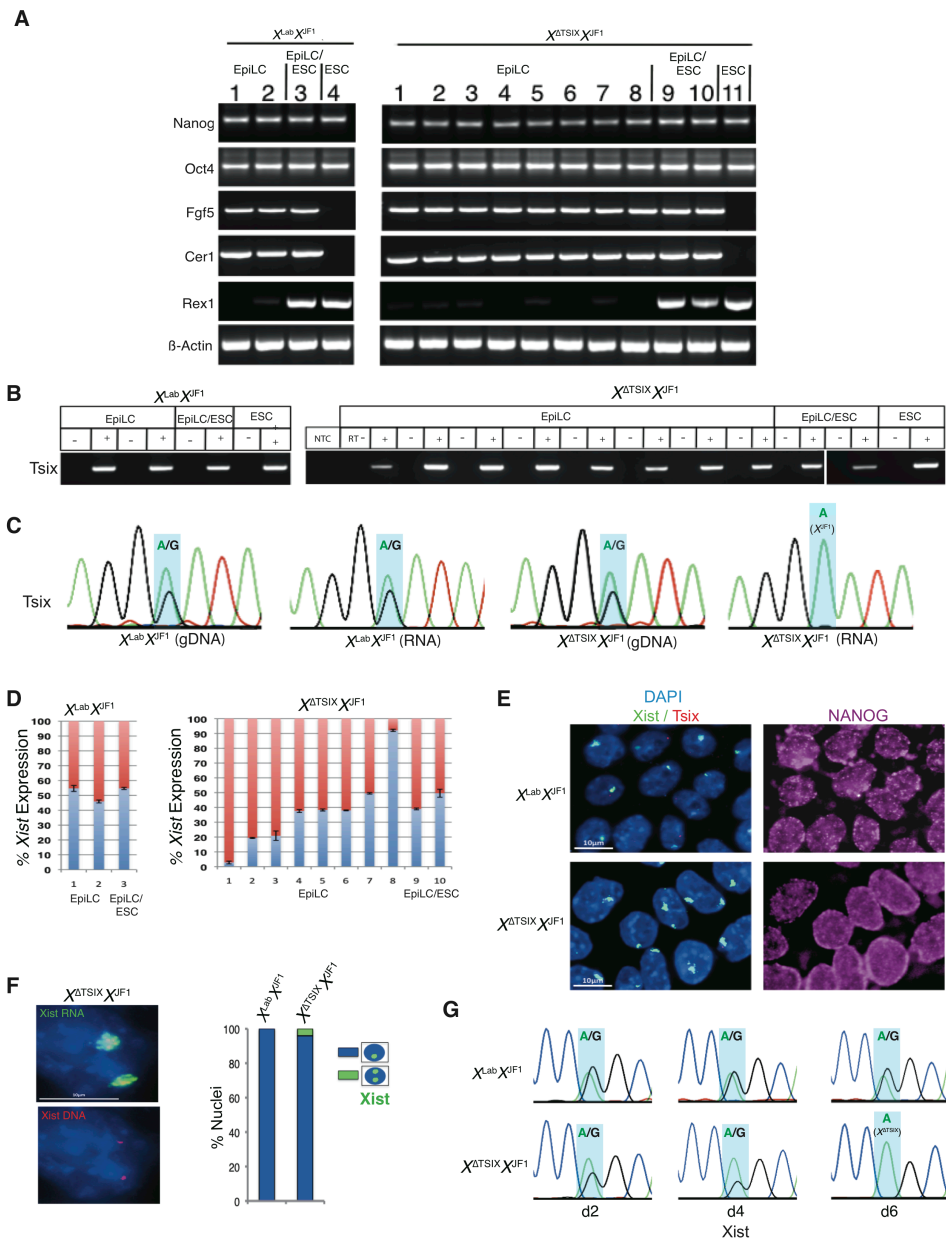


Figure 3.13: Characterization of female ESC-derived EpiLCs. (A) Marker analysis by RT-PCR of female EpiLCs. *Fgf5* and *Cer1* are expressed only in EpiLCs whereas high *Rex1* expression marks ESCs. ‘EpiLC’ samples are individual fields in tissue culture wells containing largely if not exclusively cells morphologically resembling EpiLCs. ‘EpiLC/ESC’ samples are of entire tissue culture wells in which ESCs were being converted to EpiLCs. These samples display faint *Rex1* expression, indicative of residual undifferentiated ESCs in the wells. ‘ESC’ samples are cells from unconverted ESC wells. (B) RT-PCR detection of *Tsix* expression (exon 4). (C) Representative Sanger sequencing chromatograms demonstrating exclusive expression of *Tsix* from the WT X^{IF1} in *Tsix*-mutant ESCs. Blue highlights mark a SNP that differs between the $X^{Lab} / X^{\Delta six}$ and X^{IF1} mouse strains. (D) Pyrosequencing of *Xist* cDNAs quantifies *Xist* expression in the EpiLCs. Error bars represent the standard deviation of 3 independent Pyrosequencing results. The average expression of the two *Xist* alleles is not significantly different between the two genotypes ($p = 0.13$, Welch’s Two-sample T Test). (E) Strand-specific RNA FISH detection of *Xist* (green) and *Tsix* (red) combined with IF detection of *NANOG* in EpiLCs. A few cells display two *Xist* RNA coats, presumably reflecting ectopic *Xist* induction from the $X^{\Delta six}$ due to further differentiation of EpiLCs. Scale bars, 10 μm . (F) Quantification of *Xist* RNA coated nuclei in $X^{Lab} X^{IF1}$ and

$X^{\Delta Tsix}X^{JFI}$ EpiLC lines. Scale bars, 10 μm . Only cells with two Xist loci detected by DNA FISH (left) following RNA FISH were counted; $n=100$ nuclei/cell line. (G) Representative Sanger sequencing chromatograms of Xist cDNAs amplified from differentiating ESCs (2d = EpiLC stage, 4d and 6d, further differentiation after the EpiLC stage). Blue highlights mark a SNP that differs between the $X^{Lab} / X^{\Delta Tsix}$ and X^{JFI} mouse strains. By d6, Xist expression is detected only from the $X^{\Delta Tsix}$ in $X^{\Delta Tsix}X^{JFI}$ cells.

3-9: Concluding Remarks

Tsix repression of Xist at the onset of X-inactivation has been invoked previously to support a role for the Tsix locus in X-chromosome counting and/or choice (Clerc and Avner, 1998; Cohen et al., 2007; Debrand et al., 1999; Lee, 2000; Lee and Lu, 1999; Lee, 2005; Morey et al., 2004; Navarro et al., 2010; Sado et al., 2001; Vigneau et al., 2006). In the counting step, the cell senses the number of X-chromosomes; only if there are two or more Xs do the cells proceed to the choice and inactivation steps (Grumbach et al., 1963; LYON, 1962). In the choice step, one of the two X-chromosomes is selected for silencing; only then does X-inactivation ensue (Rastan, 1983; Takagi, 1980). In this model of random X-inactivation, counting must precede choice, with the last step being inactivation itself. Thus, XY male epiblast cells do not undergo X-inactivation because the cells ‘count’ only one X-chromosome, which would preclude both the choice and inactivation steps.

Our data, however, rule out a function for Tsix in X-chromosome counting, in agreement with Monkhorst *et al.*, (Monkhorst et al., 2008). In a diploid male or female cell, the counting process protects one X-chromosome from inactivation; a defect in counting is therefore expected to result in inactivation of the single X-chromosome in males at some frequency (Avner and Heard, 2001). The absolute absence of Xist RNA coating and X-inactivation in undifferentiated $X^{\Delta Tsix}Y$ EpiSCs is evidence that the Tsix RNA is not part of the counting mechanism. Xist is only induced when $X^{\Delta Tsix}Y$ EpiSCs differentiate. That not all differentiating $X^{\Delta Tsix}Y$ cells express Xist may reflect intercellular variability in the levels of an Xist activating factor (see below).

Our findings also exclude a primary role for Tsix in the choice of which X undergoes inactivation. Biased X-inactivation in Tsix-heterozygous cells occurs through a secondary cell selection effect, rather than through primary inactivation of the $X^{\Delta Tsix}$ at the onset of X-inactivation (Fig. 3.14). Tsix therefore constitutes a failsafe mechanism that prevents ectopic Xist induction and inactivation of the active X-chromosome, but only *after* X-inactivation has initiated normally (Fig. 3.14). Thus, Tsix is required not to establish but to maintain the randomized pattern of X-inactivation. This protective function of Tsix in the epiblast lineage appears to be conserved in extra-embryonic cell types. Stem cells of the trophectoderm lineage, which undergoes imprinted X-inactivation of the paternal X-chromosome, similarly ectopically silence the $X^{\Delta Tsix}$ only upon differentiation both *in vivo* and *in vitro* (Maclary et al., 2014).

Tsix is expressed in pluripotent cells, but it is only required to silence Xist as these cells differentiate. Tsix expression in epiblast precursor cells in E4.5 embryos as well as in EpiSCs and EpiLCs may prime the epiblast cells to forestall inactivation of the active X-chromosome upon impending differentiation. In support of this idea, Tsix is robustly expressed in ESCs yet its loss does not lead to ectopic Xist induction in pluripotent cells of either sex, as shown here and in earlier studies (Cohen et al., 2007; Debrand et al., 1999; Lee and Lu, 1999; Luikenhuis et al., 2001; Minkovsky et al., 2013; Morey et al., 2004; Ohhata et al., 2006).

If Tsix does not regulate X-chromosome counting or choice, then alternate mechanisms must explain why X-inactivation does not occur in males and does so randomly in females. We favor a parsimonious model of random inactivation whereby a dose-dependent X-linked activity triggers inactivation only in females. For example, the increased dosage of an X-linked factor in XX compared to XY cells at the onset of inactivation when both Xs are active may facilitate X-inactivation by stochastically and directly activating Xist on one of the two X-chromosomes in

females, as has been proposed (but debated) for RNF12 (Barakat et al., 2011; Gontan et al., 2012; Jonkers et al., 2009; Shin et al., 2014). The lower level of such a factor may explain why Xist is ectopically induced from the mutant X in only some $X^{\Delta Tsix}Y$ embryonic cells, but in all $X^{\Delta Tsix}X$ embryonic cells. Xist may also be expressed to a lesser extent in individual $X^{\Delta Tsix}Y$ cells compared to female cells, resulting in a comparatively reduced degree of X-linked gene silencing in males and potentially explaining why differentiating Tsix-mutant female but not male EpiSCs are subject to cell selection. Future work will clarify the underlying reasons for this difference.

Our work lends caution to the modeling of X-inactivation kinetics in differentiating ESCs. Depending on the ESC differentiation regimen, aberrantly inactivated cells may be rapidly outcompeted by appropriately inactivated ones, thus masking a defect in the initiation phase of X-inactivation. Conversely, errors in X-inactivation that manifest only during the maintenance phase are difficult to distinguish from those that occur at the onset due to the asynchronous differentiation of ESCs. Such a scenario may resolve the seemingly discordant observations of the Tsix-mutant X-chromosome appearing to be both susceptible and resistant to Xist induction in differentiating ESCs. Directed differentiation of ESCs into EpiLCs may be one route to capturing cells just after X-inactivation has initiated. Conversion of ESCs into EpiLCs, however, is also subject to key shortcomings. Not all ESCs differentiate into EpiLCs, thus resulting in a heterogeneous population of cells; and, when they do, the EpiLCs are only transiently present (Buecker et al., 2014; Hayashi et al., 2011).

Our data instead highlight the utility of EpiSCs as a model system to uncouple the onset of random X-inactivation from differentiation of pluripotent cells. A comparison of X-inactivation defects in Tsix-mutant EpiSCs with embryonic epiblasts suggests that EpiSCs can capture a window in differentiation of naïve pluripotent epiblast cells immediately after X-

inactivation has initiated. Whereas *Tsix*-heterozygous embryonic epiblasts display ectopic *Xist* induction beginning at ~E5.25 stage of embryogenesis, sex and genotype-matched EpiSCs do not. Upon differentiation, however, these EpiSCs exhibit *Xist* RNA coating of both Xs, mimicking the pattern of ectopic *Xist* induction in the mutant epiblasts as the embryos develop from E5.25, just after random X-inactivation has commenced, to E6.5, a stage by which ectopic *Xist* induction is almost undetectable. By E6.5, *Tsix* heterozygote epiblasts are comprised almost exclusively of cells in which the $X^{\Delta Tsix}$ is the inactive-X, due to rapid selection against cells that had originally chosen the WT X for silencing but subsequently ectopically induced *Xist* and underwent inactivation of the $X^{\Delta Tsix}$. Thus, the pattern of inactivation changes rapidly within ~1 day of development, at a stage of embryogenesis that is not easily accessible. By mirroring early epiblast cells just after they have undergone X-inactivation, EpiSCs are a valuable resource to tease apart defects in the initiation of X-inactivation from differentiation of the pluripotential epiblast cells.

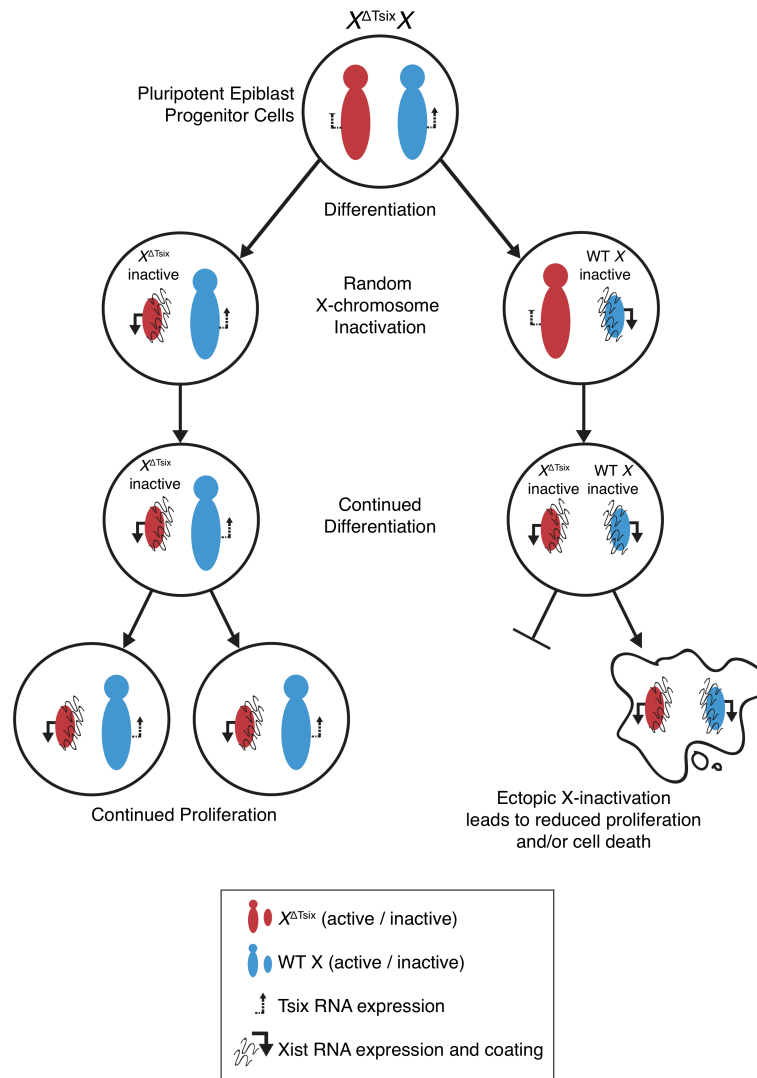


Figure 3.14: A model of *Tsix* function in X-inactivation. At the onset of X-inactivation, *Tsix* heterozygous epiblast cells undergo stochastic X-inactivation indistinguishable from WT epiblasts. Upon continued differentiation of the epiblast cells, the $X^{\Delta Tsix}$ ectopically induces Xist RNA. In female cells that had originally inactivated the WT X-chromosome, ectopic Xist induction accompanies the initiation of X-inactivation a second time (of the $X^{\Delta Tsix}$), resulting in two inactive-Xs. As a result of a paucity of X-linked gene expression, these cells are selected away due both to reduced proliferation and induced cell death. Thus, the developing embryo is ultimately populated only with cells that had originally inactivated the $X^{\Delta Tsix}$.

3-10: Materials and Methods

Ethics Statement.

This study was performed in strict accordance with the recommendations in the Guide for the Care and Use of Laboratory Animals of the National Institutes of Health. All animals were handled according to protocols approved by the University Committee on Use and Care of Animals (UCUCA) at the University of Michigan (protocol #PRO00004007).

Mice.

The generation of mice harboring the *Tsix*^{AA2Δ1.7} mutation has been described previously (Kalantry and Magnuson, 2006; Maclary et al., 2014; Sado et al., 2001). The *M. molossinus* JF1 strain was sourced from Jackson Laboratories (JF1/ms), and has been described previously (Maclary et al., 2014; Takada et al., 2013).

Embryo Dissections and Processing.

Pre-, peri-, and post-implantation stage embryos were isolated essentially as described (Maclary et al., 2014). Dissections were carried out in 1X PBS (Invitrogen, #14200075) containing 6% bovine serum albumin (BSA; Invitrogen, #15260037). Individual implantation sites were cut from the uterine limbs, and decidua were removed with forceps. Embryos were dissected from the decidua, and the Reichert's membranes surrounding post-implantation embryos were removed using fine forceps. For separation of extra-embryonic and epiblast portions of embryos, fine forceps were used to physically bisect the embryos at the junction of the extra-embryonic ectoderm and epiblast. Epiblast fragments were plated on gelatinized

coverslips for immunofluorescence and/or RNA FISH or collected for mRNA extraction. Extra-embryonic portions of the embryo were lysed to extract DNA to confirm sex and genotype.

Derivation, Culture, Differentiation, and Characterization of Epiblast Stem Cell (EpiSC)

Lines.

EpiSCs were derived from pre-, peri-, and post-implantation stages essentially as described (Brons et al., 2007; Najm et al., 2011; Tesar et al., 2007). EpiSCs derived from different stages of embryogenesis (See Table 3-1) did not display any noticeable differences in Xist induction and X-inactivation patterns. For derivation of EpiSCs from pre- and peri-implantation mouse embryos, individual embryos were plated on quiescent mouse embryonic fibroblast (MEF) feeder cells in K15F5 medium containing Knockout DMEM (GIBCO, #10829-018) supplemented with 15% Knockout Serum Replacement (KSR; GIBCO, #A1099201), 5% ESC-qualified fetal bovine serum (FBS; GIBCO, #104390924), 2 mM L-glutamine (GIBCO, #25030), 1X nonessential amino acids (GIBCO, #11140-050), and 0.1 mM 2-mercaptoethanol (Sigma, #M7522). After 5–6 days, blastocyst outgrowths were dissociated partially with 0.05% trypsin (Invitrogen, #25300-054). The partial dissociates were plated individually into a 1.9 cm² well containing MEF feeder layer and cultured for an additional 4–6 days in K15F5 medium. The culture was then passaged by a brief exposure (2–3 min) to 0.05% trypsin/EDTA with gentle pipetting to prevent complete single-cell dissociation of pluripotent clusters, and plated into a 9.6 cm² well containing MEF feeders in K15F5 medium. Morphologically distinct mouse EpiSC colonies became evident over the next 4–8 days and were subcloned from a mixed population of cells, including ESCs. EpiSC colonies were manually dissociated into small clusters using a glass needle and plated into 1.9 cm² wells containing MEF feeders in EpiSC cell medium consisting of Knockout DMEM supplemented with 20% KSR, 2 mM Glutamax (GIBCO,

#35050061), 1X nonessential amino acids, 0.1 mM 2-mercaptoethanol, and 10 ng/ml FGF2 (R&D Systems, #233-FB).

For derivation of EpiSCs from postimplantation mouse embryos, the epiblast layer was microdissected from E5.5 embryos and plated on MEF cells in EpiSC medium and cultured for 3-4 days to form a large EpiSC colony. EpiSC colonies were then manually dissociated into small clusters using a glass needle and plated into 1.9 cm² wells containing MEF feeders in EpiSC cell medium. EpiSCs were passaged every third day using 1.5 mg/ml collagenase type IV (GIBCO, #17104-019) with pipetting into small clumps.

Differentiation of EpiSCs was achieved by growing the EpiSCs on gelatin-coated tissue culture dishes in EpiSC medium lacking FGF2. Expression of pluripotency markers Oct4, Nanog; mesodermal marker Brachyury; neuroectodermal marker β -III tubulin; and hepatocyte marker FoxA2 was assessed by RT-PCR using Invitrogen SuperScript III One-Step RT-PCR System (Invitrogen, #12574-026). Primer sequences were designed using the primer bank web software (<http://pga.mgh.harvard.edu/primerbank/>; PrimerBank ID: *Oct4*:356995852c2; *Nanog*: 153791181c2; *Brachyury*:118130357c1; *β -III tubulin*:12963615a1; *FoxA2*:153945803c1). Fgf5 forward primer: CTGTACTGCAGAGTGGGCATCGG; Fgf5 reverse primer: GACTTCTGCGAGGCTGCGACAGG. Cer1 forward primer: CTCTGGGGAAGGCAGACCTAT; Cer1 reverse primer: CCACAAACAGATCCGGCTT. Rex1 forward primer: TGGAAGCGAGTTCCTTCTC; Rex1 reverse primer: GCCGCCTGCAAGTAATGAG. All primer pairs except Tsix (exon 4) spanned an intron, thereby distinguishing cDNA from genomic DNA amplification. Nevertheless, control reactions lacking reverse transcriptase for each sample were performed to rule out genomic DNA contamination.

For IF and/or RNA FISH, EpiSCs were cultured on gelatin-coated glass coverslips. The cells were then permeabilized through sequential treatment with ice-cold cytoskeletal extraction buffer (CSK:100 mM NaCl, 300 mM sucrose, 3 mM MgCl₂, and 10 mM PIPES buffer, pH 6.8) for 30 sec, ice-cold CSK buffer containing 0.4% Triton X-100 (Fisher Scientific, #EP151) for 30 sec, followed twice with ice-cold CSK for 30 sec each. After permeabilization, cells were fixed by incubation in 4% paraformaldehyde for 10 min. Cells were then rinsed 3X in 70% ethanol and stored in 70% ethanol at -20°C prior to IF and/or RNA FISH.

Immunofluorescence (IF).

Cells mounted on glass coverslips were washed 3X in PBS for 3 min each while shaking. Coverslips were then incubated in blocking buffer consisting of 0.5 mg/mL BSA (New England Biolabs, #B9001S), 50 ug/mL yeast tRNA (Invitrogen, #15401-029), 80 units/mL RNaseOUT (Invitrogen, #10777-019), and 0.2% Tween 20 (Fisher, #BP337-100) in 1X PBS in a humid chamber for 30 min at 37°C. The samples were next incubated with primary antibody diluted in blocking buffer for 1 hr in the humid chamber at 37°C. The H3-K27me₃ antibody (Millipore, #07-449) was used at a 1:2500 dilution. The samples were then washed 3X in PBS/0.2% Tween 20 for 3 min each while shaking. After a 5 min incubation in blocking buffer at 37°C in the humid chamber, the samples were incubated in blocking buffer containing a 1:300 dilution of fluorescently-conjugated secondary antibody (Alexa Fluor, Invitrogen) for 30 min in the humid chamber at 37°C, followed by three washes in PBS/0.2% Tween 20 while shaking for 3 min each. The samples were then processed for RNA FISH.

RNA Fluorescence in situ Hybridization (RNA FISH).

Double-stranded RNA FISH (dsRNA FISH) was performed as previously described (16, 45, 77). The dsRNA FISH probes were made by randomly-priming DNA templates using BioPrime DNA Labeling System (Invitrogen, #18094011). Probes were labeled with Fluorescein-12-dUTP (Invitrogen), Cy3-dCTP (GE Healthcare, #PA53021). Labeled probes from multiple templates were precipitated in a 0.3M sodium acetate solution (Teknova, #S0298) along with 300 µg of yeast tRNA (Invitrogen, #15401-029) and 150 µg of sheared, boiled salmon sperm DNA (Invitrogen, #15632-011). The solution was then spun at 15,000 rpm for 20 min at 4°C. The pellet was washed consecutively with 70% ethanol and 100% ethanol. The pellet was dried, then re-suspended in deionized formamide (ISC Bioexpress, #0606). The probe was denatured by incubating at 90°C for 10 min followed by an immediate 5 min incubation on ice. A 2X hybridization solution consisting of 4X SSC, 20% Dextran sulfate (Millipore, #S4030), and 2.5 mg/ml purified BSA (New England Biolabs, #B9001S) was added to the denatured solution. All probes were stored at -20°C until use.

Strand-specific RNA FISH (ssRNA FISH) probes were labeled with Cy5 CTP (GE Healthcare, # 25801086) or Cy3 CTP (GE Healthcare, # 25801086) using Invitrogen MAXIscript Kit (Invitrogen, #AM-1324). Labeled probes were column purified (Roche, #11814427001) and precipitated in an 0.25M ammonium acetate solution as described above for the dsRNA FISH probes. Probes were resuspended as described for dsRNA FISH probes and stored at -20°C .

Cells or embryo fragments mounted on coverslips were dehydrated through 2 min incubations in 70%, 85%, 95%, and 100% ethanol solutions and subsequently air-dried. The

coverslips were then hybridized to the probe overnight in a humid chamber at 37°C. The samples were then washed 3X for 7 min each while shaking at 39°C with 2XSSC/50% formamide, 2X with 2X SSC, and 2X with 1X SSC. A 1:250,000 dilution of DAPI (Invitrogen, #D21490) was added to the third 2X SSC wash. The cells were then mounted in Vectashield (Vector Labs, #H-1200).

DNA FISH.

After RNA FISH, the cells were washed with 1X PBS three times and then incubated in PBS for 5 min at room temperature. The cells were then refixed with 1% (wt/vol) PFA containing 0.5% (vol/vol) Tergitol and 0.5% (vol/vol) Triton X-100 for 10 min at room temperature. The cells were next dehydrated through an ethanol series (70%, 85%, and 100% ethanol, 2 min each) and air dried for 15 mins. The cells were then treated with RNase A (1.25 ug/ul) at 37°C for 30 min. The cells were again dehydrated through the ethanol series as described above. The samples were then denatured in a prewarmed solution of 70% formamide in 2x SSC on a glass slide stationed on top of a heat block set at 95°C for 11 min followed immediately by dehydration through a -20°C-chilled ethanol series (70%, 85%, 95%, and 100% ethanol, 2 min each). The cells were then air dried for 15 min followed by probe hybridization overnight at 37°C. The BAC template used for Xist DNA FISH is RP24-287F13 (Children's Hospital of Oakland Research Institute). The next day, the samples were washed twice with prewarmed 50% formamide/2X SSC solution at 39°C and 2X with 2X SSC, 7 min each.

Quantification of Allele-specific Expression.

Allele-specific expression was quantified using Qiagen PyroMark sequencing platform. Amplicons containing SNPs were designed using the PyroMark Assay Design software. cDNAs were synthesized using Invitrogen SuperScript III One-Step RT-PCR System (Invitrogen, #12574-026). Following the PCR reaction, 5 ul of a total of 25 uL of reaction was run on a 3% agarose gel to assess the efficacy of amplification. The samples were then prepared for pyrosequencing according to the standard recommendations for use with the PyroMark Q96 ID sequencer. For *Xist*, the following primers were used: forward, CAAGAAGAAGGATTGCCTGGATTT; reverse, 5'-biotin-GCGAGGACTTGAAGAGAAGTTCTG; sequencing, CAAACAATCCCTATGTGA. For *Atrx*, the following primers were used: forward: ATAGCTTCAGATTCTGATGAAACC; reverse: 5'-biotin-ACATCGTTGTCACTGCCACTT; sequencing: TAAGCTCAGATGAAAAGA. For *Rnf12*, the following primers were used: forward: 5'-Biotin-TGCAGCCAACAAGTGAAATTCC; reverse: TATCTGCTGTCTCAGGGTCACATG; sequencing: TAGAACTTCCTTCAGGC. All three amplicons span intron (s), thus permitting discrimination of RNA vs. any contaminating genomic DNA amplification due to size differences. Control reactions lacking reverse transcriptase for each sample were also performed to rule out genomic DNA contamination.

Cell Proliferation and Viability.

Live/Dead cell viability assay (Life technologies cat. #L3224) was performed as described previously (Gayen et al., 2015). 50,000 EpiSCs were plated on gelatinized plate and differentiated as described above. Cells were counted using the Trypan blue (Invitrogen cat. #15250061) exclusion assay with Invitrogen Countess Automated Cell Counter (cat. # C10227).

Cell viability was calculated both for adherent cells, harvested via trypsinization, and cells in suspension, harvested by centrifugation of culture media. Data were collected from three independent differentiation experiments.

Microscopy.

Samples were imaged using a Nikon Eclipse TiE inverted microscope with a Photometrics CCD camera. The images were deconvolved and uniformly processed using NIS-Elements software.

Statistics.

$p=0.01$ was used as the cutoff for statistical significance. Tests used to calculate statistical significance are indicated in the corresponding figure legends.

Chapter 4: A Strand-Specific and Allele-Specific RNA-Seq Pipeline to Identify Novel Regulators of X-inactivation

4-1: Introduction

My studies of the role of Tsix RNA in imprinted and random X-chromosome inactivation have indicated that current models of X-inactivation are insufficient to explain the initiation of epigenetic silencing during embryonic development (Gayen et al., 2015; Kalantry et al., 2009; Maclary et al., 2014). I hypothesize, based on assessment of Tsix mutant embryos as well as evolutionary analysis of the X-chromosome, that previously unidentified X-linked factors play key roles in X-inactivation. We believe that these novel factors include both novel lncRNAs that regulate gene expression regionally in *cis*, and escapers of X-inactivation that function in *trans*.

Evolutionary analysis of the X chromosome suggests that X-inactivation may be triggered regionally (Jegalian and Page, 1998; Lahn and Page, 1999; Sandstedt and Tucker, 2004): The X and Y are hypothesized to have evolved from a pair of identical autosomes (Graves and Schmidt, 1992; Jegalian and Page, 1998), and dosage compensation may have evolved in a piecemeal fashion as genes were slowly lost from the Y-chromosome (Bellott et al., 2014; Jegalian and Page, 1998; Lahn and Page, 1999). Based on the nucleotide divergence between X and Y homologs, genes on the X chromosome can be divided into discrete groups, or evolutionary strata (Bellott et al., 2014; Cortez et al., 2014; Lahn and Page, 1999). Genes belonging to the oldest evolutionary strata were the first to diverge on the Y chromosome and

were likely to be the first genes to undergo dosage compensation on the X-chromosome (Jegalian and Page, 1998). As gene loss and the subsequent need for dosage compensation arose regionally, I hypothesize that X-inactivation may be triggered regionally, by novel *cis*-acting long non-coding RNAs. Long non-coding RNAs they are believed to influence regional epigenetic states through recruitment of chromatin modifying complexes, and have been implicated in the regulation of imprinted loci and establishment of parent-of-origin specific expression patterns, making them prime candidates for *cis* regulators of X-chromosome inactivation (Bartholdi et al., 2009; Delaval and Feil, 2004; Hung and Chang, 2010; Lee, 2009; O'Neill, 2005).

Whereas evolutionary considerations point novel to *cis* acting players in X-chromosome inactivation, analysis of X-linked gene silencing in *Tsix*-mutant embryos and stem cells indicate a role for *trans*-acting X-linked genes that escape X-inactivation in mediating silencing (Gayen et al., 2016), (Gayen et al., in prep). During our investigations of the role of *Tsix* in random X-inactivation, we observed that, though loss of *Tsix* leads to ectopic *Xist* RNA induction upon differentiation in both male and female cells, the frequency of *Xist* induction differed between male and female cells (Gayen et al., 2015). We subsequently utilized these ES cells and Epiblast Stem Cells harboring mutations in the *Tsix* lncRNA to evaluate both the frequency of *Xist* RNA induction and sufficiency of *Xist* RNA to silence X-linked genes. We found that a higher frequency of $X^{\Delta Tsix}Y$ male cells displayed ectopic *Xist* RNA coating compared to $X^{\Delta Tsix}X$ female cells (Gayen et al., 2016). This increase reflects the inability of $X^{\Delta Tsix}Y$ cells to efficiently silence X-linked genes compared to $X^{\Delta Tsix}X$ cells, despite equivalent *Xist* induction and coating. Silencing of genes on both Xs results in significantly reduced proliferation and increased cell death in $X^{\Delta Tsix}X$ female cells relative to $X^{\Delta Tsix}Y$ male cells (Gayen et al., 2016). Thus, whereas

Xist RNA can inactivate the X-chromosome in females it may not do so in males.

We further found comparable silencing in differentiating $X^{\Delta Tsix}Y$ and 39, $X^{\Delta Tsix}$ ($X^{\Delta Tsix}O$) ESCs, excluding the Y-chromosome and instead implicating the X-chromosome dose as the source of the sex-specific differences (Gayen et al., 2016). In the *Tsix* mutants, the differences in Xist induction and X-linked gene silencing must be genetically attributed to the sex chromosomes, as both $X^{\Delta Tsix}X$ and $X^{\Delta Tsix}Y$ cells have identical complements of autosomes, and since differentiating $X^{\Delta Tsix}O$ ESCs behave similarly to $X^{\Delta Tsix}Y$ ESCs, a protective effect of the Y-chromosome can be excluded as the source of sex-specific differences (Gayen et al., 2016). Instead, the data implicate the presence of the second X-chromosome as the source of the increased permissiveness for ectopic X-linked gene silencing in females compared to males. Most X-linked genes in females with an inactive X-chromosome are expressed at levels equal to that in males (Deng and Disteche, 2010; Deng et al., 2011; Disteche, 2012). A subset of X-linked genes, however, escape X-inactivation in female cells and are capable of being expressed from both X-chromosomes despite inactivation of one of the two Xs (Berletch et al., 2010; Marks et al., 2015). Due to expression from both alleles, these X-inactivation escapees are expressed at higher levels in females compared to males (Berletch et al., 2015a). Since $X^{\Delta Tsix}X$ female embryonic epiblast cells and EpiSCs harbor an inactivated X-chromosome prior to ectopic inactivation of the active $X^{\Delta Tsix}$ X-chromosome, the increased dosage of one or more X-inactivation escapees are prime candidates as *trans*-acting factors that help trigger X-linked gene silencing (Gayen et al., 2016).

In order to discover and characterize putative novel regulators of X-inactivation, I sought to establish a pipeline able to identify both escapers of X-inactivation and novel non-coding RNAs. Recent advances in next-generation sequencing have revolutionized genetic analysis. To

delineate both novel lncRNAs and escapers of X-inactivation, we turned to high-throughput RNA-Sequencing, which is able to provide an unbiased survey of global gene expression in cell lines and embryos. Here, I outline an RNA-Seq approach for comprehensive transcriptome analysis, including approaches for both novel transcript identification and allelic expression analysis. Through this approach, I aim to identify novel *cis* and *trans* acting regulators of X-inactivation.

4-2: Sample Derivation, Library Preparation, and Sequencing

Allele-specific expression analysis, whether through high-throughput sequencing or single-gene approaches, relies on the presence of polymorphic sites in the genome to distinguish the two alleles. To generate polymorphic samples, I use two genetically divergent inbred mouse lines, the 129/S1 *Mus musculus* strain and the JF1 *Mus molossinus* strain. These strains were selected based on the sequence divergence between the two genomes and the availability of whole-genome sequencing data for both strains (Keane et al., 2011; Takada et al., 2013; Yalcin et al., 2011). I have identified 413,974 SNPs on the X-chromosome that differ between the two strains and we find that, for known genes included in the NCBI RefSeq annotation, 89% of X-chromosome genes contain at least one polymorphic site, allowing for allele-specific expression analysis of most transcripts (Keane et al., 2011; Pruitt et al., 2014; Takada et al., 2013; Yalcin et al., 2011).

I set up matings of these divergent mouse strains to generate F1 hybrid embryos, which will harbor a paternally-inherited X-chromosome from one mouse strain and a maternally-inherited X-chromosome from the other. Thus, strain-specific single nucleotide polymorphisms (SNPs) can be identified and traced back to either the maternally-inherited or paternally-inherited genome. In cells and embryos that undergo imprinted X-inactivation, the paternally-inherited X

will always be inactive. Knowing the strain source of the paternal X-chromosome, I can then associate specific single nucleotide polymorphisms with the paternal-X, and thus the inactive-X. Blastocyst stage hybrid embryos, which undergo imprinted X-inactivation (Kay et al., 1994; Mak et al., 2004; Takagi et al., 1978), can be sequenced directly, or cell lines can be derived from individual embryos. Trophoblast stem cells (TSCs), which are derived from the trophectodermal lineage of the early embryo, and extra-embryonic endoderm (XEN) cells, which are derived from the primitive endoderm lineage of the embryo, stably maintain imprinted X-inactivation in culture, facilitating allele specific analysis of wild-type samples (Kunath et al., 2005; Maclary et al., 2014; Tanaka et al., 1998). To assess embryonic cell lineages, such as epiblast stem cells (EpiSCs), which normally undergo random X-inactivation, genetic mutations can be introduced to bias X-inactivation (Berletch et al., 2015b; Marks et al., 2015; Tesar et al., 2007). Isolated wild-type extra-embryonic tissues of later-stage embryos, which maintain imprinted X-inactivation, or epiblast-derived tissues in embryos harboring mutations that bias random X-inactivation, could be sequenced using these methods as well.

For sequencing, either total RNA or mRNA is extracted from embryos and cell lines. I have primarily opted to isolate mRNA, as the protein-coding genes that could function as *trans*-acting regulators of X-inactivation are expected to be polyadenylated, and most lncRNAs are known to be polyadenylated as well (Guttman et al., 2010). Following mRNA extraction, strand-specific RNA-Sequencing libraries are prepared. Strand-specific sequencing is critical for identification of lncRNAs and putative epigenetic initiators, as sense/antisense transcription from the same genomic locus is a feature of many expressed lncRNAs and imprinted genes (Ogawa and Lee, 2003a; Su et al., 2010). Without a strand-specific library, it is impossible to distinguish bi-directional transcription at these loci.

Of the many protocols available for strand-specific library preparation, dUTP incorporation provides an accurate and reliable for strand-specific library preparation that is compatible with paired-end sequencing (Borodina et al., 2011; Levin et al., 2010; Parkhomchuk et al., 2009). The dUTP library preparation method allows for strand-specificity by incorporating uracil during second-strand cDNA synthesis in lieu of thymidine. Second-strand cDNA is then degraded following adapter ligation so that only the first-strand cDNA is ultimately sequenced, thus generating strand-specific sequence data. (Borodina et al., 2011; Parkhomchuk et al., 2009).

Following library preparation, samples are sequenced on the Illumina HiSeq platform. I have opted for 100-basepair paired-end sequencing reads, as using long paired-end reads provides additional information for accurate assembly and identification of novel splice isoforms and transcripts (Williams et al., 2014). The additional sequence information contained in long reads can also assist improving the percentage of uniquely mapped reads (Williams et al., 2014). Following sequencing, I perform preliminary quality control of data using FastQC, which will flag anomalies in sequence content, GC content, or decreases in quality score towards the ends of reads that require trimming (Andrews, 2010).

4-3: Reference Genome Assembly and Allele-specific Mapping

Allele-specific RNA-Seq analysis presents unique challenges. Analysis relies on mapping of short reads to the reference genome, and RNA-Seq read aligners typically allow a small number of mismatches within alignments between the read and reference sequence. These mismatches permit mapping of reads containing polymorphisms or sequencing errors. Though mismatches are permitted, reads that contain mismatches to the reference sequence are less likely to be aligned to the reference genome. For quantification of allele-specific expression, mapping

bias towards the reference allele can lead to inaccuracies in observed allelic balance when reads are mapped to a single reference genome, with the reference allele overrepresented among mapped reads (Degner et al., 2009; Stevenson et al., 2013). To diminish reference mapping bias, I built *in silico* strain-specific references for both the 129/S1 and JF1 genomes. Read mapping to strain-specific or species specific reference genomes is a strategy that has previously been used to identify imprinted genes in both mice and *drosophila* as well as to characterize X-inactivation in mouse stem cells (Berletch et al., 2015b; Calabrese et al., 2012; Coolon et al., 2012; Finn et al., 2014). I generated strain-specific reference genomes by substituting strain-specific SNPs identified by whole-genome sequencing into appropriate sites in the reference genome using VCFtools (Danecek et al., 2011). Then, reads are mapped separately to the 129/S1 and JF1 reference genomes. Importantly, though use of a strain-specific reference genome minimizes mapping bias, it does not eliminate it entirely since, in addition to SNPs, different mouse strains harbor indels and structural variations.

I mapped reads to the strain-specific reference genomes using the rapid spliced aligner STAR (Dobin and Gingeras, 2015). A systematic comparison of numerous read mappers indicates that STAR yields accurate alignment of a high proportion of both spliced and unspliced RNA-Seq reads (Engström et al., 2013). During alignment to strain-specific reference genomes, I required a perfect match between the read sequence and reference sequence (zero mismatches in alignment); thus, reads overlapping polymorphic sites in the reference genome will only overlap that SNP in one of the two allele-specific references, allowing for rapid downstream quantification of allele-specific reads. During mapping, STAR truncates reads for which it is unable to find a perfect full-length alignment, and will then map these “clipped” reads. For my stringent mapping protocol, this allows for a higher percentage of reads to be mapped, even if

sequencing errors are present: in RNA-Seq data, as sequence quality of reads frequently diminishes toward the end of long reads. This read trimming also may assist in diminishing reference mapping bias due to indels, as some reads aligning near indels can be truncated to permit mapping; STAR does permit small insertions and deletions in full-length mapped reads as well.

When setting STAR mapping parameters, in addition to requiring a perfect match between the read and reference genome, I provided a reference genome annotation from Ensembl to serve as a splice junction database. The use of a splice junction database assists in accurate mapping of spliced reads to known genes and gene models. STAR is also able to identify splice junctions *de novo*; I permitted *de novo* splice junction identification to allow assembly of novel transcripts, but required a minimum of 3 reads supporting each novel junction with a consensus splice donor and acceptor site, and five reads supporting novel splice junctions without consensus donor and acceptor sites. This allows for discovery of novel splice junctions in known or novel transcripts, but restricts spurious prediction of splice junctions from single reads.

Following read mapping to both reference genomes, I divided into three groups: reads that do not cover polymorphic sites (“non-allelic reads”), reads overlapping SNP sites that map to the JF1 reference genome, and reads overlapping SNP sites that map to the 129 reference genome. Both nonallelic and allelic reads were compiled into a single non-redundant alignment file for transcriptome annotation and novel transcript discovery (see section 4-4). For allele-specific analysis (section 4-5), only reads overlapping polymorphic sites were used.

4-4: Transcriptome Annotation and Novel Transcript Discovery

RNA-Seq allows for comprehensive analysis of transcriptional profiles based on sequencing of short reads from fragmented RNA. Analysis pipelines typically rely on assembly

of transcripts from these short reads. For differential expression analysis of known genes, reads are associated with known genes based on map coordinates from a reference annotation. Reference transcript assemblies for commonly used model organisms, including mouse, are available from numerous sources, and typically include known protein coding genes and long non-coding transcripts, as well as an assortment of predicted transcripts, such as those identified by the RIKEN pipeline or through expressed sequence tags. Each annotation differs: RefSeq includes validated genes and a small number of gene models, whereas the Ensembl genome annotation includes additional gene models and predicted transcripts, curated in part from UniProt and HAVANA manual annotation (Cunningham et al., 2015; Pruitt et al., 2014). Since RNA-Seq provides an unbiased snapshot of cellular transcription, recent studies of mammalian transcriptomes have shown, however, many sequencing reads typically map outside of annotated regions in the reference assembly (ENCODE Project Consortium et al., 2007; Trapnell et al., 2012). One current challenge in biology is identifying and annotating these putative novel transcripts from sequencing data, and distinguishing novel transcripts from polymerase read-through or other transcriptional “noise”.

Cufflinks, part of an RNA-Seq analysis suite, provides a method for identifying novel transcripts from a reference-mapped assembly (Trapnell et al., 2012; 2010). Cufflinks includes flexible options for building transcripts and annotating novel transcripts based on the reference genome, with the goal of identifying the minimum possible set of transcriptional units that could explain mapped reads within the RNA-Seq dataset (Trapnell et al., 2010). The Cufflinks pipeline is capable of identifying both fully novel transcriptional units as well as putative anti-sense transcripts and novel splice variants.

Briefly, to assemble transcripts, Cufflinks assesses the numbers of reads mapped to

specific regions of the reference genome. A set minimum number of reads must map to any putative region in order for the cluster of mapped reads to be considered a transcript. I set 5 reads as the minimum for a transcript to be called; this low threshold is likely to yield false-positive transcript calls, however, with biological replicates, these can be filtered out while avoiding the possibility of missing transcripts, like lncRNAs, that may be expressed at very low levels. I then compared assembled transcripts to a reference transcriptome annotation. For this comparison, I opted to utilize the Ensembl mm9 build transcriptome annotation (Cunningham et al., 2015). Whereas the Ensembl transcriptome contains redundancies in annotations, it also includes the most comprehensive panel of predicted genes and gene models. Cufflinks comparison of assembled transcripts and the reference annotation sorts assembled transcripts into numerous categories using 11 different class codes (Trapnell et al., 2012). These codes identify known genes and gene variants, putative novel transcripts, and assembled reads that likely represent polymerase run-on or spurious transcription.

To prioritize putative novel transcripts for follow-up, I first filtered transcripts by class code. I kept novel intergenic transcripts, antisense transcripts, and transcripts that are fully intronic. Transcripts that have exonic overlap in the same direction as known transcripts and putative polymerase run-on fragments were excluded. I next filtered transcripts based on comparison between multiple biological replicates, only transcripts that appear in multiple cell lines are targeted for follow-up. I additionally filtered by expression level, transcript length, and intron-exon structure, prioritizing transcripts that are highly expressed, greater than 500 base pairs, or show evidence of splicing structure. My interests focus particularly on long non-coding RNAs, which may function as *cis*-acting regulators of epigenetic inheritance; To identify and prioritize putative lncRNAs, I predicted protein coding potential based on RNA sequence using

Coding Potential Calculator (CPC) (Kong et al., 2007). CPC evaluates the presence and coverage of open reading frames in transcript sequences and provides a coding score. Specifically, CPC looks for a single open reading frame that covers the majority of the sequence length, as well as the presence of in-frame start and stop codons (Kong et al., 2007). Following identification of transcripts, the transcript annotation file is used to identify allele-specific expression of both known and novel genes.

4-5: Allele-specific Transcriptome Analysis

From our set of mapped reads and a list of SNP sites that differ between the 129/S1 and JF1 genomes, I counted the number of overlapping reads mapping to the 129 genome and the number of overlapping reads mapping to the JF1 genome using Bedtools (Quinlan and Hall, 2010). For each SNP, I calculated inactive-X expression, calculating the number of allele-specific reads mapped to the inactive-X strain divided by the total number of allele specific reads overlapping the SNP in both strains. For samples with imprinted X-inactivation, including blastocysts, TSCs, and XEN cells, this will be the paternal strain. For samples that typically would undergo random X-inactivation, such as ES cells or EpiSCs, the strain and parent of origin for the inactive-X depends on the cell line and on how biased X-inactivation was achieved. Once allelic expression calculations have been made for individual polymorphic sites, I compare SNP sites to a reference transcriptome annotation to identify transcript-level allele-specific expression.

From the transcriptome annotation, I generated a non-redundant set of exons, and identify polymorphic sites within each exon using Bedtools (Quinlan and Hall, 2010). To calculate allelic expression for a given gene, I averaged the percent expression from the inactive allele for all SNPs that reside within exon boundaries for that single gene. For some genes with low

expression levels, or for SNPs near the end of transcripts, where read coverage can be inconsistent, the numbers of SNP overlapping reads can be quite low. To avoid biasing gene-level allelic expression calls based on low coverage SNPs, which may not be accurate reflections of true allelic balance, I set a threshold for the minimum number of reads covering each polymorphic site. Our preliminary data analysis utilizes thresholds of 10 reads per SNP or 5 reads per SNP, I find that these coverage thresholds yield similar results, however, including SNPs with only 5 allele-specific reads increases variability in average allelic expression within single genes (See Chapter 5). Analyzing the variability between allelic expression calls for all SNPs within a given gene can be highly informative both for understanding gene expression and for filtering potential incorrect polymorphism calls from whole-genome sequencing. Assessing variability between SNPs in the same transcript provides confidence in allelic expression calls, and can identify individual SNPs that behave abnormally. SNPs that do not match the allelic balance of other polymorphic sites in the same transcript may arise from alternative splicing, or could represent errors in SNP calls from whole genome sequencing, variants that differ between our samples and those for which whole-genome sequencing was performed, or regions harboring small indels or structural rearrangements that lead to reference mapping bias. Depending on context and the consistency of read mapping, these sites may be excluded from analysis.

Based on calculated allele-specific expression levels, I have identified escapers of X-inactivation and inactive-X specific transcripts. Early surveys of escape from X-inactivation frequently used a threshold of 10% inactive-X expression as the definition of escape (Carrel and Willard, 2005; Marks et al., 2015; Yang et al., 2010). This definition is advantageous in that it is simple and will typically encompass the genes for which escape from X-inactivation is substantial enough to impact gene dosage in a biologically relevant way, such as sex-specific

increases in expression in females compared to males. Sequencing based approaches to surveying escape from X-inactivation, however, have made it increasingly apparent that escape from X-inactivation occurs on a broad spectrum. Some X-linked genes are very strictly silenced, however, many show low levels of transcription from the inactive X-chromosome; this basal inactive-X transcription ranges from vanishingly small, contributing less than a percent of the total expression level of the gene, to modest: in my preliminary data analysis, a number of genes fall in the range of 1-10% inactive-X expression. This low level of inactive-X expression may not indicate a functional increase in dosage in females, however, it is clear that the regulation of these genes differs from those that are strictly silenced, and does not preclude that this low-level escape from X-inactivation serves a biological purpose, even if dosage is not substantially altered. Given this spectrum of escape, alternative approaches to defining escape genes have recently been developed, utilizing binomial models to predict whether the inactive-X contribution of a given gene is significant (Berletch et al., 2015b; Calabrese et al., 2012). These models have the advantage of identifying broad ranges of inactive-X contribution that differ from expectations, even at low levels. For future studies, the choice of how to define escape from X-inactivation depends largely on the goals of the specific project.

4-6: Strategies for Follow-up Characterization of Gene Expression

Following identification of novel lncRNAs and escapers of X-inactivation in WT cells by RNA-Seq, it is critical to confirm these expression patterns using alternative approaches. I have previously analyzed expression of X-linked genes in populations of cells using RT-PCR followed by Sanger sequencing (Gayen et al., 2015; Maclary et al., 2014). Design of RT-PCR primers flanking SNP sites can identify monoallelic versus biallelic expression from the maternal or paternally-inherited X-chromosomes. I and other members of the lab have also optimized a

more quantitative approach for allele-specific expression of X-linked genes using pyrosequencing (Gayen et al., 2015; 2016). Pyrosequencing again relies on design of an RT-PCR amplicon flanking a SNP site, followed by quantitative analysis of the relative proportions of each allele present based on quantification of pyrophosphate release during nucleotide incorporation (Kreutz et al., 2015). In addition to these sequencing-based approaches to analyze populations of cells, I will use RNA fluorescence *in situ* hybridization (FISH) to confirm allele-specific expression at the single-cell level. For escapees, this will help to clarify whether escape occurs at a low level in all cells, or if genes of interest escape X-inactivation in every cell within a population. I will develop specific oligonucleotide probes that hybridize to genes of interest, and perform RNA-FISH for these genes of interest in conjunction with Xist RNA, which marks the inactive-X, as commonly used in our publications (see, for example, (Hinten et al., 2016)). From RNA FISH stains, I can assess allele-specific expression by counting colocalization of genes of interest with Xist RNA coating. An RNA FISH approach uniquely allows for assessment of gene expression in non-hybrid genetic backgrounds, to determine if any gene expression pattern changes result from hybrid genetic background. Additionally, I have recently optimized a protocol for allele-specific RNA FISH for Xist, which stains Xist RNA from the *M. molossinus* derived X-chromosome and the *M. musculus* derived X-chromosome in separate colors (Levesque et al., 2013). This novel approach permits follow-up of novel transcript expression in randomly inactivated populations of cells. This is particularly important for analysis of any novel transcripts identified in lineages that typically undergo random X-inactivation, such as EpiSCs. Analysis of novel factors on the single-cell level in WT, randomly-inactivated cells can distinguish if these transcripts are expressed in WT cells, or if they are restricted to mutant cell lines and, if so, if they show any strain bias in inactive-X expression.

4-7: Applications for Allele-Specific RNA-Seq Analysis and Future Goals

I and other members of the lab have generated numerous cell lines and embryos from F1 hybrid crosses of *M. molossinus* and *M. musculus* mice. Preliminarily, I aim to comprehensively identify escapers of X-inactivation and novel lncRNAs in cell lines representative of all three lineages of the blastocyst-stage mouse embryo: TSCs, XEN cells, and EpiSCs. TSCs are derived from the trophoctodermal lineage, which will give rise to the placenta in later stage embryos (Tanaka et al., 1998). XEN cells are derived from the primitive endoderm lineage, which gives rise to the yolk sac (Kunath et al., 2005). Both TSCs and XEN cells stably maintain imprinted X-inactivation in culture. EpiSCs arise from the inner cell mass of the early embryo, and are representative of randomly inactivated populations (Tesar et al., 2007). I have derived and sequenced nine lines of WT hybrid TSCs and nine lines of wild-type hybrid XEN cells. For each cell type, these lines include six female cell lines, three derived from a *M. molossinus* dam crossed to an *M. musculus* sire and three derived from a *M. musculus* dam crossed to an *M. molossinus* sire. Using these reciprocal crosses, we can discern escape from X-inactivation or inactive-X specific expression from strain-specific differences in expression. I have additionally sequenced three male cell lines for each cell type, to allow for differential expression analysis between female and male cells and identification of female-specific or female-upregulated transcripts. For EpiSCs, I have sequenced twelve cell lines: nine female lines with biased X-inactivation and three male lines, for comparative analysis. Of the nine female cell lines, six harbor mutations in the Tsix lncRNA; five of these cell lines have the *M. musculus*-derived Tsix mutant X inactivated in all cells, whereas one has the *M. molossinus*-derived X-chromosome inactivated. The other three cell lines harbor mutations in the Xist lncRNA, in these cells, the

wild-type *M. molossinus*-derived X is inactivated. In these cells, I am currently working to identify novel lncRNAs and escapers of X-inactivation.

In addition to sequencing of WT cells, I have leveraged this allele-specific expression analysis pipeline to characterize X-inactivation status in mutant embryos and stem cells. I have performed allele-specific RNA-Seq of TSCs bearing mutations in EED, the core component of the chromatin modifying complex Polycomb Repressive Complex 2 (see Chapter 5). Through this analysis, I have identified a limited defect in X-linked gene expression upon loss of EED. I have also sequenced XEN cells harboring mutations in EED. In collaboration with other members of the lab, I am currently pursuing RNA-Seq analysis of individual blastocyst-stage embryos harboring mutations in multiple components of PRC2, to develop a comprehensive understanding of the role of PRC2 in initiation of imprinted X-inactivation.

Chapter 5: Repression of Basally Transcribed Inactive X-linked genes by PRC2 and Xist RNA

This chapter will be submitted for publication as: Maclary E., Hinten M., Sethuraman S., Harris C., and Kalantry S., “Repression of Basally Transcribed Inactive X-linked genes by PRC2 and Xist RNA”. This chapter was written by E.M., M.H., and S.K. Data presented in this chapter was primarily collected and analyzed by E.M. and M.H.; M.H. performed experiments and analyzed all data presented in figures 5.1 and 5.2, with the exception of figure 5.1D; E.M. performed experiments and analyzed data presented in figures 5.1D, 5.3-5.13 and tables 5.1-5.6; S.S. assisted with bioinformatic analysis; C.H. derived and maintained *Eed^{fl/fl}* mice and assisted with cell line derivation and culture.

5-1: Introduction

Post-translational modifications of histones in chromatin are capable of transmitting epigenetic transcriptional states across cell division (Margueron and Reinberg, 2011; Ragunathan et al., 2015; Zhang et al., 2015). The histone H3-K27me3 modification constitutes a key chromatin modification. H3-K27me3 is deposited at target loci by the Polycomb repressive complex 2 (PRC2), a large evolutionarily conserved multimeric protein complex (Cao et al., 2002; Czermin et al., 2002; Kuzmichev et al., 2002; Müller et al., 2002; Tie et al., 2001). In mammals, PRC2 and H3-K27me3 are implicated in many physiological processes, including in

pluripotency, differentiation, tumorigenesis, and X-chromosome inactivation (Brockdorff, 2013; Laugesen and Helin, 2014; Margueron and Reinberg, 2011).

Mammalian PRC2 consists of the core components EZH2, EED, and SUZ12 (Cao et al., 2002; Kuzmichev et al., 2002). EZH2 is the enzymatic subunit of PRC2 that catalyzes H3K27me₃, a mark that is associated with gene silencing (Di Croce and Helin, 2013; Margueron and Reinberg, 2011; Zhang et al., 2015). The PRC2 protein EED acts to propagate H3-K27me₃ at target loci (Margueron et al., 2009). PRC2 binds to pre-deposited H3-K27me₃ in S-phase and in turn stimulates EZH2 to catalyze H3-K27me₃ on newly deposited histones (Hansen et al., 2008; Margueron et al., 2009). In the absence of EED, H3-K27me₃ catalysis is ablated and the levels of the other core PRC2 proteins are reduced, indicating that PRC2 does not assemble (Montgomery et al., 2005). Thus, EED is required for PRC2 recruitment, stability, and robust enzymatic catalysis of H3-K27me₃.

X-chromosome inactivation has provided essential insights into PRC2 function (Brockdorff, 2013; Froberg et al., 2013; Pontier and Gribnau, 2011). X-inactivation is an evolutionarily conserved epigenetic process in mammals that equalizes X-linked gene dosage between *XX* females and *XY* males (BEUTLER et al., 1962; LYON, 1961). Two different forms of X-inactivation characterize the early mouse embryo. The initial form is imprinted X-inactivation, in which all cells of the pre-implantation mouse embryo exclusively inactivate the paternally-inherited X-chromosome (Kay et al., 1994; Mak et al., 2004; Takagi et al., 1978). In later stage embryos, imprinted inactivation of the paternal-X is maintained in the trophectoderm and primitive-endoderm derived placental and yolk-sac cells (Takagi and Sasaki, 1975; West et al., 1977; 1978). The epiblast progenitor cells that give rise to the embryo proper, on the other

hand, reactivate the paternal-X and subsequently randomly inactivate either the paternal or the maternal X-chromosome (Mak et al., 2004).

At the onset of both random and imprinted X-inactivation, PRC2 proteins and H3-K27me3 are enriched on the inactive X-chromosome (Erhardt et al., 2003; Mak et al., 2002; Okamoto et al., 2004; Plath et al., 2003; Silva et al., 2003). PRC2 is proposed to be recruited to the inactive X-chromosome by the Xist long non-coding (lnc) RNA (Sunwoo et al., 2015; Zhao et al., 2008), which is only transcribed from the inactive X-chromosome and is necessary for stable X-inactivation (Kalantry et al., 2009; Marahrens et al., 1997; Penny et al., 1996). By virtue of its early enrichment on the inactive-X and its gene silencing function, PRC2 is thought to be critical for the stable silencing of X-linked genes (Plath et al., 2003; Silva et al., 2003). In agreement with this idea, loss-of-function studies suggest that PRC2 is required in imprinted mouse X-inactivation (Wang et al., 2001). The extra-embryonic tissues in *Eed*^{-/-} mouse embryos and *Eed*^{-/-} trophoblast stem cells (TSCs) are defective in maintaining silencing of paternal X-linked genes (Kalantry et al., 2006; Wang et al., 2001). Although EED loss compromises imprinted X-inactivation, whether PRC2 is required for silencing of all or only some X-linked genes is not known. In this study, we generated F1 hybrid *Eed*^{-/-} TSC lines harboring polymorphic X-chromosomes, thus enabling a comprehensive analysis of X-linked gene expression by allele-specific RNA-Seq. *Eed*^{-/-} TSCs lack H3-K27me3 and Xist RNA coating. Despite the absence of H3-K27me3 and Xist RNA coating, fewer than one-fifth of the X-linked genes are derepressed from the inactive X-chromosome in *Eed*^{-/-} TSCs. Analysis of ChIP-Seq profiles of transcriptional machinery and histone modifications in wild-type (WT) TSCs demonstrates that the derepressed genes in *Eed*^{-/-} TSCs display hallmarks of open chromatin and basal transcriptional activity on the inactive-X. X-linked genes that are completely silenced,

however, are refractory to the loss of EED, H3-K27me3, and Xist RNA. Thus, PRC2 and Xist RNA are required to prevent upregulation of genes that are transcribed at low levels or are primed for expression but are dispensable for the continued silencing of genes that are stably inactivated.

5-2: Loss of H3-K27me3 Enrichment and Xist RNA Coating on the Inactive X-chromosome in *Eed*^{-/-}TSCs.

From a conditionally-mutant *Eed* mouse strain, we generated *Eed*^{fl/fl} TSC line, in which a portion of one of the evolutionarily conserved WD40 repeats (WD3) is flanked by *loxP* sequences (Fig. 5.1A). WD40 domains have been shown to be necessary for EED to interact with the PRC2 enzyme EZH2 (Denisenko et al., 1998; Han et al., 2007), which catalyzes H3-K27me3. A perturbation of the WD40 may therefore disrupt essential PRC2 interactions and function. From *Eed*^{fl/fl} TSCs, we generated three *Eed*^{-/-} TSC subclones. In *Eed*^{fl/fl} and *Eed*^{-/-} TSC lines, we first assessed enrichment of EED protein and H3-K27me3 by immunofluorescence (IF). In the same cells, we also assessed Xist RNA expression by FISH; Xist RNA accumulation marks the inactive X-chromosome (Brown et al., 1992; Clemson et al., 1996; Jonkers et al., 2008). As expected, in *Eed*^{fl/fl} cells EED and H3-K27me3 are enriched on the Xist RNA-coated inactive paternal X-chromosome. *Eed*^{-/-} TSCs, by contrast, lack EED and H3-K27me3 enrichment as well as Xist RNA coating (Fig. 5.1B). Thus, EED absence results in the loss of H3-K27me3 enrichment on and Xist RNA coating of the paternal X-chromosome that is subject to imprinted X-inactivation, consistent with previous data (Kalantry et al., 2006).

To test that the absence of Xist RNA coating in *Eed*^{-/-} TSCs did not reflect loss of the Xist locus, we tested whether the TSCs harbored two Xist loci by DNA FISH. A vast majority of the

cells in both the *Eed^{fl/fl}* and *Eed^{-/-}* TSC lines exhibited two Xist loci (Fig. 5.1C). We also investigated X-chromosomal ploidy by X-chromosome paint, which showed that most cells of both genotypes harbored two X-chromosomes (Fig. 5.1D).

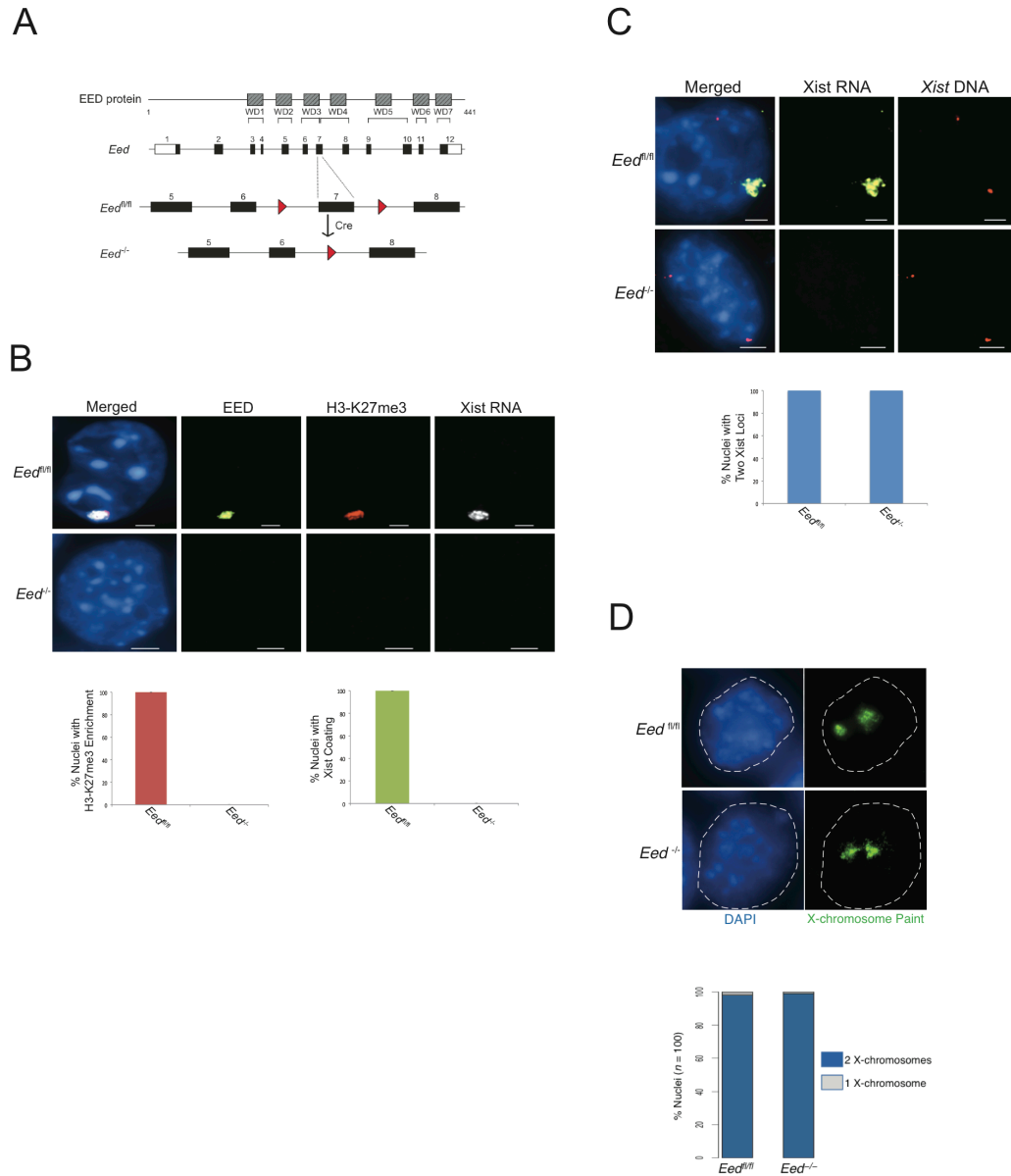


Figure 5.1: Absence of H3-K27me3 enrichment and Xist RNA coating on the inactive X-chromosome in *Eed^{-/-}* TSCs. (A) Diagram of conditional *Eed* mutation. (B) Detection of EED (in green) and H3-K27me3 (red) by immunofluorescence (IF) and Xist RNA (white) by RNA FISH in *Eed^{fl/fl}* and *Eed^{-/-}* TSCs. Nuclei are stained blue with DAPI. Scale bar, 2 μ m. Bottom, quantifications of numbers of nuclei with H3-K27me3 enrichment and Xist RNA coating in *Eed^{fl/fl}* and *Eed^{-/-}* TSCs. (C) Combined Xist RNA FISH and Xist DNA FISH in *Eed^{fl/fl}* and *Eed^{-/-}* TSCs. Xist RNA is detected in green and Xist DNA in red (pinpoints). Nuclei are stained blue with DAPI. Scale bar, 2 μ m. Right, quantification of Xist DNA FISH data. (D) Detection of X-chromosomes via X-chromosome

paint (DNA FISH) in *Eed*^{fl/fl} and *Eed*^{-/-} TSC lines. Top, representative nucleus from each genotype. Bottom, quantification of X-chromosome number. 100 nuclei were counted from a representative cell line of each genotype.

5-3: RNA FISH in *Eed*^{-/-} TSCs Reveals Limited Derepression of X-linked genes

To test whether X-inactivation is compromised in *Eed*^{-/-} TSCs, we assayed the expression by RNA FISH of four X-linked genes subject to X-inactivation, *Atrx*, *Rnf12*, *Pdhal*, and *Pgkl*. Both the parental *Eed*^{fl/fl} parental TSC line and the three derived *Eed*^{-/-} TSC lines displayed monoallelic expression of *Atrx*, *Rnf12*, and *Pdhal* (Fig. 5.2). All three genes appeared to be silenced on one allele in *Eed*^{-/-} TSCs, presumably the inactive paternal-X, despite the absence of H3-K27me3 and Xist RNA coating. The fourth X-linked gene, *Pgkl*, however, was monoallelically expressed in *Eed*^{fl/fl} TSCs but biallelically expressed in *Eed*^{-/-} TSCs (Fig. 5.2). *Pgkl*, therefore, is no longer silenced on the inactive-X when EED is deleted. In summary, these results imply that some genes, but not others, are subject to derepression from the previously inactive paternal X-chromosome when *Eed* is deleted.

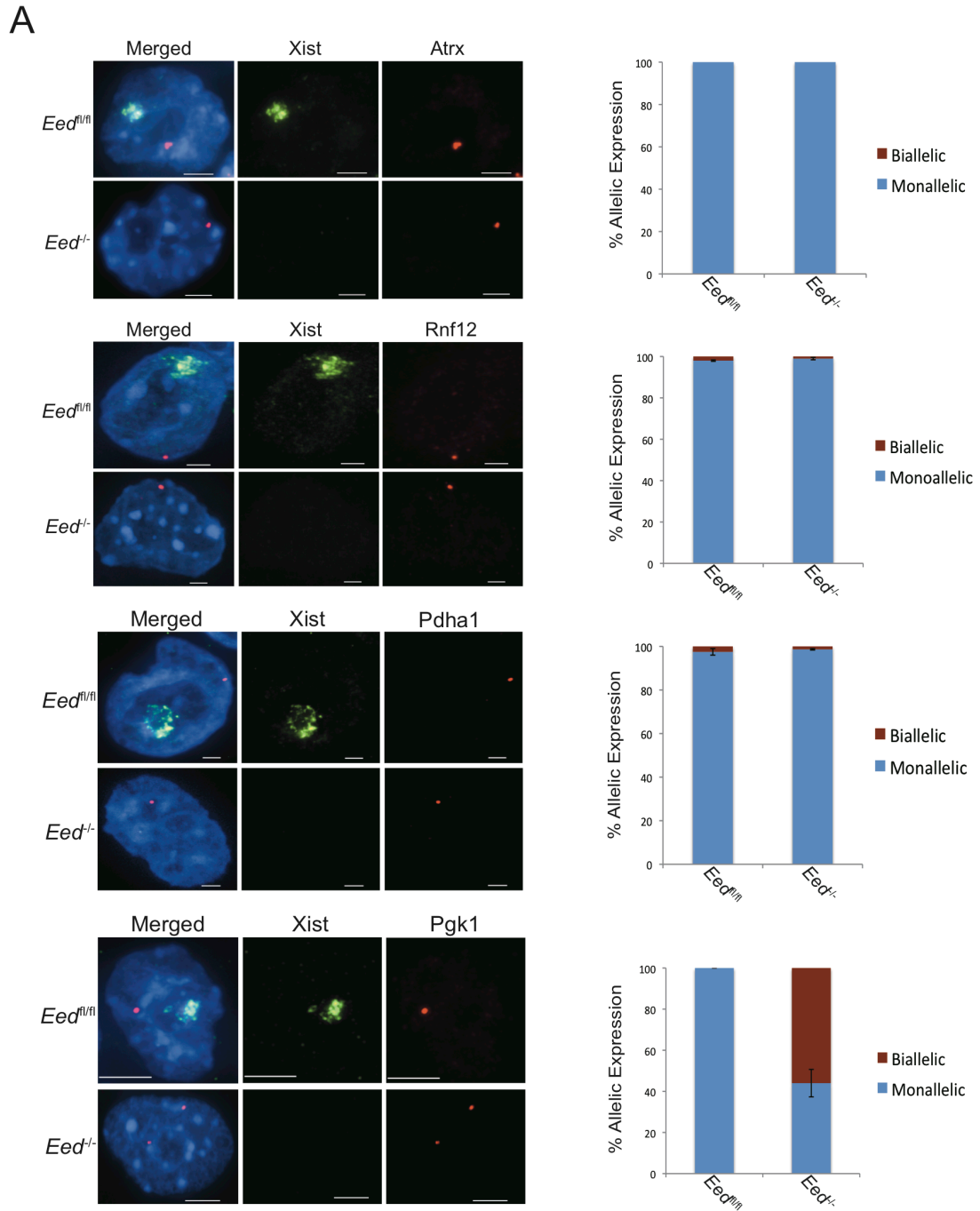


Figure 5.2: RNA FISH analysis of X-linked gene expression in *Eed^{-/-}* TSCs. Left, RNA FISH detection of Xist RNA coating (green) and RNAs of four X-linked gene (*Atrx*, *Rnf12*, *Pdha1*, and *Pgk1*, red) in *Eed^{fl/fl}* and *Eed^{-/-}* TSCs. Nuclei are stained blue with DAPI. Scale bar, 2 μ m. Right, quantifications of the RNA FISH data. Whereas *Atrx*, *Rnf12*, and *Pdha1* remain silenced in *Eed^{-/-}* TSCs, *Pgk1* is derepressed from the inactive-X in the absence of EED.

5-4: X-chromosome-wide Identification of Derepressed Genes in *Eed*^{-/-} TSCs

To comprehensively identify genes across the inactive paternal X-chromosome that require PRC2 and Xist RNA coating for stable silencing, we performed RNA-Seq on *Eed*^{+/+} and *Eed*^{fl/fl} (both classified as control WT genotype hereafter) as well as on *Eed*^{-/-} TSCs. Both the WT and mutant TSC lines are F1 hybrid and harbor polymorphic X-chromosomes, with the maternal-X derived from the *Mus musculus* 129/S1 mouse strain and the paternal-X from the *Mus molossinus* JF1/Ms strain. The genomes of the 129/S1 and JF1/Ms strains are highly divergent and contain many defined single nucleotide polymorphisms (SNPs) (Keane et al., 2011; Takada et al., 2013; Yalcin et al., 2011). Since TSCs undergo imprinted X-inactivation, the JF1/Ms-derived paternal X-chromosome is the inactive-X and the 129/S1-derived maternal X-chromosome is the active-X. We were thus able to exploit the strain-specific SNPs to interrogate parent-of-origin-specific expression of X-linked genes across the X-chromosome. For RNA-Seq analysis, we generated 100-base pair paired-end reads from strand-specific libraries to facilitate accurate allele-specific mapping of sequencing reads (see detailed discussion in Methods).

We first assessed EED mRNA expression in *Eed*^{-/-} TSCs in the RNA-Seq data. Compared to *Eed*^{fl/fl} TSCs, *Eed* was negligibly detected in *Eed*^{-/-} TSCs. Notably, reads mapping to the deleted *Eed* exon 7 were missing entirely in *Eed*^{-/-} TSCs (Fig. 5.3A). The RNA-Seq data also showed that Xist RNA was robustly expressed in *Eed*^{fl/fl} TSCs but was significantly reduced in *Eed*^{-/-} TSCs, in agreement with the RNA FISH results (Fig. 5.3B). For allele-specific analysis, we identified 413,974 SNPs on the X-chromosome based on previously published whole-genome sequencing of the divergent strains used to generate the TSCs (Keane et al., 2011; Takada et al., 2013; Yalcin et al., 2011). From the RefSeq mm9 genome annotation, 89% of the non-redundant set of X-linked genes contained at least one SNP (Fig. 5.3C).

To map RNA-Seq reads in an allele-specific manner, we created *in silico* strain-specific reference genomes by substituting SNPs from the 129/S1 and JF1/Ms mouse strains into the reference genome from the C57BL/6J strain. We then separately mapped the RNA-Seq reads to each strain-specific reference genome using STAR, permitting zero mismatches between the 100 base pair paired-end reads and the strain-specific genomes. Reads expressed from the JF1/Ms allele that overlapped SNP sites would map uniquely to the JF1/Ms reference, while reads expressed from the 129/S1 allele would map only to the 129/S1 genome, facilitating quantification of allelic expression. Use of *in silico* strain-specific reference genomes also minimizes the mapping bias that can skew read counts towards the reference allele when mapping to a single reference genome (Degner et al., 2009), though due to structural rearrangements and indels between genomes reference mapping bias cannot be eliminated entirely (see detailed discussion in Methods). For each gene, we identified reads overlapping known SNPs and calculated the percent inactive-X expression by averaging the fraction of reads that mapped to the paternal (JF1/Ms) allele at all SNP sites with $\geq 10X$ read coverage in that gene (Fig. 5.4).

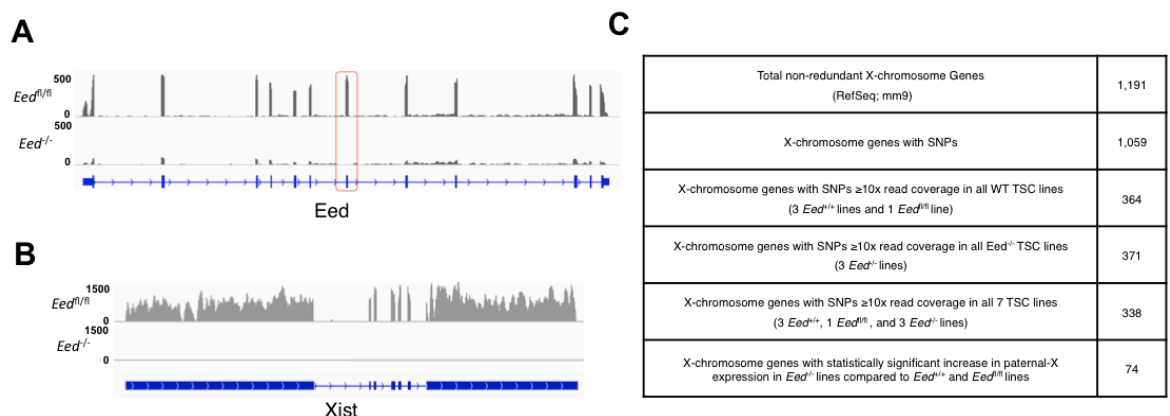


Figure 5.3: RNA-Seq profiling of X-linked gene expression in *Eed*^{+/+}, *Eed*^{fl/fl}, and *Eed*^{-/-} TSCs. (A) RNA-Seq detects robust expression of full-length *Eed* mRNA in *Eed*^{fl/fl} TSCs. In *Eed*^{-/-} TSCs, minimal levels of *Eed* mRNA are observed, lacking expression altogether from the excised exon 7 (red box). (B) Xist RNA expression in *Eed*^{fl/fl} and *Eed*^{-/-} TSCs. (C) Table summarizing allele-specific RNA-Seq analysis of X-linked genes.

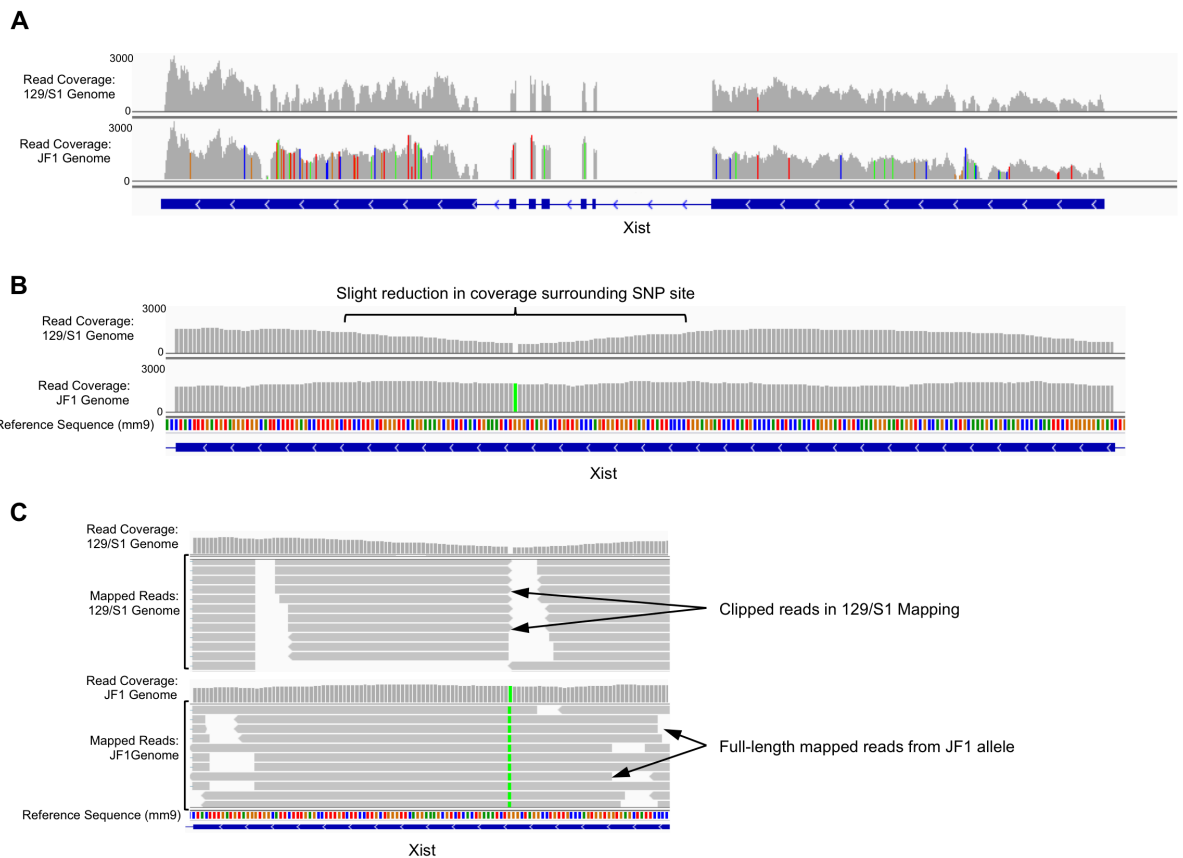


Figure 5.4: Allelic Read Mapping with STAR. All panels show varying resolutions of read and read coverage data at the *Xist* locus from a representative wild-type sample mapped separately to the 129/S1 and JF1 *in silico* genomes. Because *Xist* RNA is expressed from the inactive-X, we expect reads overlapping SNP sites to map to the JF1 reference genome exclusively. We observe a decrease in read coverage surrounding SNP sites in the 129/S1 mapping, as well as the presence of clipped reads adjacent to the SNP site.

To evaluate allele-specific expression in the TSCs, we first identified genes that contained at least one SNP with $\geq 10X$ read coverage. Three hundred and sixty-four and 371 genes in the four WT TSC lines and three *Eed*^{-/-} TSC lines, respectively, satisfied the 10X coverage threshold (Fig. 5.3C). We assessed relative expression of genes from the inactive paternal vs. the active maternal X-chromosome by calculating the proportion of SNP-overlapping reads mapping to the paternal vs. the maternal allele in every TSC line. As expected for TSCs, most genes are expressed almost exclusively from the maternally-inherited active X-chromosome. A small subset of genes, however, showed substantial expression from the

paternal-X in WT *Eed*^{+/+} and *Eed*^{fl/fl} TSCs (Fig. 5.5A; see Table 5-1 at end of chapter for allelic information for all genes and TSC lines). Genes expressed from the inactive-X are known as escapers of X-inactivation (reviewed in (Berletch et al., 2010; Peeters et al., 2014)). Levels of inactive-X expression vary widely between genes. Based on average paternal-X expression in our wild-type cells, we identify 65 genes with less than 1% expression from the inactive-X, 215 genes expressed at very low, but detectable, levels from the inactive X-chromosome (i.e., 1-5% of total expression from the inactive-X), and 84 genes displaying more substantial levels of inactive-X expression (>5%). We defined X-inactivation escapees as genes whose paternal allele expression is $\geq 10\%$ of total expression. The 10% threshold has previously been used to define escape genes in both mouse and human (Balaton et al., 2015; Carrel and Willard, 2005; Cotton et al., 2013; Marks et al., 2015; Yang et al., 2010). Using this threshold, we found that 20 of 364 genes (5%) escape X-inactivation in all three *Eed*^{+/+} and the sole *Eed*^{fl/fl} TSCs (Fig. 5.5A). This set includes genes previously shown to escape X-inactivation such as *Kdm5c* and *Eif2s3x* (Balaton et al., 2015; Berletch et al., 2015b; Calabrese et al., 2012; Yang et al., 2010). Included are also genes that escape X-inactivation in TSCs but not in other tissues, such as *Yipf6* (Calabrese et al., 2012). An additional 12 genes not previously reported to escape X-inactivation display $\geq 10\%$ of total expression from the paternal X-chromosome in all four WT TSC lines; these unique escapers include genes such as *Dusp9* and *Atp7a*. Both tissue-specific differences and strain-specific differences in escape from X-inactivation may explain why these genes have not previously been identified as escapees.

We next interrogated expression from the paternal X-chromosome in *Eed*^{-/-} TSCs. Compared to the WT TSCs, a substantially higher number of genes were expressed from the paternal allele in all three *Eed*^{-/-} TSCs (112/371, or 30%) (Fig. 5.5B; see also Table 5.1).

Contained within this subset are most of the genes that escape X-inactivation in the four WT TSCs (18 out of 20 escape genes). The two escapees unique to WT TSCs do not reach the required 10x depth of coverage at SNP sites in *Eed*^{-/-} TSCs to permit calculation of allelic expression ratio, but do show expression from the paternal-X in the mutant cells. An additional 94 genes that are X-inactivated in the WT TSCs were expressed from the paternal X-chromosome in the three *Eed*^{-/-} TSCs. Overall, *Eed*^{-/-} TSCs displayed a much higher percentage of genes that are expressed from the paternal X-chromosome (30%) compared to WT TSCs (5%).

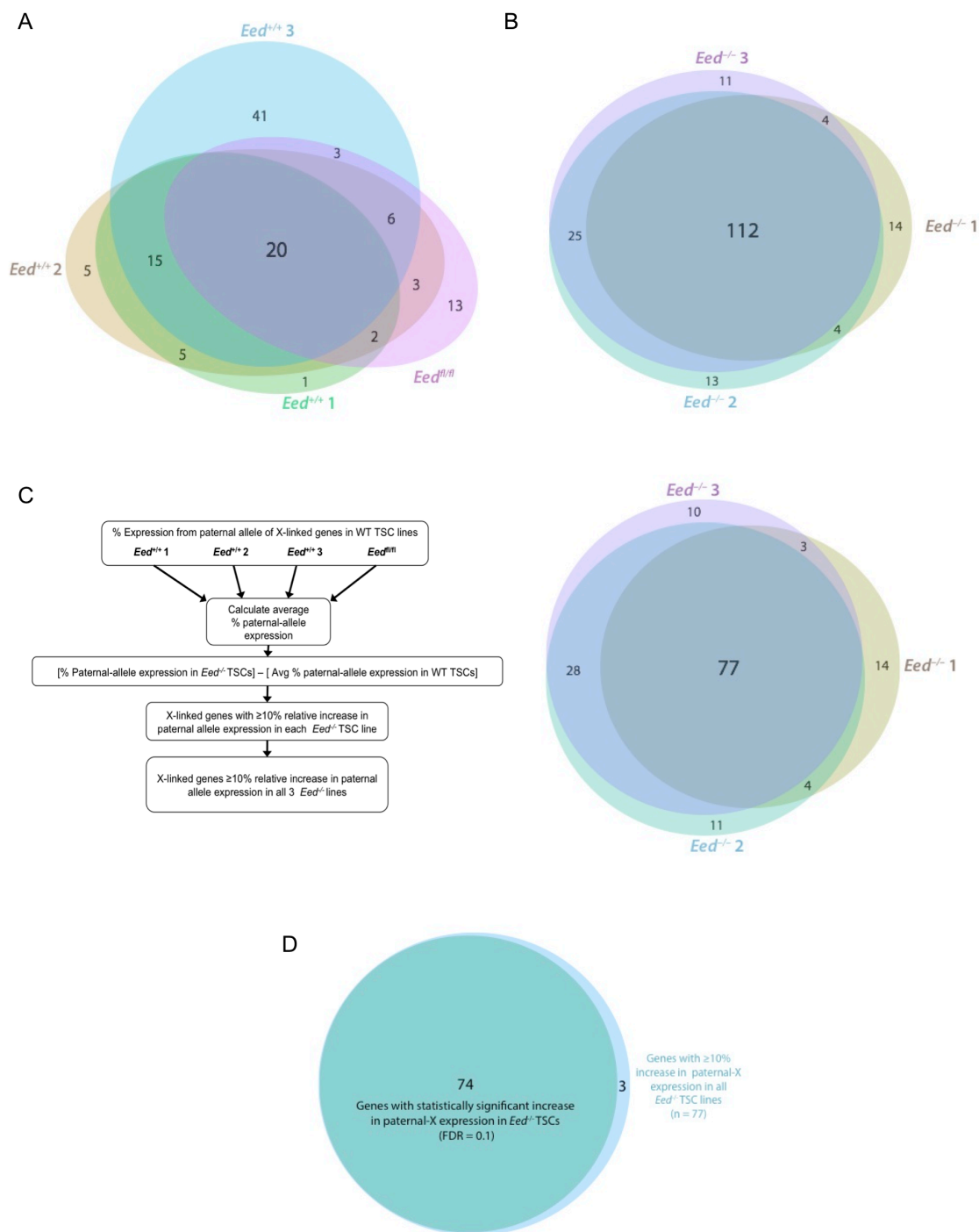


Figure 5.5: Identification and characterization paternal-X expression in *Eed^{+/+}*, *Eed^{fl/fl}*, and *Eed^{-/-}* TSCs. (A) Euler diagram assessing escape from X-inactivation, defines as ≥10% expression from the paternal-X, in three *Eed^{+/+}* TSC lines and one *Eed^{fl/fl}* TSC line. All four wild-type lines show a low level of escape from X-inactivation, with 20 genes (5%) consistently escaping X-inactivation in all four cell lines. (B) Euler diagram assessing escape from X-inactivation in three *Eed^{-/-}* TSC lines. Upon loss of EED, all cell lines show a higher percentage of genes escaping X-inactivation, with 106 (28%) of genes escaping in all three cell lines. (C) Comparison of percent paternal-X

expression in *Eed*^{-/-} TSCs compared to WT TSCs. Percent paternal-X expression for individual *Eed*^{-/-} lines was compared to the average percent paternal-X expression in WT TSCs (left). In each line, genes that showed $\geq 10\%$ increase in paternal-X expression compared to the average level in WT cells were identified. Right, Euler diagram comparing the genes displaying a $\geq 10\%$ increase in paternal-X expression in each *Eed*^{-/-} line. Seventy-seven genes consistently show an increase in paternal-X expression level in all three *Eed*^{-/-} cell lines. (D) Identification of genes showing a statistically significant difference in percent paternal-X expression in *Eed*^{-/-} TSCs compared to WT TSCs. Percent paternal-X expression in the four WT cell lines and three *Eed*^{-/-} lines was compared by T-test for the 77 genes found to show a consistent increase in paternal-X expression in *Eed*^{-/-} lines. Of these, 74 genes were found to show a statistically significant increase in paternal-X expression in *Eed*^{-/-} TSCs, following Benjamini-Hochberg correction for multiple testing (FDR=0.1).

We next calculated the extent of upregulation of genes that were expressed from the paternal-X in *Eed*^{-/-} TSCs (Fig. 5.5C). We compared the ratio of paternal to total (paternal + maternal) allelic expression for a common set of 338 X-linked genes with $\geq 10X$ read coverage in each of the three *Eed*^{-/-} TSC lines to the average percent paternal allele expression in the four WT lines (Fig. 5.5C). We defined genes whose expression from the paternal allele was increased by $\geq 10\%$ in *Eed*^{-/-} TSCs compared to the standard level of paternal allele expression observed in WT TSCs as candidate derepressed X-linked genes in the mutants. A total of 77 out of the 338 genes, or 23%, reached this threshold. Seventy-two of the 77 genes are inactivated in WT TSCs. The remainder escaped X-inactivation in the WT TSCs, but were nevertheless expressed from the paternal allele at a higher level in *Eed*^{-/-} TSCs.

For the set of genes that reached the threshold for calculating allelic expression in only WT or only *Eed*^{-/-} TSCs (7% and 9% of genes with allelic information, respectively), the ratios of paternal allele:total expression could not be compared. These genes reach the 10X coverage threshold in all WT lines or all mutant lines, however, one or more TSC lines does not reach the required level of SNP coverage in the other genotype. For these subsets of genes, we calculated the percent paternal allele expression in the individual genotypes. Of the 26 genes that are uniquely expressed with ≥ 10 reads overlapping at least one SNP site in the WT TSC lines, only one, *Xist*, was expressed from the paternal allele.

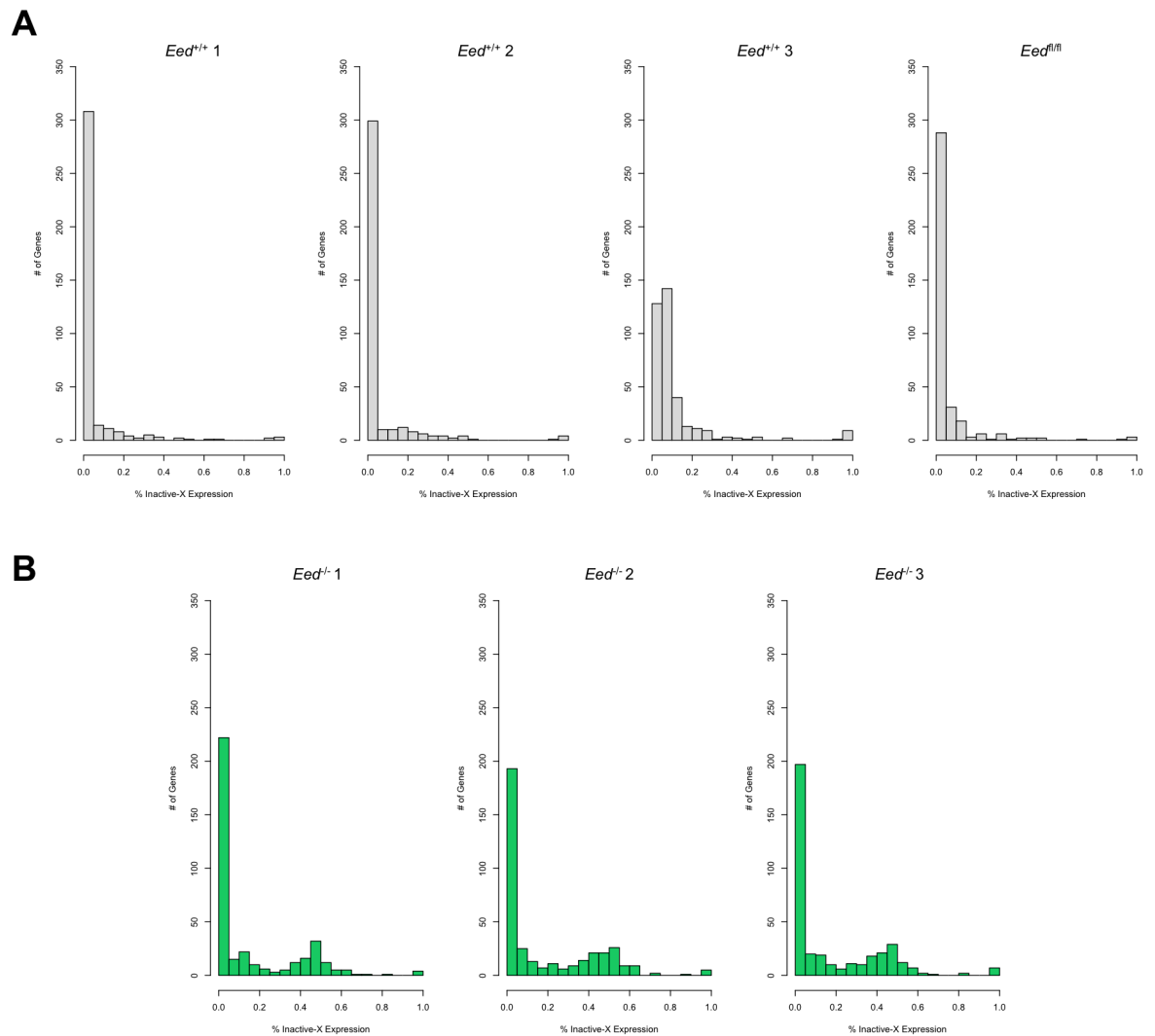


Figure 5.6: Distribution of Allelic Expression Profiles for X-linked Genes in Individual Cell Lines. (A) Allelic distribution profiles for 364 genes reaching the 10X coverage threshold in all WT cell lines. Lines show varying distributions of allelic expression, however, genes show predominantly <10% paternal-X expression. (B) Allelic distribution profiles for 371 genes reaching the 10X coverage threshold in all *Eed*^{-/-} lines. A greater proportion of genes in *Eed*^{-/-} TSCs show >10% expression from the paternal-X.

For the 33 genes that reached ≥ 10 read coverage threshold only in *Eed*^{-/-} TSCs, a higher proportion of the X-linked genes were expressed from the paternal allele (9, or 27%). These results are consistent with our observations of increased escape in *Eed*^{-/-} TSCs within the set of 368 genes that reach the 10X read coverage threshold in all seven lines. Distributions of allelic expression for each WT and *Eed*^{-/-} TSC line are plotted in Figure 5.6.

For genes with $\geq 10\%$ increase in paternal-X expression in all *Eed*^{-/-} TSC lines compared to the WT TSC lines, we performed T-tests to calculate the statistical significance of the change in allelic expression. Of the 77 genes that demonstrated an increase in expression from the paternal-X in all three *Eed*^{-/-} TSC lines, 74 displayed a statistically significant difference between the proportion of paternal-X expression in *Eed*^{-/-} TSC lines vs. the control WT TSC lines (FDR = 0.1) (Fig. 5.5D; Table 5.1).

In principle, the relative increase in expression from the paternal-X allele in *Eed*^{-/-} TSCs could be driven by one of two major mechanisms: either increased expression of the paternal-X allele or reduced expression from the maternal-X allele. In order to distinguish between these two possibilities, we performed differential analysis of X-linked gene expression between WT and *Eed*^{-/-} TSCs (Love et al., 2014). For genes whose shift in allelic expression is driven by derepression of the paternal-X allele, both the percent of total expression contributed by the paternal allele as well as the total expression itself are expected to increase, since these genes are now expressed from both the maternal and paternal X-chromosomes. SNP-containing reads provide only sparse coverage of genes, thus, SNP-overlapping reads alone cannot be used for differential expression analysis. We therefore calculated read coverage of the entire gene, including reads overlapping both polymorphic and non-polymorphic sites. From the total read counts, we calculated paternal-X expression by multiplying the number of mapped reads for each gene by the proportion of SNP containing reads mapping to the paternal X-chromosome (See detailed description in Methods). We then performed differential expression analysis on these calculated paternal-X expression levels between the four WT TSC lines and the three *Eed*^{-/-} TSC lines (See Table 5.2 at end of chapter; Fig. 5.7A) (Love et al., 2014). The majority of X-linked genes exhibiting a relative increase in expression from the paternal allele also showed an

increase in the absolute expression from the paternal X-chromosome (65/74, or 85%). The remaining 11 genes displayed either negligible changes in the absolute level of paternal-X expression or a decrease in paternal-X expression. In these genes, the observed shift in the proportion of paternal allele expression is likely due to down-regulation of the maternal allele.

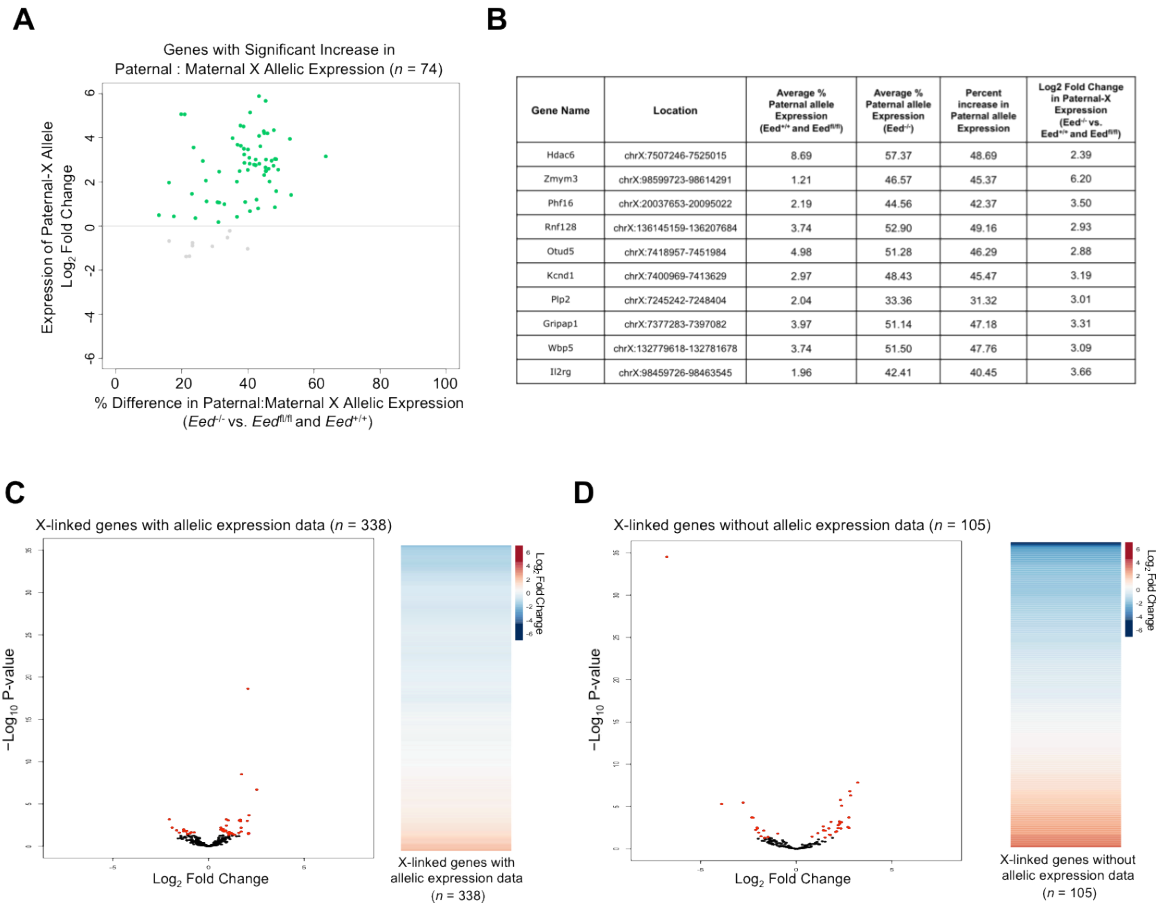


Figure 5.7: Differential Expression Analysis of X-linked Genes. (A) Plot of \log_2 fold change between genotypes in the expression of paternal X-chromosome genes (Y axis) versus percent difference in paternal allele expression (X axis) for the 74 X-linked genes exhibiting a relative increase in the proportion of paternal:maternal allele expression, as calculated by DESeq2. (B) Table summarizing the 10 X-linked genes that show the greatest increase in paternal allele expression in *Eed*^{-/-} TSCs. (C) Differential expression analysis of X-linked genes. Heat maps and volcano plots illustrating differential expression results for genes with allelic expression data ($n = 338$) and genes without allelic expression data ($n = 105$). Both groups show similar percentages of upregulated and downregulated genes, as well as similar \log_2 fold change magnitudes for genes that are differentially expressed. In volcano plots, each points indicates a single gene; red points indicate genes that are significantly differentially expressed between WT and *Eed*^{-/-} TSCs ($p < 0.05$ following BH correction for multiple testing).

We therefore defined paternally derepressed genes as the set of 65 X-linked genes (19% of the 338 genes assayed) that exhibit both relative and absolute upregulation of the paternal allele in *Eed*^{-/-} TSCs compared to WT TSCs. The ten highest derepressed X-linked genes in *Eed*^{-/-} TSCs are summarized in Fig. 5.7B. To confirm that the gene-specific derepression observed is not simply a function of the thresholds set for read coverage and allelic balance, we additionally assessed expression from the paternal X-chromosome in *Eed*^{+/+}, *Eed*^{fl/fl}, and *Eed*^{-/-} TSC lines at a less stringent coverage threshold, requiring only 5X coverage of SNPs. The lower stringency criteria yielded derepression of a similar subset of paternal X-linked genes in *Eed*^{-/-} TSCs (21%) (Fig. 5.8; see Table 5.3 at end of chapter).

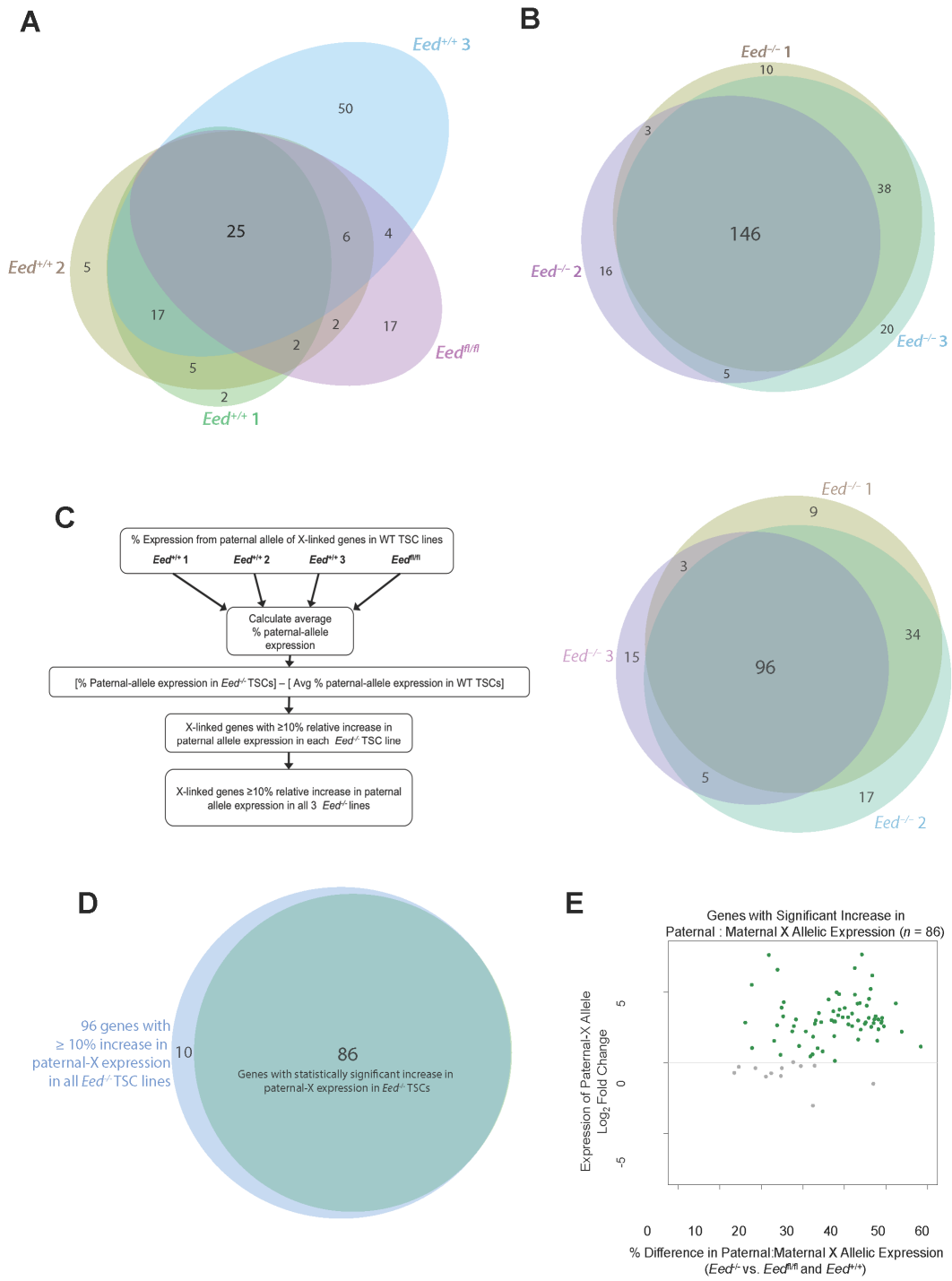


Figure 5.8: Identification and characterization paternal-X expression in *Eed*^{+/+}, *Eed*^{fl/fl}, and *Eed*^{-/-} TSCs at a 5X read coverage threshold. (A) Euler diagram assessing escape from X-inactivation, defined as $\geq 10\%$ expression from the paternal-X, in three *Eed*^{+/+} TSC lines and one *Eed*^{fl/fl} TSC line. (B) Euler diagram assessing escape from X-inactivation in three *Eed*^{-/-} TSC lines. (C) Comparison of percent paternal-X expression in *Eed*^{-/-} TSCs compared to WT TSCs. Percent paternal-X expression for individual *Eed*^{-/-} lines was compared to the average percent paternal-X expression in WT TSCs (left). In each line, genes that showed $\geq 10\%$ increase in paternal-X expression compared to the average level in WT cells were identified. Right, Euler diagram comparing the genes displaying a $\geq 10\%$ increase in paternal-X expression in each *Eed*^{-/-} line. (D) Identification of genes showing a statistically significant difference in percent paternal-X expression in *Eed*^{-/-} TSCs compared to WT TSCs. Percent paternal-X expression in the four WT cell lines and three *Eed*^{-/-} lines was compared by T-test, and P-values were corrected for multiple testing (FDR=0.1). (E) Plot of \log_2 fold change between genotypes in the expression of paternal X-chromosome genes (Y axis) versus percent difference in paternal allele expression (X axis) for X-linked genes exhibiting a relative increase in the proportion of paternal:maternal allele expression, as calculated by DESeq2.

To extend the allelic expression calculations and differential expression analysis above, we evaluated derepression of all RefSeq X-linked genes, including non-SNP containing genes, in *Eed*^{-/-} TSCs. We first tabulated X-linked genes with at least five reads mapped annotated exons in at least one of the seven cell lines. Expression of four hundred forty three X-linked genes surpassed 0.2 RPKM in all seven cell lines, a threshold established based on the minimum expression levels of genes that harbored SNPs. In addition to the 338 genes that contained SNPs with $\geq 10X$ coverage threshold, we identified 82 expressed SNP-containing genes that did not reach the 10X coverage threshold at SNP sites and 23 expressed genes that lacked SNPs altogether. Compared to WT TSCs, *Eed*^{-/-} TSCs displayed a statistically significant upregulation of 43 X-linked genes (10% of expressed X-chromosome genes; FDR=0.05). This number differs from the 65 derepressed genes previously identified for two reasons: First, derepressed genes were identified on the basis of calculated paternal-X expression, while this number takes into account changes in maternal expression as well. Second, some derepressed genes show only modest upregulation (1.1 to 1.5-fold increase in paternal-X expression). These modest fold changes are consistent with a 10% or greater increase in paternal-X expression, but, depending on variability between cell lines and total read coverage of each gene, does not necessarily represent a statistically significant increase in expression. To understand if loss of EED affects

the 338 genes with SNPs and the 105 genes without SNPs differently, we calculated differential expression of X-linked genes in both groups. Of the 338 allelically analyzed genes, 31, or 9%, were significantly upregulated (Fig. 5.7C). Of the 105 genes without allelic information, a slightly higher percentage was significantly upregulated (12 genes or 11%) (Fig. 5.7D). We also identified statistically significant downregulation of 31 X-linked genes in *Eed*^{-/-} TSCs (7% of expressed X-chromosome genes). Once again, the percentage of downregulated X-linked genes with SNPs is similar to the percentage of downregulated genes that lacked SNPs (Fig. 5.7C-D). The downregulation of X-linked genes in *Eed*^{-/-} TSCs may be indirect, for example due to the induction of transcriptional silencers in the absence of EED.

We next validated the allele-specific RNA-Seq data by RT-PCR followed by Sanger sequencing. We selected six genes distributed across the X-chromosome, *Hdac6*, *Wdr13*, *Med12*, *Pgk1*, *Wbp5*, and *Rnf128*, that are found by RNA-Seq to be derepressed from the paternal X-chromosome in *Eed*^{-/-} TSCs (Fig. 5.9A). We also chose six X-linked genes, *C330007P06Rik*, *Atp11c*, *Fam3a*, *Rnf12*, *Atrx*, and *Pdhal*, that stably maintain silencing of the paternal allele in *Eed*^{-/-} TSCs (Fig. 5.9A). For each gene, we selected amplicons spanning SNPs that differ between the 129/S1 and JF1/Ms mouse strains and performed RT-PCR followed by Sanger sequencing (see Table 5.4 at end of chapter for primer and SNP information). For all six genes derepressed in *Eed*^{-/-} TSCs, the Sanger chromatograms exhibited expression from only the maternal (active)-X allele in all four WT TSC lines but biallelic expression in all three *Eed*^{-/-} TSC lines, consistent with the RNA-Seq data (Fig. 5.9B). For the six X-linked genes for which there was no allelic shift in the RNA-Seq data, the WT as well as the *Eed*^{-/-} TSCs displayed expression from only the maternal allele (Fig. 5.9C). We also validated the presence of the genomic loci of the genes assayed by RT-PCR. Sanger sequencing of PCR amplified genomic

DNAs from WT and *Eed*^{-/-} TSC lines, using amplicons spanning the same polymorphic sites assayed by RT-PCR, demonstrated that both alleles of all the genes tested were intact in all TSC lines (Fig 5.10 A-B).

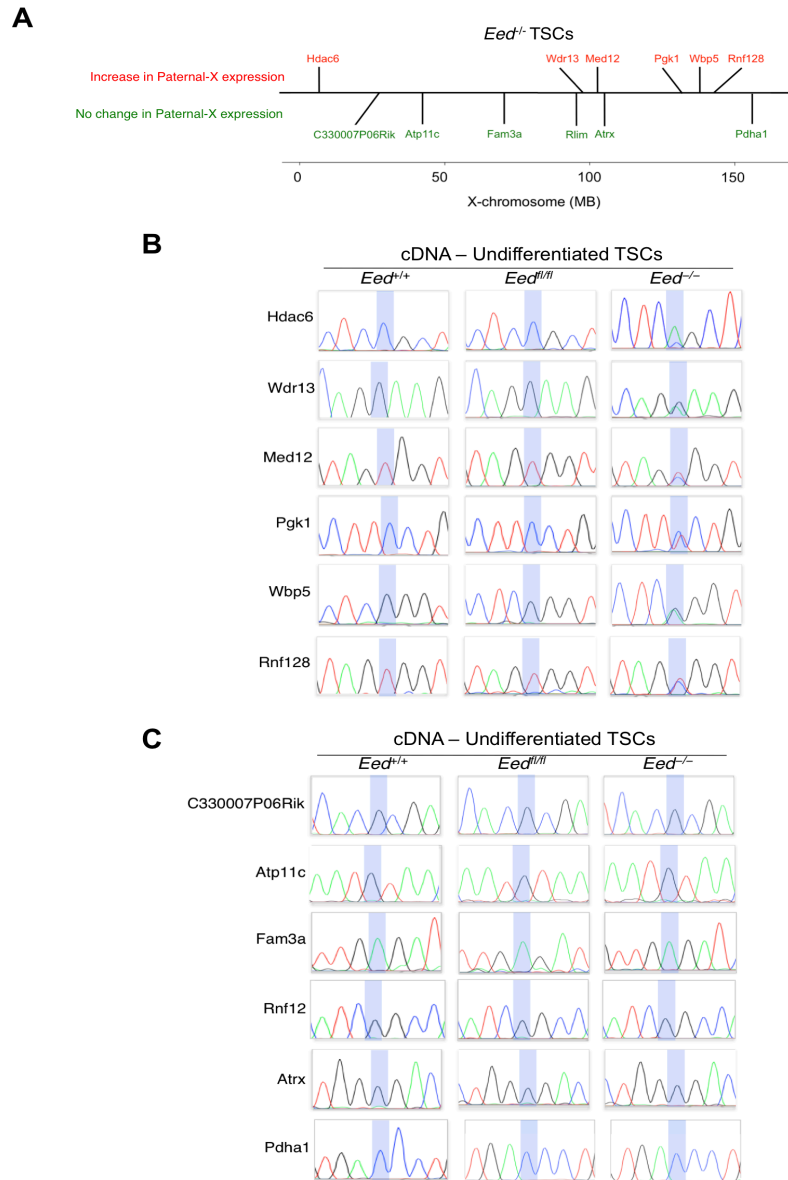


Figure 5.9: Validation of RNA-Seq results by RT-PCR and Sanger sequencing. (A) Schematic of chromosomal locations of genes selected for validation. From RNA-Seq data, six X-linked genes that display an increase in paternal allele expression in *Eed*^{-/-} TSCs (top, red) and six genes that show no allelic shift in *Eed*^{-/-} TSCs (bottom, green) were selected. (B) Sanger sequencing chromatograms of amplified cDNAs from *Hdac6*, *Wdr13*, *Med12*, *Pgl1*, *Wbp5*, and *Rnf128*. All 6 genes are derepressed from the paternal X-chromosome in *Eed*^{-/-} TSCs by RNA-Seq. Blue highlights mark SNPs that differ between the 129/S1 strain (maternally-inherited X-chromosome in all TSC lines) and the JF1/Ms strain (paternally-inherited X-chromosome in all TSC lines). (C) Sanger sequencing

chromatograms from RT-PCR products for *C330007P06Rik*, *Atp11c*, *Fam3a*, *Rnf12*, *Atrx*, and *Pdha1*. These six X-linked genes exhibit no change in paternal allele expression in *Eed*^{-/-} TSCs by RNA-Seq.

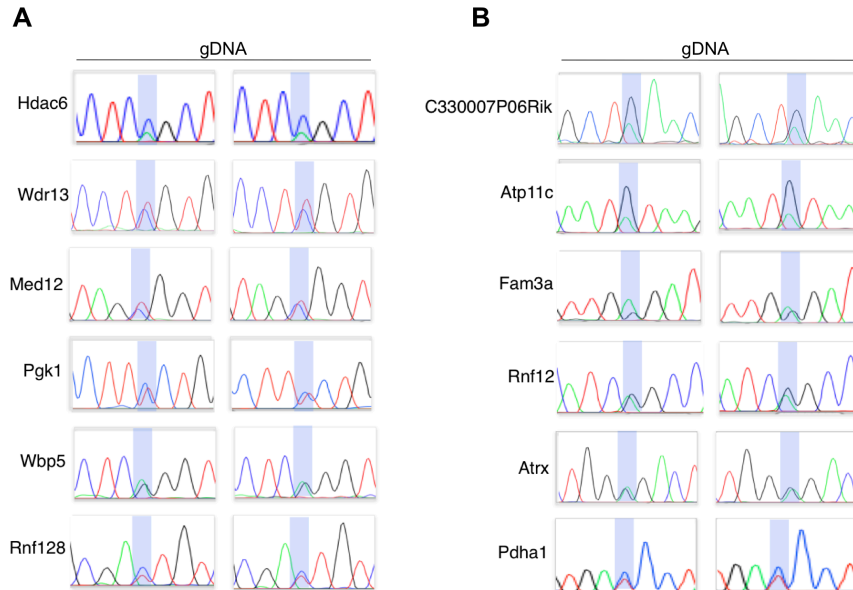


Figure 5.10: Genomic PCR for selected X-linked genes validates the presence of both alleles in DNA samples from WT and *Eed*^{-/-} TSCs

5-5: Characterization of Derepressed Genes

RNA-Seq analysis of WT and *Eed*^{-/-} TSCs identified a small subset of genes that are derepressed from the inactive-X upon loss of EED, which abrogates H3-K27me3 and Xist RNA expression. We next sought to determine if these genes shared any unifying features in WT TSCs, which may predict their derepression when EED is abrogated. We first tested if the derepressed X-linked genes were clustered in specific regions of the X-chromosome, which may suggest that those regions are particularly sensitive to loss of EED, H3-K27me3, or Xist RNA coating. The derepressed genes were distributed along the length of the X-chromosome, and did not occupy any one specific region (Fig. 5.11A). A subset of the derepressed genes, however, was clustered near the centromere and in a few other regions of the X-chromosome. We reasoned that the three-dimensional structure of the X-chromosome might explain such non-

linear arrangement of the clusters. We took advantage of published allele-specific Hi-C data from mouse embryonic stem cells (ESCs) (Dixon et al., 2012; Minajigi et al., 2015). The allele-specific Hi-C data identifies topologically associated domains (TADs) on the active and inactive X-chromosomes. In mouse cells, the active-X forms a series of well-defined TADs. The inactive-X, on the other hand, is structured into two large superdomains that meet at a “hinge” region centered on the *Dxz4* minisatellite repeat, rather than into the discrete TADs that characterize the active-X. When Xist RNA is knocked-down in X-inactivated cells, the inactive X-chromosome now takes on a conformation more similar to the active-X (Minajigi et al., 2015). We hypothesized that the derepressed X-linked genes in *Eed*^{-/-} TSCs may occupy regions that correspond to specific TADs on the active X-chromosome. The spike of derepressed genes near the centromere indeed occupies a single TAD on the active X-chromosome in WT ESCs and in X-inactivated cells in which Xist RNA is knocked-down (Minajigi et al., 2015). Nevertheless, many derepressed X-linked genes do not appear to cluster in specific TADs or lie in or near defined TAD boundaries (Fig. 5.12).

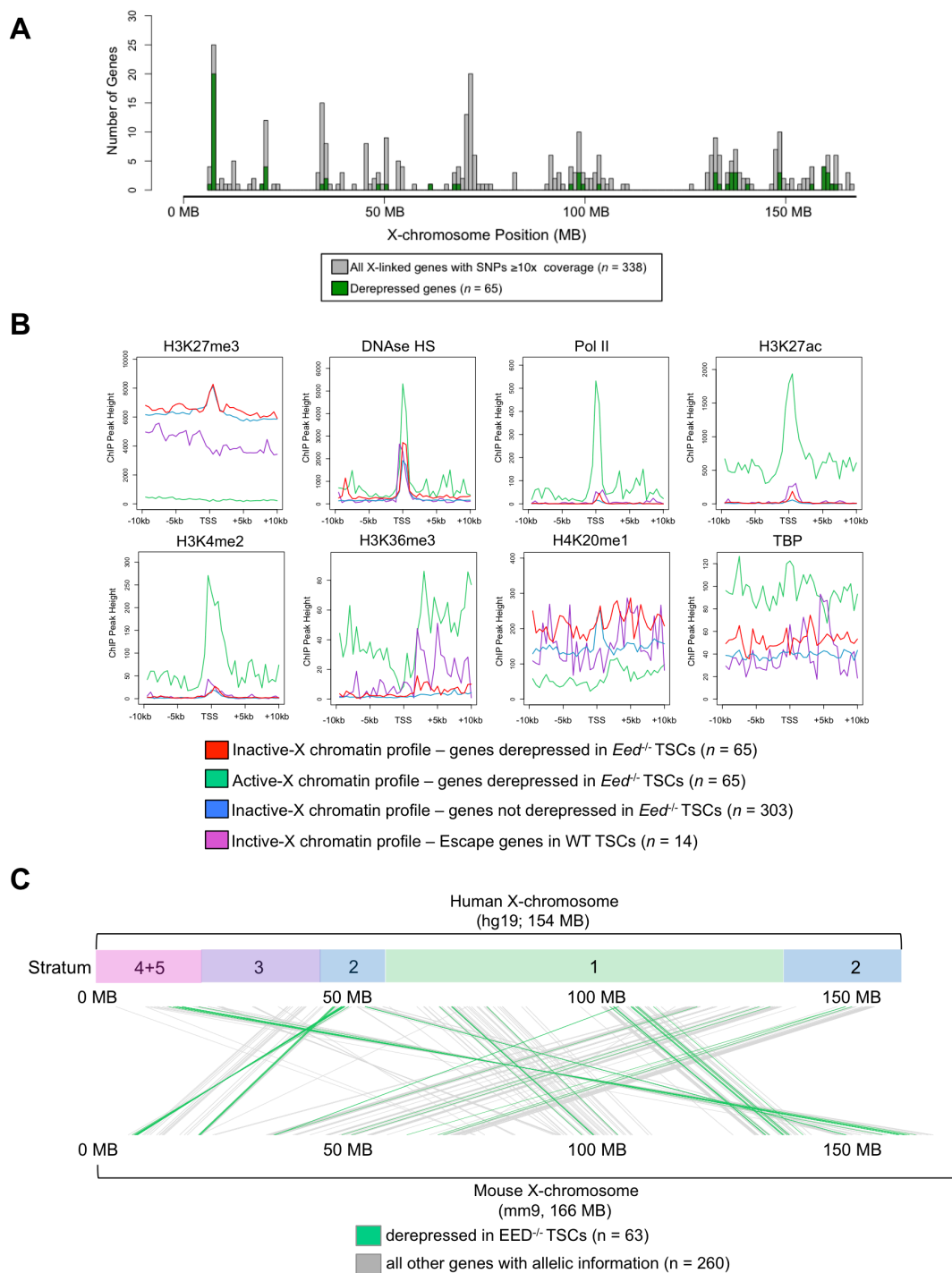


Figure 5.11: Chromatin context and genomic location of derepressed X-linked genes (A) Histogram indicating the location of all 338 X-linked genes with informative SNPs at $\geq 10\times$ coverage (gray bars) and the 65 upregulated genes whose relative expression from the paternal allele is significantly increased (green bars). Derepressed X-linked genes are distributed across the length of the X-chromosome. (B) Allelic profiles of H3-K27me3, DNase hypersensitivity, PolII occupancy, H3K27ac, H3K4me2, H3K36me3, Tata binding protein (TBP) occupancy and CTCF occupancy were calculated from previously published ChIP-seq data from F1 hybrid C57Bl/6J x CAST/EiJ

TSCs (Calabrese et al. 2012). Plots show average chromatin modification or occupancy profiles 10kb upstream and 10kb downstream of the transcription start site for the inactive X-chromosome for derepressed genes, non-derepressed genes, and escapers of X-inactivation. The active-X chromatin profile for the 65 genes derepressed from the inactive-X is also shown for comparison. (B) Plot illustrating the location of homologous human X-linked genes compared to mouse X-linked genes with an increase in paternal allele expression in *Eed*^{-/-} TSCs (green lines) versus all X-linked genes with $\geq 5X$ coverage (gray lines). Genes that require EED and/or Xist RNA for repression do not exhibit any significant clustering pattern within the ancient evolutionary strata of the human X-chromosome.

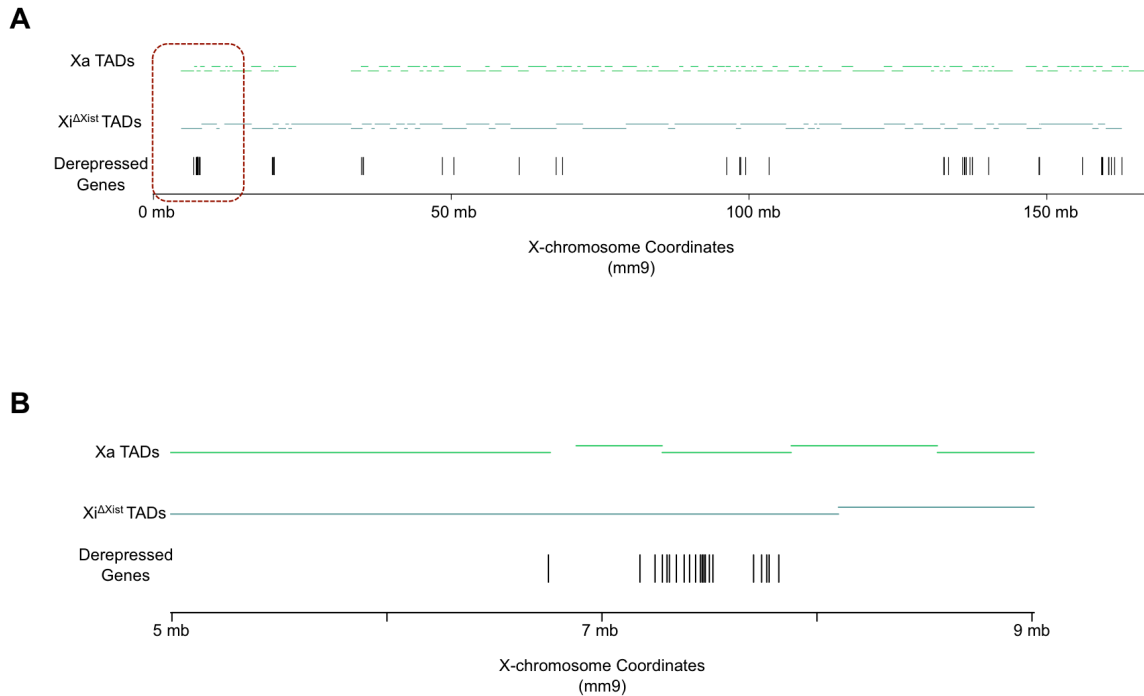


Figure 5.12: Locations of X-chromosome Topologically Associated Domains compared to derepressed genes. Horizontal lines mark TADs identified in previously published data (Dixon et al., 2012; Minajigi et al., 2015). Derepressed genes (locations indicated by vertical lines) do not cluster in individual TADs or at TAD boundaries.

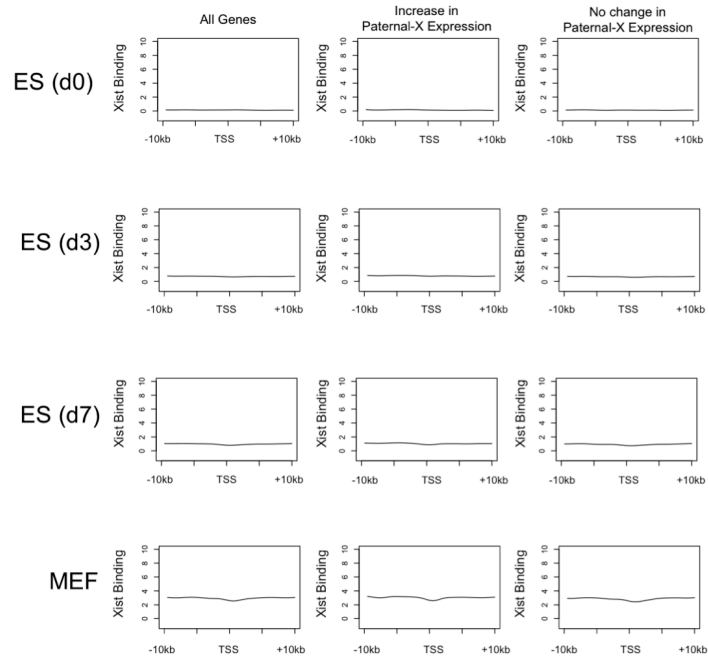
We next interrogated if the genes that require EED, H3-K27me3, or Xist RNA to maintain repression share known chromatin features in WT TSCs. We reasoned that the chromatin context could indicate whether genes were susceptible to reactivation upon loss of EED and Xist RNA coating. Due to the essential role of EED in H3-K27me3 catalysis, and the proposed silencing function of H3-K27me3, we first hypothesized that genes sensitive to EED loss are normally occupied by higher levels of H3-K27me3 compared to genes whose inactive-X

expression is unchanged. Using published H3-K27me3 chromatin immunoprecipitation-sequencing (ChIP-Seq) data from WT F1 hybrid TSCs (Calabrese et al., 2012), we examined H3-K27me3 profile in WT and *Eed*^{-/-} TSCs at the transcription start sites (TSSs) of the allelically analyzed X-chromosome genes. As a frame of reference, we also assessed H3-K27me3 ChIP-Seq profile of the active X-chromosome alleles of the set of 65 X-linked genes that are derepressed in *Eed*^{-/-} TSCs and of the 20 genes that escape X-inactivation in WT TSCs. Consistent with the enrichment of H3-K27me3 on the inactive X-chromosome that is detected cytologically, genes on the inactive-X displayed a high average level of H3-K27me3 that peaks at the TSSs. In contrast to this H3-K27me3 enrichment, TSSs of genes that escape X-inactivation displayed a reduced average H3-K27me3 level. On the active X-chromosome, H3-K27me3 occupancy is very low, correlating with transcriptional competency of genes on that X-chromosome (Fig. 5.11B). Notably, H3-K27me3 is not present at higher levels at TSSs of X-linked genes that are derepressed in *Eed*^{-/-} TSCs compared to genes that remain silenced, suggesting that H3-K27me3 levels alone do not dictate susceptibility to reactivation (Fig. 5.11B).

We next tested whether the derepression of X-linked genes in *Eed*^{-/-} TSCs correlated with the preferential binding of Xist RNA to those genes in WT cells, since Xist RNA expression is lost in *Eed*^{-/-} TSCs. Using previously published CHART-Seq (capture hybridization analysis of RNA targets with deep sequencing) data assessing where Xist was bound on the inactive-X (Simon et al., 2013), we did not find Xist RNA to be enriched at X-linked genes that were derepressed vs. genes that remained silenced in *Eed*^{-/-} TSCs (Fig. 5.13). Thus, Xist RNA enrichment does not appear to be predictive of derepression of X-linked genes upon EED loss.

A

Xist Binding: Transcription Start Site



B

Xist Binding: Gene Body

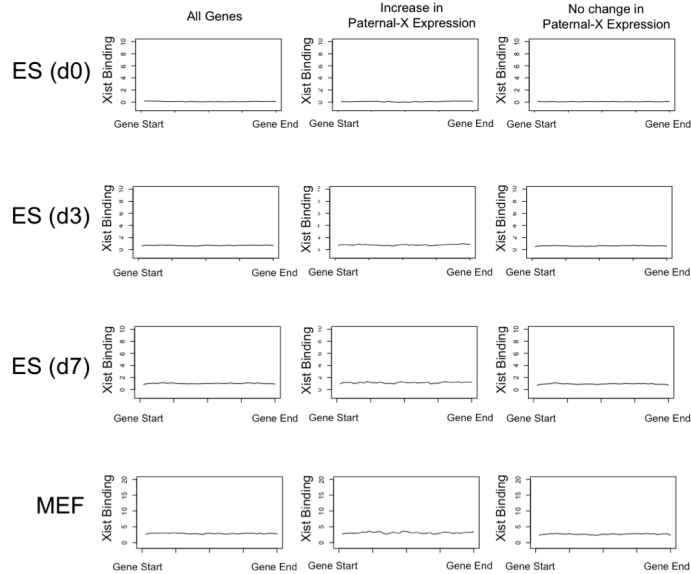


Figure 5.13: Xist RNA binding pattern is not predictive of derepression of paternal X-linked genes in *Eed*^{-/-} TSCs. (A) Xist RNA binding profiles 10kb upstream and 10kb downstream of the transcription start in ESCs 0, 3, or 7 days following Xist induction and fully X-inactivated terminally differentiated fibroblast (MEFs), as assessed by CHART-seq (Simon *et al.* 2013). d, day after Xist induction. Binding patterns are shown for all genes with allelic information, genes with an increase in paternal-X expression in *Eed*^{-/-} TSCs, and genes with no change in allelic expression in *Eed*^{-/-} TSCs. Genes with an increase in paternal-X expression exhibit no detectable difference in Xist accumulation compared to genes with no change in allelic expression pattern. (B) Xist RNA binding profiles within gene bodies in ESCs 0, 3, or 7 days following Xist induction and fully X-inactivated mouse embryonic fibroblast

(MEF) cells, as assessed by CHART-seq (Simon *et al.* 2013). Binding patterns are shown for all genes with allelic information, genes with an increase in paternal-X expression in *Eed*^{-/-} TSCs, and genes with no change in allelic expression in *Eed*^{-/-} TSCs. Genes with an increase in paternal-X expression display no detectable difference in Xist accumulation compared to genes with no change in allelic expression.

We additionally hypothesized that reactivation may be influenced by when during evolution X-linked genes became subject to dosage compensation. The X- and Y- chromosomes are believed to have evolved from a pair of identical autosomes (Graves and Schmidt, 1992; Jegalian and Page, 1998; Ohno, 1967). As the proto-X and proto-Y diverged, the proto Y-chromosome lost many of its genes. The loss of genes on the proto Y-chromosome is believed to have driven gradual dosage compensation on the X-chromosome, which likely occurred in a piecemeal fashion (Bellott *et al.*, 2014; Jegalian and Page, 1998; Lahn and Page, 1999). Intriguingly, the region of the X-chromosome with higher than average H3-K27me3 density lies within the ancestral region of the human X-chromosome, which is thought to have undergone dosage compensation first, based on analysis of nucleotide divergence between *X* and *Y* homologs (Lahn and Page, 1999; Vallot *et al.*, 2015). This ancestral segment of the X-chromosome is enriched for genes most susceptible to reactivation upon a reduction in H3-K27me3 levels that characterizes the inactive-X during the culture of human embryonic stem cells (hESCs) (Vallot *et al.*, 2015). Additionally, based on gene coordinates, Xist appears to reside within the group of genes that underwent dosage compensation early, if not first, during the evolution of the sex chromosomes (Bellott *et al.*, 2014; Cortez *et al.*, 2014). We therefore hypothesized that Xist may play a more prominent role in the silencing of genes in the evolutionary older group of X-linked genes, since genes in the older groups may have been under the influence of Xist RNA longer.

On the human X-chromosomes, the group of genes that underwent dosage compensation at similar times during evolution, termed evolutionary strata, are collinear with map position

(Bellott et al., 2014; Cortez et al., 2014; Lahn and Page, 1999) . In the mouse, by contrast, the X-chromosome has undergone numerous rearrangements. Analysis of nucleotide divergence, however, has demonstrated that mouse X-chromosome genes correspond to human X-chromosome evolutionary strata, despite the rearrangements (Sandstedt and Tucker, 2004). To identify whether each derepressed gene is a member of one of the ancient evolutionary strata or one of the newer strata, we converted the mouse gene coordinates for all X-linked genes with allelic information to human coordinates. Comparison of the derepressed paternal X-linked genes in *Eed*^{-/-} TSCs to human evolutionary strata, however, showed that the genes were not concentrated in a specific evolutionary stratum (Fig. 5.11C). This indicates that the genes dependent on EED, H3-K27me3, and Xist RNA coating for silencing may not have become dosage compensated together but rather did so at distinct periods during evolution.

To determine if chromatin features in WT cells other than H3-K27me3 levels or Xist RNA enrichment predict the derepression of X-linked genes in *Eed*^{-/-} TSCs, we interrogated a panel of chromatin modifications and indicators of chromatin structure, focusing now on markers of active transcription. Again using published allele-specific ChIP-seq as well as DNase-Seq data from WT F1 hybrid TSCs (Calabrese et al., 2012), we assessed profiles of histone H3-K27ac, H3-K4me2, H3-K36me3, H4-K20me1, DNase hypersensitivity, PolII occupancy, and TBP binding at TSSs of the 338 allelically analyzed X-chromosome genes in WT and *Eed*^{-/-} TSCs. We again assessed if in the WT TSCs the average profile of these chromatin features was similar or differed in the set of genes that were derepressed vs. the set that remained silenced on the inactive-X in *Eed*^{-/-} TSCs. As a frame of reference, we also examined the chromatin state on the active X-chromosome in WT TSCs of the 65 genes derepressed in *Eed*^{-/-} TSCs and of the 20 genes that escape X-inactivation (Fig. 5.11B).

DNase hypersensitivity marks nucleosome-free regions of DNA, and is characteristic of regulatory elements and TSSs of active genes (Song et al., 2011). In agreement, DNase hypersensitivity is a prominent feature of TSSs on the active X-chromosome (Fig. 5.11B) (Calabrese et al., 2012). On the inactive-X, DNase hypersensitivity is greatly reduced at silenced genes, whereas genes that escape X-inactivation exhibit an intermediate level of DNase hypersensitivity. In WT TSCs, DNase hypersensitivity of genes on the inactive-X that become derepressed parallels that of escape genes, suggesting that the chromatin at TSSs of derepressed genes is more open compared to genes that remain silenced in *Eed*^{-/-} TSCs. Similarly, in F1 WT TSCs Pol II occupancy, H3-K27 acetylation, and H3-K4me2, all indicators of active transcription and open chromatin, TSSs at genes that are derepressed in *Eed*^{-/-} TSCs again mimic escapees. Binding of TBP (TATA-binding protein), another indicator of active transcription, also exhibits an intermediate pattern of enrichment on the inactive-X in WT TSCs at genes that are derepressed in *Eed*^{-/-} TSCs, with occupancy higher than in silenced genes but lower than at genes on the active-X. H3-K36me3, a chromatin modification that is enriched in the gene bodies of actively transcribed genes, is also enriched at derepressed compared to silenced genes. However, H3-K36me3 enrichment is far lower in derepressed genes than in escape genes, suggesting that the derepressed genes are normally not transcribed at the frequency of escape genes.

We additionally assessed histone H4-K20me1 levels in F1 WT TSCs, and observed that whereas peak height at TSSs was indistinguishable between derepressed and silenced X-linked genes the derepressed genes had higher H4-K20me1 deposition flanking TSSs (Fig. 5.11B). H4-K20me1 is enriched on the inactive-X as detected by IF, consistent with a role in transcriptional repression (Kalakonda et al., 2008; Karachentsev et al., 2005; Kohlmaier et al., 2004). H4-

K20me1, however, has also been associated with transcriptional activation (Barski et al., 2007; Vakoc et al., 2006; Wang et al., 2008). H4-K20me1 may therefore have context-dependent roles, perhaps contingent on other surrounding chromatin modifications; or, H4-K20me1 may be an intermediate to the catalysis of H4-K20me2/3 (Oda et al., 2009). If H4-K20me1 at TSSs functions as a mark of active chromatin, it could mark genes that are lowly transcribed from the normally inactive-X and which are derepressed in *Eed*^{-/-} TSCs, like Pol II, TBP and DNase hypersensitivity. Alternatively, if H4-K20me1 contributes to transcriptional repression, as the enrichment on the inactive-X might suggest, then its loss may predispose certain X-linked genes to derepression. *Eed*^{-/-} TSCs have previously been shown to lose H4-K20me1 enrichment from the inactive-X (Kalantry et al., 2006), potentially triggering derepression of a small subset of genes that depend on this histone modification for transcriptional silencing.

Together, the ChIP-Seq analysis shows that in WT TSCs H3-K27me3 profiles do not differ between genes that are derepressed vs. genes that remain silenced in *Eed*^{-/-} TSCs. However, derepressed genes in *Eed*^{-/-} TSCs are characterized by markers of open chromatin compared to genes that remain silenced. The data therefore imply that the derepressed genes are poised for transcriptional activation upon loss of EED, H3-K27me3, and Xi st RNA. Alternatively, Pol II and H3-K36me3 presence at the derepressed genes suggest that these genes may in fact be transcribed from the inactive-X at low levels, but whose transcriptional activity is upregulated in *Eed*^{-/-} TSCs.

To evaluate the basal transcription of the X-linked genes that become derepressed upon EED loss, we ranked the 65 genes that are derepressed in *Eed*^{-/-} TSCs by their average paternal-X expression in WT TSCs (Fig. 5.14). We found that, based on the 10% threshold used previously to define escapers of X-inactivation, the majority of the derepressed genes (84%) fall below this

threshold in WT TSCs. Transcription from the inactive-X, however, occurs on a broad and highly variable spectrum (Calabrese et al., 2012). Whereas few derepressed genes show >10% expression from the paternal-X in WT TSCs, many show a low, but detectable, level of inactive-X expression, ranging from 1-10% of total expression from the paternal X-chromosome (Calabrese et al., 2012). To determine if genes that are derepressed in *Eed*^{-/-} TSCs display, on average, higher levels of basal inactive-X transcription than genes that remain silenced, we ranked all 338 genes for which allelic information was available by percent paternal-X expression in WT TSCs, and divided this ranked list into five quintiles, each containing 67-68 genes (Fig. 5.14). We evaluated the range of percent paternal-X expression for each quintile, and identified the number of derepressed genes in each group (Fig. 5.14). Through this analysis, we found that the derepressed X-linked genes are not evenly distributed between the quintiles ($p = 0.0011$, Fisher's exact test). Derepressed genes are underrepresented in quintile 1, which encompasses genes ranging from 0% to 1% paternal-X expression in WT TSCs and includes 7 derepressed genes, but are over-represented in quintile 4, which encompasses genes that display 3-6% inactive-X expression in WT TSCs and includes 25 derepressed genes. To determine if the presence of marks of open chromatin and active transcription at genes in WT TSCs that are derepressed in *Eed*^{-/-} TSCs was driven by this low-level transcription from the inactive paternal-X in WT TSCs, we separately evaluated the average chromatin profiles for genes in each quintile (Fig. 5.14). We found that derepressed genes in quintile 5, which harbors genes with >6% paternal-X expression in WT TSCs and thus includes escape genes, show the highest levels of Pol II occupancy, H3-K27ac, H3-K4me2, and H3-K36me3, whereas quintiles with lower levels of expression exhibit reduced levels of these features of active transcription.

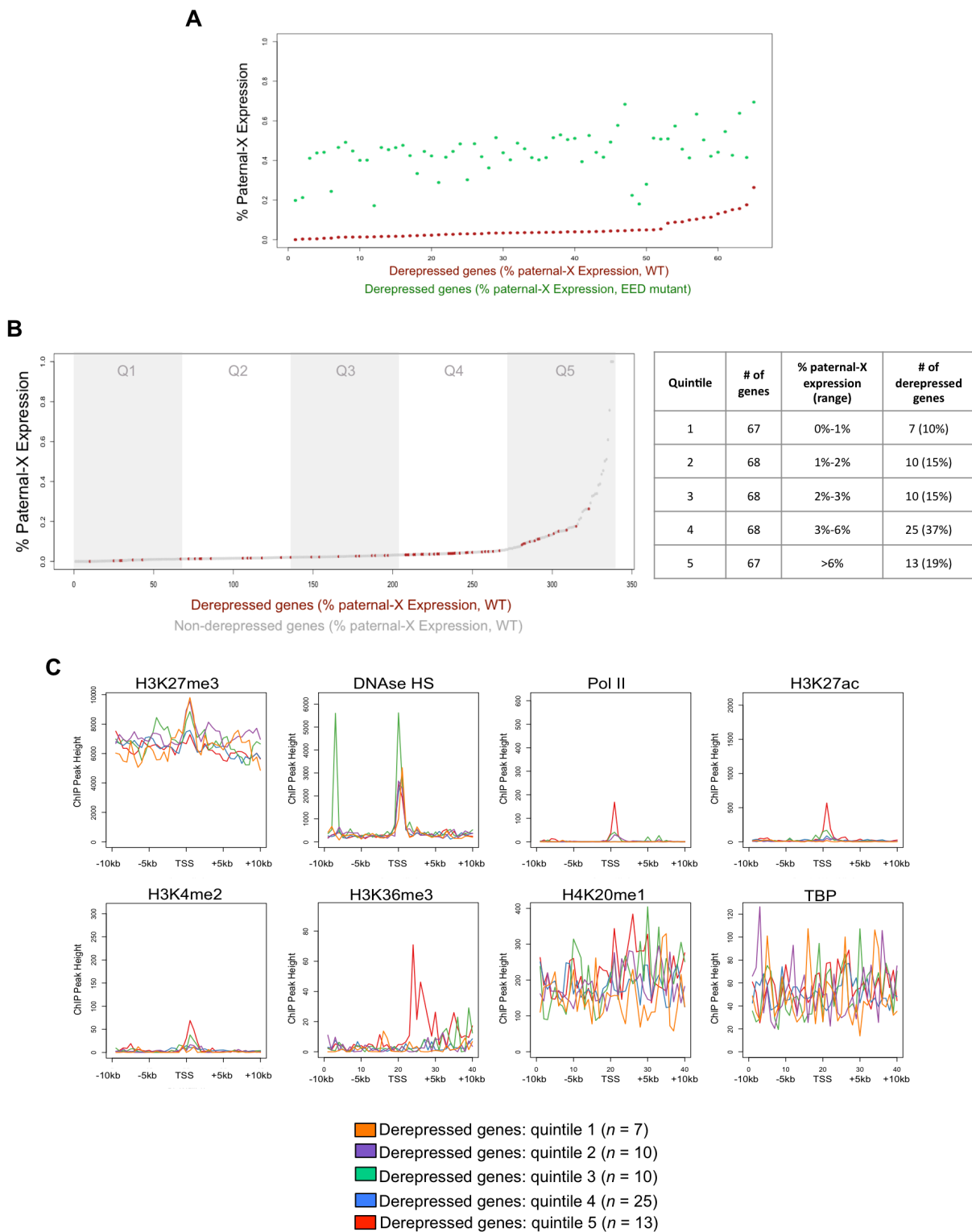


Figure 5.14: Assessment of Basal Transcription at Derepressed X-chromosome Genes. (A) Ranking of derepressed X-linked genes. The X-axis indicates the rank order of each gene from least to most paternal-X expression in WT cells. The Y-axis indicates percent paternal-X expression for individual genes in WT (red dots) or *Eed*^{-/-} (green) TSCs. (B) Paternal-X contribution for all expressed X-linked genes in WT TSCs. The X-axis indicates the rank order of each gene from least to most paternal-X expression in WT cells. Gray dots indicate genes that are not derepressed, while red dots mark genes that are derepressed in *Eed*^{-/-} TSCs. The Y-axis depicts percent paternal-X expression for each gene. Based on percent paternal-X expression, expressed genes can be divided into 5 quintiles. Derepressed genes are overrepresented in quintile 4, indicating that derepressed genes show, on average, a

higher level of basal transcription from the paternal-X in WT TSCs. (C) Average chromatin modification profiles surrounding the transcription start sites for derepressed genes in each quintile.

5-6: Discussion

The Polycomb PRC2 complex and the H3-K27me3 histone modification it catalyzes are associated with gene silencing in wide variety of contexts, including in X-inactivation (Brockdorff, 2013; Laugesen and Helin, 2014; Margueron and Reinberg, 2011). PRC2 proteins and H3-K27me3 are recruited to the prospective inactive-X at the beginning of X-inactivation (Erhardt et al., 2003; Mak et al., 2002; Okamoto et al., 2004; Plath et al., 2003; Silva et al., 2003). As a result, PRC2 has been proposed to contribute to gene silencing on the inactive-X (Plath et al., 2003; Silva et al., 2003). In agreement, EED, a core subunit of PRC2, is necessary to maintain silencing of X-linked genes during imprinted mouse X-inactivation (Kalantry et al., 2006; Wang et al., 2001). Here, we sought to delineate the repertoire of X-linked genes that require EED for silencing on the inactive X-chromosome, using the imprinted X-inactivation model system.

Imprinted X-inactivation offers a unique opportunity to assess allele-specific expression of X-linked genes. Since the paternal X-chromosome is exclusively inactivated in cells that undergo imprinted X-inactivation, strain-specific SNPs can be exploited to comprehensively identify transcripts originating from the active and the inactive X-chromosome by RNA-Seq. In cells that undergo imprinted X-inactivation, i.e., mouse TSCs, transcripts expressed from the inactive-X harbor paternal-specific SNPs, whereas RNAs expressed from the active-X contain maternal-specific SNPs. Compared to imprinted X-inactivation, random X-inactivation is more difficult to study by high-throughput approaches. In a randomly inactivated population of cells, parent-of-origin specific SNPs will not correspond exclusively to the active- or the inactive X-chromosome, since some cells will have inactivated the maternal- and some the paternal-X.

Eed^{-/-} TSCs lose Xist RNA coating on the inactive-X, suggesting that PRC2 induces Xist RNA expression (Fig. 5.1; see also (Kalantry et al., 2006)). Analysis of differentiating female ESCs, which undergo random X-inactivation, previously revealed that the Xist promoter undergoes a transient heterochromatinization prior to X-inactivation and Xist induction (Sun et al., 2006; Zhao et al., 2008). This heterochromatic state is characterized by H4 hypoacetylation, a reduction in H3-K4 dimethylation, and an increase in PRC2-catalyzed H3-K27me3. The marking of the Xist chromatin in this manner may be necessary for Xist RNA expression, potentially explaining why the absence of EED and H3-K27me3 abrogates Xist RNA expression.

Despite the loss of both H3-K27me3 and Xist RNA expression, only a subset of the genes on the inactive-X is reactivated. Overall, 19% of the genes containing SNPs displayed loss of silencing on the normally inactivated paternal X-chromosome in *Eed*^{-/-} TSCs. These genes are distributed across the X-chromosome, with no obvious linear clustering. Derepressed genes also do not appear to be associated with changes in three-dimensional conformation of the X-chromosome, based on assessment of topologically associated domains; Genes that are derepressed in *Eed*^{-/-} TSCs do not appear to cluster in individual TADs any more than they do so linearly, nor do they appear to be enriched at TAD boundaries, which could be disrupted upon loss of H3-K27me3 and Xist RNA.

An altered local chromatin state in the derepressed genes would be consistent with the reactivation of X-linked genes with high H3-K27me3 that is lost in hESCs under prolonged culture (Vallot et al., 2015). H3-K27me3 levels, however, did not differ significantly between X-linked genes that are derepressed vs. silenced in TSCs. Xist RNA binding at gene promoters and in gene bodies also did not correlate with derepression of inactivated X-linked genes.

We next examined which evolutionary strata that the reactivated genes fall into on the X-chromosome. Prior work has suggested that the requirement for Xist RNA in X-linked gene silencing may depend on the length of time a gene has been subject to dosage compensation during evolution (Kalantry et al., 2009). However, the derepressed genes in *Eed*^{-/-} TSCs did not correlate with membership in the ancient evolutionary strata on the X-chromosome.

In addition to loss of H3-K27me3 and Xist RNA accumulation from the inactive-X, *Eed*^{-/-} TSCs are also devoid of enrichment of other histone variants and chromatin modifications that are enriched on the inactive-X chromosome, including histone H2a ubiquitination that is catalyzed by PRC1, MacroH2a, and, as discussed above, H4-K20me1 (Kalantry et al., 2006). One or more of these chromatin modifications and histone variants may be required to maintain silencing of the X-linked genes that are derepressed from the inactive X-chromosome in *Eed*^{-/-} TSCs. The reactivated X-linked genes may also accumulate activating chromatin modifications following loss of H3-K27me3, whereas genes that maintain silencing do not. To gain insight into these possibilities, we looked beyond the classic markers of the inactive-X, H3-K27me3 and Xist RNA, and assessed ChIP-seq data for a panel of chromatin modifications that mark active transcription, as well as PolIII occupancy and DNase-seq data. Through this analysis, we found that derepressed genes showed an enrichment of activating marks. We observed that escape from X-inactivation is not a binary readout in WT TSCs. Rather, whereas few genes are transcribed from the inactive-X at high levels, many show a low basal level of transcription. Although not all genes that are derepressed from the paternal-X in *Eed*^{-/-} TSCs are transcribed from the paternal-X in WT TSCs, derepressed genes are overrepresented among the set that is transcribed at a low level from the inactive-X in WT TSCs. This baseline expression level appears to correlate with the enrichment of marks of open chromatin and active transcription in WT TSCs.

Since many of these genes harbor marks of active chromatin and are occupied by RNA Pol II in WT TSCs, they may be prone to induction from the inactive-X upon loss of EED and Xist RNA. Notably, the X-linked genes that escape from X-inactivation in *Eed*^{-/-} TSCs, but do not reach the 10X threshold of SNP coverage to accurately calculate allelic balance in WT TSCs also show baseline levels of inactive-X expression in WT cells. Several of these genes reach 5X coverage in one or more WT cell lines and, in all cases, harbor reads mapping to the paternal X-chromosome. Intriguingly, however, many genes that do show low-level expression from the inactive-X remain silenced upon loss of EED or Xist RNA, suggesting that other factor(s) must continue to constrain transcriptional activity at these genes.

Our previous analysis of *Eed*^{-/-} TSCs concluded that EED is required to maintain silencing on the inactive-X only upon differentiation of trophoblast progenitor cells *in vivo* and *in vitro* (Kalantry et al., 2006). Our results herein instead show that EED is also required to maintain silencing of a subset of X-linked genes on the inactive-X in undifferentiated TSCs. The earlier study assessed expression of a limited number of X-linked genes and may therefore have missed the X-inactivation defects in undifferentiated TSCs. Intriguingly, the loss of dosage compensation of the derepressed genes is not catastrophic, since *Eed*^{-/-} TSCs are viable and can proliferate. This suggests that undifferentiated TSCs may be insensitive to the dosage imbalance between the sexes of the subset of derepressed X-linked genes in *Eed*^{-/-} TSCs. Though these genes may not be required to be dosage compensated in undifferentiated TSCs, their dose may need to be balanced later during differentiation of the trophoblast lineage. Consistent with a differentiation-dependent requirement for correct dosage compensation, *Eed*^{-/-} TSCs are blocked in differentiation (Kalantry et al., 2006).

X-linked gene silencing defects observed in *Eed*^{-/-} TSCs may also characterize random X-inactivation. Notably, our previous work has shown that EED loss does not alter random X-inactivation, based again on the expression analysis of a limited number of X-linked genes (Kalantry and Magnuson, 2006). Profiling of the whole X-chromosome in *Eed*^{-/-} epiblast lineage by allele-specific RNA-Seq, however, may reveal a gene-specific requirement for EED in random X-inactivation much as in imprinted X-inactivation. Whereas the analysis of a randomly inactivated population of cells is not directly feasible by sequencing-based approaches like allele-specific RNA-Seq, sequencing of single cells or of a population of cells in which random X-inactivation has been biased is possible (Berletch et al., 2015b; Calabrese et al., 2012; Carrel and Willard, 2005; Marks et al., 2015; Yang et al., 2010). If one or the other X-chromosome is preferentially inactivated in cells that are normally randomly inactivated, then allele-specific RNA-Seq can be exploited to catalog gene expression defects across the X-chromosome in an *Eed*^{-/-} background.

By comprehensively analyzing defects in imprinted X-inactivation arising from loss of the essential Polycomb protein EED in TSCs, we have found that, despite the loss of the classic gene silencing elements Xist RNA and H3-K27me4, only a subset of genes on the paternal X-chromosome are subject to derepression in *Eed*^{-/-} TSCs. The continued stable silencing of majority of genes on the paternal X-chromosome in *Eed*^{-/-} TSCs implies that factors in addition to PRC2, H3-K27me3, and Xist RNA must play a role in the maintenance of X-inactivation. Silencing may be maintained in part by the suite of factors recently shown to interact with Xist RNA (Chan et al., 2011; Chu et al., 2015; McHugh et al., 2015; Minajigi et al., 2015; Minkovsky et al., 2015; Moindrot et al., 2015; Monfort et al., 2015). Critically, we find that derepressed genes in *Eed*^{-/-} TSCs display hallmarks of open chromatin and basal transcriptional activity from

the inactive-X, while X-linked genes that are completely silenced are refractory to loss of EED, H3-K27me3, and Xist RNA. This points to an intriguing new role for PRC2 in regulating gene expression, in which PRC2-catalyzed H3-K27me3 may be responsible for minimizing the expression levels of basally transcribed genes without establishing stringent X-linked gene silencing. Based on our current analysis of allele-specific expression and chromatin profiles, we hypothesize that susceptibility to reactivation is a gene-intrinsic property that is influenced by the local chromatin context. Depending on local chromatin structure, different factors may be responsible for maintaining repression of different gene sets. Future work will further explore both the role of PRC2 in regulating basally transcribed genes and the mechanisms that maintain silencing of stringently silenced X-linked genes.

5-7: Materials and Methods

Ethics Statement.

This study was performed in strict accordance with the recommendations in the Guide for the Care and Use of Laboratory Animals of the National Institutes of Health. All animals were handled according to protocols approved by the University Committee on Use and Care of Animals (UCUCA) at the University of Michigan (protocol #PRO00006455).

Mice.

Mice harboring a conditional mutation in *Eed* were generated by the University of Michigan Transgenic Animal Model Core using *Eed*^{tm1a(EUCOMM)Wtsi} targeted ES cells (EUCOMM). Briefly, ES cells were injected into blastocysts, and implanted into pseudopregnant

females. Mice with high percentages of chimerism were bred and assessed for germline transmission. To generate homozygous EED mutant mice harboring polymorphic X-chromosomes, first, male and female mice on a B6 *Mus musculus* background carrying the conditional mutant allele for EED were intercrossed ($EED^{fl/+}$ x $EED^{fl/+}$) to achieve homozygosity. To obtain mice conditionally mutant for EED and on the JF1 *Mus molossinus* divergent background, we bred $EED^{fl/fl}$ males (B6 *Mus musculus* background) to WT JF1 *Mus molossinus* females. This gave us F1 hybrid $EED^{fl/+}$ males that possessed an X-chromosome from the JF1 *Mus molossinus* background (X^{JF1}/Y). Such males were backcrossed to WT JF1 *Mus molossinus* females to derive $EED^{fl/+}$ females that were a mix of B6 *Mus musculus* and JF1 *Mus molossinus* and also harbored two X-chromosomes from the JF1 *Mus molossinus* background (X^{JF1}/X^{JF1}). $EED^{fl/+}; X^{JF1}/X^{JF1}$ females were bred against $EED^{fl/+}; X^{JF1}/Y$ males to derive $EED^{fl/fl}; X^{JF1}/Y$ males. To obtain our female embryos used for TS cell derivation, we crossed an $EED^{fl/fl}$ female on the B6 *Mus musculus* background with an $EED^{fl/fl}$ male that was a mix of B6 *Mus musculus* and JF1 *Mus molossinus* but possessed an X-chromosome from the JF1 *Mus molossinus* background (X^{JF1}/Y). The JF1/Ms strain has been described previously.

TS cell derivation and culture.

Blastocysts were dissected out of pregnant mice 3.5 dpc and plated in 4 well dishes preseeded with MEFs. Hatched embryos were cultured in standard TS medium supplemented with 1.5x FGF4 and Heparin for 4-5 days until blastocyst outgrowths were of ideal size. Blastocysts were then trypsinized in 0.05% Trypsin-EDTA, neutralized with TS media supplemented with 1.5x FGF4 and Heparin, and cultured in 96 well dishes. Once lines were well established genotyping PCRs confirmed a female $Eed^{fl/fl}$ line. Cell lines were then cultured in standard TS media supplemented with FGF4 and Heparin. RNA was harvested from TS cells using Trizol

(Invitrogen, #15596-018) and RT-PCR was performed as described below. For RNA FISH and/or IF, TS cells were split onto gelatin-coated glass coverslips and allowed to grow for 3-6 days. The cells were then permeabilized through sequential treatment with ice-cold cytoskeletal extraction buffer (CSK; 100 mM NaCl, 300 mM sucrose, 3 mM MgCl₂, and 10 mM PIPES buffer, pH 6.8) for 30 seconds, ice-cold CSK buffer containing 0.4% Triton X-100 (Fisher Scientific, #EP151) for 30 seconds, followed twice with ice-cold CSK for 30 seconds. After permeabilization, cells were fixed by incubation in 4% paraformaldehyde for 10 minutes at RT. Cells were then rinsed 3 times each in 70% ethanol and stored in 70% ethanol at -20°C prior to IF and/or RNA FISH. For differentiation of TS cells, cells were split onto gelatinized dishes or coverslips and cultured for 6 days (d6) in media without FGF4 or heparin. On d6 of differentiation, RNA was harvested or cells were processed as described above for IF and RNA FISH.

Generation of stable $Eed^{-/-}$ TSCs.

$EED^{fl/fl}$ TSCs were plated at a 1:24-1:48 dilution into 6 well dishes pre-seeded with MEFs and allowed to adhere until the next day. Cells were then transduced with Ad5-CMV-Cre (Adenovirus type 5, University of Michigan Viral Vector Core adenoviral construct, 4×10^{12} particles/mL) at an MOI of 1000. Once cell colonies were large enough, they were subcloned into 96 well dishes pre-seeded with MEFs and re-transduced 24 hours later with Adeno-Cre at MOI of 1000. Following this expanded 96 well samples were split to 6 well dishes pre-seeded MEFs and again transduced 24 hours later. A portion of each 96 well samples was lysed for DNA genotyping to assess the efficiency of Cre-mediated deletion of the *Eed* floxed alleles.

Subcloning, transduction, and genotyping procedures were repeated until a pure population of *Eed*^{-/-} TSCs was achieved. *Eed*^{-/-} TSCs were maintained in culture as described above.

Immunofluorescence.

Sample coverslips containing CSK-treated and 4% PFA-fixed cells were placed in a 6-well dish that contained 2ml of 1X PBS in each well. Samples were then washed briefly with 3 changes of 1X PBS to remove ethanol followed by three successive washes with 1X PBS for 3 minutes each on a rocker. Samples were blocked for 30 minutes at 37°C in 50 µl pre-warmed blocking buffer in a humid chamber. Samples were then incubated for 1 hour at 37°C in 50 uL diluted primary antibody (dilution depends on primary antibody used, 1:500 EED primary Ab, previously used in (Kalantry et al., 2006; Plath et al., 2003; Shen et al., 2008; Silva et al., 2003; Valk-Lingbeek et al., 2004; Wang et al., 2001); 1:5000 H3-K27me3 primary Ab: polyclonal Rabbit anti-mouse, Millipore, #ABE44) in a humid chamber. After incubation, samples were washed 3 times with 1X PBS/0.2% Tween-20 for 3 min each on a rocker. Coverslips were then placed back in 50 uL pre-warmed blocking buffer in a humid chamber for 5 minutes at 37°C followed by an additional incubation at for 30 minutes at 37°C in 50 uL diluted secondary antibody. Alexa Fluor conjugated secondary antibodies were used at a 1:300 dilution. Following secondary incubation, coverslips were washed 3 times with 1X PBS/0.2% Tween-20 for 3 min each on a rocker. Samples were incubated in 100 µl of 2% PFA on a glass plate wrapped in parafilm for 10 minutes at room temperature. Following this, samples were dehydrated through room temperature ethanol series (5 minutes each for 70%, 85%, 95% and 100% ethanol). Coverslips were allowed to dry for 15 minutes after the 100% ethanol wash, followed by hybridizing the samples overnight with the appropriate RNA FISH probe. After hybridization,

samples were washed for 7 minutes at 39°C 3 times each in 2X SSC/50% formamide, followed by three 7 minute washes at 39°C in 2X SSC (1:100,000-1:200,000 dilution of DAPI added at third wash of 2X SSC), followed by two 7 minute washes at 39°C in 1X SSC. Sample coverslips were then mounted onto glass microscope slides with Vectashield. Coverslips were sealed to the glass slides with clear nail polish.

RNA FISH.

Samples were dehydrated through room temperature ethanol series (5 minutes each for 70%, 85%, 95% and 100% ethanol). Coverslips were allowed to dry for 15 minutes at room temperature after the 100% ethanol wash, followed by hybridizing the samples overnight with the appropriate RNA FISH probe. After the hybridization, samples were washed for 7 minutes at 39°C 3 times each in 2X SSC/50% formamide, followed by three 7 minute washes at 39°C in 2X SSC (1:100,000-1:200,000 dilution of DAPI added at third wash of 2X SSC), followed by two 7 minute washes at 39°C in 1X SSC. Sample coverslips were then mounted onto glass microscope slides with Vectashield. Coverslips were sealed to the glass slides with clear nail polish.

DNA FISH.

After RNA FISH and imaging of the samples, a razor blade was used to cut away the nail polish used to seal the coverslip to the slide. Coverslips were submerged in a solution of 2X SSC. While the sample was still submerged the coverslips were gently peeled of the slide. Coverslips were washed with 1X PBS three times quickly and then incubated in 1X PBS for 5 minutes at room temperature. Samples were then re-fixed in 1% PFA containing 0.5% Tergitol and 0.5% Triton X-100 (vol/vol) for 10 minutes at room temperature. A dehydration step was

performed with the coverslips by moving them through a room-temperature ethanol series (70%, 85%, and 100% ethanol) for 2 minutes each. Coverslips were then air dried at for 15 minutes at room temperature. Following a drying period, samples were RNase treated with 1.25 $\mu\text{g}/\mu\text{l}$ RNase A (Roche, #10109142001) in 2X SSC, incubating for 30 minutes at 37°C. Coverslips were dehydrated through a room-temperature ethanol series (85%, 95%, and 100% ethanol) for 2 min each followed by air drying at for 15 minutes at room temperature. Samples were then denatured in a pre-warmed solution of 2X SSC/70% formamide on a glass slide or glass plate stationed on top of a heat block for 11 minutes set at 95°C. Samples were immediately dehydrated through a -20°C ethanol series (70%, 85%, 95%, and 100% ethanol) for 2 min each followed by a final drying period for 15 minutes at room temperature. Samples were then hybridized to the appropriate DNA probes overnight. After the hybridization, samples were washed for 7 minutes at 39°C 2 times each in 2X SSC/50% formamide, followed by two 7 minute washes at 39°C in 2X SSC (1:100,000-1:200,000 dilution of DAPI added at first wash of 2X SSC). Sample coverslips were then mounted onto glass microscope slides with Vectashield. Coverslips were sealed to the glass slides with clear nail polish.

RNA-sequencing.

Total RNA was isolated from TRIZOL according to manufacturers instructions and submitted to the University of Michigan DNA Sequencing Core for Poly-A Purification and Strand-specific library preparation using the Illumina TruSeq Library Preparation Kit. Libraries were sequenced on the Illumina HiSeq2000 platform to generate 100 basepair paired-end reads. Increased sequence length increases the likelihood of finding a single unique map location, minimizing multi-mapping reads; as such, these long reads can permit robust allele-specific

mapping, even in genes belonging to multi-gene families. RNA-seq reads were mapped in an allele-specific manner to identify the allelic contribution of the paternally-inherited inactive-X to the transcriptome. Briefly, we generated *in silico* strain-specific reference genomes by substituting SNP data from whole-genome sequencing of the 129/S1 and JF1/Ms strains into the mm9 mouse reference genome build (Keane et al., 2011; Takada et al., 2013; Yalcin et al., 2011). Use of strain-specific references minimizes reference allele mapping bias, which can result from mapping polymorphic reads to a single reference genome (Degner et al., 2009). Strain-specific references do not completely eliminate reference mapping bias, however, due to the presence of structural variations and small indels between the genomes of the two strains. Sequencing reads were separately mapped to each strain-specific reference genome using STAR (Dobin et al., 2013), allowing 0 mismatches in mapped reads to ensure allele-specific mapping of SNP containing reads to only one strain-specific reference genome. STAR was selected for read mapping, in part, due to improved ability to handle structural variability and indels, with the goal of again reducing reference mapping bias; STAR is a spliced aligner capable of detecting structural variations, and is able to handle small insertions and deletions during read mapping. STAR additionally permits soft-clipping of reads during mapping, trimming the ends of long reads that cannot be perfectly mapped to the reference genome. This would permit reads flanking indels to be clipped if indels fall near the ends of reads, thus preserving mapability at SNPs that may be near indels. All multi-mapping reads were excluded from both differential expression and allele-specific analysis. For differential expression analysis, all reads (non-SNP-overlapping reads, as mapped to the 129 genome + SNP reads with the 129 allele + SNP reads with the JF1 allele) were merged into a single alignment file and the number of reads per RefSeq annotated gene was counted using HTSeq (Anders et al., 2015), and differential expression analysis was

performed using DESeq2 (Love et al., 2014). For allelic expression analysis, only sequencing reads overlapping known polymorphic sites that differ between the 129/S1 and JF1/Ms genomes were retained. For each polymorphic site, reads mapping to the 129/S1 and JF1/Ms genomes were counted, and the proportion of reads from each X-chromosome identified. Allelic expression was calculated individually for each polymorphic site; for genes containing multiple SNPs, the paternal-X percentage for all SNPs was averaged to calculate gene-level allelic expression. To calculate paternal-X expression for DESeq2 analysis, we took the total read counts from HTSeq and multiplied the number of mapped reads for each gene by the proportion of SNP containing reads mapping to the paternal X-chromosome, calculating

$$\left\{ \text{total reads} \times \left(\frac{\text{paternal reads}}{\text{maternal reads} + \text{paternal reads}} \right) \right\}$$

We then performed differential expression analysis for the paternal-X expression level using DESeq2 (Love et al., 2014).

Allele-specific Reverse Transcriptase Polymerase Chain Reaction (RT-PCR).

Total RNA was isolated from TRIZOL following manufacturers instructions. SuperScript III One-Step RT-PCR Kit with Platinum *Taq* enzyme mixture (Invitrogen, #12574-035) was used to prepare and amplify the complimentary DNA (cDNA). See Table 5.4 for primer and SNP information for each amplicon. Amplified cDNAs were run on agarose gels and purified using the Clontech NucleoSpin Kit (Clontech, #740609). The purified cDNAs were then sequenced and sequencing traces were examined for single nucleotide polymorphisms (SNPs) characteristic of the *M. molossinus*-derived X^{JF1} chromosome and the *M. musculus*-derived X^{Lab} chromosomes.

PCR.

For DNA isolation, cell pellets from TSCs were lysed in buffer composed of 50mM KCl, 10mM Tris-Cl (pH 8.3), 2.5mM MgCl₂, 0.1mg/ml gelatin, 0.45%NP-40, and 0.45% Tween-20. Cells in lysis buffer were incubated at 50°C overnight, then stored at 4⁰C until use. Genomic PCR reactions were carried out in ChromaTaq buffer (Denville Scientific) with 1.5mM Magnesium Chloride using RadiantTaq DNA polymerase (Alkali Scientific, #C109). Primers and SNPs are described in Table 5.4.

X-Chromosome Paint.

Fixed and permeabilized TS Cells on coverslips were denatured in a pre-warmed solution of 2X SSC/70% formamide at 95°C, as with DNA FISH (above). Samples were immediately dehydrated through a -20°C ethanol series (70%, 85%, 95%, and 100% ethanol) for 2 min each followed by a final drying period for 15 min at room temperature. Dried coverslips were inverted onto a glass slide with 8 µl of XCyting X-chromosome Paint (Metasystems, #D-1420-050-F1). Coverslip and probe were then denatured together for an additional 2 min at 75⁰C, then placed in a humid chamber for overnight hybridization at 37⁰C. Hybridized samples were washed once for 2 min at 75C in 0.4X SSC, pH7, with a 1:250,000 dilution of DAPI, then once for 30 sec in 2x SSC with 0.2% Tergitol. Samples were then rinsed briefly with ddH₂O to prevent formation of salt crystals and allowed to air dry briefly. Dried samples were mounted on glass slides with VectaShield and sealed with clear nailpolish.

Microscopy.

Stained samples were imaged using a Nikon Eclipse TiE inverted microscope with a Photometrics CCD camera. The images were deconvolved and uniformly processed using NIS-Elements software.

Profiling of Chromatin Modifications.

DNase-Seq data and ChIP-Seq data for H3K27me3, PolII, H3K27ac, H3K4me2, H3K36me3, H4K20me1, and TBP were sourced from a study of TSCs by Calabrese *et al.* (Calabrese et al., 2012) as a part of GEO data set GSE39406. Wiggle tracks for total H3-K27me3 coverage were cross-referenced with allele-specific read calls. For regions containing SNPs, the proportion of inactive-X expression of a given peak was calculated based on the percentage of inactive X-specific reads overlapping SNP sites within the peak. ChIP-seq data assigned to the inactive-X was subdivided into 50bp bins along the span of the X-chromosome. Allelic ChIP-seq peak depth surrounding the transcription start site of genes was calculated by averaging the 50bp bins into 500bp sections spanning from 10kb upstream to 10kb downstream of the transcription start site.

Analysis of Xist binding profiles.

Xist RNA binding data was sourced from a CHART-Seq study by Simon *et al.* (Simon et al., 2013) as a part of GEO data set GSE48649. Bedgraph tracks for allelic Xist binding were subdivided into 50bp bins along the span of the X-chromosome. CHART-Seq read depth surrounding the transcription start site of genes was calculated by averaging the 50bp bins into 500bp sections spanning from 10kb upstream to 10kb downstream of the transcription start site

of each gene. CHART-Seq values for individual genes were then averaged for each bin. CHART-Seq read depth within gene bodies was calculated by averaging 50bp bins into 40 bins of even length spanning the transcription start site to the transcription termination site of individual genes. CHART-Seq values for individual genes were then averaged for each bin.

Analysis of Evolutionary Strata.

X-chromosome gene coordinates from all exons of the Ensembl mouse annotation for the mm9 genome build were lifted over to the human genome (hg19 build) using UCSC's LiftOver tool. For mouse X-chromosome genes with coordinates mapped back to the human X-chromosome, gene locations were plotted based on the start coordinate of both mouse and human genes. Genes were assigned to evolutionary strata based on human coordinates, with stratum boundaries defined based on previously published analysis of the Y chromosome (Bellott et al., 2014; Cortez et al., 2014; Lahn and Page, 1999).

Table 5.1: Allelic Expression of X-linked Genes: 10X Read Coverage Threshold

Gene Name	B		C		D		E		F		G		H		I		J		K		L		M		N			
	WT 1	WT 2	WT 3	Eed ^{0/1}	WT Average	Consistent Escape in WT?	Eed ^{+/+} 1	Eed ^{+/+} 2	Eed ^{+/+} 3	Eed ^{+/+} Average	Consistent escape in Eed ^{+/+}	WT vs. Eed ^{+/+} P Value (T Test)	Adjusted P Value															
1																												
2																												
3																												
4	Hdac6	0.091	0.090	0.096	0.071	0.087	No	0.579	0.582	0.561	0.574	Yes	2.04794E-07	7.358E-06														
5	Zmyrn3	0.002	0.000	0.042	0.005	0.012	No	0.471	0.475	0.452	0.466	Yes	3.22468E-07	1.2093E-05														
6	Phf16	0.011	0.005	0.056	0.015	0.033	No	0.456	0.456	0.431	0.446	Yes	1.1327E-06	2.8318E-05														
7	Tcf3	0.006	0.010	0.037	0.080	0.033	No	0.537	0.508	0.500	0.515	Yes	3.76681E-06	4.7085E-05														
8	Rnf128	0.017	0.030	0.083	0.020	0.037	No	0.557	0.514	0.516	0.529	Yes	2.8787E-06	4.7085E-05														
9	Cttd5	0.034	0.014	0.086	0.066	0.050	No	0.537	0.510	0.491	0.513	Yes	3.54533E-06	4.7085E-05														
10	Kcnd1	0.000	0.000	0.065	0.054	0.030	No	0.471	0.508	0.475	0.484	Yes	4.9641E-06	5.3187E-05														
11	Plp2	0.002	0.002	0.047	0.030	0.020	No	0.336	0.350	0.314	0.334	Yes	6.62706E-06	6.2129E-05														
12	Gripap1	0.008	0.019	0.087	0.044	0.040	No	0.480	0.514	0.540	0.511	Yes	1.02749E-05	8.5624E-05														
13	Wbp5	0.007	0.002	0.080	0.062	0.037	No	0.507	0.536	0.503	0.515	Yes	1.2459E-05	9.3442E-05														
14	Itih9	0.000	0.000	0.056	0.023	0.020	No	0.451	0.423	0.426	0.424	Yes	2.52478E-05	0.00014566														
15	Ftsj1	0.000	0.001	0.079	0.009	0.009	No	0.434	0.446	0.389	0.423	Yes	2.14551E-05	0.00014566														
16	Wdr45	0.006	0.000	0.056	0.046	0.027	No	0.468	0.412	0.457	0.446	Yes	2.50716E-05	0.00014566														
17	Wdr13	0.000	0.000	0.042	0.025	0.017	No	0.496	0.450	0.448	0.465	Yes	4.55013E-05	0.00023274														
18	Gpkow	0.161	0.205	0.109	0.152	0.157	Yes	0.635	0.630	0.651	0.638	Yes	4.65488E-05	0.00031874														
19	Trapla	0.000	0.000	0.160	0.032	0.048	No	0.714	0.722	0.614	0.684	Yes	6.79979E-05	0.00031874														
20	Pqk1	0.003	0.001	0.107	0.027	0.034	No	0.437	0.508	0.518	0.487	Yes	7.50658E-05	0.00033117														
21	Ccdc22	0.012	0.000	0.118	0.085	0.054	No	0.523	0.519	0.482	0.508	Yes	0.000104968	0.00043737														
22	Rbm41	0.003	0.002	0.068	0.088	0.040	No	0.580	0.526	0.488	0.526	Yes	0.000115444	0.00045557														
23	Ccdc120	0.003	0.145	0.057	0.090	0.111	No	0.504	0.516	0.491	0.504	Yes	0.000165925	0.00062222														
24	Ubal	0.015	0.009	0.083	0.057	0.041	No	0.488	0.427	0.407	0.441	Yes	0.00021222	0.00072348														
25	Zrsr2	0.078	0.196	0.107	0.141	0.131	No	0.447	0.473	0.404	0.442	Yes	0.000206312	0.00072348														
26	Pqbp1	0.001	0.008	0.063	0.070	0.035	No	0.465	0.501	0.474	0.459	Yes	0.000229	0.00074674														
27	3830417A13Rik	0.010	0.029	0.096	0.025	0.040	No	0.360	0.381	0.394	0.381	Yes	0.00024293	0.00075716														
28	Tbc1d25	0.000	0.000	0.051	0.000	0.013	No	0.533	0.533	0.489	0.491	Yes	0.000281641	0.00084492														
29	Piga	0.008	0.128	0.075	0.121	0.083	No	0.520	0.446	0.563	0.509	Yes	0.000472521	0.00131256														
30	Gata1	0.093	0.093	0.140	0.119	0.117	No	0.495	0.554	0.483	0.511	Yes	0.000470855	0.00131256														
31	Txling	0.000	0.017	0.018	0.031	0.017	No	0.458	0.454	0.422	0.483	Yes	0.00051985	0.00139246														
32	Pim2	0.212	0.206	0.074	0.065	0.139	No	0.580	0.577	0.479	0.546	Yes	0.000563688	0.00145781														
33	Slc35a2	0.015	0.025	0.056	0.037	0.033	No	0.451	0.471	0.394	0.439	Yes	0.001050686	0.0026101														
34	Timm17b	0.007	0.008	0.069	0.082	0.042	No	0.460	0.436	0.353	0.419	Yes	0.001148443	0.0026101														
35	2610029G23Rik	0.097	0.167	0.050	0.210	0.131	No	0.456	0.428	0.476	0.476	Yes	0.001122252	0.0026101														
36	Eif2s3x	0.388	0.419	0.360	0.436	0.388	Yes	0.619	0.621	0.594	0.611	Yes	0.001117723	0.0026101														
37	Psmad10	0.000	0.000	0.041	0.013	0.013	No	0.368	0.447	0.385	0.400	Yes	0.001218701	0.00268831														
38	Rp2h	0.000	0.000	0.007	0.009	0.004	No	0.384	0.442	0.406	0.411	Yes	0.001450466	0.00310814														
39	Pcsk1n	0.000	0.006	0.164	0.030	0.050	No	0.614	0.648	0.470	0.577	Yes	0.001593649	0.0033201														
40	5530601H04Rik	0.131	0.235	0.210	0.241	0.204	Yes	0.488	0.417	0.405	0.437	Yes	0.001680754	0.00340693														
41	Gemin8	0.111	0.115	0.216	0.010	0.113	No	0.375	0.440	0.448	0.421	Yes	0.002056876	0.00405962														
42	Erc6f1	0.064	0.251	0.122	0.241	0.169	No	0.488	0.551	0.484	0.507	Yes	0.002227955	0.00428375														
43	Rhox6	0.015	0.026	0.056	0.077	0.044	No	0.421	0.541	0.516	0.493	Yes	0.002710934	0.005083														
44	Cdk16	0.005	0.003	0.067	0.045	0.030	No	0.376	0.490	0.391	0.419	Yes	0.003070156	0.00561614														
45	Car5b	0.002	0.067	0.044	0.020	0.033	No	0.415	0.370	0.301	0.362	Yes	0.00395754	0.00706704														
46	Rhox9	0.020	0.016	0.076	0.047	0.040	No	0.422	0.557	0.537	0.505	Yes	0.00433658	0.00730432														
47	Star8	0.172	0.171	0.227	0.033	0.151	No	0.357	0.439	0.482	0.426	Yes	0.004224792	0.00730432														
48	Kdm5c	0.143	0.152	0.196	0.202	0.173	Yes	0.458	0.428	0.361	0.415	Yes	0.004382591	0.00730432														
49	2900056M20Rik	0.000	0.000	0.080	0.332	0.103	No	0.663	0.645	0.594	0.634	Yes	0.004938323	0.00805161														
50	Tbc1d8b	0.009	0.004	0.010	0.006	0.007	No	0.429	0.504	0.391	0.441	Yes	0.00581269	0.00927557														
51	Cd9912	0.001	0.000	0.025	0.170	0.049	No	0.295	0.305	0.239	0.280	Yes	0.005987683	0.00935576														
52	Med12	0.000	0.000	0.051	0.012	0.016	No	0.548	0.455	0.392	0.465	Yes	0.006737911	0.01031313														
53	Mbn13	0.004	0.010	0.126	0.007	0.037	No	0.457	0.478	0.307	0.414	Yes	0.007065411	0.01059812														
54	Porcn	0.000	0.000	0.017	0.000	0.004	No	0.388	0.516	0.410	0.438	Yes	0.007652554	0.01111663														
55	Ctbs2	0.000	0.004	0.053	0.011	0.017	No	0.558	0.479	0.392	0.476	Yes	0.007707533	0.01111663														
56	Syap1	0.002	0.022	0.061	0.021	0.027	No	0.455	0.474	0.416	0.416	Yes	0.011218587	0.01587536														
57	Capn6	0.000	0.000	0.326	0.033	0.090	No	0.369	0.523	0.479	0.457	Yes	0.012186441	0.01692561														
58	Usp11	0.000	0.000	0.035	0.018	0.013	No	0.493	0.324	0.386	0.401	Yes	0.01370361	0.01868674														
59	Tceal8	0.000	0.000	0.013	0.000	0.003	No	0.207	0.261	0.169	0.212	Yes	0.014895495	0.01984972														
60	Tspyl2	0.001	0.004	0.021	0.072	0.025	No	0.367	0.221	0.288	0.288	Yes	0.015085788	0.01984972														
61	Mospd2	0.000	0.003	0.073	0.114	0.048	No	0.150	0.264	0.257	0.224	Yes	0.018903549	0.02444424														

1	A		B		C		D		E		F		G		H		I		J		K		L		M		N	
	Gene Name	WT 1	WT 2	WT 3	Eed ^{fl/fl}	WT Average	Consistent Escape in WT?	Eed ^{+/+} 1	Eed ^{+/+} 2	Eed ^{+/+} 3	Eed ^{+/+} Average	Consistent escape in Eed ^{+/+}	WT vs. Eed ^{+/+} P Value (T Test)	Adjusted P Value														
62	Rps4x	0.049	0.293	0.103	0.301	0.187	No	0.484	0.491	0.464	0.479	Yes	0.019486325	0.02477075														
63	Isc22d3	0.010	0.007	0.044	0.134	0.049	No	0.174	0.186	0.179	0.180	Yes	0.020775445	0.02596931														
64	Atg4a	0.000	0.012	0.073	0.053	0.034	No	0.430	0.495	0.283	0.403	Yes	0.021294296	0.02618151														
65	Cln5	0.002	0.000	0.083	0.031	0.029	No	0.329	0.548	0.573	0.484	Yes	0.022376012	0.02706776														
66	Bex1	0.001	0.001	0.052	0.342	0.099	No	0.387	0.391	0.460	0.413	Yes	0.027040049	0.03219053														
67	Yfp6	0.235	0.371	0.143	0.223	0.243	Yes	0.437	0.360	0.397	0.405	Yes	0.03601812	0.04220873														
68	Rhox4d	0.000	0.000	0.000	0.000	0.000	No	0.260	0.211	0.124	0.198	Yes	0.037836325	0.04299582														
69	Tmsb15b2	0.000	0.000	0.000	0.052	0.013	No	0.608	0.448	0.437	0.448	Yes	0.037401005	0.04299582														
70	Id5	0.011	0.006	0.088	0.012	0.029	No	0.229	0.432	0.246	0.302	Yes	0.042963682	0.04809367														
71	Nup62cl	0.000	0.000	0.072	0.333	0.101	No	0.334	0.334	0.333	0.334	Yes	0.060615878	0.06685575														
72	Ebp	0.000	0.004	0.064	0.008	0.008	No	0.115	0.290	0.325	0.244	Yes	0.067518064	0.07234078														
73	Plac1	0.091	0.064	0.165	0.733	0.263	No	0.548	0.717	0.818	0.694	Yes	0.0671087	0.07234078														
74	Oat	0.042	0.398	0.234	0.351	0.256	No	0.473	0.460	0.476	0.470	Yes	0.074176173	0.07835511														
75	AB330080D01Rik	0.011	0.008	0.098	0.024	0.035	No	0.154	0.559	0.495	0.403	Yes	0.095795749	0.09851141														
76	Rbbp7	0.001	0.002	0.083	0.056	0.036	No	0.647	0.203	0.392	0.414	Yes	0.095034036	0.15709621														
77	Taf1	0.054	0.461	0.364	0.479	0.340	No	0.523	0.529	0.529	0.526	Yes	0.155001594	0.15709621														
78	Rhox4c	0.950	0.310	0.237	0.940	0.609	Yes	0.821	0.964	0.971	0.919	Yes	0.210443323	0.21044332														
79	Gm6036	0.000	0.000	0.000	0.000	0.000	No	0.000	0.000	0.000	0.000	No	NA	NA														
80	Gria3	0.000	0.000	0.000	0.000	0.000	No	0.000	0.000	0.000	0.000	No	NA	NA														
81	Hs6st2	0.000	0.000	0.000	0.000	0.000	No	0.000	0.000	0.000	0.000	No	NA	NA														
82	LOC100504564	0.000	0.000	0.000	0.000	0.000	No	0.000	0.000	0.000	0.000	No	NA	NA														
83	Pja1	0.000	0.000	0.000	0.000	0.000	No	0.000	0.000	0.000	0.000	No	NA	NA														
84	Pixna3	0.000	0.000	0.000	0.000	0.000	No	0.000	0.000	0.000	0.000	No	NA	NA														
85	Rhox4g	0.000	0.000	0.000	0.000	0.000	No	0.000	0.003	0.000	0.001	No	NA	NA														
86	Trappc2	0.000	0.000	0.000	0.000	0.000	No	0.000	0.000	0.011	0.004	No	NA	NA														
87	Gpr173	0.000	0.000	0.000	0.000	0.000	No	0.176	0.163	0.026	0.122	No	NA	NA														
88	2810403D21Rik	0.000	0.000	0.000	0.000	0.000	No	NA	NA	NA	NA	No	NA	NA														
89	Gpr64	0.000	0.000	0.000	0.000	0.000	No	NA	NA	NA	NA	No	NA	NA														
90	Srxp2	0.000	0.000	0.000	0.000	0.000	No	NA	NA	NA	NA	No	NA	NA														
91	Tspan6	0.000	0.000	0.000	0.000	0.000	No	NA	NA	NA	NA	No	NA	NA														
92	LOC100046796	0.000	0.000	0.000	0.001	0.000	No	0.000	0.000	0.000	0.000	No	NA	NA														
93	Col4a5	0.000	0.000	0.000	0.001	0.000	No	0.000	0.000	0.000	0.000	No	NA	NA														
94	Timp1	0.000	0.000	0.001	0.000	0.000	No	0.000	0.069	0.004	0.024	No	NA	NA														
95	Tmem47	0.000	0.002	0.000	0.000	0.000	No	NA	NA	NA	NA	No	NA	NA														
96	Bgn	0.000	0.000	0.000	0.001	0.000	No	0.000	0.000	0.001	0.000	No	NA	NA														
97	Dock11	0.000	0.000	0.003	0.000	0.001	No	0.001	0.303	0.072	0.125	No	NA	NA														
98	Armcx3	0.000	0.004	0.000	0.000	0.001	No	0.000	0.000	0.000	0.000	No	NA	NA														
99	Fgf	0.005	0.000	0.000	0.000	0.001	No	NA	NA	NA	NA	No	NA	NA														
100	41157	0.000	0.005	0.000	0.000	0.001	No	0.000	0.176	0.001	0.059	No	NA	NA														
101	Sept6	0.000	0.005	0.000	0.000	0.001	No	0.000	0.176	0.001	0.059	No	NA	NA														
102	Apln	0.005	0.000	0.000	0.000	0.001	No	NA	NA	NA	NA	No	NA	NA														
103	Gpc4	0.000	0.000	0.000	0.005	0.001	No	0.028	0.145	0.109	0.094	No	NA	NA														
104	Lrch2	0.006	0.000	0.000	0.000	0.001	No	NA	NA	NA	NA	No	NA	NA														
105	Cask	0.000	0.000	0.003	0.004	0.002	No	0.006	0.000	0.000	0.002	No	NA	NA														
106	LOC100503437	0.007	0.000	0.000	0.000	0.002	No	0.000	0.000	0.000	0.000	No	NA	NA														
107	Yy2	0.000	0.000	0.000	0.009	0.002	No	0.000	0.000	0.051	0.017	No	NA	NA														
108	Sicl6a2	0.000	0.000	0.009	0.000	0.002	No	NA	NA	NA	NA	No	NA	NA														
109	Mid1p1	0.000	0.000	0.010	0.000	0.002	No	0.000	0.000	0.000	0.000	No	NA	NA														
110	Nono	0.000	0.000	0.009	0.001	0.002	No	0.012	0.017	0.018	0.016	No	NA	NA														
111	Fhl1	0.000	0.000	0.011	0.000	0.003	No	0.000	0.085	0.030	0.038	No	NA	NA														
112	Jil3ra1	0.000	0.000	0.006	0.006	0.003	No	0.000	0.036	0.046	0.027	No	NA	NA														
113	C1galt1c1	0.000	0.003	0.011	0.000	0.003	No	0.000	0.016	0.007	0.008	No	NA	NA														
114	Taf9b	0.000	0.000	0.000	0.000	0.004	No	0.000	0.052	0.133	0.069	No	NA	NA														
115	Alg13	0.000	0.000	0.015	0.000	0.004	No	NA	NA	NA	NA	No	NA	NA														
116	Pir	0.000	0.000	0.016	0.000	0.004	No	0.000	0.000	0.228	0.076	No	NA	NA														
117	Tspan7	0.000	0.000	0.011	0.017	0.004	No	NA	NA	NA	NA	No	NA	NA														
118	Prps2	0.000	0.000	0.011	0.006	0.004	No	0.000	0.251	0.143	0.131	No	NA	NA														
119	C330007P06Rik	0.002	0.001	0.010	0.006	0.005	No	0.001	0.001	0.001	0.001	No	NA	NA														

1	A		B		C		D		E		F		G		H		I		J		K		L		M		N	
	Gene Name	WT 1	WT 2	WT 3	Eed ^{fl/fl}	WT Average	Consistent Escape in WT?	Eed ^{fl/fl} 1	Eed ^{fl/fl} 2	Eed ^{fl/fl} 3	Eed ^{fl/fl} Average	Consistent escape in Eed ^{fl/fl} ?	WT vs. Eed ^{fl/fl} P Value (T Test)	Adjusted P Value														
120	Mum1l1	0.012	0.004	0.004	0.000	0.005	No	0.228	0.050	0.142	0.140	No	NA	NA														
121	Fam123b	0.000	0.000	0.026	0.000	0.006	No	0.000	0.000	0.000	0.000	No	NA	NA														
122	Mecp2	0.000	0.000	0.024	0.000	0.007	No	0.000	0.000	0.000	0.000	No	NA	NA														
123	Sh3kbp1	0.015	0.008	0.000	0.006	0.007	No	0.029	0.080	0.024	0.044	No	NA	NA														
124	Brc3	0.000	0.013	0.016	0.000	0.007	No	0.000	0.000	0.000	0.000	No	NA	NA														
125	Rps6ka3	0.000	0.000	0.029	0.000	0.007	No	0.000	0.000	0.000	0.000	No	NA	NA														
126	LOC100503426	0.002	0.000	0.019	0.007	0.007	No	0.036	0.147	0.085	0.089	No	NA	NA														
127	Phf6	0.000	0.000	0.024	0.001	0.008	No	0.004	0.004	0.000	0.000	No	NA	NA														
128	Magee1	0.005	0.002	0.029	0.000	0.009	No	NA	NA	NA	NA	No	NA	NA														
129	Pcdh19	0.011	0.009	0.014	0.000	0.009	No	0.000	0.000	0.000	0.000	No	NA	NA														
130	Phka2	0.000	0.000	0.030	0.005	0.009	No	0.000	0.000	0.000	0.000	No	NA	NA														
131	Tsr2	0.000	0.000	0.035	0.000	0.009	No	0.000	0.002	0.000	0.001	No	NA	NA														
132	Tex13	0.000	0.000	0.030	0.006	0.009	No	0.090	0.121	0.145	0.119	No	NA	NA														
133	Rhox4a	0.000	0.008	0.011	0.019	0.009	No	0.010	0.032	0.111	0.051	No	NA	NA														
134	Ubi4	0.003	0.002	0.033	0.000	0.009	No	0.000	0.000	0.000	0.000	No	NA	NA														
135	Ngr1ap1	0.000	0.002	0.028	0.007	0.009	No	0.247	0.006	0.064	0.106	No	NA	NA														
136	Phka1	0.000	0.000	0.034	0.005	0.010	No	0.000	0.004	0.026	0.010	No	NA	NA														
137	Lamp2	0.001	0.001	0.020	0.018	0.010	No	0.000	0.003	0.002	0.001	No	NA	NA														
138	2900062L11Rik	0.000	0.000	0.033	0.007	0.010	No	0.002	0.027	0.038	0.022	No	NA	NA														
139	Atp11c	0.000	0.000	0.040	0.010	0.010	No	0.000	0.000	0.000	0.000	No	NA	NA														
140	Tbl1x	0.007	0.000	0.034	0.001	0.010	No	0.008	0.000	0.005	0.000	No	NA	NA														
141	Phf8	0.000	0.000	0.043	0.000	0.011	No	0.000	0.000	0.000	0.000	No	NA	NA														
142	Magt1	0.001	0.000	0.024	0.018	0.011	No	0.332	0.005	0.000	0.116	No	NA	NA														
143	Mpp1	0.000	0.000	0.043	0.000	0.011	No	0.000	0.000	0.007	0.000	No	NA	NA														
144	Eif1ax	0.000	0.000	0.041	0.002	0.011	No	0.085	0.203	0.426	0.238	No	NA	NA														
145	Msn	0.000	0.001	0.042	0.000	0.011	No	0.000	0.001	0.000	0.000	No	NA	NA														
146	Cxx1b	0.000	0.002	0.000	0.042	0.011	No	0.000	0.000	0.043	0.014	No	NA	NA														
147	Naa10	0.000	0.000	0.033	0.010	0.011	No	0.000	0.000	0.000	0.000	No	NA	NA														
148	261002M06Rik	0.000	0.000	0.044	0.000	0.011	No	0.023	0.000	0.000	0.008	No	NA	NA														
149	Prickle3	0.000	0.000	0.032	0.013	0.011	No	0.049	0.110	0.266	0.141	No	NA	NA														
150	Alga4-2	0.000	0.000	0.047	0.000	0.012	No	0.163	0.108	0.175	0.148	Yes	NA	NA														
151	Prkx	0.000	0.002	0.045	0.000	0.012	No	0.000	0.000	0.000	0.000	No	NA	NA														
152	Fam120c	0.000	0.000	0.048	0.000	0.012	No	NA	NA	NA	NA	No	NA	NA														
153	Slc7a3	0.000	0.000	0.048	0.000	0.012	No	NA	NA	NA	NA	No	NA	NA														
154	Fundc1	0.000	0.002	0.025	0.022	0.012	No	0.000	0.402	0.356	0.253	No	NA	NA														
155	Stag2	0.000	0.000	0.046	0.004	0.013	No	0.000	0.000	0.000	0.000	No	NA	NA														
156	Htatsf1	0.003	0.002	0.046	0.000	0.013	No	0.000	0.000	0.002	0.001	No	NA	NA														
157	Tmem164	0.001	0.000	0.042	0.007	0.013	No	0.003	0.000	0.000	0.001	No	NA	NA														
158	Lage3	0.000	0.000	0.050	0.001	0.013	No	0.000	0.000	0.000	0.000	No	NA	NA														
159	Plb3	0.000	0.000	0.003	0.048	0.013	No	0.139	0.230	0.045	0.138	No	NA	NA														
160	Eda2r	0.003	0.002	0.028	0.018	0.013	No	0.010	0.343	0.382	0.245	No	NA	NA														
161	Tab3	0.001	0.002	0.048	0.003	0.013	No	0.001	0.000	0.001	0.001	No	NA	NA														
162	Pgrmc1	0.001	0.000	0.050	0.002	0.013	No	0.001	0.003	0.002	0.002	No	NA	NA														
163	Suv39h1	0.000	0.004	0.044	0.005	0.013	No	0.022	0.000	0.000	0.007	No	NA	NA														
164	Mtmr1	0.000	0.000	0.051	0.004	0.014	No	0.002	0.000	0.004	0.002	No	NA	NA														
165	Gyk	0.000	0.000	0.052	0.003	0.014	No	0.033	0.525	0.365	0.308	No	NA	NA														
166	Hsd17b10	0.003	0.003	0.050	0.000	0.014	No	0.000	0.000	0.004	0.001	No	NA	NA														
167	Armcx5	0.000	0.005	0.051	0.000	0.014	No	0.000	0.000	0.000	0.000	No	NA	NA														
168	Cenpi	0.000	0.004	0.053	0.000	0.014	No	0.000	0.000	0.000	0.000	No	NA	NA														
169	Zkda	0.000	0.000	0.057	0.000	0.014	No	0.008	0.001	0.011	0.006	No	NA	NA														
170	Igsec2	0.000	0.029	0.028	0.000	0.014	No	0.139	0.032	0.053	0.075	No	NA	NA														
171	Rbm10	0.000	0.000	0.055	0.003	0.014	No	0.035	0.032	0.077	0.048	No	NA	NA														
172	Fam3a	0.006	0.010	0.038	0.003	0.014	No	0.000	0.000	0.000	0.000	No	NA	NA														
173	Gprasp1	0.000	0.000	0.054	0.004	0.014	No	0.001	0.001	0.001	0.001	No	NA	NA														
174	Elf4	0.001	0.001	0.053	0.003	0.014	No	0.000	0.020	0.026	0.015	No	NA	NA														
175	Mtmr1	0.000	0.000	0.054	0.004	0.015	No	0.000	0.000	0.005	0.002	No	NA	NA														
176	Pkfb1	0.000	0.000	0.054	0.004	0.015	No	0.005	0.000	0.000	0.000	No	NA	NA														
177	Praf2	0.000	0.000	0.048	0.012	0.015	No	0.005	0.462	0.174	0.214	No	NA	NA														

1	Gene Name	B		C		D		E		F		G		H		I		J		K		L	M	N
		WT 1	WT 2	WT 3	Eed ^{off} /h	WT Average	Consistent Escape in WT?	Eed ^{off} -1	Eed ^{off} -2	Eed ^{off} -3	Eed ^{off} -Average	Consistent escape in Eed ^{off} -?	WT vs. Eed ^{off} - P Value (T Test)	Adjusted P Value										
178	Xlf3a	0.000	0.000	0.057	0.004	0.015	No	0.003	0.001	0.002	0.002	No	NA	NA	NA	NA	NA	NA	NA	NA	NA	NA	NA	
179	Bcor	0.006	0.001	0.049	0.005	0.015	No	0.000	0.000	0.000	0.000	No	NA	NA	NA	NA	NA	NA	NA	NA	NA	NA	NA	
180	Maoa	0.000	0.000	0.061	0.000	0.015	No	0.000	0.000	0.000	0.000	No	NA	NA	NA	NA	NA	NA	NA	NA	NA	NA	NA	
181	Itm2a	0.000	0.000	0.062	0.000	0.015	No	0.462	0.000	0.015	0.159	No	NA	NA	NA	NA	NA	NA	NA	NA	NA	NA	NA	
182	Xk	0.000	0.000	0.062	0.000	0.016	No	0.000	0.000	0.000	0.000	No	NA	NA	NA	NA	NA	NA	NA	NA	NA	NA	NA	
183	Idh3g	0.000	0.000	0.061	0.001	0.016	No	0.000	0.000	0.000	0.000	No	NA	NA	NA	NA	NA	NA	NA	NA	NA	NA	NA	
184	Trak1	0.004	0.000	0.058	0.001	0.016	No	0.001	0.002	0.001	0.001	No	NA	NA	NA	NA	NA	NA	NA	NA	NA	NA	NA	
185	Maged1	0.001	0.001	0.055	0.006	0.016	No	0.001	0.006	0.003	0.003	No	NA	NA	NA	NA	NA	NA	NA	NA	NA	NA	NA	
186	Hcfc1	0.000	0.001	0.061	0.001	0.016	No	0.000	0.001	0.000	0.000	No	NA	NA	NA	NA	NA	NA	NA	NA	NA	NA	NA	
187	Abcd7	0.017	0.002	0.038	0.006	0.016	No	0.020	0.010	0.023	0.018	No	NA	NA	NA	NA	NA	NA	NA	NA	NA	NA	NA	
188	Msi3	0.004	0.014	0.048	0.000	0.016	No	0.058	0.059	0.013	0.043	No	NA	NA	NA	NA	NA	NA	NA	NA	NA	NA	NA	
189	Rlim	0.003	0.003	0.054	0.007	0.016	No	0.028	0.032	0.046	0.035	No	NA	NA	NA	NA	NA	NA	NA	NA	NA	NA	NA	
190	A230072C01Rik	0.000	0.000	0.067	0.000	0.017	No	0.000	0.000	0.000	0.000	No	NA	NA	NA	NA	NA	NA	NA	NA	NA	NA	NA	
191	G6pdx	0.000	0.008	0.059	0.000	0.017	No	0.003	0.008	0.002	0.004	No	NA	NA	NA	NA	NA	NA	NA	NA	NA	NA	NA	
192	Mbtps2	0.010	0.000	0.057	0.000	0.017	No	0.000	0.014	0.000	0.005	No	NA	NA	NA	NA	NA	NA	NA	NA	NA	NA	NA	
193	Mcts1	0.005	0.000	0.062	0.000	0.017	No	0.000	0.000	0.000	0.000	No	NA	NA	NA	NA	NA	NA	NA	NA	NA	NA	NA	
194	Zfp275	0.000	0.000	0.043	0.025	0.017	No	0.000	0.000	0.000	0.000	No	NA	NA	NA	NA	NA	NA	NA	NA	NA	NA	NA	
195	Slc25a14	0.032	0.007	0.029	0.000	0.017	No	0.035	0.438	0.440	0.304	No	NA	NA	NA	NA	NA	NA	NA	NA	NA	NA	NA	
196	Dnase1l1	0.000	0.000	0.069	0.000	0.017	No	0.000	0.000	0.000	0.000	No	NA	NA	NA	NA	NA	NA	NA	NA	NA	NA	NA	
197	Zbtb33	0.004	0.001	0.060	0.005	0.018	No	0.000	0.000	0.002	0.001	No	NA	NA	NA	NA	NA	NA	NA	NA	NA	NA	NA	
198	Rpgr	0.000	0.000	0.071	0.000	0.018	No	0.000	0.007	0.143	0.050	No	NA	NA	NA	NA	NA	NA	NA	NA	NA	NA	NA	
199	Klh13	0.004	0.002	0.059	0.007	0.018	No	0.002	0.001	0.010	0.004	No	NA	NA	NA	NA	NA	NA	NA	NA	NA	NA	NA	
200	Rap9	0.000	0.002	0.071	0.000	0.018	No	0.000	0.002	0.000	0.001	No	NA	NA	NA	NA	NA	NA	NA	NA	NA	NA	NA	
201	Ublin2	0.000	0.000	0.073	0.000	0.018	No	0.000	0.000	0.000	0.000	No	NA	NA	NA	NA	NA	NA	NA	NA	NA	NA	NA	
202	Gpc3	0.000	0.000	0.074	0.000	0.019	No	NA	NA	NA	NA	No	NA	NA	NA	NA	NA	NA	NA	NA	NA	NA	NA	
203	Pdk3	0.021	0.002	0.027	0.026	0.019	No	0.014	0.031	0.018	0.021	No	NA	NA	NA	NA	NA	NA	NA	NA	NA	NA	NA	
204	Brwd3	0.002	0.001	0.068	0.006	0.019	No	0.441	0.001	0.005	0.149	No	NA	NA	NA	NA	NA	NA	NA	NA	NA	NA	NA	
205	Nrk	0.004	0.011	0.057	0.004	0.019	No	0.007	0.005	0.004	0.005	No	NA	NA	NA	NA	NA	NA	NA	NA	NA	NA	NA	
206	Lomf3	0.000	0.001	0.076	0.000	0.019	No	0.000	0.003	0.010	0.004	No	NA	NA	NA	NA	NA	NA	NA	NA	NA	NA	NA	
207	Atp6ap1	0.003	0.001	0.065	0.009	0.020	No	0.001	0.000	0.001	0.001	No	NA	NA	NA	NA	NA	NA	NA	NA	NA	NA	NA	
208	Acot9	0.003	0.002	0.062	0.012	0.020	No	0.447	0.001	0.001	0.160	No	NA	NA	NA	NA	NA	NA	NA	NA	NA	NA	NA	
209	Hprt	0.000	0.000	0.077	0.001	0.020	No	0.000	0.018	0.000	0.006	No	NA	NA	NA	NA	NA	NA	NA	NA	NA	NA	NA	
210	Eik1	0.000	0.000	0.048	0.033	0.020	No	0.065	0.222	0.024	0.104	No	NA	NA	NA	NA	NA	NA	NA	NA	NA	NA	NA	
211	Sat1	0.000	0.005	0.066	0.010	0.020	No	0.005	0.000	0.000	0.002	No	NA	NA	NA	NA	NA	NA	NA	NA	NA	NA	NA	
212	Rap2c	0.000	0.000	0.081	0.000	0.020	No	0.002	0.000	0.000	0.001	No	NA	NA	NA	NA	NA	NA	NA	NA	NA	NA	NA	
213	Bcap31	0.001	0.001	0.053	0.026	0.020	No	0.000	0.002	0.002	0.001	No	NA	NA	NA	NA	NA	NA	NA	NA	NA	NA	NA	
214	Zfx	0.000	0.001	0.083	0.000	0.021	No	0.035	0.072	0.054	0.053	No	NA	NA	NA	NA	NA	NA	NA	NA	NA	NA	NA	
215	Renbp	0.000	0.002	0.079	0.003	0.021	No	0.000	0.000	0.000	0.000	No	NA	NA	NA	NA	NA	NA	NA	NA	NA	NA	NA	
216	Cstf2	0.004	0.003	0.076	0.001	0.021	No	0.000	0.002	0.000	0.001	No	NA	NA	NA	NA	NA	NA	NA	NA	NA	NA	NA	
217	Alfm1	0.002	0.002	0.075	0.005	0.021	No	0.000	0.013	0.014	0.009	No	NA	NA	NA	NA	NA	NA	NA	NA	NA	NA	NA	
218	Mospd1	0.004	0.008	0.064	0.009	0.021	No	0.104	0.517	0.350	0.324	Yes	NA	NA	NA	NA	NA	NA	NA	NA	NA	NA	NA	
219	Ocr1	0.003	0.000	0.064	0.018	0.021	No	0.106	0.494	0.443	0.443	Yes	NA	NA	NA	NA	NA	NA	NA	NA	NA	NA	NA	
220	Amnecr1	0.000	0.000	0.086	0.000	0.021	No	0.000	0.000	0.004	0.001	No	NA	NA	NA	NA	NA	NA	NA	NA	NA	NA	NA	
221	Smc1a	0.002	0.001	0.084	0.000	0.022	No	0.000	0.000	0.000	0.000	No	NA	NA	NA	NA	NA	NA	NA	NA	NA	NA	NA	
222	Emd	0.000	0.000	0.081	0.006	0.022	No	0.000	0.000	0.000	0.000	No	NA	NA	NA	NA	NA	NA	NA	NA	NA	NA	NA	
223	Apex2	0.009	0.000	0.079	0.000	0.022	No	0.010	0.000	0.000	0.000	No	NA	NA	NA	NA	NA	NA	NA	NA	NA	NA	NA	
224	1600014k23Rik	0.019	0.014	0.055	0.000	0.022	No	0.000	0.000	0.200	0.067	No	NA	NA	NA	NA	NA	NA	NA	NA	NA	NA	NA	
225	Maged2	0.001	0.020	0.061	0.006	0.022	No	0.001	0.000	0.000	0.000	No	NA	NA	NA	NA	NA	NA	NA	NA	NA	NA	NA	
226	Nkrf	0.000	0.000	0.089	0.000	0.022	No	0.000	0.000	0.000	0.000	No	NA	NA	NA	NA	NA	NA	NA	NA	NA	NA	NA	
227	Shroom2	0.002	0.000	0.082	0.004	0.022	No	0.004	0.008	0.016	0.008	No	NA	NA	NA	NA	NA	NA	NA	NA	NA	NA	NA	
228	Acs4	0.001	0.002	0.073	0.013	0.022	No	0.018	0.007	0.016	0.014	No	NA	NA	NA	NA	NA	NA	NA	NA	NA	NA	NA	
229	C77370	0.000	0.000	0.090	0.000	0.022	No	NA	NA	NA	NA	No	NA	NA	NA	NA	NA	NA	NA	NA	NA	NA	NA	
230	2610030H06Rik	0.007	0.002	0.072	0.016	0.023	No	0.172	0.000	0.002	0.058	No	NA	NA	NA	NA	NA	NA	NA	NA	NA	NA	NA	
231	Rbm2c	0.001	0.003	0.054	0.028	0.023	No	0.009	0.029	0.033	0.024	No	NA	NA	NA	NA	NA	NA	NA	NA	NA	NA	NA	
232	Usp9x	0.005	0.002	0.075	0.009	0.023	No	0.005	0.094	0.125	0.092	No	NA	NA	NA	NA	NA	NA	NA	NA	NA	NA	NA	
233	Cfp	0.000	0.000	0.092	0.000	0.023	No	0.038	0.183	0.089	0.089	No	NA	NA	NA	NA	NA	NA	NA	NA	NA	NA	NA	
234	Haus7	0.000	0.004	0.064	0.025	0.023	No	0.000	0.003	0.000	0.001	No	NA	NA	NA	NA	NA	NA	NA	NA	NA	NA	NA	
235	Ap1s2	0.006	0.000	0.087	0.000	0.023	No	0.000	0.000	0.003	0.001	No	NA	NA	NA	NA	NA	NA	NA	NA	NA	NA	NA	

1	Gene Name	B		C		D		E		F		G		H		I		J		K		L	M	N
		WT 1	WT 2	WT 3	Eed ^{off}	WT Average	Consistent Escape in WT?	Eed ^{+/+} 1	Eed ^{+/+} 2	Eed ^{+/+} 3	Eed ^{+/+} Average	Consistent escape in Eed ^{-/-} ?	WT vs. Eed ^{-/-} P Value (T Test)	Adjusted P Value										
236	Dlg3	0.003	0.024	0.043	0.023	0.023	No	0.516	0.011	0.009	0.179	No	NA	NA										
237	Chm	0.004	0.013	0.047	0.031	0.024	No	0.002	0.001	0.000	0.001	No	NA	NA										
238	Xiap	0.003	0.019	0.062	0.011	0.024	No	0.000	0.137	0.001	0.047	No	NA	NA										
239	Iaz	0.000	0.000	0.096	0.000	0.024	No	0.000	0.000	0.000	0.000	No	NA	NA										
240	Pola1	0.000	0.000	0.097	0.000	0.024	No	0.000	0.000	0.008	0.003	No	NA	NA										
241	Ndufr1	0.035	0.021	0.039	0.002	0.024	No	0.000	0.015	0.005	0.006	No	NA	NA										
242	Eras	0.004	0.000	0.085	0.009	0.024	No	NA	NA	NA	NA	No	NA	NA										
243	Mid2	0.005	0.007	0.008	0.079	0.025	No	0.113	0.114	0.106	0.111	Yes	NA	NA										
244	Chic1	0.000	0.000	0.099	0.000	0.025	No	0.030	0.000	0.039	0.023	No	NA	NA										
245	Atg6ap2	0.005	0.002	0.066	0.026	0.025	No	0.000	0.001	0.003	0.001	No	NA	NA										
246	Fancb	0.000	0.000	0.091	0.000	0.025	No	NA	NA	NA	NA	No	NA	NA										
247	Zdhxc9	0.002	0.003	0.057	0.038	0.025	No	0.088	0.489	0.362	0.313	No	NA	NA										
248	Rbm3	0.000	0.007	0.093	0.002	0.026	No	0.068	0.052	0.029	0.050	No	NA	NA										
249	Wdr44	0.000	0.005	0.098	0.000	0.026	No	0.000	0.000	0.000	0.000	No	NA	NA										
250	Ndufrb11	0.022	0.011	0.054	0.017	0.026	No	0.040	0.053	0.040	0.045	No	NA	NA										
251	Las1	0.006	0.010	0.062	0.025	0.026	No	0.003	0.000	0.007	0.003	No	NA	NA										
252	Dkc1	0.005	0.000	0.099	0.000	0.026	No	0.000	0.000	0.000	0.000	No	NA	NA										
253	Ube2a	0.006	0.000	0.075	0.024	0.026	No	0.000	0.044	0.000	0.015	No	NA	NA										
254	1110012L19Rik	0.003	0.002	0.064	0.036	0.026	No	0.037	0.435	0.326	0.266	No	NA	NA										
255	Cox7b	0.001	0.001	0.090	0.015	0.027	No	0.485	0.022	0.019	0.176	No	NA	NA										
256	RbmX	0.000	0.005	0.087	0.016	0.027	No	0.015	0.009	0.000	0.008	No	NA	NA										
257	Gnl3l	0.001	0.001	0.091	0.016	0.027	No	0.443	0.002	0.006	0.151	No	NA	NA										
258	Esx1	0.000	0.000	0.109	0.000	0.027	No	0.000	0.001	0.001	0.001	No	NA	NA										
259	Mimgt1	0.002	0.001	0.096	0.010	0.027	No	0.000	0.385	0.233	0.315	No	NA	NA										
260	Mageb16	0.009	0.008	0.093	0.000	0.027	No	0.030	0.000	0.004	0.011	No	NA	NA										
261	Slc25a43	0.000	0.000	0.090	0.020	0.027	No	0.000	0.594	0.067	0.220	No	NA	NA										
262	Ofd1	0.007	0.010	0.091	0.004	0.028	No	0.044	0.016	0.068	0.042	No	NA	NA										
263	Foxo4	0.002	0.002	0.108	0.000	0.028	No	0.000	0.004	0.003	0.003	No	NA	NA										
264	Vbp1	0.000	0.005	0.099	0.012	0.029	No	0.000	0.000	0.000	0.000	No	NA	NA										
265	Zip182	0.000	0.000	0.117	0.000	0.029	No	0.000	0.000	0.000	0.000	No	NA	NA										
266	Upr3b	0.004	0.000	0.077	0.037	0.029	No	0.014	0.318	0.009	0.113	No	NA	NA										
267	Zip280c	0.002	0.003	0.031	0.082	0.029	No	0.084	0.082	0.088	0.088	No	NA	NA										
268	Fam122b	0.016	0.013	0.090	0.003	0.031	No	0.013	0.072	0.074	0.053	No	NA	NA										
269	Bhlhb9	0.000	0.000	0.126	0.000	0.031	No	0.002	0.000	0.001	0.001	No	NA	NA										
270	Ribc1	0.000	0.017	0.110	0.000	0.032	No	0.000	0.000	0.000	0.000	No	NA	NA										
271	Nkap	0.022	0.024	0.068	0.014	0.032	No	0.041	0.037	0.044	0.041	No	NA	NA										
272	6720401G13Rik	0.023	0.029	0.038	0.039	0.032	No	0.000	0.000	0.000	0.000	No	NA	NA										
273	Apoal	0.000	0.010	0.120	0.000	0.032	No	0.000	0.000	0.000	0.000	No	NA	NA										
274	Fgd1	0.007	0.043	0.080	0.000	0.033	No	0.015	0.000	0.000	0.005	No	NA	NA										
275	Zip449	0.000	0.000	0.130	0.000	0.033	No	0.000	0.048	0.019	0.022	No	NA	NA										
276	2210013021Rik	0.000	0.000	0.132	0.000	0.033	No	0.000	0.000	0.000	0.000	No	NA	NA										
277	Nsdh1	0.004	0.004	0.079	0.046	0.033	No	0.000	0.437	0.417	0.285	No	NA	NA										
278	LOC100504671	0.000	0.000	0.092	0.042	0.034	No	0.126	0.519	0.539	0.395	Yes	NA	NA										
279	4933407K13Rik	0.000	0.000	0.134	0.000	0.034	No	NA	NA	NA	NA	No	NA	NA										
280	Ikbkg	0.034	0.034	0.063	0.000	0.034	No	0.001	0.000	0.046	0.016	No	NA	NA										
281	Armcx2	0.067	0.059	0.114	0.000	0.035	No	0.000	0.000	0.125	0.042	No	NA	NA										
282	Lpar4	0.005	0.072	0.064	0.000	0.035	No	NA	NA	NA	NA	No	NA	NA										
283	Fam199x	0.008	0.022	0.085	0.025	0.035	No	0.040	0.646	0.549	0.411	No	NA	NA										
284	Slc9a6	0.000	0.000	0.080	0.052	0.035	No	0.480	0.480	0.428	0.304	No	NA	NA										
285	Pp1s1	0.000	0.005	0.125	0.012	0.036	No	0.000	0.006	0.003	0.003	No	NA	NA										
286	Pdha1	0.002	0.001	0.115	0.024	0.036	No	0.003	0.003	0.010	0.005	No	NA	NA										
287	Akap17b	0.004	0.005	0.110	0.025	0.036	No	0.002	0.362	0.040	0.135	No	NA	NA										
288	Med14	0.010	0.009	0.063	0.062	0.036	No	0.003	0.003	0.022	0.026	No	NA	NA										
289	Hmgn5	0.000	0.000	0.146	0.000	0.037	No	0.020	0.000	0.026	0.015	No	NA	NA										
290	Atrx	0.001	0.000	0.072	0.076	0.037	No	0.066	0.070	0.073	0.070	No	NA	NA										
291	Gpm6b	0.023	0.000	0.000	0.130	0.038	No	0.000	0.099	0.300	0.133	No	NA	NA										
292	Cxx1c	0.000	0.000	0.044	0.109	0.038	No	0.040	0.000	0.142	0.061	No	NA	NA										
293	Abcd1	0.012	0.000	0.127	0.016	0.039	No	0.001	0.000	0.000	0.000	No	NA	NA										

1	A		B		C		D		E		F		G		H		I		J		K		L		M		N	
	Gene Name	WT 1	WT 2	WT 3	Eed ^{off} /n	WT Average	Consistent Escape in WT?	Eed ^{off} 1	Eed ^{off} 2	Eed ^{off} 3	Eed ^{off} Average	Consistent escape in Eed ^{off} 1-3	WT vs. Eed ^{off} P Value (T Test)	Adjusted P Value														
294	Usp27x	0.003	0.000	0.152	0.002	0.039	No	0.000	0.000	0.021	0.007	No	NA	NA														
295	Tceanc	0.010	0.022	0.097	0.028	0.039	No	0.404	0.357	0.022	0.261	No	NA	NA														
296	Prrg3	0.000	0.000	0.064	0.101	0.041	No	0.000	0.097	0.100	0.099	No	NA	NA														
297	Rpl36a	0.004	0.011	0.089	0.068	0.043	No	0.000	0.000	0.000	0.000	No	NA	NA														
298	Morc4	0.007	0.010	0.147	0.008	0.043	No	0.023	0.594	0.550	0.389	No	NA	NA														
299	Nkt2	0.015	0.018	0.068	0.071	0.043	No	0.167	0.000	0.073	0.080	No	NA	NA														
300	Shroom4	0.013	0.013	0.083	0.071	0.045	No	0.085	0.392	0.454	0.310	No	NA	NA														
301	Efnb1	0.033	0.000	0.109	0.038	0.045	No	0.000	0.000	0.008	0.003	No	NA	NA														
302	Gm4779	0.000	0.000	0.182	0.000	0.045	No	0.016	0.024	0.043	0.028	No	NA	NA														
303	8030474K03R1K	0.000	0.125	0.048	0.010	0.046	No	0.012	0.025	0.055	0.031	No	NA	NA														
304	1810030007R1K	0.037	0.002	0.046	0.100	0.046	No	0.007	0.387	0.160	0.185	No	NA	NA														
305	Amtot	0.003	0.025	0.120	0.013	0.047	No	0.368	0.001	0.006	0.006	No	NA	NA														
306	Apoo	0.003	0.002	0.123	0.062	0.048	No	0.138	0.494	0.418	0.350	Yes	NA	NA														
307	Bcor1l	0.013	0.007	0.095	0.079	0.048	No	0.120	0.315	0.336	0.257	Yes	NA	NA														
308	BC023829	0.000	0.000	0.183	0.011	0.049	No	0.000	0.000	0.000	0.000	No	NA	NA														
309	Himgb3	0.000	0.000	0.195	0.000	0.049	No	0.000	0.000	0.000	0.000	No	NA	NA														
310	Athae6	0.023	0.016	0.108	0.048	0.049	No	0.003	0.001	0.000	0.002	No	NA	NA														
311	Thoc2	0.000	0.001	0.196	0.002	0.050	No	0.000	0.002	0.000	0.001	No	NA	NA														
312	Ddk3x	0.056	0.025	0.121	0.003	0.051	No	0.000	0.002	0.001	0.001	No	NA	NA														
313	Gm9	0.050	0.044	0.097	0.015	0.052	No	0.062	0.184	0.088	0.088	No	NA	NA														
314	4933402E13R1K	0.013	0.019	0.179	0.000	0.053	No	NA	NA	NA	NA	No	NA	NA														
315	Pztd11	0.000	0.134	0.073	0.005	0.053	No	0.000	0.000	0.000	0.000	No	NA	NA														
316	Mcart6	0.002	0.000	0.147	0.000	0.055	No	0.127	0.375	0.283	0.262	Yes	NA	NA														
317	Diap2	0.016	0.015	0.084	0.108	0.056	No	0.125	0.116	0.000	0.000	No	NA	NA														
318	BC022960	0.000	0.167	0.058	0.000	0.056	No	0.000	0.013	0.000	0.004	No	NA	NA														
319	Flina	0.056	0.056	0.095	0.031	0.059	No	0.014	0.008	0.032	0.018	No	NA	NA														
320	Trimr8a1	0.000	0.000	0.204	0.034	0.060	No	0.000	0.000	0.000	0.000	No	NA	NA														
321	Ddx26b	0.019	0.027	0.189	0.023	0.065	No	0.000	0.434	0.470	0.301	No	NA	NA														
322	Sms	0.047	0.083	0.131	0.000	0.065	No	0.000	0.000	0.023	0.008	No	NA	NA														
323	Xlr5a	0.111	0.077	0.072	0.000	0.065	No	0.000	0.005	0.022	0.009	No	NA	NA														
324	Hdx	0.000	0.000	0.267	0.000	0.067	No	NA	NA	NA	NA	No	NA	NA														
325	Tmeim29	0.054	0.034	0.000	0.188	0.069	No	0.406	0.241	0.180	0.241	Yes	NA	NA														
326	Kdm6a	0.000	0.153	0.089	0.000	0.070	No	0.000	0.001	0.000	0.000	No	NA	NA														
327	Cxx1a	0.000	0.000	0.288	0.000	0.072	No	0.000	0.000	0.048	0.016	No	NA	NA														
328	Ncrna00086	0.000	0.000	0.285	0.009	0.074	No	0.016	0.245	0.139	0.133	No	NA	NA														
329	Sh3bgrl	0.041	0.040	0.185	0.037	0.076	No	0.399	0.040	0.029	0.156	No	NA	NA														
330	Xlr3c	0.012	0.012	0.277	0.074	0.094	No	0.003	0.003	0.018	0.007	No	NA	NA														
331	Gla	0.100	0.098	0.070	0.122	0.098	No	0.105	0.108	0.105	0.106	Yes	NA	NA														
332	Trmt2b	0.093	0.100	0.102	0.111	0.101	No	0.091	0.083	0.091	0.088	No	NA	NA														
333	Utp14a	0.120	0.152	0.115	0.082	0.117	No	0.126	0.506	0.459	0.364	Yes	NA	NA														
334	Hmrph2	0.136	0.140	0.059	0.142	0.119	No	0.139	0.144	0.142	0.142	Yes	NA	NA														
335	Dcaf12l1	0.000	0.000	0.476	0.006	0.120	No	0.002	0.004	0.022	0.009	No	NA	NA														
336	Huwe1	0.138	0.141	0.202	0.011	0.123	No	0.004	0.007	0.012	0.008	No	NA	NA														
337	Hccs	0.138	0.216	0.130	0.013	0.125	No	0.010	0.000	0.033	0.014	No	NA	NA														
338	Atp7a	0.101	0.115	0.190	0.126	0.133	Yes	0.498	0.218	0.187	0.301	Yes	NA	NA														
339	Rps6ka6	0.216	0.226	0.088	0.009	0.135	No	NA	NA	NA	NA	No	NA	NA														
340	Zxdh	0.178	0.200	0.199	0.000	0.144	No	NA	NA	NA	NA	No	NA	NA														
341	Klf4	0.129	0.232	0.215	0.007	0.146	No	0.007	0.000	0.011	0.006	No	NA	NA														
342	Rpl10	0.002	0.501	0.083	0.003	0.147	No	0.002	0.002	0.002	0.002	No	NA	NA														
343	Xlr3b	0.127	0.190	0.276	0.012	0.151	No	0.024	0.010	0.023	0.019	No	NA	NA														
344	Wnk3-ps	0.144	0.156	0.216	0.092	0.152	No	0.090	0.083	0.091	0.088	No	NA	NA														
345	Cui4b	0.103	0.103	0.291	0.118	0.154	Yes	0.103	0.105	0.113	0.107	Yes	NA	NA														
346	Fundc2	0.317	0.201	0.099	0.000	0.154	No	0.000	0.000	0.000	0.000	No	NA	NA														
347	Morf4l2	0.287	0.260	0.059	0.057	0.166	No	0.120	0.523	0.528	0.390	Yes	NA	NA														
348	Snx12	0.190	0.190	0.296	0.003	0.170	No	0.007	0.013	0.063	0.028	No	NA	NA														
349	C430049B03R1K	0.209	0.205	0.222	0.049	0.171	No	0.025	0.479	0.451	0.319	Yes	NA	NA														
350	Slah1b	0.020	0.259	0.094	0.329	0.176	No	0.157	0.216	0.418	0.264	Yes	NA	NA														
351	Armck1	0.174	0.138	0.210	0.252	0.193	Yes	NA	NA	NA	NA	No	NA	NA														

Gene Name	B		C		D		E		F		G		H		I		J		K		L	M	N	
	WT 1	WT 2	WT 3	Eed ^{off} /n	WT Average	Consistent Escape in WT?	Eed ^{+/+} 1	Eed ^{+/+} 2	Eed ^{+/+} 3	Eed ^{+/+} Average	Consistent escape in Eed ^{+/+} ?	WT vs. Eed ^{+/+} P Value (T Test)	Adjusted P Value											
1																								
2																								
3																								
352	B230206f22Rik	0.277	0.290	0.193	0.218	Yes	0.197	0.264	0.284	0.248	Yes	NA	NA	NA	NA	NA	NA	NA	0.248	Yes	NA	NA	NA	
353	Midi1	0.378	0.299	0.253	0.116	Yes	0.111	0.247	0.244	0.201	Yes	NA	NA	NA	NA	NA	NA	NA	0.201	Yes	NA	NA	NA	
354	Fmr1	0.321	0.328	0.380	0.019	Yes	0.328	0.380	0.019	0.020	No	NA	NA	NA	NA	NA	NA	NA	0.019	No	NA	NA	NA	
355	Zfp185	0.333	0.385	0.441	0.012	No	0.000	0.001	0.011	0.004	No	NA	NA	NA	NA	NA	NA	NA	0.004	No	NA	NA	NA	
356	Gdi1	0.342	0.303	0.425	0.237	Yes	0.169	0.170	0.176	0.172	Yes	NA	NA	NA	NA	NA	NA	NA	0.172	Yes	NA	NA	NA	
357	Rhox4b	0.351	0.365	0.189	0.415	Yes	0.108	0.207	0.283	0.152	Yes	NA	NA	NA	NA	NA	NA	NA	0.152	No	NA	NA	NA	
358	Bex2	0.357	0.417	0.257	0.320	Yes	0.227	0.136	0.275	0.213	Yes	NA	NA	NA	NA	NA	NA	NA	0.213	Yes	NA	NA	NA	
359	Sic10a3	0.500	0.500	0.530	0.000	No	0.500	0.500	0.469	0.490	No	NA	NA	NA	NA	NA	NA	NA	0.490	Yes	NA	NA	NA	
360	Gspt2	0.693	0.310	0.700	0.043	No	0.000	0.000	0.028	0.009	No	NA	NA	NA	NA	NA	NA	NA	0.009	No	NA	NA	NA	
361	BC065397	0.641	1.000	0.048	0.130	No	0.060	0.545	0.410	0.339	No	NA	NA	NA	NA	NA	NA	NA	0.339	No	NA	NA	NA	
362	Pnck	0.500	0.500	0.543	0.467	Yes	0.500	0.500	0.500	0.500	Yes	NA	NA	NA	NA	NA	NA	NA	0.500	Yes	NA	NA	NA	
363	Dusp9	0.502	0.499	0.532	0.511	Yes	0.499	0.500	0.499	0.500	Yes	NA	NA	NA	NA	NA	NA	NA	0.500	Yes	NA	NA	NA	
364	Rhox4e	0.906	0.902	0.672	0.547	Yes	0.757	0.987	0.984	0.984	Yes	NA	NA	NA	NA	NA	NA	NA	0.984	Yes	NA	NA	NA	
365	Xist	0.985	0.987	0.984	0.982	Yes	0.984	0.987	0.984	0.984	Yes	NA	NA	NA	NA	NA	NA	NA	0.984	Yes	NA	NA	NA	
366	Dynt3	1.000	1.000	1.000	1.000	Yes	1.000	1.000	1.000	1.000	Yes	NA	NA	NA	NA	NA	NA	NA	1.000	Yes	NA	NA	NA	
367	LOC100503459	1.000	1.000	1.000	1.000	Yes	1.000	1.000	1.000	1.000	Yes	NA	NA	NA	NA	NA	NA	NA	1.000	Yes	NA	NA	NA	
368	1600025M17Rik	NA	NA	NA	NA	NA	NA	NA	NA	NA	NA	NA	NA	NA	NA	NA	NA	NA	NA	NA	NA	NA	NA	
369	170000805Rik	NA	NA	NA	NA	NA	NA	NA	NA	NA	NA	NA	NA	NA	NA	NA	NA	NA	NA	NA	NA	NA	NA	
370	6530401D17Rik	NA	NA	NA	NA	NA	NA	NA	NA	NA	NA	NA	NA	NA	NA	NA	NA	NA	NA	NA	NA	NA	NA	
371	Fndc3c1	NA	NA	NA	NA	NA	NA	NA	NA	NA	NA	NA	NA	NA	NA	NA	NA	NA	NA	NA	NA	NA	NA	
372	Gabre	NA	NA	NA	NA	NA	NA	NA	NA	NA	NA	NA	NA	NA	NA	NA	NA	NA	NA	NA	NA	NA	NA	
373	Gm14685	NA	NA	NA	NA	NA	NA	NA	NA	NA	NA	NA	NA	NA	NA	NA	NA	NA	NA	NA	NA	NA	NA	
374	Gprasp2	NA	NA	NA	NA	NA	NA	NA	NA	NA	NA	NA	NA	NA	NA	NA	NA	NA	NA	NA	NA	NA	NA	
375	Itgb1bp2	NA	NA	NA	NA	NA	NA	NA	NA	NA	NA	NA	NA	NA	NA	NA	NA	NA	NA	NA	NA	NA	NA	
376	Klhl15	NA	NA	NA	NA	NA	NA	NA	NA	NA	NA	NA	NA	NA	NA	NA	NA	NA	NA	NA	NA	NA	NA	
377	L1cam	NA	NA	NA	NA	NA	NA	NA	NA	NA	NA	NA	NA	NA	NA	NA	NA	NA	NA	NA	NA	NA	NA	
378	Map3k15	NA	NA	NA	NA	NA	NA	NA	NA	NA	NA	NA	NA	NA	NA	NA	NA	NA	NA	NA	NA	NA	NA	
379	Mtap7d2	NA	NA	NA	NA	NA	NA	NA	NA	NA	NA	NA	NA	NA	NA	NA	NA	NA	NA	NA	NA	NA	NA	
380	Nhs12	NA	NA	NA	NA	NA	NA	NA	NA	NA	NA	NA	NA	NA	NA	NA	NA	NA	NA	NA	NA	NA	NA	
381	Nudt11	NA	NA	NA	NA	NA	NA	NA	NA	NA	NA	NA	NA	NA	NA	NA	NA	NA	NA	NA	NA	NA	NA	
382	Pfzd4	NA	NA	NA	NA	NA	NA	NA	NA	NA	NA	NA	NA	NA	NA	NA	NA	NA	NA	NA	NA	NA	NA	
383	Rhox12	NA	NA	NA	NA	NA	NA	NA	NA	NA	NA	NA	NA	NA	NA	NA	NA	NA	NA	NA	NA	NA	NA	
384	Sic9a7	NA	NA	NA	NA	NA	NA	NA	NA	NA	NA	NA	NA	NA	NA	NA	NA	NA	NA	NA	NA	NA	NA	
385	Sym1	NA	NA	NA	NA	NA	NA	NA	NA	NA	NA	NA	NA	NA	NA	NA	NA	NA	NA	NA	NA	NA	NA	
386	Xir5b	NA	NA	NA	NA	NA	NA	NA	NA	NA	NA	NA	NA	NA	NA	NA	NA	NA	NA	NA	NA	NA	NA	
387	Zdhhc15	NA	NA	NA	NA	NA	NA	NA	NA	NA	NA	NA	NA	NA	NA	NA	NA	NA	NA	NA	NA	NA	NA	
388	Dgkck-2	NA	NA	NA	NA	NA	NA	NA	NA	NA	NA	NA	NA	NA	NA	NA	NA	NA	NA	NA	NA	NA	NA	
389	Syp	NA	NA	NA	NA	NA	NA	NA	NA	NA	NA	NA	NA	NA	NA	NA	NA	NA	NA	NA	NA	NA	NA	
390	Klf8	NA	NA	NA	NA	NA	NA	NA	NA	NA	NA	NA	NA	NA	NA	NA	NA	NA	NA	NA	NA	NA	NA	
391	Pip1	NA	NA	NA	NA	NA	NA	NA	NA	NA	NA	NA	NA	NA	NA	NA	NA	NA	NA	NA	NA	NA	NA	
392	LOC100503525	NA	NA	NA	NA	NA	NA	NA	NA	NA	NA	NA	NA	NA	NA	NA	NA	NA	NA	NA	NA	NA	NA	
393	Ppp1r3f	NA	NA	NA	NA	NA	NA	NA	NA	NA	NA	NA	NA	NA	NA	NA	NA	NA	NA	NA	NA	NA	NA	
394	Fhd3c2	NA	NA	NA	NA	NA	NA	NA	NA	NA	NA	NA	NA	NA	NA	NA	NA	NA	NA	NA	NA	NA	NA	
395	AU015836	NA	NA	NA	NA	NA	NA	NA	NA	NA	NA	NA	NA	NA	NA	NA	NA	NA	NA	NA	NA	NA	NA	
396	Reps2	NA	NA	NA	NA	NA	NA	NA	NA	NA	NA	NA	NA	NA	NA	NA	NA	NA	NA	NA	NA	NA	NA	
397	Foxp3	NA	NA	NA	NA	NA	NA	NA	NA	NA	NA	NA	NA	NA	NA	NA	NA	NA	NA	NA	NA	NA	NA	
398	4930524123Rik	NA	NA	NA	NA	NA	NA	NA	NA	NA	NA	NA	NA	NA	NA	NA	NA	NA	NA	NA	NA	NA	NA	
399	Gm5637	NA	NA	NA	NA	NA	NA	NA	NA	NA	NA	NA	NA	NA	NA	NA	NA	NA	NA	NA	NA	NA	NA	
400	Gm5946	NA	NA	NA	NA	NA	NA	NA	NA	NA	NA	NA	NA	NA	NA	NA	NA	NA	NA	NA	NA	NA	NA	

Table 5.2: Differential Expression Analysis of X-chromosome Genes

Gene Name	B		C		D		E		F		G		H		I	
	DESeq2 Results: Log ₂ Fold Change	Total X-chromosome P Value	Adjusted P Value	DESeq2 Results: Log ₂ Fold Change	Adjusted P Value	DESeq2 Results: Log ₂ Fold Change	Adjusted P Value	Calculated P Value	Adjusted P Value	Average Paternal-X Expression (WT)	Adjusted P Value	Average Paternal-X Expression (WT)	Average Paternal-X Expression (Eq ² *)			
1																
2																
3	Gpr173	1.272450182	0.0049603562	0.050386825	7.718384231	0.000277712	0.001943985			0.0000	0.0000	0.1219				
4	Rp2h	0.02619322	0.92717172	0.970251633	7.67882734	1.58E-11	2.49E-09			0.0039	0.0039	0.4107				
5	Dock11	1.118642845	0.010951033	0.018951033	6.91171934	0.000252432	0.084182302			0.0009	0.0009	0.1253				
6	Porcn	1.694914351	0.000934006	0.016201624	6.71179505	4.51E-06	6.76E-05			0.0042	0.0042	0.4379				
7	Rhox4d	0.432676517	0.33532364	0.650166096	6.600259606	0.002583791	0.009805953			0.0000	0.0000	0.1981				
8	Zmyx3	1.850514863	1.21E-13	6.32E-11	6.197297076	9.63E-06	0.000126457			0.0121	0.0121	0.4657				
9	Tceal8	0.575366057	0.201237007	0.498854185	5.29805025	0.001971255	0.007918635			0.0031	0.0031	0.2122				
10	Ctps2	0.137382528	0.000161534	0.004410526	5.242070982	1.85E-05	0.002035533			0.0171	0.0171	0.4764				
11	Mbnl3	2.26065894	0.001105698	0.018201834	4.996758005	0.000628395	0.003534722			0.0366	0.0366	0.4140				
12	Psmid10	1.138396525	1.07E-06	8.18E-05	4.874534994	0.001476564	0.006839966			0.0134	0.0134	0.4003				
13	Wdr13	1.071536656	0.0008341	0.014928533	4.834866006	0.003336895	0.01155079			0.0166	0.0166	0.4646				
14	Prps2	0.35451545	0.41055336	0.696468299	4.800497748	0.012888862	0.03355365			0.0042	0.0042	0.1315				
15	Tbc1d25	1.23697977	0.000262203	0.006461648	4.540112254	NA	NA			0.0127	0.0127	0.4913				
16	3830417A13Rik	2.361628345	1.59E-07	1.66E-05	4.496205999	5.38E-09	2.83E-07			0.0397	0.0397	0.3937				
17	Atg4a	1.328652229	0.000469206	0.009883696	4.308802609	0.000256837	0.001881482			0.0343	0.0343	0.4027				
18	Gpc4	0.442669341	0.323099486	0.637901022	4.267723783	0.031301899	0.067075498			0.0014	0.0014	0.0942				
19	Tbc1d8b	0.506559916	0.19844229	0.494551627	4.237305442	0.000142157	0.001243872			0.0071	0.0071	0.4413				
20	Pcsk1n	1.335691341	0.006776439	0.061755712	4.217141587	NA	NA			0.0500	0.0500	0.5771				
21	Elf1ax	0.222062598	0.642521713	0.816538909	4.216106513	0.000651436	0.00360004			0.0108	0.0108	0.2379				
22	Mum1l	1.032521569	0.05828618	0.242314601	4.082397463	0.001730688	0.007468036			0.0050	0.0050	0.1404				
23	Med12	1.140480147	0.002228423	0.029327057	4.055648653	0.031771264	0.067621272			0.0159	0.0159	0.4653				
24	Rhox4g	-0.154845543	0.78422538	0.900887547	3.931309551	0.150553307	0.24201497			0.0000	0.0000	0.0110				
25	Ebp	0.243222553	0.410099555	0.696186769	3.917979695	0.000923378	0.004691356			0.0078	0.0078	0.2436				
26	Ftsl1	0.644199012	0.009631991	0.077876886	3.894358384	NA	NA			0.0224	0.0224	0.4228				
27	Fam199x	1.089502307	0.028637932	0.157805179	3.868027298	0.000817048	0.004219181			0.0351	0.0351	0.4114				
28	Tceanc	1.741606806	0.003914457	0.043161361	3.8607059818	0.004383648	0.014235559			0.0411	0.0411	0.2607				
29	Usp11	-0.11519663	0.812312985	0.918409612	3.784126787	0.009067612	0.025055245			0.0134	0.0134	0.4013				
30	Rbbp7	0.884728435	0.052756627	0.228913927	3.759111443	0.003271234	0.01155079			0.0355	0.0355	0.4140				
31	Sic25a14	0.870002133	0.020807059	0.123898538	3.735290365	0.005435854	0.016818788			0.0171	0.0171	0.3042				
32	Trappc2	-0.615799875	0.055612006	0.236056423	3.685786068	0.178352538	0.280905247			0.0000	0.0000	0.0059				
33	Praf2	0.594439543	0.099216466	0.333706269	3.664601553	0.050505299	0.097007129			0.0149	0.0149	0.2137				
34	Il2rg	0.785892691	0.167752604	0.451815127	3.662717516	0.002478127	0.009519636			0.0196	0.0196	0.4241				
35	Pikna3	0.662341298	0.069154718	0.268834222	3.611218179	0.187479924	NA			0.0000	0.0000	0.0010				
36	Trap1a	0.635901028	0.030172563	0.163311249	3.588511654	NA	NA			0.0480	0.0480	0.6835				
37	Gm4779	2.084886285	0.002909683	0.035222213	3.581865475	0.005615275	0.017172929			0.0455	0.0455	0.0278				
38	Phf16	0.379944616	0.472657148	0.734938307	3.498571314	0.001284971	0.006240619			0.0219	0.0219	0.4456				
39	Apoa	0.733188968	0.037450084	0.186839089	3.466664736	0.006149037	0.017934692			0.0475	0.0475	0.3502				
40	Nono	-0.113877977	0.620542933	0.802806761	3.381297604	0.000502397	0.002985943			0.0025	0.0025	0.0158				
41	Uba1	0.649810964	0.003274076	0.038536055	3.374070657	1.29E-06	2.26E-05			0.0411	0.0411	0.4410				
42	Morc4	0.162869142	0.810872292	0.918407342	3.333314694	0.012759941	0.0335365			0.0430	0.0430	0.3892				
43	Gripap1	0.868675719	5.81E-05	0.001966766	3.310764241	1.43E-05	0.000173664			0.0397	0.0397	0.5114				
44	Bcor1l	2.152802493	1.03E-23	2.38E-20	3.296853912	0.000404479	0.002498252			0.0495	0.0495	0.2570				
45	Tex13	1.349991433	NA	NA	3.291248024	0.007661454	0.021547838			0.0091	0.0091	0.1187				
46	Ocr1	0.78384518	0.019521838	0.123279314	3.270657457	0.000190441	0.00157866			0.0214	0.0214	0.3477				
47	Sic35a2	0.859719228	0.001374402	0.021162536	3.23738163	5.54E-07	1.25E-05			0.0334	0.0334	0.4388				
48	Syap1	0.468946206	0.197217707	0.49293779	3.23714114	0.001979635	0.007918635			0.0266	0.0266	0.4163				
49	Dlg3	0.31042037	0.371067194	0.67827464	3.209944019	NA	NA			0.0233	0.0233	0.1785				
50	Kcnd1	0.899514067	0.00705206	0.063243893	3.193097051	0.028128904	0.061962271			0.0297	0.0297	0.4843				
51	Pgk1	-0.223165775	0.609060196	0.79507918	3.188517177	0.003808072	0.012761093			0.0345	0.0345	0.4875				
52	Sic25ea3	-0.024711567	0.949726045	0.980088219	3.167758234	0.115265773	0.19606878			0.0275	0.0275	0.2203				

I	A		B		C		D		E		F		G		H		I	
	Gene Name	DESeq2 Results: Log ₂ Fold Change	Total X-chromosome P Value	Adjusted P Value	DESeq2 Results: Log ₂ Fold Change	Calculated P Value	Adjusted P Value	DESeq2 Results: Log ₂ Fold Change	Adjusted P Value	Adjusted P Value	Adjusted P Value	Average Paternal-X Expression (WT)	Average Paternal-X Expression	Average Paternal-X Expression (WT)	Average Paternal-X Expression			
2	Fundc1	0.349897263	0.367709496	0.675052161	3.10658111	0.092449008	0.163603582	0.0123	0.0123	0.0123	0.0123	0.0123	0.0123	0.0123	0.0123	0.0123	0.0123	0.2527
53	Wbp5	0.636953353	0.003871482	0.042947068	3.087535081	0.004356514	0.014235559	0.0374	0.0374	0.0374	0.0374	0.0374	0.0374	0.0374	0.0374	0.0374	0.0374	0.5150
54	Tspyl2	-1.001895841	0.003947395	0.043373462	3.087535081	0.043373462	0.033536536	0.0246	0.0246	0.0246	0.0246	0.0246	0.0246	0.0246	0.0246	0.0246	0.0246	0.2883
55	Gyk	-0.143033863	0.760533888	0.891218114	3.049158352	0.080553051	0.144995492	0.0137	0.0137	0.0137	0.0137	0.0137	0.0137	0.0137	0.0137	0.0137	0.0137	0.3078
56	Gemin8	1.06173666	0.004865388	0.049637913	3.030660488	NA	NA	NA	NA	NA	NA	NA	NA	NA	NA	NA	NA	0.4212
57	Plp2	-0.047308285	0.836893763	0.927986693	3.010596422	0.01096294	0.029770053	0.0204	0.0204	0.0204	0.0204	0.0204	0.0204	0.0204	0.0204	0.0204	0.0204	0.3336
58	Cdk16	0.98262834	5.68E-06	0.000317271	3.009006573	0.000242798	0.001881482	0.0301	0.0301	0.0301	0.0301	0.0301	0.0301	0.0301	0.0301	0.0301	0.0301	0.4190
59	Cdc22	1.029666442	3.62E-05	0.001360775	3.003939305	0.013085521	0.033786387	0.0536	0.0536	0.0536	0.0536	0.0536	0.0536	0.0536	0.0536	0.0536	0.0536	0.5079
60	Eda2r	-0.009566307	0.981797822	0.992613512	2.979914972	0.024264467	0.05498782	0.0129	0.0129	0.0129	0.0129	0.0129	0.0129	0.0129	0.0129	0.0129	0.0129	0.2450
61	Zdhhc9	0.521995615	0.214473949	0.516961728	2.968851746	0.00237299	0.009228295	0.0250	0.0250	0.0250	0.0250	0.0250	0.0250	0.0250	0.0250	0.0250	0.0250	0.3130
62	1110012119RIK	0.5187102	0.165682812	0.448618406	2.95469741	0.016697018	0.041090319	0.0263	0.0263	0.0263	0.0263	0.0263	0.0263	0.0263	0.0263	0.0263	0.0263	0.2661
63	Wdr45	0.417300925	0.230247195	0.535709159	2.935572324	0.001498798	0.00684234	0.0269	0.0269	0.0269	0.0269	0.0269	0.0269	0.0269	0.0269	0.0269	0.0269	0.4457
64	Rnf128	0.470950614	0.049210672	0.220711719	2.929941494	1.87E-05	0.00203533	0.0374	0.0374	0.0374	0.0374	0.0374	0.0374	0.0374	0.0374	0.0374	0.0374	0.5290
65	Itnm2a	-0.553085725	0.355848176	0.664698741	2.900330213	NA	NA	NA	NA	NA	NA	NA	NA	NA	NA	NA	NA	0.1590
66	Timm17b	0.928043362	0.000223233	0.005657676	2.885545127	0.000614002	0.003516557	0.0415	0.0415	0.0415	0.0415	0.0415	0.0415	0.0415	0.0415	0.0415	0.0415	0.4163
67	Otdud5	0.85672535	0.009704681	0.078199889	2.881861477	0.000740585	0.003953968	0.0498	0.0498	0.0498	0.0498	0.0498	0.0498	0.0498	0.0498	0.0498	0.0498	0.5128
68	Rbm41	0.851179979	0.015320399	0.106001288	2.843700659	0.036359246	0.074371184	0.0402	0.0402	0.0402	0.0402	0.0402	0.0402	0.0402	0.0402	0.0402	0.0402	0.5259
69	Txlng	0.508136117	0.164178312	0.446364859	2.822796533	NA	NA	0.0165	0.0165	0.0165	0.0165	0.0165	0.0165	0.0165	0.0165	0.0165	0.0165	0.4544
70	Fhl1	0.52696045	0.059042842	0.2443949	2.785675233	0.128671059	0.21100956	0.0029	0.0029	0.0029	0.0029	0.0029	0.0029	0.0029	0.0029	0.0029	0.0029	0.0382
71	Ngrap1	0.177893315	0.343013982	0.653461142	2.782814046	0.05016094	0.096936785	0.0094	0.0094	0.0094	0.0094	0.0094	0.0094	0.0094	0.0094	0.0094	0.0094	0.1057
72	Rhox6	0.338304299	0.623107638	0.804636548	2.772603	0.006465401	0.018514557	0.0436	0.0436	0.0436	0.0436	0.0436	0.0436	0.0436	0.0436	0.0436	0.0436	0.4927
73	Rhox9	-0.171986011	0.811385844	0.918407342	2.75429733	0.019664774	0.047649259	0.0396	0.0396	0.0396	0.0396	0.0396	0.0396	0.0396	0.0396	0.0396	0.0396	0.5052
74	BC065397	1.027811099	0.008624164	0.072155958	2.730804932	0.037590825	0.076394257	0.4548	0.4548	0.4548	0.4548	0.4548	0.4548	0.4548	0.4548	0.4548	0.4548	0.3386
75	C430049B03RIK	0.765926887	0.260628772	0.573053214	2.726744691	0.028691946	0.062489337	0.1712	0.1712	0.1712	0.1712	0.1712	0.1712	0.1712	0.1712	0.1712	0.1712	0.3187
76	A830080D01RIK	0.150117376	0.614181063	0.798803477	2.713839431	0.001764139	0.007509512	0.0360	0.0360	0.0360	0.0360	0.0360	0.0360	0.0360	0.0360	0.0360	0.0360	0.4027
77	Mospd1	-0.041999841	0.928673364	0.971175841	2.64803555	0.010913554	0.029770053	0.0213	0.0213	0.0213	0.0213	0.0213	0.0213	0.0213	0.0213	0.0213	0.0213	0.3238
78	Ids	0.292697744	0.422075004	0.706726295	2.614115606	0.000480891	0.002913088	0.0292	0.0292	0.0292	0.0292	0.0292	0.0292	0.0292	0.0292	0.0292	0.0292	0.3023
79	Pqbp1	0.806399381	3.18E-05	0.001233264	2.608045668	0.018715783	0.04570133	0.0355	0.0355	0.0355	0.0355	0.0355	0.0355	0.0355	0.0355	0.0355	0.0355	0.4590
80	Acof9	-0.099181705	0.791916105	0.9095354	2.604827744	NA	NA	0.0198	0.0198	0.0198	0.0198	0.0198	0.0198	0.0198	0.0198	0.0198	0.0198	0.1596
81	Rhox9	-0.171986011	0.811385844	0.918407342	2.597429733	0.019664774	0.047649259	0.0396	0.0396	0.0396	0.0396	0.0396	0.0396	0.0396	0.0396	0.0396	0.0396	0.5052
82	Slc9a6	0.434998932	0.306718002	0.622504576	2.567973974	0.10219067	0.178833673	0.0351	0.0351	0.0351	0.0351	0.0351	0.0351	0.0351	0.0351	0.0351	0.0351	0.3041
83	Brdw3	0.055013081	0.86855368	0.94048517	2.555099727	NA	NA	0.0191	0.0191	0.0191	0.0191	0.0191	0.0191	0.0191	0.0191	0.0191	0.0191	0.1489
84	Nsdh1	0.263246418	0.597651631	0.789731425	2.545340004	0.122578387	0.205383999	0.0331	0.0331	0.0331	0.0331	0.0331	0.0331	0.0331	0.0331	0.0331	0.0331	0.2846
85	Ddx26b	0.685542677	0.091414149	0.319107066	2.511591217	0.033277844	0.069584829	0.0647	0.0647	0.0647	0.0647	0.0647	0.0647	0.0647	0.0647	0.0647	0.0647	0.3014
86	Timp1	-0.74839404	0.293289361	0.609790146	2.4942786	0.107685928	0.187409212	0.0003	0.0003	0.0003	0.0003	0.0003	0.0003	0.0003	0.0003	0.0003	0.0003	0.0245
87	Hdac6	1.02271859	0.001724205	0.024842024	2.388103652	0.000712081	0.003867337	0.0881	0.0881	0.0881	0.0881	0.0881	0.0881	0.0881	0.0881	0.0881	0.0881	0.5737
88	Clicn5	0.363566587	0.378320609	0.68455221	2.363702469	0.118312643	0.199296699	0.0291	0.0291	0.0291	0.0291	0.0291	0.0291	0.0291	0.0291	0.0291	0.0291	0.4836
89	Magt1	-0.761906802	0.070678283	0.272597474	2.235153426	NA	NA	0.0107	0.0107	0.0107	0.0107	0.0107	0.0107	0.0107	0.0107	0.0107	0.0107	0.1162
90	Stard8	1.099503542	0.06200485	0.251870358	2.234291661	0.014472552	0.036281	0.1510	0.1510	0.1510	0.1510	0.1510	0.1510	0.1510	0.1510	0.1510	0.1510	0.4261
91	Tnm29	0.517188806	0.048591968	0.2195601	2.230797771	0.00455071	0.014627281	0.0689	0.0689	0.0689	0.0689	0.0689	0.0689	0.0689	0.0689	0.0689	0.0689	0.2414
92	Gpko	1.059058687	2.82E-05	0.001125654	2.216238791	0.001555099	0.006997946	0.1567	0.1567	0.1567	0.1567	0.1567	0.1567	0.1567	0.1567	0.1567	0.1567	0.6383
93	8030474K03RIK	2.114795501	0.002285242	0.029755273	2.203815233	0.074980286	0.136524799	0.0457	0.0457	0.0457	0.0457	0.0457	0.0457	0.0457	0.0457	0.0457	0.0457	0.0308
94	Cox7b	-0.906099127	0.054393066	0.233186606	2.143563493	NA	NA	0.0265	0.0265	0.0265	0.0265	0.0265	0.0265	0.0265	0.0265	0.0265	0.0265	0.1755
95	Elk1	0.534033235	0.031668573	0.168089524	2.107272923	0.232222919	0.336177913	0.0202	0.0202	0.0202	0.0202	0.0202	0.0202	0.0202	0.0202	0.0202	0.0202	0.1038
96	Mmg1	-0.290089554	0.445169313	0.7236043281	2.073761494	0.224365403	0.327199547	0.0298	0.0298	0.0298	0.0298	0.0298	0.0298	0.0298	0.0298	0.0298	0.0298	0.2334
97	Ii13ra1	-0.034891843	0.942973032	0.978773214	2.051194633	0.294008554	0.405252895	0.0031	0.0031	0.0031	0.0031	0.0031	0.0031	0.0031	0.0031	0.0031	0.0031	0.0274
98	Iqsec2	1.701757283	1.89E-05	0.000832179	1.901999905	0.159670809	0.255311192	0.0143	0.0143	0.0143	0.0143	0.0143	0.0143	0.0143	0.0143	0.0143	0.0143	0.0746
99	Ccdc120	0.984154603	0.005912566	0.056841946	1.901738481	0.060755141	0.114598021	0.1115	0.1115	0.1115	0.1115	0.1115	0.1115	0.1115	0.1115	0.1115	0.1115	0.5035
100	Gnl3l	0.230721464	0.445482952	0.723814251	1.861765055	NA	NA	0.0296	0.0296	0.0296	0.0296	0.0296	0.0296	0.0296	0.0296	0.0296	0.0296	0.1505
101	Car5b	0.016899691	0.970685898	0.98775457	1.8588812	0.19111396	0.293662915	0.0331	0.0331	0.0331	0.0331	0.0331	0.0331	0.0331	0.0331	0.0331	0.0331	0.3621
102	Pir	-0.194398332	0.666178591	0.831941722	1.8400989	NA	NA	0.0039	0.0039	0.0039	0.0039	0.0039	0.0039	0.0039	0.0039	0.0039	0.0039	0.0761

Gene Name	B		C		D		E		F		G		H		I	
	DESeq2 Results: Log ₂ Fold Change	Total X-chromosome P Value	Adjusted P Value	DESeq2 Results: Log ₂ Fold Change	Adjusted P Value	DESeq2 Results: Log ₂ Fold Change	Adjusted P Value	DESeq2 Results: Log ₂ Fold Change	Adjusted P Value	DESeq2 Results: Log ₂ Fold Change	Adjusted P Value	DESeq2 Results: Log ₂ Fold Change	Adjusted P Value	Average Paternal-X Expression (WT)	Average Paternal-X Expression (Eq ^{+/+})	
103	0.808653899	NA	NA	1.804621663	NA	NA	1.804621663	NA	NA	NA	NA	NA	0.0229	0.0886		
104	0.459718807	0.350338179	0.659491758	1.769181475	0.659491758	0.659491758	1.769181475	0.659491758	0.333432901	0.445048152	0.445048152	0.0735	0.1334			
105	0.495455179	0.166346382	0.449247365	1.680926846	0.449247365	0.449247365	1.680926846	0.449247365	0.06745412	0.124988516	0.124988516	0.1660	0.3905			
106	0.572614468	0.022602382	0.135076139	1.664212082	0.135076139	0.135076139	1.664212082	0.135076139	0.070256988	0.129420768	0.129420768	0.0830	0.5094			
107	-0.908986132	0.140560633	0.409380634	1.611880254	0.409380634	0.409380634	1.611880254	0.409380634	0.404421283	0.51997022	0.51997022	0.0037	0.0686			
108	0.191222535	0.801289947	0.912521574	1.578473225	0.912521574	0.912521574	1.578473225	0.912521574	0.187272017	0.289170026	0.289170026	0.2633	0.6944			
109	0.158388688	0.632985491	0.811220339	1.56399048	0.811220339	0.811220339	1.56399048	0.811220339	0.336228297	0.446885711	0.446885711	0.0490	0.2798			
110	0.326430561	0.186070086	0.477905222	1.26220351	0.477905222	0.477905222	1.26220351	0.477905222	0.473257334	0.586913623	0.586913623	0.0143	0.0480			
111	-0.183761262	0.716945996	0.863610057	1.235486869	0.863610057	0.863610057	1.235486869	0.863610057	0.294612422	0.405252895	0.405252895	0.0449	0.3104			
112	0.142798306	0.663502865	0.82969719	1.170722838	0.82969719	0.82969719	1.170722838	0.82969719	0.265037994	0.376067424	0.376067424	0.0229	0.0915			
113	0.753085227	0.001034145	0.017444812	1.159163649	0.017444812	0.017444812	1.159163649	0.017444812	NA	NA	NA	0.1032	0.6339			
114	0.283831882	0.292398741	0.608784672	1.144883803	0.608784672	0.608784672	1.144883803	0.608784672	0.381175071	0.496157634	0.496157634	0.0112	0.1415			
115	1.176206908	0.002795874	0.0343421	1.062701283	0.0343421	0.0343421	1.062701283	0.0343421	0.429669459	0.543557749	0.543557749	0.0548	0.2616			
116	0.866931615	0.000170232	0.004605777	1.047507464	0.004605777	0.004605777	1.047507464	0.004605777	NA	NA	NA	0.0992	0.4126			
117	0.37080859	0.284836308	0.600606762	0.905260605	0.600606762	0.600606762	0.905260605	0.600606762	0.488984189	0.601679764	0.601679764	0.0464	0.1847			
118	0.434716142	0.545457212	0.77703645	0.82388068	0.77703645	0.77703645	0.82388068	0.77703645	0.682137414	0.787081632	0.787081632	0.0899	0.4570			
119	-0.312881489	0.200817672	0.498051734	0.75554698	0.498051734	0.498051734	0.75554698	0.498051734	0.579329331	0.696521906	0.696521906	0.0476	0.2237			
120	-0.333468608	0.270081795	0.585077379	0.699359464	0.585077379	0.585077379	0.699359464	0.585077379	0.623238266	0.72711131	0.72711131	0.0164	0.0433			
121	0.369142634	0.203057573	0.501398415	0.678055172	0.501398415	0.501398415	0.678055172	0.501398415	NA	NA	NA	0.0486	0.0622			
122	0.463832561	0.01344681	0.09700543	0.611162023	0.09700543	0.09700543	0.611162023	0.09700543	0.416851886	0.533773757	0.533773757	0.1306	0.4415			
123	0.952509005	0.000407262	0.00888428	0.576700179	0.00888428	0.00888428	0.576700179	0.00888428	0.425618412	0.540919111	0.540919111	0.1732	0.4147			
124	-1.03255377	0.064235435	0.252554075	0.491224323	0.252554075	0.252554075	0.491224323	0.252554075	0.78316259	0.856584083	0.856584083	0.0382	0.0606			
125	0.036871706	0.959221661	0.984201623	0.428309539	0.984201623	0.984201623	0.428309539	0.984201623	0.802596091	0.871785409	0.871785409	0.0473	0.1250			
126	-0.414234579	0.384041796	0.690336645	0.421834402	0.690336645	0.690336645	0.421834402	0.690336645	0.762609841	0.845852465	0.845852465	0.0076	0.0288			
127	-0.071428082	0.82118808	0.9222630358	0.386593015	0.9222630358	0.9222630358	0.386593015	0.9222630358	NA	NA	NA	0.0294	0.1133			
128	-0.211286966	0.563644718	0.789731425	0.371622265	0.789731425	0.789731425	0.371622265	0.789731425	0.70113559	0.80605004	0.80605004	0.0488	0.1798			
129	-0.199550031	0.533116708	0.769133664	0.319253805	0.769133664	0.769133664	0.319253805	0.769133664	NA	NA	NA	0.0210	0.0535			
130	0.839142289	0.025688372	0.14650037	0.262518797	0.14650037	0.14650037	0.262518797	0.14650037	0.756692513	0.845241637	0.845241637	0.0009	0.0009			
131	-1.103594959	0.046796973	0.214315529	0.230200709	0.214315529	0.214315529	0.230200709	0.214315529	NA	NA	NA	0.0128	0.1382			
132	2.449994304	1.10E-09	2.30E-07	0.217007649	2.30E-07	2.30E-07	0.217007649	2.30E-07	0.776544016	0.855284493	0.855284493	0.3378	0.2127			
133	0.242893564	0.38400017	0.690336645	0.198829409	0.690336645	0.690336645	0.198829409	0.690336645	NA	NA	NA	0.0248	0.0232			
134	-1.018599168	0.007356189	0.066086516	0.157528995	0.066086516	0.066086516	0.157528995	0.066086516	0.912677536	0.945702052	0.945702052	0.0359	0.1348			
135	0.93625606	0.001858425	0.026054451	0.152440708	0.026054451	0.026054451	0.152440708	0.026054451	0.897968505	0.933531614	0.933531614	0.1393	0.5456			
136	0.164983046	0.467363526	0.732029497	0.141309679	0.732029497	0.732029497	0.141309679	0.732029497	NA	NA	NA	0.0294	0.0847			
137	0.345943528	0.366357164	0.673681949	0.138291508	0.673681949	0.673681949	0.138291508	0.673681949	0.957378509	0.969692059	0.969692059	0.0064	0.0000			
138	1.66678484	1.47E-05	0.000686425	0.137402486	0.000686425	0.000686425	0.137402486	0.000686425	0.859465373	0.903682544	0.903682544	0.5025	0.5000			
139	-0.034860543	0.907311081	0.960516883	0.06210411	0.960516883	0.960516883	0.06210411	0.960516883	0.941438586	0.960161642	0.960161642	0.1311	0.4762			
140	0.301766165	0.262261418	0.575307163	0.056187965	0.575307163	0.575307163	0.056187965	0.575307163	0.97533234	0.984710535	0.984710535	0.0414	0.0989			
141	1.027811099	0.008624164	0.072155508	0.022879391	0.072155508	0.072155508	0.022879391	0.072155508	0.98145946	0.987730766	0.987730766	0.4548	0.3386			
142	-0.23915787	0.366630722	0.673962573	0.015448068	0.673962573	0.673962573	0.015448068	0.673962573	0.993991884	0.994019785	0.994019785	0.0035	0.0077			
143	-0.035719822	0.923042548	0.96850896	-0.09276659	0.96850896	0.96850896	-0.09276659	0.96850896	0.922027708	0.94914617	0.94914617	0.1172	0.3636			
144	-0.412293959	0.19990431	0.496910452	-0.107581712	0.496910452	0.496910452	-0.107581712	0.496910452	0.941500965	0.960161642	0.960161642	0.0093	0.0510			
145	-0.31677372	0.306020117	0.622009173	-0.152825603	0.622009173	0.622009173	-0.152825603	0.622009173	NA	NA	NA	0.0166	0.0352			
146	0.106383173	0.840047939	0.928617145	-0.193546067	0.928617145	0.928617145	-0.193546067	0.928617145	0.847153743	0.898496394	0.898496394	0.1694	0.5075			
147	0.60094966	0.095945201	0.328621813	-0.212129798	0.328621813	0.328621813	-0.212129798	0.328621813	0.921343089	0.94914617	0.94914617	0.0177	0.0500			
148	-0.174927122	0.536253902	0.771265278	-0.218150359	0.771265278	0.771265278	-0.218150359	0.771265278	0.824375958	0.886851701	0.886851701	0.1867	0.4793			
149	0.317210078	0.17529832	0.462757049	-0.223948831	0.462757049	0.462757049	-0.223948831	0.462757049	0.759564332	0.854541465	0.854541465	0.0257	0.0446			
150	0.053027898	0.850530619	0.932977274	-0.254457501	0.932977274	0.932977274	-0.254457501	0.932977274	0.860650042	0.903682544	0.903682544	0.0135	0.0072			
151	0.031994912	0.918131801	0.966166715	-0.26904382	0.966166715	0.966166715	-0.26904382	0.966166715	0.824912852	0.886851701	0.886851701	0.0248	0.1111			
152	0.390350288	0.227822096	0.533103193	-0.291233764	0.533103193	0.533103193	-0.291233764	0.533103193	0.859433933	0.903682544	0.903682544	0.0145	0.0152			

I	A		B		C		D		E		F		G		H		I	
	Gene Name	DfSeq2 Results: Log ₂ Fold Change	Total X-chromosome P Value	Adjusted P Value	DESeq2 Results: Log ₂ Fold Change	Calculated P Value	Adjusted P Value	Paternal-X Expression	Adjusted P Value	Paternal-X Expression (WT)	Average Paternal-X Expression (Eq ^{1/2})	Adjusted P Value	Paternal-X Expression	Average Paternal-X Expression (Eq ^{1/2})				
203	Gpm6b	-1.357131256	NA	NA	-2.113503786	0.232656461	0.336177913	0.0381	0.0381	0.0381	0.336177913	0.0381	0.0381					
204	Aifm1	-0.352753699	0.137542272	0.403693739	-2.139043847	0.148083873	0.240445464	0.0213	0.0213	0.0213	0.240445464	0.0213	0.0213					
205	Dym1	-0.071171717	0.071129795	0.273706503	-2.14480181	0.005111516	0.016101277	1.0000	1.0000	1.0000	0.016101277	1.0000	1.0000					
206	Lonn3	1.723783026	0.000982065	0.01685285	-2.161263237	0.297824226	0.407889701	0.0194	0.0194	0.0194	0.407889701	0.0194	0.0194					
207	Cxx1a	-1.45259198	0.005050889	0.050981192	-2.180691717	NA	NA	0.0719	0.0719	0.0719	NA	0.0719	0.0719					
208	Pola1	-0.261603157	0.586684478	0.789731425	-2.185431604	NA	NA	0.0268	0.0268	0.0268	NA	0.0268	0.0268					
209	Gdi1	0.392274685	0.133426364	0.397026103	-2.197680102	0.003153567	0.011400109	0.3269	0.3269	0.3269	0.011400109	0.3269	0.3269					
210	Ikbkg	-0.41792346	0.154123268	0.431051782	-2.226146536	0.028764933	0.062489337	0.0335	0.0335	0.0335	0.062489337	0.0335	0.0335					
211	Cul4b	-0.568804597	0.013099388	0.095286159	-2.239961885	0.000338565	0.002269105	0.1536	0.1536	0.1536	0.002269105	0.1536	0.1536					
212	Las1	-0.367178787	0.428172022	0.712241117	-2.250585449	0.168513964	0.268890398	0.0257	0.0257	0.0257	0.268890398	0.0257	0.0257					
213	Mageb16	-0.336679001	0.33048899	0.644972096	-2.267200145	0.197997616	0.301044696	0.0292	0.0292	0.0292	0.301044696	0.0292	0.0292					
214	Gpdx	-0.21466973	0.451339496	0.72765483	-2.270877552	0.199740767	0.301044696	0.0168	0.0168	0.0168	0.301044696	0.0168	0.0168					
215	RbmX	0.446072403	0.157507719	0.435980357	-2.298811629	0.197018508	0.301044696	0.0270	0.0270	0.0270	0.301044696	0.0270	0.0270					
216	Rhox4b	0.414156923	0.297479707	0.6133664198	-2.328790136	0.0145124	0.036281	0.3301	0.3301	0.3301	0.036281	0.3301	0.3301					
217	Shroom2	-0.279502648	0.451115046	0.72746186	-2.400626296	NA	NA	0.0222	0.0222	0.0222	NA	0.0222	0.0222					
218	C1galt1c1	-0.23915787	0.366630722	0.673962573	-2.475651256	0.381715512	NA	0.0035	0.0035	0.0035	NA	0.0035	0.0035					
219	Pfkfb1	-0.024676665	0.943462572	0.978779601	-2.526219807	0.284285835	0.394493356	0.0147	0.0147	0.0147	0.394493356	0.0147	0.0147					
220	Ube2a	-1.113117422	0.000986219	0.016910206	-2.628404005	0.214302555	0.313978162	0.0262	0.0262	0.0262	0.313978162	0.0262	0.0262					
221	Msn	-0.62277367	0.065791628	0.26077367	-2.700370282	0.06160896	0.1155168	0.0108	0.0108	0.0108	0.1155168	0.0108	0.0108					
222	Phf6	0.309822756	0.439033087	0.72061998	-2.845810233	NA	NA	0.0076	0.0076	0.0076	NA	0.0076	0.0076					
223	Atrx	-1.283045641	0.001334836	0.020799278	-2.848709945	0.048841411	0.095559282	0.0371	0.0371	0.0371	0.095559282	0.0371	0.0371					
224	Hprt	-0.835643609	0.041392228	0.198875527	-2.855222766	NA	NA	0.0198	0.0198	0.0198	NA	0.0198	0.0198					
225	Gprasp1	1.611281586	1.99E-05	0.000858845	-2.880073972	0.113232049	0.195861125	0.0144	0.0144	0.0144	0.195861125	0.0144	0.0144					
226	Bhlhb9	0.259843537	0.446304039	0.72452734	-2.984192528	NA	NA	0.0314	0.0314	0.0314	NA	0.0314	0.0314					
227	Rhox4c	-0.107423979	0.816234583	0.919992212	-2.997145517	0.000814864	0.004219181	0.6091	0.6091	0.6091	0.004219181	0.6091	0.6091					
228	Gata1	-0.932142198	0.05262286	0.228632336	-3.021263789	0.020416514	0.048354901	0.1112	0.1112	0.1112	0.048354901	0.1112	0.1112					
229	Mpp1	-0.00812137	0.986737347	0.99509629	-3.054005683	NA	NA	0.0107	0.0107	0.0107	NA	0.0107	0.0107					
230	Dcaf12l1	0.33249428	0.01423478	0.100765601	-3.072393069	NA	NA	0.1204	0.1204	0.1204	NA	0.1204	0.1204					
231	A230072C01R1k	0.33249428	0.23071212	0.536076392	-3.086243531	0.272179977	NA	0.0167	0.0167	0.0167	NA	0.0167	0.0167					
232	Mid1ip1	-0.480763624	0.242731029	0.551452076	-3.086243531	0.272179977	NA	0.0024	0.0024	0.0024	NA	0.0024	0.0024					
233	Sat1	-0.845698236	0.123299082	0.379142402	-3.158354687	NA	NA	0.0202	0.0202	0.0202	NA	0.0202	0.0202					
234	Lamp2	-0.878204844	0.051228625	0.2255857	-3.186707693	0.033577441	0.069584829	0.0098	0.0098	0.0098	0.069584829	0.0098	0.0098					
235	Tmem164	0.388420205	0.088625895	0.313045656	-3.216458437	0.072144569	0.132125229	0.0126	0.0126	0.0126	0.132125229	0.0126	0.0126					
236	Armcx2	-1.496012448	0.002238296	0.029390734	-3.245173273	0.021734387	0.051057575	0.0349	0.0349	0.0349	0.051057575	0.0349	0.0349					
237	Nrk	-0.522901403	0.467257629	0.732029497	-3.27197659	0.027416091	0.061248713	0.0192	0.0192	0.0192	0.061248713	0.0192	0.0192					
238	Armcx3	-0.472503716	0.306527639	0.622345804	-3.293705312	0.239474367	NA	0.0010	0.0010	0.0010	NA	0.0010	0.0010					
239	Bgn	-1.879750023	NA	NA	-3.313718485	0.030477453	0.065756148	0.0005	0.0005	0.0005	0.065756148	0.0005	0.0005					
240	Ubqln2	-0.004497441	0.989654691	0.996013254	-3.317571986	NA	NA	0.0183	0.0183	0.0183	NA	0.0183	0.0183					
241	Pgrmc1	-0.064854949	0.786898758	0.906668361	-3.356568824	0.032773199	0.069285622	0.0133	0.0133	0.0133	0.069285622	0.0133	0.0133					
242	Xir3a	-1.158922089	0.001185787	0.019105561	-3.422194859	0.066737777	0.124392898	0.0151	0.0151	0.0151	0.124392898	0.0151	0.0151					
243	Rap2c	-0.262020484	0.47201145	0.734330113	-3.449284516	NA	NA	0.0203	0.0203	0.0203	NA	0.0203	0.0203					
244	Klhl13	-0.858894578	0.018301445	0.117814795	-3.450331917	0.003653014	0.012507601	0.0181	0.0181	0.0181	0.012507601	0.0181	0.0181					
245	Apoal	-0.275444569	0.384189577	0.690341681	-3.508028541	0.126969709	0.209400306	0.0324	0.0324	0.0324	0.209400306	0.0324	0.0324					
246	Xir3b	0.408213036	0.435822152	0.718030464	-3.52729114	0.000384482	0.002422239	0.1513	0.1513	0.1513	0.002422239	0.1513	0.1513					
247	Col4a5	-0.575426231	0.230005252	0.535571986	-3.531397005	0.205094383	NA	0.0003	0.0003	0.0003	NA	0.0003	0.0003					
248	Irak1	-0.04472628	0.829507589	0.927015119	-3.552012079	0.021943208	0.051057575	0.0157	0.0157	0.0157	0.051057575	0.0157	0.0157					
249	Ndufa1	-0.264408587	0.320723609	0.635317575	-3.582365063	0.012150094	0.032434572	0.0244	0.0244	0.0244	0.032434572	0.0244	0.0244					
250	Ammecr1	0.540955853	0.107431034	0.349923503	-3.620992525	0.113785987	0.195861125	0.0214	0.0214	0.0214	0.195861125	0.0214	0.0214					
251	Hsd17b10	-0.356008848	0.275888995	0.590140577	-3.682019781	0.058525826	0.111731122	0.0138	0.0138	0.0138	0.111731122	0.0138	0.0138					
252	Fina	-1.004063325	0.008482426	0.071515329	-3.706968554	6.59E-05	0.000610132	0.0593	0.0593	0.0593	0.000610132	0.0593	0.0593					

Gene Name	B		C		D		E		F		G		H		I	
	DESeq2 Results: Log ₂ Fold Change	Total X-chromosome P Value	Adjusted P Value	DESeq2 Results: Log ₂ Fold Change	Adjusted P Value	DESeq2 Results: Log ₂ Fold Change	Adjusted P Value	Calculated P Value	Adjusted P Value	Average Expression (WT)	Adjusted P Value	Average Expression (WT)	Average Expression (Eq ^{1/2})			
1																
2																
253	0.053216474	0.866910567	0.940253473	-3.724861708	0.000126034	9.20E-06	0.000126034	0.000126034	0.000126034	0.0358	0.000126034	0.0358	0.0054			
254	-0.185407453	0.633710214	0.811566984	-3.826716462	0.007468036	0.001729083	0.007468036	0.007468036	0.007468036	0.0651	0.007468036	0.0651	0.0076			
255	-1.647418366	0.000841982	0.01504729	-3.942725454	0.015511973	0.015511973	0.015511973	0.015511973	0.015511973	0.0000	0.015511973	0.0000	0.0000			
256	-0.95038633	0.009947405	0.079343891	-4.068598594	0.000124511	8.70E-06	0.000124511	0.000124511	8.70E-06	0.1522	0.000124511	0.1522	0.0879			
257	0.194692644	0.692140124	0.847682469	-4.209042355	0.008644313	0.002195381	0.008644313	0.008644313	0.002195381	0.0220	0.008644313	0.0220	0.0004			
258	-0.134772177	0.671196373	0.835082247	-4.215686458	NA	NA	NA	NA	NA	0.0181	NA	0.0181	0.0005			
259	0.219391171	0.632950131	0.811220339	-4.222098077	NA	NA	NA	NA	NA	0.0156	NA	0.0156	0.0000			
260	-0.12284152	0.603003643	0.79103173	-4.241671771	NA	NA	NA	NA	NA	0.0022	NA	0.0022	0.0000			
261	0.023009293	0.966583412	0.986186676	-4.276448806	NA	NA	NA	NA	NA	0.0940	NA	0.0940	0.0071			
262	-0.649399867	0.056556673	0.238119761	-4.294590234	NA	NA	NA	NA	NA	0.0145	NA	0.0145	0.0015			
263	-0.851246057	0.007831962	0.067742489	-4.366570547	0.005328187	0.001056537	0.005328187	0.005328187	0.001056537	0.1698	0.005328187	0.1698	0.0277			
264	-0.421292599	0.588007628	0.789731425	-4.473495885	0.001351438	0.00015874	0.001351438	0.001351438	0.00015874	0.0489	0.001351438	0.0489	0.0017			
265	-0.237619787	0.157358722	0.435764224	-4.537666221	0.001597133	0.001597133	0.001597133	0.001597133	0.001597133	0.0321	0.001597133	0.0321	0.0013			
266	1.321129686	0.004132581	0.044680765	-4.616099613	0.005822408	0.005822408	0.005822408	0.005822408	0.005822408	0.4365	0.005822408	0.4365	0.0094			
267	-0.230775946	0.455809351	0.728994027	-4.624452197	0.080564175	0.040154208	0.080564175	0.080564175	0.040154208	0.0218	0.080564175	0.0218	0.0035			
268	1.714461793	0.000231012	0.005833539	-4.629619094	0.013311013	0.013311013	0.013311013	0.013311013	0.013311013	0.0450	0.013311013	0.0450	0.0027			
269	-0.28829741	0.273738122	0.588555554	-4.653228999	0.007509648	0.001788011	0.007509648	0.007509648	0.001788011	0.0212	0.007509648	0.0212	0.0007			
270	-0.1111589	0.585799528	0.789731425	-4.71708065	NA	NA	NA	NA	NA	0.0156	NA	0.0156	0.0001			
271	-1.281826736	0.000609454	0.01191065	-4.737064256	0.017934692	0.006100582	0.017934692	0.017934692	0.006100582	0.0325	0.017934692	0.0325	0.0050			
272	-1.100041097	0.00320264	0.037887904	-4.756435268	0.00502883	0.00502883	0.00502883	0.00502883	0.00502883	0.0355	0.00502883	0.0355	0.0028			
273	0.087980831	0.67997604	0.841094976	-4.805497973	0.001885946	0.000263434	0.001885946	0.001885946	0.000263434	0.0651	0.001885946	0.0651	0.0091			
274	0.324155208	0.348514048	0.657510875	-4.827447077	NA	NA	NA	NA	NA	0.0100	NA	0.0100	0.0000			
275	-0.399634994	0.117195632	0.366707209	-4.842053715	0.00287747	0.00287747	0.00287747	0.00287747	0.00287747	0.0176	0.00287747	0.0176	0.0011			
276	-0.092951907	0.823890402	0.92429234	-4.923302302	NA	NA	NA	NA	NA	0.0330	NA	0.0330	0.0000			
277	-2.033156864	1.51E-05	0.000702899	-4.978533156	NA	NA	NA	NA	NA	0.1543	NA	0.1543	0.0000			
278	-0.230621381	0.450897747	0.727347098	-5.044804948	0.00255592	0.00255592	0.00255592	0.00255592	0.00255592	0.0204	0.00255592	0.0204	0.0011			
279	0.435375603	0.274746363	0.589517113	-5.046684997	0.030454902	0.011311821	0.030454902	0.030454902	0.011311821	0.0386	0.030454902	0.0386	0.0004			
280	0.697867981	0.074905821	0.282445787	-5.135464621	NA	NA	NA	NA	NA	0.0291	NA	0.0291	0.0000			
281	-0.459509151	0.392257879	0.694089751	-5.174735088	0.01400109	0.003184792	0.01400109	0.01400109	0.003184792	0.0125	0.01400109	0.0125	0.0007			
282	0.29488492	0.08174531	0.298189668	-5.30480125	NA	NA	NA	NA	NA	0.0141	NA	0.0141	0.0000			
283	-1.58966506	0.018692446	0.119637395	-5.309773388	0.012637198	0.003730982	0.012637198	0.012637198	0.003730982	0.0564	0.012637198	0.0564	0.0667			
284	-0.093059172	0.794596133	0.911065052	-5.422447513	0.007918635	0.001985943	0.007918635	0.007918635	0.001985943	0.0531	0.007918635	0.0531	0.0044			
285	-0.4505891	0.117420107	0.367133887	-5.459427037	0.008212432	0.008212432	0.008212432	0.008212432	0.008212432	0.0531	0.008212432	0.0531	0.0000			
286	-0.707163566	0.07309599	0.278190648	-5.581137372	NA	NA	NA	NA	NA	0.0221	NA	0.0221	0.0000			
287	-0.387155382	0.35787476	0.666214358	-5.5866417933	6.08E-08	6.08E-08	6.08E-08	6.08E-08	6.08E-08	0.0195	6.08E-08	0.0195	0.0006			
288	-0.350514613	0.473300294	0.73523712	-5.590562304	NA	NA	NA	NA	NA	0.0173	NA	0.0173	0.0000			
289	-0.288243585	0.390356296	0.694089751	-5.649579541	0.061757838	0.027840041	0.061757838	0.061757838	0.027840041	0.0109	0.061757838	0.0109	0.0000			
290	-0.605590191	0.051675703	0.226501139	-5.649848025	1.21E-06	3.07E-08	1.21E-06	1.21E-06	3.07E-08	0.2620	1.21E-06	0.2620	0.0189			
291	-0.107142019	0.715300925	0.86243075	-5.75906035	2.36E-06	7.50E-08	2.36E-06	2.36E-06	7.50E-08	0.1227	2.36E-06	0.1227	0.0075			
292	-0.135331386	0.815933239	0.91979711	-5.766053931	NA	NA	NA	NA	NA	0.0486	NA	0.0486	0.0000			
293	-0.937355855	0.001626206	0.023757885	-5.766657909	0.000654327	7.27E-05	0.000654327	0.000654327	7.27E-05	0.1246	0.000654327	0.1246	0.0142			
294	-0.367985453	0.413945984	0.700219437	-5.827774129	0.051057575	0.022043905	0.051057575	0.051057575	0.022043905	0.0319	0.051057575	0.0319	0.0000			
295	-0.007519885	0.982566818	0.992929335	-5.83870075	NA	NA	NA	NA	NA	0.0153	NA	0.0153	0.0000			
296	-0.106828488	0.653183203	0.823066937	-5.914663098	0.020272645	0.020272645	0.020272645	0.020272645	0.020272645	0.0066	0.020272645	0.0066	0.0000			
297	-0.108289694	NA	NA	-5.927867142	0.007533758	0.001817669	0.007533758	0.007533758	0.001817669	0.0230	0.007533758	0.0230	0.0009			
298	-0.660289679	0.01322418	0.095936996	-6.049630981	3.41E-05	2.17E-06	3.41E-05	3.41E-05	2.17E-06	0.0142	3.41E-05	0.0142	0.0020			
299	-0.310558162	0.349098805	0.658178335	-6.084652773	NA	NA	NA	NA	NA	0.0241	NA	0.0241	0.0000			
300	0.440517494	0.189471314	0.483838033	-6.126665278	NA	NA	NA	NA	NA	0.0241	NA	0.0241	0.0000			
301	-0.614128718	0.02729062	0.154625145	-6.301902593	NA	NA	NA	NA	NA	0.0265	NA	0.0265	0.0000			
302	-0.351616942	0.142396944	0.41259546	-6.344663293	2.69E-07	2.69E-07	2.69E-07	2.69E-07	2.69E-07	0.0235	2.69E-07	0.0235	0.0010			

I	A		B		C		D		E		F		G		H		I	
	Gene Name	DESeq2 Results: Log ₂ Fold Change	Total X-chromosome P Value	Adjusted P Value	DESeq2 Results: Log ₂ Fold Change	Adjusted P Value	DESeq2 Results: Log ₂ Fold Change	Adjusted P Value	DESeq2 Results: Log ₂ Fold Change	Adjusted P Value	DESeq2 Results: Log ₂ Fold Change	Adjusted P Value	DESeq2 Results: Log ₂ Fold Change	Adjusted P Value	Average Paternal-X Expression (WT)	Average Paternal-X Expression (Eq ^{1/2})		
1																		
2																		
303	Phf8	-0.319927892	0.518444896	0.761358989	-6.379453447	0.761358989	NA	NA	NA	NA	NA	NA	NA	0.0107	0.0000			
304	Zfp185	0.708769132	0.006137812	0.058107317	6.512171065	0.058107317	2.14E-05	0.000224292	2.14E-05	0.000224292	2.14E-05	0.000224292	2.14E-05	0.2927	0.0040			
305	Atfp6ap2	-0.442221827	0.229195404	0.534575442	-6.671147182	0.534575442	3.87E-07	9.39E-06	3.87E-07	9.39E-06	3.87E-07	9.39E-06	3.87E-07	0.0249	0.0012			
306	Phka2	0.545356916	0.012611031	0.032606838	-6.730648468	0.032606838	0.006296694	0.018196867	0.006296694	0.018196867	0.006296694	0.018196867	0.006296694	0.0087	0.0000			
307	Tab3	0.193678484	0.562392057	0.789731425	-6.999599446	0.789731425	NA	NA	NA	NA	NA	NA	NA	0.0133	0.0008			
308	Bcor	0.240369454	0.581991611	0.789731425	-7.088066665	0.789731425	9.31E-07	1.72E-05	9.31E-07	1.72E-05	9.31E-07	1.72E-05	9.31E-07	0.0152	0.0002			
309	Timm8a1	-0.931574343	0.038991182	0.191988487	-7.185193882	0.191988487	NA	NA	NA	NA	NA	NA	NA	0.0595	0.0000			
310	Hcfcl1	-0.086749206	0.592375506	0.789731425	-7.201618368	0.789731425	NA	NA	NA	NA	NA	NA	NA	0.0158	0.0002			
311	Klf4	-0.796268928	0.084746395	0.304505287	-7.217806799	0.304505287	2.04E-06	3.37E-05	2.04E-06	3.37E-05	2.04E-06	3.37E-05	2.04E-06	0.1456	0.0063			
312	Thoc2	-0.530053797	0.021408985	0.130565978	-7.241988842	0.130565978	NA	NA	NA	NA	NA	NA	NA	0.0497	0.0005			
313	Mct5	-0.598398759	0.038135916	0.189253345	-7.253631181	0.189253345	0.002924915	0.010968433	0.002924915	0.010968433	0.002924915	0.010968433	0.002924915	0.0168	0.0000			
314	Prkx	-0.146626351	0.60372196	0.791326261	-7.610801713	0.791326261	NA	NA	NA	NA	NA	NA	NA	0.0119	0.0000			
315	Zfp275	-0.412091598	0.230917556	0.536250746	-7.692826866	0.536250746	0.001349723	0.006345714	0.001349723	0.006345714	0.001349723	0.006345714	0.001349723	0.0168	0.0000			
316	Stag2	-0.725005704	0.001688327	0.024497483	-7.790232912	0.024497483	NA	NA	NA	NA	NA	NA	NA	0.0125	0.0000			
317	Fam3a	0.230960143	0.370060968	0.67692336	-7.83873911	0.67692336	0.000316533	0.002167564	0.000316533	0.002167564	0.000316533	0.002167564	0.000316533	0.0144	0.0000			
318	Rpl36a	-0.982523355	0.002187156	0.028930173	-7.91173753	0.028930173	2.77E-10	1.74E-08	2.77E-10	1.74E-08	2.77E-10	1.74E-08	2.77E-10	0.0430	0.0003			
319	Renbp	-0.631657082	0.188705723	0.482424593	-8.180343133	0.482424593	NA	NA	NA	NA	NA	NA	NA	0.0210	0.0001			
320	Kdm6a	-0.383008397	0.141242041	0.410495226	-8.404292851	0.410495226	1.06E-05	0.000133885	1.06E-05	0.000133885	1.06E-05	0.000133885	1.06E-05	0.0699	0.0004			
321	Ddx3x	-0.659766798	0.008255234	0.070230386	-8.947269387	0.070230386	9.94E-11	1.04E-08	9.94E-11	1.04E-08	9.94E-11	1.04E-08	9.94E-11	0.0511	0.0010			
322	Smc1a	-0.443515574	0.083517468	0.302366732	-9.011470292	0.302366732	5.27E-05	0.000503318	5.27E-05	0.000503318	5.27E-05	0.000503318	5.27E-05	0.0218	0.0000			
323	Vbp1	-0.526515282	0.140693964	0.409539941	-9.072426002	0.409539941	3.32E-05	0.000326993	3.32E-05	0.000326993	3.32E-05	0.000326993	3.32E-05	0.0295	0.0000			
324	Brrc3	-0.484076296	0.071386458	0.274440685	-10.43312916	0.274440685	2.06E-07	5.91E-06	2.06E-07	5.91E-06	2.06E-07	5.91E-06	2.06E-07	0.0071	0.0000			
325	Slc38a5	5.437520008	1.57E-15	1.13E-12	NA	1.13E-12	NA	NA	NA	NA	NA	NA	NA	NA	NA	NA	NA	
326	1700008105Rik	4.080687256	1.63E-11	5.38E-09	NA	5.38E-09	NA	NA	NA	NA	NA	NA	NA	NA	NA	NA	NA	
327	Dgkk	3.529455531	1.56E-07	1.64E-05	NA	1.64E-05	NA	NA	NA	NA	NA	NA	NA	NA	NA	NA	NA	
328	Gm614	3.368086979	2.71E-11	8.07E-09	NA	8.07E-09	NA	NA	NA	NA	NA	NA	NA	NA	NA	NA	NA	
329	Slc9a7	3.224119785	6.43E-11	1.70E-08	NA	1.70E-08	NA	NA	NA	NA	NA	NA	NA	NA	NA	NA	NA	
330	Reps2	2.947264911	2.02E-05	0.000867873	NA	0.000867873	NA	NA	NA	NA	NA	NA	NA	NA	NA	NA	NA	
331	LOC100503393	2.937139971	5.02E-10	1.14E-07	NA	1.14E-07	NA	NA	NA	NA	NA	NA	NA	NA	NA	NA	NA	
332	Dgkcl-2	2.886817663	1.68E-06	0.000122095	NA	0.000122095	NA	NA	NA	NA	NA	NA	NA	NA	NA	NA	NA	
333	Bex4	2.811088739	1.10E-09	2.30E-07	NA	2.30E-07	NA	NA	NA	NA	NA	NA	NA	NA	NA	NA	NA	
334	Gpr50	2.778589213	0.000109057	0.00326903	NA	0.00326903	NA	NA	NA	NA	NA	NA	NA	NA	NA	NA	NA	
335	Zcchc12	2.701617851	0.000284106	0.006756602	NA	0.006756602	NA	NA	NA	NA	NA	NA	NA	NA	NA	NA	NA	
336	Nlgn3	2.590279216	1.87E-06	0.00013427	NA	0.00013427	NA	NA	NA	NA	NA	NA	NA	NA	NA	NA	NA	
337	6530401D17Rik	2.388425195	7.11E-08	8.61E-06	NA	8.61E-06	NA	NA	NA	NA	NA	NA	NA	NA	NA	NA	NA	
338	Fndc3c1	2.351037413	9.53E-05	0.002920632	NA	0.002920632	NA	NA	NA	NA	NA	NA	NA	NA	NA	NA	NA	
339	Mtap7d2	2.342480962	NA	NA	NA	NA	NA	NA	NA	NA	NA	NA	NA	NA	NA	NA	NA	
340	Nap1l2	2.32122232	1.05E-08	1.73E-06	NA	1.73E-06	NA	NA	NA	NA	NA	NA	NA	NA	NA	NA	NA	
341	Nhlh2	2.298202858	7.73E-06	0.000404557	NA	0.000404557	NA	NA	NA	NA	NA	NA	NA	NA	NA	NA	NA	
342	Usp51	2.288742074	5.18E-05	0.001805588	NA	0.001805588	NA	NA	NA	NA	NA	NA	NA	NA	NA	NA	NA	
343	Klf8	2.267930237	3.93E-05	0.001436033	NA	0.001436033	NA	NA	NA	NA	NA	NA	NA	NA	NA	NA	NA	
344	Nudt10	2.205995542	4.26E-05	0.001537121	NA	0.001537121	NA	NA	NA	NA	NA	NA	NA	NA	NA	NA	NA	
345	Vsig1	2.169430148	0.002530979	0.031962832	NA	0.031962832	NA	NA	NA	NA	NA	NA	NA	NA	NA	NA	NA	
346	Zdhc1l5	2.120636353	0.000420449	0.009095759	NA	0.009095759	NA	NA	NA	NA	NA	NA	NA	NA	NA	NA	NA	
347	Syp	2.085411531	0.000400123	0.008802292	NA	0.008802292	NA	NA	NA	NA	NA	NA	NA	NA	NA	NA	NA	
348	Licam	1.913861508	0.004575205	0.047624842	NA	0.047624842	NA	NA	NA	NA	NA	NA	NA	NA	NA	NA	NA	
349	LOC100503525	1.884174395	5.93E-06	0.000330058	NA	0.000330058	NA	NA	NA	NA	NA	NA	NA	NA	NA	NA	NA	
350	Mir362	1.879685179	0.017335084	0.114213093	NA	0.114213093	NA	NA	NA	NA	NA	NA	NA	NA	NA	NA	NA	
351	Ppp1r3f	1.864956846	0.001059513	0.017711718	NA	0.017711718	NA	NA	NA	NA	NA	NA	NA	NA	NA	NA	NA	
352	Map3k15	1.809282803	1.74E-05	0.000786957	NA	0.000786957	NA	NA	NA	NA	NA	NA	NA	NA	NA	NA	NA	

	A	B	C	D	E	F	G	H	I
	Gene Name	DESeq2 Results: Log ₂ Fold Change	Total X-chromosome P Value	Adjusted P Value	DESeq2 Results: Log ₂ Fold Change	Calculated Paternal-X P Value	Adjusted P Value	Average Paternal-X Expression (WT)	Average Paternal-X Expression (Eq ^{1/2})
1									
2									
403	Gm14685	0.516914397	0.217397068	0.52051869	NA	NA	NA	NA	NA
404	Klh15	0.505783914	0.113430776	0.360276772	NA	NA	NA	NA	NA
405	Mageh1	0.487166365	0.10804629	0.351049338	NA	NA	NA	NA	NA
406	LOC100504671	0.472432497	0.332910381	0.647393071	NA	NA	NA	0.0335	0.3951
407	Fam120c	0.469292727	0.266880774	0.581704035	NA	NA	NA	NA	NA
408	Gm6036	0.456469173	0.260935878	0.573607381	NA	NA	NA	0.0000	0.0000
409	Mir224	0.429613123	0.59397103	0.789731425	NA	NA	NA	NA	NA
410	Pja1	0.405917172	0.078259166	0.290930267	NA	NA	NA	0.0000	0.0000
411	5730405015Rik	0.405399545	0.41897655	0.704057735	NA	NA	NA	NA	NA
412	Mir503	0.388292542	0.600918858	0.79004733	NA	NA	NA	NA	NA
413	4933407K13Rik	0.366166977	0.288510357	0.604135091	NA	NA	NA	NA	NA
414	Tir13	0.361714136	0.530763448	0.767501556	NA	NA	NA	NA	NA
415	Tmsb15b1	0.353583996	0.548823032	0.779493538	NA	NA	NA	NA	NA
416	Hdac8	0.33772583	0.064406161	0.257340536	NA	NA	NA	NA	NA
417	Smarca1	0.276858889	0.650597083	0.821348262	NA	NA	NA	NA	NA
418	Mir374	0.254593226	0.648970394	0.820288814	NA	NA	NA	NA	NA
419	Cited1	0.250421164	0.618767866	0.801527947	NA	NA	NA	NA	NA
420	Nxf7	0.230689924	0.659450434	0.827410919	NA	NA	NA	NA	NA
421	Apln	0.213105881	0.745963614	0.882906134	NA	NA	NA	NA	NA
422	LOC100504260	0.201307105	0.666798919	0.832390545	NA	NA	NA	NA	NA
423	Gm14535	0.187869426	0.626188156	0.807239149	NA	NA	NA	NA	NA
424	Cybb	0.14332365	0.832645258	0.927570647	NA	NA	NA	NA	NA
425	2900002K06Rik	0.113433189	0.836918451	0.927986693	NA	NA	NA	NA	NA
426	Fnd3c2	0.03606409	0.96445076	0.986011576	NA	NA	NA	NA	NA
427	LOC100503437	0.02759964	0.885989797	0.949259586	NA	NA	NA	0.0016	0.0000
428	2610030H06Rik	-0.031019846	0.938613724	0.976228478	NA	NA	NA	0.0226	0.0579
429	Dmd	-0.03589859	0.919881243	0.966954936	NA	NA	NA	NA	NA
430	Gm648	-0.039895035	0.959543018	0.984398095	NA	NA	NA	NA	NA
431	Pin4	-0.046864034	0.876221641	0.944352067	NA	NA	NA	NA	NA
432	Snora70	-0.055189159	0.895397315	0.954305636	NA	NA	NA	NA	NA
433	F8a	-0.075962661	0.826639599	0.925676862	NA	NA	NA	NA	NA
434	Gm5643	-0.13450518	0.761205287	0.891510554	NA	NA	NA	NA	NA
435	Rgag4	-0.177732498	0.719625884	0.865446427	NA	NA	NA	NA	NA
436	Lanc13	-0.214728047	0.719375387	0.865446427	NA	NA	NA	NA	NA
437	Cetn2	-0.222911608	0.633116892	0.811220339	NA	NA	NA	NA	NA
438	Gm6568	-0.24211023	0.716898688	0.863603005	NA	NA	NA	NA	NA
439	Mir421	-0.25701321	0.661162599	0.828336538	NA	NA	NA	NA	NA
440	LOC100504405	-0.2690859	0.639144588	0.81482751	NA	NA	NA	NA	NA
441	Igbb1	-0.269460757	0.37748528	0.683958152	NA	NA	NA	NA	NA
442	Arhgap4	-0.274483224	0.415042913	0.700718421	NA	NA	NA	NA	NA
443	Mam1d1	-0.298370483	0.566294259	0.789731425	NA	NA	NA	NA	NA
444	Fam50a	-0.305460365	0.28241963	0.597628049	NA	NA	NA	NA	NA
445	Gpc3	-0.350637199	0.565438735	0.789731425	NA	NA	NA	NA	NA
446	Fancb	-0.355041728	0.356667614	0.665215434	NA	NA	NA	NA	NA
447	LOC100504564	-0.364277358	0.49478152	0.749215959	NA	NA	NA	0.0000	0.0000
448	Gm1862	-0.370757378	0.436493238	0.718711128	NA	NA	NA	NA	NA
449	Mtcb1	-0.376691869	0.167535083	0.451492075	NA	NA	NA	NA	NA
450	Gm7429	-0.480062852	0.321101983	0.635764838	NA	NA	NA	NA	NA
451	Uxt	-0.498099122	0.044143878	0.207080119	NA	NA	NA	NA	NA
452	Tspan7	-0.499243256	0.334682779	0.649264022	NA	NA	NA	NA	NA

I	A		B		C		D		E		F		G		H		I	
	Gene Name	DESeq2 Results: Log ₂ Fold Change	Total X-chromosome P Value	Adjusted P Value	Adjusted P Value	DESeq2 Results: Log ₂ Fold Change	Calculated P Value	Adjusted P Value	Adjusted P Value	DESeq2 Results: Log ₂ Fold Change	P Value	Adjusted P Value	Adjusted P Value	Average Paternal-X Expression (WT)	Average Paternal-X Expression (Eeq'')	Average Paternal-X Expression (Eeq'')		
453	Ssr4	-0.5589133869	0.074396154	0.281083416	NA	NA	NA	NA	NA	NA	NA	NA	NA	NA	NA	NA		
454	Eda	-0.571687696	0.212893519	0.514429663	NA	NA	NA	NA	NA	NA	NA	NA	NA	NA	NA	NA		
455	Awat2	-0.585497697	0.283526057	0.598874413	NA	NA	NA	NA	NA	NA	NA	NA	NA	NA	NA	NA		
456	Rpf113a1	-0.626758329	0.031460473	0.167614711	NA	NA	NA	NA	NA	NA	NA	NA	NA	NA	NA	NA		
457	Hdx	-0.640744661	NA	NA	NA	NA	NA	NA	NA	NA	NA	NA	NA	NA	NA	NA		
458	Tmsb4x	-0.656131936	0.17651529	0.46441524	NA	NA	NA	NA	NA	NA	NA	NA	NA	NA	NA	NA		
459	Drp2	-0.672271215	0.029004662	0.159066129	NA	NA	NA	NA	NA	NA	NA	NA	NA	NA	NA	NA		
460	Nr0b1	-0.673442876	0.392032662	0.694089751	NA	NA	NA	NA	NA	NA	NA	NA	NA	NA	NA	NA		
461	Zic3	-0.686200994	NA	NA	NA	NA	NA	NA	NA	NA	NA	NA	NA	NA	NA	NA		
462	Xlr5c	-0.68727408	0.192339605	0.487495367	NA	NA	NA	NA	NA	NA	NA	NA	NA	NA	NA	NA		
463	2810403D21Rik	-0.687634626	0.102199864	0.340106064	NA	NA	NA	NA	NA	NA	NA	NA	NA	NA	NA	NA		
464	Slc25a5	-0.6961788	0.015453668	0.106569437	NA	NA	NA	NA	NA	NA	NA	NA	NA	NA	NA	NA		
465	Snora69	-0.721084663	0.306479399	0.622345804	NA	NA	NA	NA	NA	NA	NA	NA	NA	NA	NA	NA		
466	Gm5637	-0.722569069	0.209685812	0.50941279	NA	NA	NA	NA	NA	NA	NA	NA	NA	NA	NA	NA		
467	Yy2	-0.743520912	0.007095461	0.063496454	NA	NA	NA	NA	NA	NA	NA	NA	NA	0.0021	0.0171	NA		
468	Slc16a2	-0.764810463	0.221751245	0.525209604	NA	NA	NA	NA	NA	NA	NA	NA	NA	NA	NA	NA		
469	Was	-0.800805381	NA	NA	NA	NA	NA	NA	NA	NA	NA	NA	NA	NA	NA	NA		
470	Zmat1	-0.830893175	0.169710834	0.454503897	NA	NA	NA	NA	NA	NA	NA	NA	NA	NA	NA	NA		
471	Prdx4	-0.836892129	0.051449676	0.225965465	NA	NA	NA	NA	NA	NA	NA	NA	NA	NA	NA	NA		
472	Zfp3613	-0.859376303	0.246071386	0.555479622	NA	NA	NA	NA	NA	NA	NA	NA	NA	NA	NA	NA		
473	LOC100503459	-0.915442864	0.010600102	0.082584861	NA	NA	NA	NA	NA	NA	NA	NA	NA	1.0000	1.0000	NA		
474	Rpl39	-0.94227923	0.001044565	0.017521272	NA	NA	NA	NA	NA	NA	NA	NA	NA	NA	NA	NA		
475	Lrhd2	-0.950423006	0.051976858	0.2270092	NA	NA	NA	NA	NA	NA	NA	NA	NA	NA	NA	NA		
476	Uprt	-1.016221824	0.024631473	0.142474686	NA	NA	NA	NA	NA	NA	NA	NA	NA	NA	NA	NA		
477	Alg13	-1.01851178	NA	NA	NA	NA	NA	NA	NA	NA	NA	NA	NA	NA	NA	NA		
478	Tceal7	-1.037858081	0.031148585	0.166731366	NA	NA	NA	NA	NA	NA	NA	NA	NA	NA	NA	NA		
479	LOC100503426	-1.070442699	NA	NA	NA	NA	NA	NA	NA	NA	NA	NA	NA	0.0072	0.0891	NA		
480	3830403N18Rik	-1.096155295	0.124586096	0.381075045	NA	NA	NA	NA	NA	NA	NA	NA	NA	NA	NA	NA		
481	2310010G23Rik	-1.102612349	0.015222526	0.105564191	NA	NA	NA	NA	NA	NA	NA	NA	NA	NA	NA	NA		
482	Pak3	-1.123876084	0.022193262	0.133446976	NA	NA	NA	NA	NA	NA	NA	NA	NA	NA	NA	NA		
483	Aff2	-1.125712868	0.018962111	0.120695895	NA	NA	NA	NA	NA	NA	NA	NA	NA	NA	NA	NA		
484	Enox2	-1.200355173	0.01174533	0.087988112	NA	NA	NA	NA	NA	NA	NA	NA	NA	NA	NA	NA		
485	Srpx2	-1.263098023	0.022836137	0.135966059	NA	NA	NA	NA	NA	NA	NA	NA	NA	NA	NA	NA		
486	LOC100046796	-1.265677165	0.014551513	0.102485352	NA	NA	NA	NA	NA	NA	NA	NA	NA	0.0003	0.0000	NA		
487	Chst7	-1.268659899	0.076715089	0.286827972	NA	NA	NA	NA	NA	NA	NA	NA	NA	NA	NA	NA		
488	Armcx6	-1.298257427	0.01517189	0.107532411	NA	NA	NA	NA	NA	NA	NA	NA	NA	NA	NA	NA		
489	Prrg1	-1.324533362	0.044947736	0.209489436	NA	NA	NA	NA	NA	NA	NA	NA	NA	NA	NA	NA		
490	C72370	-1.373613162	0.058773555	0.243614206	NA	NA	NA	NA	NA	NA	NA	NA	NA	NA	NA	NA		
491	Pcdh19	-1.403237427	0.008553628	0.071824964	NA	NA	NA	NA	NA	NA	NA	NA	NA	NA	NA	NA		
492	Hs6st2	-1.434723413	0.019893772	0.124663002	NA	NA	NA	NA	NA	NA	NA	NA	NA	0.0000	0.0000	NA		
493	Slc7a3	-1.446584679	0.004218491	0.045347688	NA	NA	NA	NA	NA	NA	NA	NA	NA	NA	NA	NA		
494	Xlr4a	-1.535132597	NA	NA	NA	NA	NA	NA	NA	NA	NA	NA	NA	NA	NA	NA		
495	Maob	-1.578833931	0.01054091	0.082306252	NA	NA	NA	NA	NA	NA	NA	NA	NA	NA	NA	NA		
496	Armcx1	-1.631842774	0.000534998	0.010884397	NA	NA	NA	NA	NA	NA	NA	NA	NA	NA	NA	NA		
497	Tspan6	-1.631920997	0.00545685	0.053725218	NA	NA	NA	NA	NA	NA	NA	NA	NA	NA	NA	NA		
498	1600025MI7Rik	-1.747879751	0.019328826	0.122398896	NA	NA	NA	NA	NA	NA	NA	NA	NA	NA	NA	NA		
499	Phma5	-1.830056498	0.009372687	0.076509131	NA	NA	NA	NA	NA	NA	NA	NA	NA	NA	NA	NA		
500	Fgf	-1.906854056	NA	NA	NA	NA	NA	NA	NA	NA	NA	NA	NA	NA	NA	NA		
501	Rhox12	-1.943431134	0.008324183	0.070725006	NA	NA	NA	NA	NA	NA	NA	NA	NA	NA	NA	NA		
502	Tceal1	-1.947745636	0.000734882	0.01362081	NA	NA	NA	NA	NA	NA	NA	NA	NA	NA	NA	NA		

	A	B	C	D	E	F	G	H	I
	Gene Name	DESeq2 Results: Log ₂ Fold Change	Total X-chromosome P Value	Adjusted P Value	DESeq2 Results: Log ₂ Fold Change	Calculated Paternal-X P Value	Adjusted Paternal-X P Value	Average Paternal-X Expression (WT)	Average Paternal-X Expression (Eq ^{1/2})
1									
2									
503	Lpar4	-2.022510659	0.000155371	0.004267029	NA	NA	NA	NA	NA
504	Gpr64	-2.099682955	0.000271325	0.006589732	NA	NA	NA	NA	NA
505	Tmem47	-2.238791153	3.85E-06	0.000235732	NA	NA	NA	NA	NA
506	A630033H2ORik	-2.301627037	3.83E-06	0.000235534	NA	NA	NA	NA	NA
507	Eras	-2.661359618	7.21E-08	8.69E-06	NA	NA	NA	NA	NA
508	LOC100504521	-3.794392088	4.60E-07	4.19E-05	NA	NA	NA	NA	NA
509	Taf7l	-3.888548946	4.57E-08	5.91E-06	NA	NA	NA	NA	NA
510	Xist	-6.9791348	5.77E-42	4.01E-38	NA	NA	NA	NA	NA

1	A		B		C		D		E		F		G		H		I		J		K		L		M		N	
	Gene Name	WT 1	WT 2	WT 3	Eed ^{fl/fl}	WT Average	Consistent Escape in WT?	Eed ^{-/-} 1	Eed ^{-/-} 2	Eed ^{-/-} 3	Eed ^{-/-} Average	Consistent escape in Eed ^{-/-}	WT vs. Eed ^{-/-} P Value (T Test)	Adjusted P Value														
64	Tspyl2	0.00444444	0.00120482	0.0205529	0.0722994	0.02462539	No	0.27738	0.20651	0.36696	0.288330333	Yes	0.015085788	0.0279458														
65	Car5b	0.062972	0.00202284	0.01998	0.169312	0.254779	No	0.26417	0.30802	0.41788	0.30286667	Yes	0.015705534	0.0286246														
66	AU015836	0.00442799	0.00101126	0.392551	0.00949756	0.09949756	No	0.391275	0.585379	0.60309	0.526564333	Yes	0.016323639	0.02927711														
67	Mospd2	0.00308642	0	0.0728309	0.114318	0.04755883	No	0.257119	0.164401	0.149547	0.223689	Yes	0.018903549	0.03337658														
68	Rp4x	0.293464	0.0491144	0.102779	0.301316	0.18366834	No	0.46358	0.490606	0.483606	0.479264	Yes	0.019486325	0.03387623														
69	Isr2d3	0.00653595	0.0462348	0.0645766	0.134084	0.06360784	No	0.179298	0.186111	0.174138	0.179849	Yes	0.020964677	0.03589407														
70	Atg4a	0.0116279	0	0.0727679	0.0527778	0.0342934	No	0.283333	0.494681	0.430128	0.402714	Yes	0.021294296	0.03591426														
71	C1cn5	0	0.00192391	0.0761195	0.0310243	0.02726693	No	0.585169	0.529996	0.329691	0.481618667	Yes	0.02325252	0.03864135														
72	R9g4	0	0	0	0	0	No	0.145833	0.25525	0.25625	0.212536	Yes	0.024487084	0.0401024														
73	Bex1	0.00138008	0.0011926	0.0517257	0.342394	0.0991731	No	0.459342	0.391296	0.386514	0.412581333	Yes	0.027040049	0.04365036														
74	Siab1b	0.185168	0.017051	0.0944415	0.329199	0.15646488	No	0.410128	0.440101	0.357741	0.405391333	Yes	0.027863616	0.04372704														
75	Vrip6	0.352935	0.214089	0.113972	0.223061	0.22601425	Yes	0.410128	0.386799	0.437403	0.411443333	Yes	0.027689946	0.0437304														
76	G53001106Rik	0.2	0.4	0.518007	0.0833333	0.30033508	No	0.590476	0.71875	1	0.769742	Yes	0.036195102	0.05602804														
77	Tmsb15b2	0	0	0	0.0520925	0.01302313	No	0.437191	0.607785	0.298419	0.447798333	Yes	0.037401005	0.05711235														
78	Mid2	0.0275253	0.00490196	0.0345238	0.102778	0.04243227	No	0.116326	0.120313	0.11842	0.116160333	Yes	0.038618141	0.05741908														
79	Gdi1	0.303389	0.284851	0.425178	0.237147	0.31264125	Yes	0.175764	0.169849	0.168982	0.171531667	Yes	0.038549439	0.05741908														
80	Id5	0.0214486	0.0102248	0.0914018	0.0121899	0.03381628	No	0.245664	0.44218	0.228766	0.30487	Yes	0.049835746	0.07313557														
81	LOC100503525	0	0	0	0	0	No	0.4375	0.372222	0.160714	0.323478667	Yes	0.060681694	0.08679787														
82	Nup62c1	0.00022538	0	0.07121668	0.333333	0.10143129	No	0.333333	0.334262	0.334262	0.333942333	Yes	0.060615878	0.08679787														
83	Gabre	0	0	0	0.371429	0.09285725	No	0.408696	0.4	0.25	0.352898667	Yes	0.06363793	0.08988858														
84	Efp	0.00362319	0	0.0192633	0.0083333	0.00780496	No	0.325171	0.290222	0.115377	0.24359	Yes	0.067518064	0.09304319														
85	Plac1	0.0639967	0.0906162	0.165167	0.733333	0.26327823	No	0.818182	0.717265	0.547682	0.694376333	Yes	0.0671087	0.09304319														
86	Diap2	0.0133929	0.0141414	0.0841471	0.107955	0.0549091	No	0.1125	0.116379	0.21566	0.12126333	Yes	0.06841651	0.09314537														
87	P1p1	0	0	0.0797203	0.0714286	0.03778723	No	0.615238	0.667079	0.231566	0.504627667	Yes	0.073247237	0.09737574														
88	Bex2	0.416667	0.357143	0.257143	0.320225	0.3377945	Yes	0.275722	0.135975	0.226998	0.212748333	Yes	0.07245259	0.09737574														
89	Oat	0.398387	0.240242	0.234498	0.350737	0.256416	No	0.467169	0.460329	0.427681	0.469726333	Yes	0.074176173	0.09746404														
90	Bcor1	0.00621118	0.0111742	0.0998001	0.0786729	0.0489646	No	0.335783	0.315363	0.119949	0.257031667	Yes	0.080881375	0.10505282														
91	201000103Rik	0.4	0.0666667	0.103535	0.220842	0.19776093	No	0.300136	0.440245	0.59246	0.444280333	Yes	0.086509154	0.11108562														
92	Rhox4d	0	0	0	0	0	No	0.124008	0.210515	0.38228	0.238934333	Yes	0.087816605	0.11149749														
93	Rbbp7	0.00191638	0.00148898	0.041387	0.059265	0.02517972	No	0.392045	0.203299	0.646775	0.414039667	Yes	0.092360719	0.11596401														
94	A830080D1Rik	0.00829632	0.010849	0.09991	0.0236824	0.03568443	No	0.495203	0.568717	0.154078	0.402666	Yes	0.09585293	0.119606529														
95	Mcart6	0	0.0718142	0.206159	0.0833333	0.09032663	No	0.363281	0.187412	0.189474	0.246722333	Yes	0.097099716	0.112626378														
96	Apoo	0.0015015	0.00347856	0.122921	0.0622332	0.0475357	No	0.418174	0.494033	0.138292	0.350166333	Yes	0.098772062	0.12001337														
97	LOC100504671	0	0	0.0923949	0.0416127	0.0335019	No	0.53944	0.51941	0.126388	0.395079333	Yes	0.111309717	0.13380849														
98	Ocr1	0.00680272	0.00314728	0.0642105	0.018166	0.02308163	No	0.443214	0.493611	0.107301	0.348042	Yes	0.113672152	0.13521003														
99	Mospd1	0.00781886	0.00441993	0.0637928	0.00929231	0.02133098	No	0.350004	0.517283	0.104018	0.323768333	Yes	0.126020745	0.14833692														
100	Taf1	0.461244	0.0538832	0.363908	0.479433	0.35961705	No	0.522771	0.529036	0.544742	0.532183	Yes	0.145551498	0.16955999														
101	Utp14a	0.151825	0.12021	0.114737	0.0818657	0.11715943	No	0.459226	0.505887	0.125787	0.363633333	Yes	0.173972615	0.20060108														
102	Fnd3c2	0.0397036	0.0768163	0.117848	0.325	0.139884198	No	1	0.340781	0.342649	0.561143333	Yes	0.18774672	0.21429676														
103	Dusp9	0.499318	0.501742	0.532048	0.511417	0.51113125	Yes	0.49881	0.500319	0.499422	0.499517	Yes	0.21669839	0.24486918														
104	Atf7a	0.106585	0.114303	0.183339	0.14264	0.13637275	Yes	0.198648	0.214795	0.498435	0.303959333	Yes	0.224684039	0.25137917														
105	Mon4f2	0.260418	0.286656	0.0592931	0.0574806	0.16596193	No	0.528323	0.522612	0.120439	0.390458	Yes	0.23269685	0.25779161														
106	Cul4b	0.10334	0.102566	0.290919	0.210427	0.176813	Yes	0.113482	0.104668	0.119237	0.112462333	Yes	0.253994169	0.2786538														
107	Rhox4e	0.902439	0.90625	0.672414	0.54717	0.75706825	Yes	0.805195	0.321429	0.538462	0.555028667	Yes	0.297452623	0.32319372														
108	Hnrpht2	0.139538	0.135546	0.0593329	0.141928	0.11908623	No	0.141986	0.143836	0.138776	0.141532667	Yes	0.342974185	0.36910555														
109	Gla	0.0980587	0.0996434	0.0701964	0.115836	0.09593363	No	0.105263	0.107256	0.105263	0.106094	Yes	0.362568615	0.38651183														
110	Mid1	0.28056	0.368813	0.234817	0.173995	0.28454625	Yes	0.249084	0.289844	0.106689	0.215205667	Yes	0.514418434	0.54326433														
111	Armcx1	0.138057	0.17381	0.167879	0.220139	0.17497125	Yes	0.1875	0.208333	0.166667	0.1875	Yes	0.573624037	0.6001807														
112	Rhox4c	0.95	0.236607	0.166607	0.13218	0.452462	Yes	0.323529	0.321212	0.410714	0.351818333	Yes	0.591933365	0.613636566														
113	Sic10a3	0.5	0.53	0.53	0.333333	0.46583325	Yes	0.46875	0.5	0.5	0.489583333	Yes	0.637565666	0.65495475														
114	B230206F22Rik	0.295652	0.332837	0.201874	0.139735	0.2425245	Yes	0.305849	0.297761	0.195019	0.266209667	Yes	0.69363364	0.70555099														
115	BC065597	0.142857	0.641026	0.0465292	0.0742754	0.2261719	No	0.487265	0.286519	0.125952	0.293245333	Yes	0.71138756	0.71773923														
116	Pnck	0.5	0.5	0.543478	0.466667	0.50253625	Yes	0.5	0.5	0.5	0.5	Yes	0.882280979	0.88228098														
117	6530401D17Rik	0	0	0	0	0	No	0.00840336	0.00986399	0	0.006089103	No	NA	NA														
118	LOC100504519	0	0	0	0	0	No	0.407879	0.491604	0	0.299827667	No	NA	NA														
119	Gor173	0	0	0	0.0175439	0.153535	No	0.07132167	0.0441176	0	0.07132167	No	NA	NA														
120	Pak3	0	0	0	0.119048	0.25	No	0.119048	0.25	0	0.123016	No	NA	NA														
121	Mfap7d2	0	0	0	0.00681696	0	No	0.00681696	0	0.0258333	0.01088342	No	NA	NA														
122	Rhox4g	0	0	0	0.00383142	0.0291262	No	0.00383142	0.0291262	0	0.010985873	No	NA	NA														
123	Nudt11	0	0	0	0.00714732	0	No	0.00714732	0	0	0.00238244	No	NA	NA														

1	Gene Name	Proportion Paternal-X Expression		Eed ^{60/11}	WT Average	Consistent Escape in WT?	Proportion Paternal-X Expression			Consistent escape in Eed ^{1/2}	WT vs. Eed ^{1/2} P Value (T Test)	Adjusted P Value
		WT 1	WT 2				WT 3	Eed ^{1/1}	Eed ^{1/2}			
124	Cdkl5	0	0	0	0	No	0.047619	0	0	0	0.015873	NA
125	Smarca1	0	0	0	0	No	0.025641	0	0	0	0.008547	NA
126	Pixra3	0	0	0	0	No	0	0.00265252	0	0	0.000884173	NA
127	Pdzd4	0	0	0	0	No	0.04	0	0	0	0.0133333333	NA
128	Trappc2	0	0	0	0	No	0.0175857	0	0	0	0.0058619	NA
129	LOC100503043	0	0	0	0	No	0.00277008	0	0	0	0.000923336	NA
130	Syn1	0	0	0	0	No	0	0.03	0	0	0.01	NA
131	Dmd	0	0	0	0	No	0	0	0	0	0	NA
132	Gm1862	0	0	0	0	No	0	0	0	0	0	NA
133	Gm6036	0	0	0	0	No	0	0	0	0	0	NA
134	Gpr64	0	0	0	0	No	0	0	0	0	0	NA
135	Gna3	0	0	0	0	No	0	0	0	0	0	NA
136	H6sst2	0	0	0	0	No	0	0	0	0	0	NA
137	LOC100504564	0	0	0	0	No	0	0	0	0	0	NA
138	Pipa1	0	0	0	0	No	0	0	0	0	0	NA
139	Zc4h2	0	0	0	0	No	0	0	0	0	0	NA
140	2810403D21RIK	0	0	0	0	No	NA	NA	NA	NA	NA	NA
141	A630033H20RIK	0	0	0	0	No	NA	NA	NA	NA	NA	NA
142	Armcx6	0	0	0	0	No	NA	NA	NA	NA	NA	NA
143	Dpp2	0	0	0	0	No	NA	NA	NA	NA	NA	NA
144	Mam1d1	0	0	0	0	No	NA	NA	NA	NA	NA	NA
145	Maob	0	0	0	0	No	NA	NA	NA	NA	NA	NA
146	Rab39b	0	0	0	0	No	NA	NA	NA	NA	NA	NA
147	Srpx2	0	0	0	0	No	NA	NA	NA	NA	NA	NA
148	Tlr13	0	0	0	0	No	NA	NA	NA	NA	NA	NA
149	Tmsb15b1	0	0	0	0	No	NA	NA	NA	NA	NA	NA
150	Tspan6	0	0	0	0	No	NA	NA	NA	NA	NA	NA
151	Uprt	0	0	0	0	No	NA	NA	NA	NA	NA	NA
152	LOC100046796	0	0	0	0.00115741	No	0.00028935	0	0	0	0	NA
153	Col4a5	0	0	0	0.00127714	No	0.00031929	0	0	0	0.029097117	NA
154	Timp1	0.00027597	0.0001759	0.000728494	0.00023652	No	0.00033954	0.0833549	0	0	0.000381722	NA
155	Tmem47	0.00149925	0	0	0	No	0.00037481	0	0	0	0	NA
156	Bon	0.00034244	0.00038271	0.000128271	0.00101471	No	0.00046703	0.303409	0.00093985	0.123510283	0.00093985	NA
157	Dock11	0	0	0.00318089	0	No	0.00079522	0	0.00284091	0.000946697	0.00284091	NA
158	Cask	0	0	0.0014245	0.00211416	No	0.00088467	0	0	0	0	NA
159	Armcx3	0.00396825	0	0	0	No	0.00099206	0	0	0	0.092039667	NA
160	Flgf	0	0.00419287	0	0	No	0.00104822	0	0	0	0	NA
161	Lrch2	0	0.00510204	0	0	No	0.00127551	0	0	0	0	NA
162	L1cam	0	0	0.00531674	0	No	0.00132919	0.00462963	0.000661376	0	0.001763669	NA
163	Gpc4	0	0	0.00546448	0.00136612	No	0.00136612	0.109091	0.145455	0.0280374	0.094194467	NA
164	LOC100503437	0	0	0.00657895	0	No	0.00164474	0	0	0	0	NA
165	Sic16a2	0	0	0.0075188	0	No	0.0018797	0.025	0.0625481	0.0138889	0.033812333	NA
166	A230072C01RIK	0	0	0.00833333	0	No	0.00208333	0	0	0	0	NA
167	Yy2	0	0	0	0.00854701	No	0.00213675	0.0512821	0	0	0.017094033	NA
168	Mid1ip1	0	0	0.0097561	0.00243903	No	0.00243903	0	0	0	0	NA
169	Nono	0.0002262	0.00030869	0.00879943	0.00055244	No	0.0183279	0.016706	0.0123294	0.015787767	0.015787767	NA
170	Fhl1	0	0.00042194	0.0110507	0	No	0.0286816	0.0708768	0	0	0.0335037	NA
171	Ilt3ra1	0	0	0.00626974	0.00555556	No	0.0459324	0.0362336	0	0	0.027388667	NA
172	Sept6	0.00469688	0	0	0.0075188	No	0.0044329	0.0044329	0	0	0.067668967	NA
173	Taf9b	0	0	0.0124717	0.00311793	No	0.00305392	0.0761905	0.0166667	0.05908533	0.0166667	NA
174	C1gat1c1	0.00294985	0	0.0110193	0	No	0.00349229	0.00680272	0.0748684	0.0166667	0.007732473	NA
175	Birc3	0.00699301	0	0.00786689	0	No	0.00371498	0	0	0	0	NA
176	Alg13	0	0	0.0151515	0	No	0.00378788	0.087484	0.05	0	0.045828	NA
177	Fam123b	0	0	0.0154545	0	No	0.00386363	0.01	0	0	0.003333333	NA
178	Pir	0	0	0.015625	0	No	0.00390625	0.228205	0	0	0.076068333	NA
179	Klhl15	0	0	0.016129	0	No	0.00403225	0	0	0	0	NA
180	Prps2	0	0	0.0106097	0.00576481	No	0.00403633	0.14317	0.247808	0	0.130326	NA
181	Mum1l1	0.00347594	0.00953415	0.00347222	0	No	0.00412058	0.132803	0.0468682	0.237265	0.138978733	NA
182	Tspan7	0	0	0	0.0166667	No	0.00416668	0.01	0	0	0.003333333	NA
183	C330007P06RIK	0.0009678	0.00197628	0.0102466	0.00633989	No	0.00098814	0.000834028	0.00104493	0.0009557	0.0009557	NA

1	Gene Name	Proportion Paternal-X Expression		Eed ^{6/11}	WT Average	Consistent Escape in WT?	Proportion Paternal-X Expression		Eed ¹	Eed ²	Eed ³	Consistent escape in Eed ¹⁻³	WT vs. Eed ¹⁻³ P Value (T Test)	Adjusted P Value
		WT 1	WT 2				WT 3	Eed ¹						
184	Arhaqa4	0	0.022222	0	0.00555555	No	0	0	0.0137649	0.0585052	0.0124421	0.0282374	NA	NA
185	Magee1	0.00168919	0.00532454	0.0156695	0.00567031	No	0	0	0.0137649	0.0585052	0.0124421	0.0282374	NA	NA
186	Mecp2	0	0.00205761	0.0244836	0.00665303	No	0	0	0	0	0	0	NA	NA
187	Tsr2	0	0.0278121	0.00695303	0.00695303	No	0	0	0.00126984	0.166667	0.012987	0.00475228	NA	NA
188	Apln	0	0.004329	0.0238095	0.00703463	No	0	0	0.07341	0.166667	0.080025667	0.00025667	NA	NA
189	Sfn3kb1	0.00764892	0.0145863	0	0.00593996	No	0	0	0.0237757	0.0714429	0.0282877	0.041168767	NA	NA
190	Rps6kb3	0	0	0.0285714	0.00714285	No	0	0	0	0	0	0	NA	NA
191	Fam120c	0	0.0285714	0	0.00714285	No	0	0	0.00699301	0.0830732	0.03002207	0.03002207	NA	NA
192	LOC100503426	0.00047461	0.00240817	0.019006	0.00703258	No	0	0	0.0754543	0.0358895	0.079890267	0.079890267	NA	NA
193	Fnf2	0	0.0289765	0.00133333	0.00757746	No	0	0	0.00416667	0	0.00138889	0	NA	NA
194	Eno2	0	0.0333333	0.00238095	0.00833333	No	0	0	0.166667	0.37963	0	0.182099	NA	NA
195	Stag2	0	0.0309659	0.00833671	0.00833671	No	0	0	0	0	0	0	NA	NA
196	Cxx1b	0	0	0.0087585	0.0087585	No	0	0	0.0284455	0	0	0.009481833	NA	NA
197	Zxda	0	0.0350907	0	0.00877268	No	0	0	0.00250627	0.00556174	0.00724389	0.003435445	NA	NA
198	Rnox4a	0.00625	0.0106383	0.0188568	0.00893628	No	0	0	0.0740741	0.0315657	0.00520833	0.03649377	NA	NA
199	Tex13	0	0.029231	0.00649351	0.00910415	No	0	0	0.145233	0.121196	0.0897401	0.118723033	NA	NA
200	Afp11c	0	0.0365122	0	0.00912805	No	0	0	0	0	0	0	NA	NA
201	Ngr1p1	0.00106999	0.00015731	0.00745967	0.00926957	No	0	0	0.064208	0.00591792	0.246892	0.10567264	NA	NA
202	Ubi4	0.00196464	0.0027933	0.0328638	0.00940544	No	0	0	0	0	0	0	NA	NA
203	Suv39h1	0.00416667	0.0294584	0.00549451	0.0097799	No	0	0	0.00163117	0.00264628	0.0217391	0.007246367	NA	NA
204	Lamp2	0.00053554	0.000882	0.0200894	0.00979291	No	0	0	0.00163117	0.00264628	0.0217391	0.007246367	NA	NA
205	Xk	0	0.0393068	0	0.0098267	No	0	0	0	0	0	0	NA	NA
206	2900062L1IRIK	0	0.0325143	0.0068609	0.0098438	No	0	0	0.0378827	0.0271463	0.00227273	0.02243391	NA	NA
207	Pcdh19	0.00759878	0.0104797	0.010989	0.01024307	No	0	0	0.00757576	0	0	0.002525253	NA	NA
208	Tbfx	0	0.00652063	0.0337175	0.00095057	No	0	0	0.00543478	0	0.00836146	0.004598747	NA	NA
209	Phf8	0	0.0429086	0	0.01027115	No	0	0	0	0	0	0	NA	NA
210	Magt1	0.00010101	0.00126672	0.0240406	0.0175347	No	0	0	0.0108449	0.00548323	0.332205	0.11617771	NA	NA
211	Mpp1	0	0.0429497	0.01073743	0.01073743	No	0	0	0.00670326	0	0	0.002234442	NA	NA
212	Eif1ax	0	0.0412924	0.0018989	0.01079782	No	0	0	0.025877	0.203164	0.084564	0.237868333	NA	NA
213	Msn	0.00055704	0.0424938	0.00016213	0.01082539	No	0	0	0.00204414	0.000561026	0.00043253	0.000412564	NA	NA
214	Naa10	0	0.0333333	0.0101523	0.0108714	No	0	0	0	0	0	0	NA	NA
215	Xr3a	0	0.0405611	0.00369563	0.01106418	No	0	0	0.00144928	0.00144928	0.00324675	0.002048437	NA	NA
216	Prickl8	0	0.0322268	0.0125026	0.01120472	No	0	0	0.265514	0.109688	0.0491504	0.1414508	NA	NA
217	Prxk	0.00201207	0.0454023	0	0.01185359	No	0	0	0	0	0	0	NA	NA
218	B630019K06RIK	0	0.047619	0	0.01190475	No	0	0	0	0	0	0	NA	NA
219	Slc7a3	0	0.047619	0	0.01190475	No	0	0	NA	NA	NA	NA	NA	NA
220	Fundc1	0.00186567	0	0.0232624	0.0123212	No	0	0	0.355854	0.402245	0	0.252699667	NA	NA
221	Hlatsf1	0.00186285	0.00262096	0.04559	0.01251845	No	0	0	0.00208664	0	0	0.000695547	NA	NA
222	Pis3	0	0.00260417	0.047619	0.01255579	No	0	0	0.0447977	0.172794	0.104545	0.1073789	NA	NA
223	Tmem164	0	0.00149414	0.00658722	0.01261712	No	0	0	0.000412371	0.000412371	0.0034787	0.001297024	NA	NA
224	Lae3	0.0004842	0	0.0498208	0.01273408	No	0	0	0	0	0	0	NA	NA
225	261002M06RIK	0	0.0515805	0	0.01289513	No	0	0	0	0	0.0181818	0.0060606	NA	NA
226	Eda2r	0.00246548	0.00332511	0.0178816	0.01290157	No	0	0	0.381872	0.342974	0.0101719	0.245005967	NA	NA
227	Mtmr1	0	0.0483383	0.00352734	0.01296641	No	0	0	0.00383598	0	0.00227273	0.002036237	NA	NA
228	Tab3	0.00182081	0.00054466	0.0480196	0.01327023	No	0	0	0.00111957	0.000327761	0.00094012	0.000795816	NA	NA
229	Parrnc1	0	0.0008547	0.00210526	0.01333402	No	0	0	0.00156365	0.00259455	0.0005291	0.001562434	NA	NA
230	Gyk	0	0.05192	0.0018797	0.01344993	No	0	0	0.353566	0.507801	0.0346939	0.298686967	NA	NA
231	Hsd17b10	0.00252908	0.002886	0.0496312	0.01376157	No	0	0	0.00380228	0	0	0.001267427	NA	NA
232	Gprasp1	0	0.0522431	0.00358584	0.01395754	No	0	0	0.00098957	0.000743833	0.00064237	0.000791923	NA	NA
233	Armcx5	0.00357634	0	0.01408116	0.01408116	No	0	0	0	0	0	0	NA	NA
234	Cenpi	0.00367199	0	0.0529776	0.0141624	No	0	0	0	0	0	0	NA	NA
235	Rbm10	0	0.0546336	0.00260417	0.01430944	No	0	0	0.0772606	0.0322711	0.0345013	0.048011	NA	NA
236	Fam3a	0.01025564	0.0059771	0.0031746	0.01437493	No	0	0	0	0	0	0	NA	NA
237	Eif4	0.00087489	0.00529957	0.003003	0.0144756	No	0	0	0.025803	0.0196653	0	0.0151561	NA	NA
238	Mtm1	0	0.0544903	0.00362319	0.01452837	No	0	0	0.004462963	0	0	0.00154321	NA	NA
239	Mbtas2	0	0.00861378	0.0501934	0.0147018	No	0	0	0	0	0.0104167	0.003472233	NA	NA
240	Pkfb1	0	0.0544495	0.00438596	0.01470887	No	0	0	0	0	0.00480769	0.001602563	NA	NA
241	Praf2	0	0.0475321	0.0121535	0.0149214	No	0	0	0.174333	0.462019	0.00473186	0.21369462	NA	NA
242	Bcor	0.00059301	0.00621472	0.0487018	0.01518095	No	0	0	0.00043478	0	0.00022624	0.00020342	NA	NA
243	Abcb7	0.00226757	0.0168698	0.00356562	0.01524401	No	0	0	0.023005	0.0101119	0.0284674	0.020530467	NA	NA

1	A		B		C		D		E		F		G		H		I		J		K		L		M		N	
	Gene Name	WT 1	WT 2	WT 3	Eed ^{fl/fl}	WT Average	Consistent Escape in WT?	Eed ^{-/-} 1	Eed ^{-/-} 2	Eed ^{-/-} 3	Eed ^{-/-} Average	Consistent escape in Eed ^{-/-} ?	WT vs. Eed ^{-/-} P Value (T Test)	Adjusted P Value														
244	Maos	0	0	0.0610873	0	0.01527183	No	0	0	0	No	NA	NA															
245	Itm2a	0	0	0.0615385	0	0.01538463	No	0.0147059	0	0.462185	0.158963633	NA	NA															
246	Phka2	0	0	0.0471917	0.0144841	0.01541895	No	0	0	0	No	NA	NA															
247	Idh3g	0	0	0.0609553	0.00143678	0.01559802	No	0.00084175	0	0.00018708	No	NA	NA															
248	Itih1	0	0.00383302	0.057583	0.00108401	0.01566883	No	0.00235781	0.00093371	0.001377756	No	NA	NA															
249	Ritm	0.00252803	0.00253292	0.0511847	0.00671832	0.01574099	No	0.0458994	0.0279758	0.035214567	No	NA	NA															
250	Maged1	0.00055773	0.0013199	0.0554375	0.00569231	0.01575186	No	0.00326392	0.00081152	0.003366415	No	NA	NA															
251	Hfcf1	0.00094502	0.00040092	0.0611984	0.00054177	0.01577153	No	0.000562365	0	0.000187455	No	NA	NA															
252	Ammecc1	0	0	0.0643116	0.0160779	0.0160779	No	0.00409836	0	0.00136612	No	NA	NA															
253	G6pdx	0.00645161	0	0.0589768	0	0.0163571	No	0.00170068	0.00833333	0.00255102	No	NA	NA															
254	Zbtb33	0.00056689	0.00437797	0.0555839	0.0051357	0.01641612	No	0.00228418	0	0.001074677	No	NA	NA															
255	Maged2	0.0195789	0.0013947	0.0404412	0.0004329	0.01643595	No	0	0.00132802	0.000442673	No	NA	NA															
256	Mg13	0.0139204	0.00378788	0.0480418	0	0.01643752	No	0.0132386	0.058802	0.0578197	No	NA	NA															
257	Mct5	0	0.000536193	0.0618557	0	0.01680441	No	0	0	0	No	NA	NA															
258	Zfp275	0	0	0.042734	0.0245039	0.01680948	No	0	0	0	No	NA	NA															
259	Slc25a14	0.00675676	0.0323427	0.0292208	0	0.01708007	No	0.439753	0.436321	0.027619	0.301231	NA	NA															
260	Dnae1l1	0	0	0.0693766	0	0.01734415	No	0	0	0	No	NA	NA															
261	Cox7b	0.00031382	0.00014757	0.0599336	0.0100013	0.01759907	No	0.0194707	0.0219914	0.397504	0.146322033	NA	NA															
262	Gpm6b	0	0.0226481	0.0102041	0.0388889	0.01793528	No	0.0428571	0.0552728	0.0277778	0.041969233	NA	NA															
263	Klhl13	0.00231163	0.00408932	0.05925	0.00682718	0.01811953	No	0.0101935	0.0010806	0.00217391	0.00445849	NA	NA															
264	Rarb9	0.00183315	0	0.0707382	0	0.01814243	No	0.00154321	0	0.000514403	No	NA	NA															
265	Ubp1n2	0	0	0.0730651	0	0.01826628	No	0	0.00416667	0	0.00138889	No	NA	NA														
266	Lpar4	0.0410831	0.00396825	0.0289256	0	0.01849424	No	NA	NA	NA	NA	NA	NA															
267	Gpc3	0	0.0740741	0	0.01851853	0.01851853	No	0.0344828	0.0833333	0	0.039272033	NA	NA															
268	Nis	0	0.0744379	0	0.01860948	0.01860948	No	0	0	0.00304446	0.00101482	NA	NA															
269	Phka1	0	0	0.076661	0.00421053	0.01871916	No	0.0315519	0.00345211	0	0.011668003	NA	NA															
270	Pdk3	0.00242869	0.0205775	0.0265079	0.0257079	0.0188055	No	0.0176594	0.0312627	0.0137722	0.0208981	NA	NA															
271	Lorrf3	0.00116144	0	0.0740761	0.01880939	0.01880939	No	0.00998623	0.00265152	0	0.0044212583	NA	NA															
272	Brd3	0.00055698	0.00245499	0.0676621	0.00576966	0.01911414	No	0.00452096	0.000986193	0.441071	0.148859384	NA	NA															
273	Nrk	0.0131351	0.003807	0.0574609	0.00437434	0.01923934	No	0.00396825	0.00481686	0.00738967	0.006391593	NA	NA															
274	Atg6ap1	0.00066199	0.00309442	0.0654015	0.00835883	0.01950418	No	0.00083963	0.00213129	0.00089225	0.006484335	NA	NA															
275	Hprt	0.00035063	0	0.077356	0.00140647	0.0197828	No	0.0082806	0	0	0.06093533	NA	NA															
276	Aco9	0.00193436	0.00346393	0.0621091	0.0116825	0.01979747	No	0.030475	0.0014581	0.446904	0.159612367	NA	NA															
277	Elk1	0	0.0480889	0.0325646	0.02016338	0.01849424	No	0.0241546	0.021938	0.0434963	0.096529633	NA	NA															
278	Satl	0.00487805	0	0.0660131	0.00995025	0.02021035	No	0	0.00534759	0.00178253	0	NA	NA															
279	Rap2c	0	0	0.0813179	0	0.02032948	No	0	0	0.00223214	0.000744047	NA	NA															
280	Bcap3l	0.001321	0.00097752	0.0534031	0.0257649	0.02036663	No	0.00187266	0.00151286	0	0.001128507	NA	NA															
281	Zfx	0.00105927	0	0.0828584	0.02097942	0.02097942	No	0.0536928	0.071909	0.0347916	0.053464467	NA	NA															
282	Renbp	0.0023183	0.00029577	0.0785071	0.00299635	0.02102938	No	0.00309215	0	0.00103072	0	NA	NA															
283	Acsl4	0.00225583	0.0005531	0.0684209	0.0133413	0.02114278	No	0.0155244	0.00690731	0.0161002	0.01284397	NA	NA															
284	Cstf2	0.00337484	0.00418571	0.0761416	0.00091743	0.0211549	No	0	0.00222222	0	0.00074074	NA	NA															
285	Rbm2	0.002849	0.00652612	0.0476545	0.0276711	0.02117518	No	0.0334329	0.0398804	0.00824176	0.02218502	NA	NA															
286	Alfr1	0.00222222	0.00231481	0.0754918	0.00510204	0.02128272	No	0.0136222	0.0134449	0	0.009023733	NA	NA															
287	Smc1a	0.00098238	0.00178904	0.0844384	0	0.02180245	No	0	0	0	0	NA	NA															
288	Emd	0	0	0.0812887	0.00598802	0.02181918	No	0	0	0	0	NA	NA															
289	Apex2	0	0.00862069	0.0782306	0	0.02183782	No	0	0	0.0104167	0.003472233	NA	NA															
290	1600014K23Rik	0.0140956	0.0187261	0.0546634	0	0.02187128	No	0.05	0	0	0.016666667	NA	NA															
291	Nkrf	0	0.0885668	0	0.0221417	0.0221417	No	0	0	0	0	NA	NA															
292	Ndufa1	0.0212114	0.0263241	0.0388216	0.00235571	0.0221782	No	0.00461361	0.0146845	0	0.006432703	NA	NA															
293	2610030H06Rik	0.00200583	0.00098425	0.0716504	0.014892	0.022389312	No	0.0162611	0.00046618	0.171672	0.057941509	NA	NA															
294	Shroom2	0	0.0020643	0.0832729	0.00422171	0.022389312	No	0.0121701	0.00782137	0.00391356	0.007968343	NA	NA															
295	C77370	0	0	0.0897925	0	0.02244813	No	0.0512511	0	0	0.0170837	NA	NA															
296	Usp9p	0.00203954	0.0050786	0.0752757	0.00922598	0.02290496	No	0.175093	0.0944097	0.00514381	0.091548837	NA	NA															
297	Cfp	0	0	0.0916667	0	0.02291668	No	0.0447635	0.0384615	0	0.088639	NA	NA															
298	Haus7	0.00357171	0	0.0636442	0.0249475	0.02304085	No	0.00273973	0	0.000913243	0	NA	NA															
299	Dlg3	0.0242959	0.00255272	0.042875	0.022784	0.02312691	No	0.0070922	0.00917736	0.516107	0.177458853	NA	NA															
300	Fancd	0	0	0.093548	0	0.023387	No	0.272484	0.353948	0	0.208810667	NA	NA															
301	Chm	0.0127056	0.00372057	0.047045	0.0307284	0.023354989	No	0	0.00128205	0.00160256	0.000961537	NA	NA															
302	Chic1	0.00740741	0	0.0869712	0	0.02359465	No	0.0270833	0.0204082	0.0165289	0.021340133	NA	NA															
303	Xiap	0.0190369	0.00310781	0.0622221	0.0108931	0.02381498	No	0.00117983	0.137186	0.00118948	0.046518437	NA	NA															

1	Gene Name	Proportion Paternal-X Expression		Eed ^{60/11}	WT Average	Consistent Escape in WT?	Proportion Paternal-X Expression			Consistent escape in Eed ^{1/2}	WT vs. Eed ^{1/2} P Value (T Test)	Adjusted P Value
		WT 1	WT 2				WT 3	Eed ^{1/1}	Eed ^{1/2}			
304	Taz	0	0	0.0963684	0.0240921	No	0	0	0	0	NA	NA
305	Las1l	0.00965217	0.00591864	0.0621922	0.02416023	No	0.00509996	0	0.00309047	0.002730143	NA	NA
306	Pola1	0	0	0.097002	0.0242505	No	0.00780423	0	0	0.00260141	NA	NA
307	Zfp182	0	0	0.097264	0.024316	No	0	0	0	0	NA	NA
308	Esx1	0	0	0.098696	0.024674	No	0.00098232	0.00115207	0	0.000711463	NA	NA
309	Fam122b	0.01093325	0.0128175	0.0722436	0.002886	No	0.07351	0.0129702	0.0129702	0.048443967	NA	NA
310	Dkc1	0.00503291	0.004085	0.094085	0.02477948	No	0	0	0	0	NA	NA
311	Atfbap2	0.0022365	0.00477889	0.0663593	0.0260793	No	0.00278659	0.000724638	0	0.001170409	NA	NA
312	Zdhc9	0.0025378	0.00205761	0.0572106	0.0380342	No	0.362016	0.488706	0.0882788	0.313000267	NA	NA
313	Foxo4	0.00182787	0.00220264	0.095506	0.0004845	No	0.00327869	0.00396935	0.00269339	0.00331381	NA	NA
314	Wdr44	0	0	0.097076	0.02545948	No	0	0	0	0	NA	NA
315	Ndufrb11	0.0111553	0.0215054	0.0537076	0.0165623	No	0.0399882	0.0534789	0.0402453	0.0445708	NA	NA
316	Nsdh1	0.0029491	0.00387597	0.0628491	0.034577	No	0.433434	0.436869	0	0.290101	NA	NA
317	1110012119Rik	0.00139234	0.00318221	0.0642373	0.036052	No	0.326302	0.43536	0.0367502	0.2661374	NA	NA
318	Ube2a	0	0.00634921	0.0746268	0.023974	No	0	0.044187	0	0.014729	NA	NA
319	Rbm3	0.0074421	0.00021554	0.097868	0.00201023	No	0.0293922	0.0490909	0.0795733	0.052685467	NA	NA
320	Rbm3	0.00505051	0	0.0872017	0.0156137	No	0	0.00854701	0.0148954	0.007814137	NA	NA
321	Mimgt1	0.00142857	0.0018018	0.095781	0.0101224	No	0.314757	0.385401	0	0.233386	NA	NA
322	Slc25a43	0	0.0903361	0.0195773	0.02747835	No	0.0672878	0.5937	0	0.20329267	NA	NA
323	Ofd1	0.00898755	0.005464	0.0934212	0.00290984	No	0.0831161	0.0130065	0.0327879	0.042970167	NA	NA
324	F8a	0	0	0.111111	0.0277775	No	NA	NA	NA	NA	NA	NA
325	Taf7l	0	0	0.114418	0.0278545	No	NA	NA	NA	NA	NA	NA
326	Vbp1	0.00502513	0	0.09701	0.0121581	No	0	0	0	0	NA	NA
327	Rbox12	0.0337112	0.0179239	0.0630599	0.02867375	No	0	0.389994	0	0.129998	NA	NA
328	Mageb16	0.00764818	0.00854701	0.099746	0.0289853	No	0.0003861	0	0.0304569	0.0114393	NA	NA
329	Gn13	0.00083913	0.00105097	0.09882	0.0156541	No	0.00622809	0.00196344	0.443422	0.150537843	NA	NA
330	Uplf3b	0	0.004	0.0765311	0.0371361	No	0.0087193	0.317504	0.0135135	0.113263143	NA	NA
331	Zfp280c	0.00271739	0.00203804	0.0313473	0.0816655	No	0.0876362	0.0821256	0.0842391	0.084666967	NA	NA
332	Nkap	0.024171	0.021767	0.0605884	0.0141848	No	0.00197191	0.00214947	0	0.00131386	NA	NA
333	Tecanc	0.0171871	0.00799201	0.0832544	0.03056398	No	0.0295455	0.339866	0.385356	0.251589167	NA	NA
334	Issac2	0.0196078	0	0.0138889	0.0912698	No	0.0308117	0.0318298	0.130946	0.066929167	NA	NA
335	LOC100504405	0	0	0.125	0.03125	No	NA	NA	NA	NA	NA	NA
336	Bhlhb9	0	0	0.12569	0.0314225	No	0.00103093	0	0.00238095	0.001137293	NA	NA
337	Uxt	0	0	0.126984	0.031746	No	NA	NA	NA	NA	NA	NA
338	Ribc1	0.0170627	0	0.110429	0.03187293	No	0	0	0	0	NA	NA
339	6720401G13Rik	0.0293533	0.0225834	0.0379266	0.0320209	No	0.0435805	0.0371374	0.0411329	0.040616933	NA	NA
340	Apool	0.00970874	0	0.12	0.03242719	No	0	0	0	0	NA	NA
341	Fgd1	0.0029469	0.00736671	0.0797718	0.03252135	No	0	0	0.0149573	0.004985767	NA	NA
342	Zfp449	0	0	0.130435	0.03260875	No	0.0185185	0.047619	0	0.022045833	NA	NA
343	8030474K03Rik	0.05	0	0.0714286	0.0102931	No	0.055361	0.024854	0.0121553	0.0307901	NA	NA
344	Anl2	0.0535714	0.00571429	0.072482	0.03293043	No	0.00271739	0	0	0.000905797	NA	NA
345	2210013021Rik	0	0	0.132035	0.03300875	No	0	0	0	0	NA	NA
346	Zmat1	0.00641026	0	0.128757	0.03379182	No	0	0	0.0333333	0.0111111	NA	NA
347	Fam199x	0.0220754	0.00800029	0.0830072	0.0222019	No	0.548717	0.645922	0.0374716	0.410703533	NA	NA
348	Cxx1c	0	0.0441017	0.095254	0.03483893	No	0.141746	0.0525794	0.040625	0.0783168	NA	NA
349	Med14	0.00871267	0.00983141	0.0589305	0.0621116	No	0.0217495	0.0628336	0.00256757	0.029050223	NA	NA
350	Sic9a6	0	0.00927083	0.079551	0.03514931	No	0.427682	0.479656	0.00504857	0.304128857	NA	NA
351	Prps1	0.00529801	0	0.125172	0.0116505	No	0.00294118	0.00555556	0	0.002832247	NA	NA
352	Pdha1	0.00129399	0.00230197	0.11515	0.0244266	No	0.0100711	0.00267941	0.0034627	0.005404403	NA	NA
353	Akap17b	0.00464843	0.00397279	0.11043	0.0245282	No	0.0398431	0.36246	0.00196078	0.134754627	NA	NA
354	Hmgm5	0	0	0.146341	0.03568525	No	0.025641	0	0.0196078	0.015082933	NA	NA
355	Atx	0.0003622	0.00052929	0.0718749	0.0755383	No	0.0730031	0.0702341	0.0657568	0.069664667	NA	NA
356	4933407K13Rik	0	0	0.094251	0.0555556	No	0.0555556	0.00694444	0	0.020833347	NA	NA
357	Abcd1	0	0.0116373	0.126843	0.0160534	No	0	0	0.00125313	0.00041771	NA	NA
358	Nsd27x	0	0.003125	0.152476	0.00208333	No	0.0210927	0	0	0.0070309	NA	NA
359	Nxt2	0.0181818	0.0151515	0.0684698	0.0612245	No	0.0729167	0.0625	0.0555556	0.063657433	NA	NA
360	Prg3	0	0	0.0642446	0.101323	No	0.1	0.0965517	0.1	0.098850567	NA	NA
361	Rpl36a	0.0106721	0.00430927	0.0887143	0.04297769	No	0.00045618	5.27E-05	0.00042651	0.000311809	NA	NA
362	Morc4	0.0100418	0.00720873	0.147136	0.00753553	No	0.550374	0.0234701	0.389174367	0.0234701	NA	NA
363	Rpgt	0	0	0.0472222	0.125	No	0.111111	0.116667	0	0.075926	NA	NA

1	Gene Name	Proportion Paternal-X Expression		Eed ^{6/11}	WT Average	Consistent Escape in WT?	Proportion Paternal-X Expression			Consistent escape in Eed ^{-/-} ?	WT vs. Eed ^{-/-} P Value (T Test)	Adjusted P Value
		WT 1	WT 2				WT 3	Eed ^{-/-} 1	Eed ^{-/-} 2			
364	Shroom4	0.0128831	0.0127864	0.0827853	0.0449355	No	0.454283	0.392308	0.0740901	0.3068937	NA	NA
365	Efnb1	0	0.0333333	0.108995	0.04500968	No	0.00813008	0	0	0.02271027	NA	NA
366	181L0030007Rik	0.00175439	0.0372633	0.0461466	0.04640857	No	0.160108	0.386753	0.00714087	0.18466729	NA	NA
367	Mir374	0	0.0666667	0.125	0.04791668	No	0.2	0.0625	0	0.0875	NA	NA
368	BC023829	0	0	0.18299	0.0113636	No	0.118656	0.0532873	0.0147186	0.062220633	NA	NA
369	Hmgb3	0	0	0.194577	0.04864425	No	0.00592105	0	0	0	NA	NA
370	Amod	0.0294769	0.0291291	0.120211	0.0489984	No	NA	NA	0.367887	0.125036293	NA	NA
371	Hdx	0	0	0.196495	0.04912375	No	0	0	NA	NA	NA	NA
372	Thoc2	0.00067069	0	0.196248	0.00138889	No	0	0.00111111	0	0.00037037	NA	NA
373	Ikbk1	0.03125	0.0364172	0.0926408	0.04969238	No	0.0309047	0.00909091	0.0507463	0.032977303	NA	NA
374	Mtbp1	0	0	0.2	0.05	No	NA	NA	NA	NA	NA	NA
375	Nap1l3	0	0	0	0.2	No	NA	NA	NA	NA	NA	NA
376	Ahrgef6	0.0159368	0.0230106	0.108258	0.05010848	No	0.0571429	0.00147665	0.00349231	0.020703953	NA	NA
377	Ddx3x	0.0252498	0.0557308	0.120989	0.0511458	No	0.00116654	0.00196424	0	0.001043593	NA	NA
378	Gm9	0.0442565	0.05	0.0970257	0.0151343	No	0.0184951	0.183935	0.0619151	0.088115067	NA	NA
379	Pdzf11	0.134211	0	0.0729469	0.00510204	No	0	0	0	0	NA	NA
380	Gm4779	0	0	0.215909	0.05397725	No	0.0426665	0.0243662	0.0162923	0.027775	NA	NA
381	Ddx26b	0.0234375	0.0193924	0.141886	0.0345547	No	0.469802	0.434488	0.0178571	0.307382367	NA	NA
382	BC022960	0.16741	0	0.0582196	0.0564074	No	0	0.0111111	0	0.0037037	NA	NA
383	Fina	0.0555766	0.0558245	0.095235	0.05933855	No	0.0318223	0.00755686	0.013515	0.017631387	NA	NA
384	Timm8a1	0	0	0.203912	0.05950073	No	0	0	0	0	NA	NA
385	Xir5e	0.0769231	0.0833333	0.0723421	0.06055347	No	0.0151616	0.003663	0	0.006274867	NA	NA
386	Tmem79	0.0338983	0.0540541	0	0.0688631	No	0.1875	0.137931	0.40625	0.211393667	NA	NA
387	4933402E13Rik	0.0191993	0.0131365	0.178541	0.0666667	No	0	0.00203252	0.00411702	0.002049847	NA	NA
388	Kdm6a	0.151872	0.037659	0.0891597	0.06963588	No	0	0.0010395	0	0.0003465	NA	NA
389	Armc2	0.0588235	0.0666667	0.0826821	0.0777778	No	0.1	0.107143	0	0.069047667	NA	NA
390	Cxx1a	0	0	0.287628	0.071907	No	0.0321789	0	0	0.0107263	NA	NA
391	Gprasp2	0	0	0.0973214	0.190476	No	0.0803571	0.0714286	0.0769231	0.076236267	NA	NA
392	Sms	0.0828824	0.0424242	0.134384	0.0333333	No	0.0272723	0	0.0208333	0.0145202	NA	NA
393	Sh3bgr1	0.0398594	0.0414632	0.18469	0.0758052	No	0.0286052	0.040141	0.398945	0.155897067	NA	NA
394	1600025M17Rik	0.0502008	0.027027	0.245283	0.0806277	No	1	0.636364	0	0.545454667	NA	NA
395	Trmt2b	0.0916667	0.0680556	0.0746308	0.08131555	No	0.0909091	0.0833333	0.0909091	0.088383833	NA	NA
396	Map3k15	0	0.192308	0.140132	0.08311	No	0	0	0	0	NA	NA
397	Ncrna000086	0	0	0.32828	0.00813888	No	0.139187	0.246086	0.0124875	0.132586833	NA	NA
398	Syp	0	0	0.182239	0.154762	No	0.189815	0.082013	0.0770482	0.116292067	NA	NA
399	Xir3c	0.0106498	0.0136486	0.276716	0.09001055	No	0.0164502	0.0030303	0	0.0064935	NA	NA
400	Frdc3c1	0.00793651	0.3	0.0753968	0.09583333	No	0.00444143	0.047619	0.11746	0.05650681	NA	NA
401	Dcaf2l1	0	0	0.471132	0.11920346	No	0.02166395	0.00416667	0.00189394	0.00923337	NA	NA
402	Nr0b1	0	0	0.483401	0.12085025	No	NA	NA	NA	NA	NA	NA
403	Hccs	0.216432	0.125814	0.130193	0.122366	No	0.032781	0	0.00973312	0.014170407	NA	NA
404	Huwe1	0.140675	0.137837	0.201841	0.12273183	No	0.011595	0.00666219	0.00426326	0.007506817	NA	NA
405	Siltrk4	0	0.535714	0	0.1339285	No	NA	NA	NA	NA	NA	NA
406	Zxdb	0.166667	0.177778	0.199393	0.1359595	No	0	0	0.0035461	0.001182033	NA	NA
407	Xir3b	0.166667	0.112698	0.275506	0.14180523	No	0.0231971	0.010382	0.023837	0.0191387	NA	NA
408	Rpl10	0.501209	0.00168157	0.0831327	0.00267891	No	0.00100822	0.0023315	0.0017325	0.00169074	NA	NA
409	Wnk3-ps	0.156197	0.144377	0.216404	0.15216653	No	0.0840514	0.0714286	0.0897525	0.081744167	NA	NA
410	Cybb	0.5	0.0833333	0.0578431	0.1602941	No	0	0.08	0.153846	0.077948667	NA	NA
411	Snrk12	0.189906	0.190168	0.296071	0.16974648	No	0.0547015	0.0134742	0.00610254	0.024759413	NA	NA
412	C430049603Rik	0.204924	0.208696	0.222202	0.17124658	No	0.45148	0.479048	0.0254835	0.3186705	NA	NA
413	Kif4	0.276705	0.180026	0.26139	0.1811849	Yes	0.0114359	0	0.00749232	0.006309407	NA	NA
414	Fundc2	0.167901	0.158276	0.183419	0.21073225	No	0.16	0	0	0.053333333	NA	NA
415	Vgll1	0.285714	0.285714	0.354117	0.23138625	No	NA	NA	NA	NA	NA	NA
416	Fmr1	0.327519	0.321212	0.37997	0.262049383	No	0.0202703	0.0188437	0.0176991	0.0189377	NA	NA
417	Ahrgef9	0.348611	0.315873	0.4	0.266121	No	NA	NA	NA	NA	NA	NA
418	Zfp185	0.357143	0.333333	0.476107	0.103061	Yes	0.01131305	0.000653595	0	0.003989032	NA	NA
419	Rtoy4b	0.364865	0.351351	0.189189	0.33012475	No	0.282609	0.0333333	0.108108	0.1413501	NA	NA
420	Gspit2	0.484127	0.519886	0.483333	0.382659	No	0.0283184	0	0	0.009439467	NA	NA
421	Tro	0.384615	0.267857	0.333333	0.43395125	Yes	NA	NA	NA	NA	NA	NA
422	Lanc3	0.428571	0.4	0.48	0.45214275	Yes	1	1	1	1	NA	NA
423	Dynl3	1	1	1	1	Yes	1	1	1	1	NA	NA

ID	A	B		C		D		E		F		G		H		I		J		K		L		M		N	
	Gene Name	WT 1	Proportion Paternal-X Expression		WT 2	WT 3	Eed ^{0/11}	WT Average	Consistent Escape in WT?		Eed ^{-/-} 1	Proportion Paternal-X Expression		Eed ^{-/-} 2	Eed ^{-/-} 3	Eed ^{-/-} Average		Consistent escape in Eed ^{-/-} ?		WT vs. Eed ^{-/-} P Value (T Test)	Adjusted P Value						
424	LOC100503459	1	1	1	1	1	1	Yes	1	NA	1	NA	1	1	1	1	0.43257333	Yes	NA	NA	NA	NA	NA	NA	NA		
425	Mageb16-ps1	1	1	1	1	1	1	Yes	1	NA	NA	NA	NA	NA	NA	NA	0.43257333	Yes	NA	NA	NA	NA	NA	NA	NA		
426	Klf8	NA	NA	NA	NA	NA	NA	NA	0.275028	0.137086	0.437832	0.283315333	0.321042667	0.142857	0.321042667	0.142857	0.142857	Yes	NA	NA	NA	NA	NA	NA	NA		
427	Dgkk	NA	NA	NA	NA	NA	NA	NA	0.30303	0.517241	0.142857	0.321042667	0.142857	0.142857	0.321042667	0.142857	0.142857	Yes	NA	NA	NA	NA	NA	NA	NA		
428	38330403M18Rik	NA	NA	NA	NA	NA	NA	NA	0.161905	0.495437	0.157738	0.271693333	0.271693333	0.157738	0.271693333	0.157738	0.157738	Yes	NA	NA	NA	NA	NA	NA	NA		
429	Riox4f	NA	NA	NA	NA	NA	NA	NA	0.4	0.6	0.25	0.416666667	0.416666667	0.25	0.416666667	0.25	0.416666667	Yes	NA	NA	NA	NA	NA	NA	NA		
430	Slc38a5	NA	NA	NA	NA	NA	NA	NA	0.252747	0.547025	0.5	0.43257333	0.43257333	0.5	0.43257333	0.5	0.43257333	Yes	NA	NA	NA	NA	NA	NA	NA		
431	Gm5637	NA	NA	NA	NA	NA	NA	NA	1	1	0.333333	0.777777667	0.777777667	0.333333	0.777777667	0.333333	0.777777667	Yes	NA	NA	NA	NA	NA	NA	NA		
432	Reps2	NA	NA	NA	NA	NA	NA	NA	0.359524	0.62066	0.511492	0.49725333	0.49725333	0.511492	0.49725333	0.511492	0.49725333	Yes	NA	NA	NA	NA	NA	NA	NA		
433	LOC100503212	NA	NA	NA	NA	NA	NA	NA	0.755556	0.366667	0.640625	0.587616	0.587616	0.640625	0.587616	0.587616	0.640625	Yes	NA	NA	NA	NA	NA	NA	NA		
434	Gm9112	NA	NA	NA	NA	NA	NA	NA	0.4	0.376575	0.416654	0.397743	0.416654	0.397743	0.416654	0.397743	0.416654	Yes	NA	NA	NA	NA	NA	NA	NA		
435	4930524L23Rik	NA	NA	NA	NA	NA	NA	NA	0.614015	0.531263	0.450549	0.531942333	0.531942333	0.450549	0.531942333	0.450549	0.531942333	Yes	NA	NA	NA	NA	NA	NA	NA		
436	Foxp3	NA	NA	NA	NA	NA	NA	NA	0.452729	0.60061	0.547131	0.53349	0.53349	0.547131	0.53349	0.53349	0.547131	Yes	NA	NA	NA	NA	NA	NA	NA		
437	Gm614	NA	NA	NA	NA	NA	NA	NA	0.508929	0.6	0.8	0.636309667	0.636309667	0.8	0.636309667	0.8	0.636309667	Yes	NA	NA	NA	NA	NA	NA	NA		
438	Gm5946	NA	NA	NA	NA	NA	NA	NA	1	1	1	1	1	1	1	1	1	Yes	NA	NA	NA	NA	NA	NA	NA		
439	1700008105Rik	NA	NA	NA	NA	NA	NA	NA	0	0	0	0	0	0	0	0	0	No	NA	NA	NA	NA	NA	NA	NA		
440	Alas2	NA	NA	NA	NA	NA	NA	NA	0	0	0	0	0	0	0	0	0	No	NA	NA	NA	NA	NA	NA	NA		
441	Arhgap6	NA	NA	NA	NA	NA	NA	NA	0	0	0	0	0	0	0	0	0	No	NA	NA	NA	NA	NA	NA	NA		
442	Eda	NA	NA	NA	NA	NA	NA	NA	0	0	0	0	0	0	0	0	0	No	NA	NA	NA	NA	NA	NA	NA		
443	Fgf13	NA	NA	NA	NA	NA	NA	NA	0	0	0	0	0	0	0	0	0	No	NA	NA	NA	NA	NA	NA	NA		
444	Gm14685	NA	NA	NA	NA	NA	NA	NA	0	0	0	0	0	0	0	0	0	No	NA	NA	NA	NA	NA	NA	NA		
445	Gpr50	NA	NA	NA	NA	NA	NA	NA	0	0	0	0	0	0	0	0	0	No	NA	NA	NA	NA	NA	NA	NA		
446	Nudt10	NA	NA	NA	NA	NA	NA	NA	0	0	0	0	0	0	0	0	0	No	NA	NA	NA	NA	NA	NA	NA		
447	Ophn1	NA	NA	NA	NA	NA	NA	NA	0.266667	0.502404	0	0.256357	0.256357	0	0.256357	0	0.256357	No	NA	NA	NA	NA	NA	NA	NA		
448	Pcvt1b	NA	NA	NA	NA	NA	NA	NA	0.250615	0.428571	0	0.26395333	0.26395333	0	0.26395333	0	0.26395333	No	NA	NA	NA	NA	NA	NA	NA		
449	41157	NA	NA	NA	NA	NA	NA	NA	0.004329	0.202574	0	0.067668967	0.067668967	0	0.067668967	0	0.067668967	No	NA	NA	NA	NA	NA	NA	NA		
450	Slc9a7	NA	NA	NA	NA	NA	NA	NA	0.0714286	0	0.03125	0.0342262	0.0342262	0.03125	0.0342262	0.03125	0.0342262	No	NA	NA	NA	NA	NA	NA	NA		
451	Spln4	NA	NA	NA	NA	NA	NA	NA	0	0	0	0	0	0	0	0	0	No	NA	NA	NA	NA	NA	NA	NA		
452	Srpk3	NA	NA	NA	NA	NA	NA	NA	0	0	0	0	0	0	0	0	0	No	NA	NA	NA	NA	NA	NA	NA		
453	Xlf5b	NA	NA	NA	NA	NA	NA	NA	0.00601504	0	0	0.002005013	0.002005013	0	0.002005013	0	0.002005013	No	NA	NA	NA	NA	NA	NA	NA		
454	Gm648	NA	NA	NA	NA	NA	NA	NA	0.333333	0.320062	0.00924581	0.22088027	0.22088027	0.00924581	0.22088027	0.00924581	0.22088027	No	NA	NA	NA	NA	NA	NA	NA		
455	Iqg1bp2	NA	NA	NA	NA	NA	NA	NA	0.14426	0.100992	0.0416667	0.095639567	0.095639567	0.0416667	0.095639567	0.0416667	0.095639567	No	NA	NA	NA	NA	NA	NA	NA		
456	Zdhnc15	NA	NA	NA	NA	NA	NA	NA	0.0784671	0.049062	0.0555556	0.061028233	0.061028233	0.0555556	0.061028233	0.0555556	0.061028233	No	NA	NA	NA	NA	NA	NA	NA		
457	Dgkk-2	NA	NA	NA	NA	NA	NA	NA	0.511636	0.478093	0.0552249	0.348317967	0.348317967	0.0552249	0.348317967	0.0552249	0.348317967	No	NA	NA	NA	NA	NA	NA	NA		
458	Nhs12	NA	NA	NA	NA	NA	NA	NA	0.172009	0.117827	0.0757143	0.1218501	0.1218501	0.0757143	0.1218501	0.0757143	0.1218501	No	NA	NA	NA	NA	NA	NA	NA		

Table 5.4. SNP Locations and Primer Sequences for RT-PCR and Genomic PCR Amplicons.

Gene Name	SNP Location	129 Allele	JF1 Allele	RT-PCR Primer (Forward)	RT-PCR Primer (Reverse)	Genomic PCR Primer (Forward)	Genomic PCR Primer (Reverse)
Hdac6	chrX:7524355	A	C	GGCGGACTAGAAAAGAGCCT	CCCTTGAAAGCCCCACAACCTA	CCGGTCTGGGGACTAGAA	GAAGGGGTGACTGGGGATTG
Wdr13	chrX:7706230	A	G	AGTGGACCGGAGTTTCGG	CCCACACAGTGAGGTTGTT	TGTTGACTGGCTGGAAAGGTG	TCCCACAAATGGCTCCTTGG
Medl2	chrX:98488083	A	G	AGGTTACCAAACCTGTTGCCA	GCTGCTGCCGGTATACAGAT	CCATCAACACGACCACTGTC	CTTTTGGCTCCTCAGTGC
Pgk1	chrX:103393283	C	T	GAAAGGAAAGGGAAGATGC	TGTGCCAATCTCCAATGTTGT	CCATGGTGGGTGAAATCTGC	TAAACTGTCCCTCAGTTACCCCAT
Whp5	chrX:132780961	T	C	TTTGTACCGCCACAGGCTAA	GCTTGGTTAGCCTTCCAAC	TCAATGCATTCCTGTAATCTGC	GGATGGCTTCGGTTAGCCTT
Rnfl28	chrX:136199996	G	A	TGTGGACCCGTGGCTTTTAG	TAAGCACCTGGAGACAAACCC	TGGTAAAGCCAAATTCCTACCCC	GCATAGCCAGATGTGGTGC
C330007P06R1k	chrX:34403690	G	A	GGAGCTATGCCGAAAAGTCGT	GCTTCCAAATTCAGCCAACTCC	CCGCAACCCCAACAGTGAACATA	TGGTAAATTCCTTCCAGGAGTG
Apl11c	chrX:57496031	G	A	TGAAAAGGCAGCCCCATAACA	AAGATTCCGATTCTGGCACT	TGCCATGCCCATGGAAAAATG	GCCCCATTTTCTTGTTCCTTAC
Fam3a	chrX:71638049	A	G	TCCCTACACCCAGACAAACA	TCATTGACATCTCCAGCCCAC	ACAAAACAGTGACACCCAG	CTCACGAGGAACATGAGCCCTG
Rlim	chrX:101159081	C	T	GAGCCCCGATGAAAATAGAGC	GGTCGGCACTTCTGTTACTGC	GCTCTGTTTCTCCGATGCTC	TGAAACCATCCACTAGGCCGTC
Atrx	chrX:103042079	G	A	GGGATTGCTGCTGTGAGTCT	CCACCACTTCTTGCCATCT	CTGAAATCTCCCTCCACAGCC	GGGATTGCTGCTGTGAGTCT
Pdh1a	chrX:156562514	G	A	GGGACGCTCTGTTGAGAGAGC	GCACCTCAAAGGGAGGATCA	TAGCCCTGTGAGCCTTCAGA	GCTACCCTACTCCGAGAAGAA

Chapter 6: Concluding Thoughts and Future Directions

6-1: Summary of Findings and Recent Advances

Through my studies of early mouse embryos and stem cells, I find that current models are insufficient to explain the mechanisms underlying epigenetic regulation of the X-chromosomes in mammalian development. Using a combination of novel genetic and computational approaches, I evaluated the roles of both the Tsix non-coding RNA and the chromatin modifying complex Polycomb Repressive Complex 2 (PRC2) in X-chromosome inactivation. Both Tsix RNA and PRC2 had been postulated to be central players in the initiation of X-inactivation. My studies show that factors other than Tsix and PRC2 are involved in initiating the epigenetic fates of the two X-chromosomes. To identify these novel regulators, I developed an allele-specific RNA-seq approach.

I first characterized a spatially and temporally specific role for the Tsix lncRNA during imprinted and random X-inactivation (Chapters 2 and 3, (Gayen et al., 2015; Maclary et al., 2014)). I assessed the role of Tsix RNA in all steps of X-chromosome regulation in the developing mouse embryo, including initiation and maintenance of imprinted X-inactivation, X-chromosome reactivation in the epiblast precursor cells, and the initiation and maintenance of random X-inactivation (See Fig. 1.1). I found that, during both imprinted and random X-inactivation, Tsix is not required to repress induction of Xist RNA from the active-X chromosome in undifferentiated cells (Gayen et al., 2015; Maclary et al., 2014). I instead

identified a novel role for the Tsix lncRNA. I find that Tsix is required for the proper maintenance of X-inactivation patterns in differentiating cells that have undergone X-inactivation normally (Gayen et al., 2015; Maclary et al., 2014). Notably, these studies describe a novel role not just for Tsix, but for lncRNAs broadly, as most are postulated to be initiators of epigenetic transcriptional changes, not maintenance factors (Froberg et al., 2013; Lee, 2009).

Due to the timing of Tsix RNA expression in early embryonic development and the exclusive expression of Tsix from the maternal X-chromosome, Tsix RNA expression has been postulated to be the direct readout of the imprint that protects the maternal-X from inactivation in the developing embryo. By demonstrating that Tsix is dispensable for maintaining Xist repression in undifferentiated cells, including the cells of the blastocyst-stage mouse embryo, my analysis of imprinted X-inactivation indicates that the imprint that prevents inactivation of the maternal X-chromosome in the early embryo does not act through Tsix RNA (Chapter 2, (Maclary et al., 2014)). Classic studies of androgenetic and gynogenetic embryos indicate that this imprint resides on the maternally-inherited X-chromosome, as embryos harboring two maternal X-chromosomes are refractory to X-inactivation, while embryos harboring two paternal X-chromosomes initially induce Xist RNA from both X chromosomes (Gayen et al., 2015; Goto and Takagi, 2000; Kay et al., 1994; Maclary et al., 2014; Okamoto et al., 2000; Tada et al., 2000). The identity of this maternal imprint remains a topic of much interest in current studies. One recent evaluation of blastomeres from two-cell embryos identified antagonistic transcription of both Xist and Tsix from the same chromosome, including low-level Xist RNA transcription from the maternal-X (Deuve et al., 2015; Gayen et al., 2015; Maclary et al., 2014). The authors of this study suggest that this simultaneous sense/antisense transcription could be involved in establishment of the imprint through either recruitment of chromatin modifiers or production of

endo-siRNAs (Deuve et al., 2015; Gayen et al., 2015; Maclary et al., 2014). However, these findings do not elucidate what distinguishes the maternal-X from the paternal-X in the developing embryo. Another study of Xist RNA induction from transgenes in developing embryos shows evidence of imprinted Xist RNA induction from paternally-inherited transgenes is more robust when the transgene is unpaired in the male germline during meiosis (Gayen et al., 2015; Maclary et al., 2014; Sun et al., 2015). This suggests that the paternal germline somehow differentially marks hemizygous DNA, such as the X-chromosome, for imprinted expression. This model would suggest that, in embryos with two maternal X-chromosomes, X-inactivation does not initiate because the X-chromosomes lack permissive marks to trigger Xist induction. However, Xist RNA is not always induced from unpaired paternally-inherited transgenes in the embryos studied (Froberg et al., 2013; Lee, 2009; Sun et al., 2015). Any epigenetic marks established in the male germline, therefore, are not necessarily sufficient to trigger consistent, robust, Xist induction. The inconsistency of Xist transgene induction from hemizygous transgenes, coupled with prior observations from androgenetic and gynogenetic embryos, supports the hypothesis that the maternal germline is the source of the imprint. Thus, we favor a model where the oocyte marks the maternal-X with chromosome-wide histone modifications. These maternally established marks establish an open chromatin conformation, and ensure that genes along the maternal X-chromosome remain transcriptionally competent during early embryogenesis. An oocyte-established chromatin profile may mediate monoallelic Tsix induction, but alone would be sufficient to repress Xist during the initiation of imprinted X-inactivation in the early embryo independently of Tsix RNA.

I further show that Tsix RNA is dispensable for reactivation of the inactive-X in the inner cell mass of developing embryos (Chapter 2, (Maclary et al., 2014)); Alternative factors must be

responsible for Xist repression and subsequent X-linked gene reactivation in this cell lineage (Maclary et al., 2014). Tsix induction from the inactive-X is posited to contribute to Xist repression and to the transcriptional equality of the two Xs in pluripotent cells (Goto and Takagi, 2000; Kay et al., 1994; Navarro et al., 2009; 2010; Nesterova et al., 2011; Okamoto et al., 2000; Tada et al., 2000). However, X-chromosome reactivation occurs in Tsix-mutant epiblast precursor cells (Maclary et al., 2014; Payer et al., 2013). Numerous other factors are implicated in Xist repression and are thus candidates for mediating X-chromosome reactivation, including the pluripotency factors NANOG, OCT4, and SOX2. These pluripotency factors have been shown to bind within intron 1 of *Xist* in undifferentiated ES cells (Donohoe et al., 2009; Navarro et al., 2008; 2010; Nesterova et al., 2011). Pluripotency factors are particularly intriguing candidate regulators of X-inactivation, as overexpression of OCT4 and SOX2, in conjunction with KLF4 and C-MYC, can induce reprogramming of terminally differentiated cells into induced pluripotent stem cells (iPSCs), a process that includes reactivation of the inactive X-chromosome (reviewed in (Deuve and Avner, 2011; Pasque and Plath, 2015)). Notably, however, Xist RNA induction is not impeded by expression of NANOG, OCT4, and SOX2 in epiblast cells during random X-inactivation (Pfister et al., 2007), and the first intron of *Xist* that is bound by these pluripotency factors is dispensable during X-chromosome reactivation *in vitro* and *in vivo* (Minkovsky et al., 2013). Thus, though forced overexpression of pluripotency factors can trigger large-scale epigenetic reprogramming, these factors are not required *in vivo* for the epigenetic changes that mediate X-chromosome reactivation.

Beyond pluripotency factors, the reprogramming of iPSCs may be able to provide valuable insights into the epigenetic changes underlying X-chromosome reactivation and assist in identification of potential triggers of reactivation. During reprogramming, cells sequentially

induce the expression of CDH1, NANOG, ESRRB, DPPA4, and finally PECAM1, with X-chromosome reactivation occurring between induction of DPPA4 and PECAM1 (Pasque and Plath, 2015; Pasque et al., 2014). These proteins, or their downstream targets, may help to mediate X-chromosome reactivation. X-chromosome reactivation is also associated with loss of methylation, suggesting that active demethylation may contribute to X-chromosome reactivation; TET proteins, which catalyze the oxidation of 5-methylcytosine to 5-hydroxymethylcytosine, are thus intriguing candidate regulators of reactivation. TET1 and TET2 are postulated to be drivers of epigenetic reprogramming in primordial germ cells and during iPSC generation, both processes during which X-chromosome reactivation occurs (reviewed in (Hill et al., 2014)). Both Tet1 and Tet2, however, were recently shown to be dispensable during reprogramming of differentiated cells that are X-inactivated into iPSCs (Pasque et al., 2014). Thus, the TETs may not normally reactivate the inactive-X.

The germline factor PRDM14 was identified as another candidate regulator of X-chromosome reactivation based on its expression pattern, which is spatiotemporally correlated with X-chromosome reactivation, and that it is found to be involved with epigenetic reprogramming in primordial germ cells (Payer et al., 2013; Yamaji et al., 2008; 2013). Loss of PRDM14, however, leads to a slight reduction in the efficiency of X-chromosome reactivation, but does not abrogate reactivation entirely (Payer et al., 2013). It is clear from these studies that further work is required to identify the mechanisms that drive X-chromosome reactivation during embryonic development.

Finally, I show that Tsix appears to play no role in the counting or choice steps that characterize initiation of random X-chromosome inactivation (Chapter 3, (Gayen et al., 2015)). During the counting step, the cell senses the number of X-chromosomes present; if and only if

there are two or more X-chromosomes will X-inactivation proceed. In the choice step, the cell then selects one X-chromosome to silence. The absolute absence of Xist RNA coating and X-inactivation in undifferentiated $X^{\Delta Tsix}Y$ EpiSCs is evidence that the Tsix RNA is not part of the counting mechanism (Gayen et al., 2015). That biased X-inactivation in Tsix-heterozygous cells occurs through a secondary cell selection effect, rather than through primary inactivation of the $X^{\Delta Tsix}$ at the onset of X-inactivation, precludes a role for the Tsix RNA in X-chromosome choice (Gayen et al., 2015). If Tsix does not regulate X-chromosome counting or choice, then alternate mechanisms must explain why X-inactivation does not occur in males and does so randomly in females. Further studies of Tsix mutant embryos and stem cells have identified a sex-specific difference in ectopic Xist RNA induction ectopic X-linked gene silencing on the Tsix mutant X-chromosome (Gayen et al., 2016). These data implicate a dose-dependent X-linked factor in triggering both Xist RNA coating and X-inactivation in female cells.

One previously proposed X-linked trigger of X-inactivation is RNF12, an E3 ubiquitin ligase that lies within the X-inactivation center. RNF12 may be involved in initiation of imprinted X-inactivation, by functioning as a dose-dependent activator of Xist expression. In agreement, embryos harboring maternally-inherited mutations show reduced Xist RNA induction and ultimately die due to failure of extra-embryonic tissues (Shin et al., 2010). However, RNF12 is dispensable for random X-inactivation (Shin et al., 2014), and thus cannot play a critical role in X-chromosome counting and choice. Recent data point to an escaper of X-inactivation as the dose-dependent factor that regulates X-chromosome counting (Gayen et al., 2016). Mechanistic insights into the choice of the inactive X-chromosome could come through the characterization of strain-specific differences between mouse strains, as hybrid mice often show biases in X-

chromosome choice during random X-inactivation (Chadwick et al., 2006; Gayen et al., 2015; Maclary et al., 2014; Thorvaldsen et al., 2012).

In addition to my comprehensive study of the role of Tsix RNA in imprinted and random X-inactivation, I characterized the requirement for EED, a core subunit of PRC2, in imprinted X-inactivation (Chapter 5). PRC2 is a key chromatin modifying complex that is enriched on the inactive X-chromosome and catalyzes H3-K27me₃, a histone modification associated with a repressive chromatin state (Barski et al., 2007; Froberg et al., 2013; Kouzarides, 2007; Lee, 2009). Through RNA-seq of hybrid *Eed*^{-/-} TSC lines, I comprehensively evaluated allelic X-linked gene expression. Despite the absence of H3-K27me₃ and Xist RNA coating, in *Eed*^{-/-} TSCs, less than one-fifth of the X-linked genes are derepressed from the inactive X-chromosome in *Eed*^{-/-} TSCs. I find that derepressed genes in *Eed*^{-/-} TSCs display hallmarks of open chromatin and basal transcriptional activity from the inactive-X, while X-linked genes that are completely silenced are refractory to loss of EED, H3-K27me₃, and Xist RNA. This points to an intriguing new role for PRC2 in regulating gene expression, in which PRC2-catalyzed H3-K27me₃ may be responsible for minimizing the expression levels of basally transcribed genes without establishing stringent X-linked gene silencing.

Taken together, these data highlight many gaps in our current knowledge of the mechanisms that initiate epigenetic states in the developing embryo. Recent proteomic approaches have identified numerous proteins that interact with Xist, some of which are involved in X-linked gene silencing (Chu et al., 2015; McHugh et al., 2015; Minajigi et al., 2015). However, these proteins are recruited by, and thus act downstream, of Xist RNA. These proteins, however, may not be involved in initiation of X-inactivation, which encapsulates the induction of Xist itself. We hypothesize, based on evolutionary considerations and my recent work, that two

classes of X-linked gene may be of particular interest as putative initiators of X-inactivation: lncRNAs and escapers of X-inactivation (see discussion in Chapter 4-1, (Gayen et al., 2016; Jegalian and Page, 1998)). I postulate that lncRNAs specific to the inactive-X may function regionally to initiate X-linked gene silencing in an Xist-independent manner, and that escapers of X-inactivation play a dosage-sensitive role in establishing a permissive environment for X-linked gene silencing in female cells. I present a pipeline for identifying these novel factors in mouse stem cells and embryos using a strand-specific, allele-specific RNA-seq approach (Chapter 4). This approach allows for both allele-specific analysis and novel transcript discovery, and permits evaluation of both known and novel *cis* and *trans*-acting factors, which I will characterize as part of future studies.

6-2: Current Work and Future Directions

Prior studies have sought to assess escape from X-inactivation in a variety of tissues (Berletch et al., 2015b; Calabrese et al., 2012; Yang et al., 2010). For many genes, escape from X-inactivation varies in different cell types. These studies have, however, identified a core group of dosage-sensitive regulators that appear to escape X-inactivation across tissue types, many of which still have functional homologs on the mammalian Y-chromosome (Bellott et al., 2014; Berletch et al., 2010; Calabrese et al., 2012; Yang et al., 2010). The genes that consistently escape X-inactivation in multiple cell lineages are prime candidates as regulators of X-inactivation. In addition, I have begun to comprehensively identify genes that escape X-inactivation in all cell lineages derived from the early mouse embryo: TSCs, XEN cells, and EpiSCs. I am able to identify both genes that escape in all cell lineages, and genes that show cell-type specific escape. I have also preliminarily identified a subset of genes that show strain-

specific escape from X-inactivation. These genes are expressed from the inactive-X in only in cell lines where the X-chromosome from a permissive strain is inactivated; In hybrid crosses from 129/S1 and JF1 mouse strains, I have identified both genes that escape X-inactivation only when the 129/S1 derived X is inactivated and genes that escape X-inactivation only when the JF1-derived X is inactivated. One gene of particular interest is *Zfx*, which escapes X-inactivation only when the 129/S1 strain is the inactive-X. *Zfx* is known to escape X-inactivation in humans, but prior studies in mice indicate that it does not escape X-inactivation (Adler et al., 1991; Schneider-Gädicke et al., 1989). I am currently confirming and characterizing strain-specific escape of *Zfx* using RT-PCR and RNA FISH analysis of stem cells and embryos.

Through RNA-sequencing analysis, I have also begun to identify novel non-coding RNAs that may function as putative regulators of X-inactivation. Current work aims to compare and contrast expression of novel lncRNAs between cell types and identify novel transcripts expressed across different lineages. Following computational characterization of novel non-coding RNAs, I aim to confirm their expression patterns by RT-PCR and RNA FISH. Future work will characterize the function of novel inactive-X specific non-coding RNAs in X-inactivation by knocking down or knocking out these transcripts in mouse cell lines.

I am also continuing to leverage allele-specific RNA-seq approaches to characterize the effects of mutations in known regulators of X-inactivation. In addition to sequencing of *Eed*^{-/-} TSCs (see Chapter 5), I have performed RNA-seq on *Eed*^{-/-} XEN cells. Intriguingly, preliminary analysis of EED mutant XEN cells suggests that X-linked gene silencing defects in the primitive endoderm lineage are even milder than those observed in the trophectodermal lineage (Clair Harris and Emily Maclary, unpublished data). Whereas my analysis of *Eed*^{-/-} TSCs suggests gene-intrinsic properties are responsible for susceptibility to EED loss, this preliminary data in

XEN cells indicates that the genes susceptible to reactivation respond differently in different cell types. These divergent responses between cell types may be due to differential expression of key regulators, or changes in chromatin context. Future experiments will focus on comparison of gene expression in wild-type and *Eed*^{-/-} TSCs and XEN cells, with the goal of identifying the differences in transcriptional profile that render XEN cells unresponsive to loss of EED, though a subset of genes in TSCs are affected. In conjunction with my recent work on *Eed*^{-/-} stem cells, additional work in the lab has utilized genetic approaches to dissect the specific roles of individual components of PRC2 during initiation of X-inactivation *in vivo*, by examining blastocyst stage embryos. To complement this work, we aim to complete RNA-seq analysis of individual blastocyst-stage embryos harboring mutations in *Eed*, *Ezh2*, or *Ezh1* and provide a chromosome-wide picture of any X-inactivation defects in mutant embryos.

Through these transcriptomic analyses of stem cells and early embryos, I plan to identify and characterize novel regulators of X-linked gene silencing. I anticipate that these studies will lend insight into the mechanisms that regulate X-chromosome inactivation and, in turn, assist in our understanding of the cellular processes that underlie epigenetic regulation broadly, in both development and disease.

References

- Adler, D.A., Bressler, S.L., Chapman, V.M., Page, D.C., and Disteché, C.M. (1991). Inactivation of the *Zfx* gene on the mouse X chromosome. *Proc. Natl. Acad. Sci. U.S.A.* 88, 4592–4595.
- Anders, S., Pyl, P.T., and Huber, W. (2015). HTSeq--a Python framework to work with high-throughput sequencing data. *Bioinformatics* 31, 166–169.
- Andrews, S. (2010). FastQC: A quality control tool for high throughput sequence data. Reference Source.
- Anguera, M.C., Ma, W., Clift, D., Namekawa, S., Kelleher, R.J., and Lee, J.T. (2011). *Tsx* produces a long noncoding RNA and has general functions in the germline, stem cells, and brain. *PLoS Genet.* 7, e1002248.
- Augui, S., Nora, E.P., and Heard, E. (2011). Regulation of X-chromosome inactivation by the X-inactivation centre. *Nat. Rev. Genet.* 12, 429–442.
- Avner, P., and Heard, E. (2001). X-chromosome inactivation: counting, choice and initiation. *Nat. Rev. Genet.* 2, 59–67.
- Balaton, B.P., Cotton, A.M., and Brown, C.J. (2015). Derivation of consensus inactivation status for X-linked genes from genome-wide studies. *Biol Sex Differ* 6, 35.
- Barakat, T.S., and Gribnau, J. (2012). X chromosome inactivation in the cycle of life. *Development* 139, 2085–2089.
- Barakat, T.S., Gunhanlar, N., Pardo, C.G., Achame, E.M., Ghazvini, M., Boers, R., Kenter, A., Rentmeester, E., Grootegoed, J.A., and Gribnau, J. (2011). RNF12 activates Xist and is essential for X chromosome inactivation. *PLoS Genet.* 7, e1002001.
- Baranov, V.S. (1983). Chromosomal control of early embryonic development in mice. II. Experiments on embryos with structural aberrations of autosomes 7, 9, 14 and 17. *Genet. Res.* 41, 227–239.
- Barlow, D.P. (2011). Genomic imprinting: a mammalian epigenetic discovery model. *Annu. Rev. Genet.* 45, 379–403.
- Barski, A., Cuddapah, S., Cui, K., Roh, T.-Y., Schones, D.E., Wang, Z., Wei, G., Chepelev, I., and Zhao, K. (2007). High-resolution profiling of histone methylations in the human genome. *Cell* 129, 823–837.
- Bartholdi, D., Krajewska-Walasek, M., Ounap, K., Gaspar, H., Chrzanowska, K.H., Ilyana, H., Kayserili, H., Lurie, I.W., Schinzel, A., and Baumer, A. (2009). Epigenetic mutations of the

imprinted IGF2-H19 domain in Silver-Russell syndrome (SRS): results from a large cohort of patients with SRS and SRS-like phenotypes. *J. Med. Genet.* *46*, 192–197.

Bellott, D.W., Hughes, J.F., Skaletsky, H., Brown, L.G., Pyntikova, T., Cho, T.-J., Koutseva, N., Zaghul, S., Graves, T., Rock, S., et al. (2014). Mammalian Y chromosomes retain widely expressed dosage-sensitive regulators. *Nature* *508*, 494–499.

Berletch, J.B., Ma, W., Yang, F., Shendure, J., Noble, W.S., Disteche, C.M., and Deng, X. (2015a). Escape from X inactivation varies in mouse tissues. *PLoS Genet.* *11*, e1005079.

Berletch, J.B., Ma, W., Yang, F., Shendure, J., Noble, W.S., Disteche, C.M., and Deng, X. (2015b). Identification of genes escaping X inactivation by allelic expression analysis in a novel hybrid mouse model. *Data Brief* *5*, 761–769.

Berletch, J.B., Yang, F., and Disteche, C.M. (2010). Escape from X inactivation in mice and humans. *Genome Biol.* *11*, 213.

Bernemann, C., Greber, B., Ko, K., Sternecker, J., Han, D.W., Araúzo-Bravo, M.J., and Schöler, H.R. (2011). Distinct developmental ground states of epiblast stem cell lines determine different pluripotency features. *Stem Cells* *29*, 1496–1503.

BEUTLER, E., YEH, M., and FAIRBANKS, V.F. (1962). The normal human female as a mosaic of X-chromosome activity: studies using the gene for C-6-PD-deficiency as a marker. *Proc. Natl. Acad. Sci. U.S.A.* *48*, 9–16.

Bonasio, R., Tu, S., and Reinberg, D. (2010). Molecular signals of epigenetic states. *Science* *330*, 612–616.

Borodina, T., Adjaye, J., and Sultan, M. (2011). A strand-specific library preparation protocol for RNA sequencing. *Meth. Enzymol.* *500*, 79–98.

Borsani, G., Tonlorenzi, R., Simmler, M.C., Dandolo, L., Arnaud, D., Capra, V., Grompe, M., Pizzuti, A., Muzny, D., Lawrence, C., et al. (1991). Characterization of a murine gene expressed from the inactive X chromosome. *Nature* *351*, 325–329.

Brockdorff, N., Ashworth, A., Kay, G.F., Cooper, P., Smith, S., McCabe, V.M., Norris, D.P., Penny, G.D., Patel, D., and Rastan, S. (1991). Conservation of position and exclusive expression of mouse Xist from the inactive X chromosome. *Nature* *351*, 329–331.

Brockdorff, N. (2011). Chromosome silencing mechanisms in X-chromosome inactivation: unknown unknowns. *Development* *138*, 5057–5065.

Brockdorff, N. (2013). Noncoding RNA and Polycomb recruitment. *Rna* *19*, 429–442.

Brons, I.G.M., Smithers, L.E., Trotter, M.W.B., Rugg-Gunn, P., Sun, B., Chuva de Sousa Lopes, S.M., Howlett, S.K., Clarkson, A., Ahrlund-Richter, L., Pedersen, R.A., et al. (2007). Derivation of pluripotent epiblast stem cells from mammalian embryos. *Nature* *448*, 191–195.

- Brown, C.J., and Willard, H.F. (1994). The human X-inactivation centre is not required for maintenance of X-chromosome inactivation. *Nature* 368, 154–156.
- Brown, C.J., Ballabio, A., Rupert, J.L., Lafreniere, R.G., Grompe, M., Tonlorenzi, R., and Willard, H.F. (1991a). A gene from the region of the human X inactivation centre is expressed exclusively from the inactive X chromosome. *Nature* 349, 38–44.
- Brown, C.J., Hendrich, B.D., Rupert, J.L., Lafreniere, R.G., Xing, Y., Lawrence, J., and Willard, H.F. (1992). The human XIST gene: analysis of a 17 kb inactive X-specific RNA that contains conserved repeats and is highly localized within the nucleus. *Cell* 71, 527–542.
- Brown, C.J., Lafreniere, R.G., Powers, V.E., Sebastio, G., Ballabio, A., Pettigrew, A.L., Ledbetter, D.H., Levy, E., Craig, I.W., and Willard, H.F. (1991b). Localization of the X inactivation centre on the human X chromosome in Xq13. *Nature* 349, 82–84.
- Brown, S.D. (1991). XIST and the mapping of the X chromosome inactivation centre. *Bioessays* 13, 607–612.
- Buecker, C., Srinivasan, R., Wu, Z., Calo, E., Acampora, D., Faial, T., Simeone, A., Tan, M., Swigut, T., and Wysocka, J. (2014). Reorganization of enhancer patterns in transition from naive to primed pluripotency. *Cell Stem Cell* 14, 838–853.
- Calabrese, J.M., Sun, W., Song, L., Mugford, J.W., Williams, L., Yee, D., Starmer, J., Mieczkowski, P., Crawford, G.E., and Magnuson, T. (2012). Site-specific silencing of regulatory elements as a mechanism of x inactivation. *Cell* 151, 951–963.
- Campos, E.I., Stafford, J.M., and Reinberg, D. (2014). Epigenetic inheritance: histone bookmarks across generations. *Trends Cell Biol.* 24, 664–674.
- Cao, R., Wang, L., Wang, H., Xia, L., Erdjument-Bromage, H., Tempst, P., Jones, R.S., and Zhang, Y. (2002). Role of histone H3 lysine 27 methylation in Polycomb-group silencing. *Science* 298, 1039–1043.
- Carrel, L., and Willard, H.F. (2005). X-inactivation profile reveals extensive variability in X-linked gene expression in females. *Nature* 434, 400–404.
- Chadwick, L.H., Pertz, L.M., Broman, K.W., Bartolomei, M.S., and Willard, H.F. (2006). Genetic control of X chromosome inactivation in mice: definition of the Xce candidate interval. *Genetics* 173, 2103–2110.
- Chan, K.M., Zhang, H., Malureanu, L., van Deursen, J., and Zhang, Z. (2011). Diverse factors are involved in maintaining X chromosome inactivation. *Proc. Natl. Acad. Sci. U.S.A.* 108, 16699–16704.
- Changolkar, L.N., Costanzi, C., Leu, N.A., Chen, D., McLaughlin, K.J., and Pehrson, J.R. (2007). Developmental changes in histone macroH2A1-mediated gene regulation. *Mol. Cell Biol.* 27, 2758–2764.

- Chaumeil, J., Le Baccon, P., Wutz, A., and Heard, E. (2006). A novel role for Xist RNA in the formation of a repressive nuclear compartment into which genes are recruited when silenced. *Genes Dev.* *20*, 2223–2237.
- Chu, C., Zhang, Q.C., da Rocha, S.T., Flynn, R.A., Bharadwaj, M., Calabrese, J.M., Magnuson, T., Heard, E., and Chang, H.Y. (2015). Systematic discovery of Xist RNA binding proteins. *Cell* *161*, 404–416.
- Chureau, C., Chantalat, S., Romito, A., Galvani, A., Duret, L., Avner, P., and Rougeulle, C. (2011). Ftx is a non-coding RNA which affects Xist expression and chromatin structure within the X-inactivation center region. *Hum. Mol. Genet.* *20*, 705–718.
- Clemson, C.M., McNeil, J.A., Willard, H.F., and Lawrence, J.B. (1996). XIST RNA paints the inactive X chromosome at interphase: evidence for a novel RNA involved in nuclear/chromosome structure. *J. Cell Biol.* *132*, 259–275.
- Clerc, P., and Avner, P. (1998). Role of the region 3' to Xist exon 6 in the counting process of X-chromosome inactivation. *Nat. Genet.* *19*, 249–253.
- Cohen, D.E., Davidow, L.S., Erwin, J.A., Xu, N., Warshawsky, D., and Lee, J.T. (2007). The DXPas34 repeat regulates random and imprinted X inactivation. *Dev. Cell* *12*, 57–71.
- Coolon, J.D., Stevenson, K.R., McManus, C.J., Graveley, B.R., and Wittkopp, P.J. (2012). Genomic imprinting absent in *Drosophila melanogaster* adult females. *Cell Rep* *2*, 69–75.
- Corbel, C., Diabangouaya, P., Gendrel, A.-V., Chow, J.C., and Heard, E. (2013). Unusual chromatin status and organization of the inactive X chromosome in murine trophoblast giant cells. *Development* *140*, 861–872.
- Cortez, D., Marin, R., Toledo-Flores, D., Froidevaux, L., Liechti, A., Waters, P.D., Grützner, F., and Kaessmann, H. (2014). Origins and functional evolution of Y chromosomes across mammals. *Nature* *508*, 488–493.
- Costanzi, C., and Pehrson, J.R. (1998). Histone macroH2A1 is concentrated in the inactive X chromosome of female mammals. *Nature* *393*, 599–601.
- Cotton, A.M., Ge, B., Light, N., Adoue, V., Pastinen, T., and Brown, C.J. (2013). Analysis of expressed SNPs identifies variable extents of expression from the human inactive X chromosome. *Genome Biol.* *14*, R122.
- Csankovszki, G., Panning, B., Bates, B., Pehrson, J.R., and Jaenisch, R. (1999). Conditional deletion of Xist disrupts histone macroH2A localization but not maintenance of X inactivation. *Nat. Genet.* *22*, 323–324.
- Cunningham, F., Amode, M.R., Barrell, D., Beal, K., Billis, K., Brent, S., Carvalho-Silva, D., Clapham, P., Coates, G., Fitzgerald, S., et al. (2015). Ensembl 2015. *Nucleic Acids Res.* *43*, D662–D669.

- Czermin, B., Melfi, R., McCabe, D., Seitz, V., Imhof, A., and Pirrotta, V. (2002). Drosophila enhancer of Zeste/ESC complexes have a histone H3 methyltransferase activity that marks chromosomal Polycomb sites. *Cell* *111*, 185–196.
- Danecek, P., Auton, A., Abecasis, G., Albers, C.A., Banks, E., DePristo, M.A., Handsaker, R.E., Lunter, G., Marth, G.T., Sherry, S.T., et al. (2011). The variant call format and VCFtools. *Bioinformatics* *27*, 2156–2158.
- Davidow, L.S., Breen, M., Duke, S.E., Samollow, P.B., McCarrey, J.R., and Lee, J.T. (2007). The search for a marsupial XIC reveals a break with vertebrate synteny. *Chromosome Res.* *15*, 137–146.
- Debrand, E., Chureau, C., Arnaud, D., Avner, P., and Heard, E. (1999). Functional analysis of the DXPas34 locus, a 3' regulator of Xist expression. *Mol. Cell. Biol.* *19*, 8513–8525.
- Degner, J.F., Marioni, J.C., Pai, A.A., Pickrell, J.K., Nkadori, E., Gilad, Y., and Pritchard, J.K. (2009). Effect of read-mapping biases on detecting allele-specific expression from RNA-sequencing data. *Bioinformatics* *25*, 3207–3212.
- Delaval, K., and Feil, R. (2004). Epigenetic regulation of mammalian genomic imprinting. *Curr. Opin. Genet. Dev.* *14*, 188–195.
- Deng, X., and Disteche, C.M. (2010). Genomic responses to abnormal gene dosage: the X chromosome improved on a common strategy. *PLoS Biol.* *8*, e1000318.
- Deng, X., Hiatt, J.B., Nguyen, D.K., Ercan, S., Sturgill, D., Hillier, L.W., Schlesinger, F., Davis, C.A., Reinke, V.J., Gingeras, T.R., et al. (2011). Evidence for compensatory upregulation of expressed X-linked genes in mammals, *Caenorhabditis elegans* and *Drosophila melanogaster*. *Nat. Genet.* *43*, 1179–1185.
- Denisenko, O., Shnyreva, M., Suzuki, H., and Bomsztyk, K. (1998). Point mutations in the WD40 domain of Eed block its interaction with Ezh2. *Mol. Cell. Biol.* *18*, 5634–5642.
- Deuve, J.L., and Avner, P. (2011). The Coupling of X-Chromosome Inactivation to Pluripotency. *Annu. Rev. Cell Dev. Biol.* *27*, 611–629.
- Deuve, J.L., Bonnet-Garnier, A., Beaujean, N., Avner, P., and Morey, C. (2015). Antagonist Xist and Tsix co-transcription during mouse oogenesis and maternal Xist expression during pre-implantation development calls into question the nature of the maternal imprint on the X chromosome. *Epigenetics* *10*, 931–942.
- Deys, B.F., Grzeschick, K.H., Grzeschick, A., Jaffé, E.R., and Siniscalco, M. (1972). Human phosphoglycerate kinase and inactivation of the X chromosome. *Science* *175*, 1002–1003.
- Di Croce, L., and Helin, K. (2013). Transcriptional regulation by Polycomb group proteins. *Nat. Struct. Mol. Biol.* *20*, 1147–1155.
- Disteche, C.M. (2012). Dosage compensation of the sex chromosomes. *Annu. Rev. Genet.* *46*,

537–560.

Dixon, J.R., Selvaraj, S., Yue, F., Kim, A., Li, Y., Shen, Y., Hu, M., Liu, J.S., and Ren, B. (2012). Topological domains in mammalian genomes identified by analysis of chromatin interactions. *Nature* *485*, 376–380.

Dobin, A., and Gingeras, T.R. (2015). Mapping RNA-seq Reads with STAR. *Curr Protoc Bioinformatics* *51*, 11.14.1–11.14.19.

Dobin, A., Davis, C.A., Schlesinger, F., Drenkow, J., Zaleski, C., Jha, S., Batut, P., Chaisson, M., and Gingeras, T.R. (2013). STAR: ultrafast universal RNA-seq aligner. *Bioinformatics* *29*, 15–21.

Donohoe, M.E., Silva, S.S., Pinter, S.F., Xu, N., and Lee, J.T. (2009). The pluripotency factor Oct4 interacts with Ctf and also controls X-chromosome pairing and counting. *Nature* *460*, 128–132.

Eicher, E.M., Nesbitt, M.N., and Francke, U. (1972). Cytological identification of the chromosomes involved in Searle's translocation and the location of the centromere in the X chromosome of the mouse. *Genetics* *71*, 643–648.

ENCODE Project Consortium, Birney, E., Stamatoyannopoulos, J.A., Dutta, A., Guigó, R., Gingeras, T.R., Margulies, E.H., Weng, Z., Snyder, M., Dermitzakis, E.T., et al. (2007). Identification and analysis of functional elements in 1% of the human genome by the ENCODE pilot project. *Nature* *447*, 799–816.

Engström, P.G., Steijger, T., Sipos, B., Grant, G.R., Kahles, A., Räscher, G., Goldman, N., Hubbard, T.J., Harrow, J., Guigó, R., et al. (2013). Systematic evaluation of spliced alignment programs for RNA-seq data. *Nat. Methods* *10*, 1185–1191.

Erhardt, S., Su, I.-H., Schneider, R., Barton, S., Bannister, A.J., Perez-Burgos, L., Jenuwein, T., Kouzarides, T., Tarakhovskiy, A., and Surani, M.A. (2003). Consequences of the depletion of zygotic and embryonic enhancer of zeste 2 during preimplantation mouse development. *Development* *130*, 4235–4248.

Finn, E.H., Smith, C.L., Rodriguez, J., Sidow, A., and Baker, J.C. (2014). Maternal bias and escape from X chromosome imprinting in the midgestation mouse placenta. *Dev. Biol.* *390*, 80–92.

Froberg, J.E., Yang, L., and Lee, J.T. (2013). Guided by RNAs: X-inactivation as a model for lncRNA function. *J. Mol. Biol.* *425*, 3698–3706.

Gardner, R.L., and LYON, M.F. (1971). X chromosome inactivation studied by injection of a single cell into the mouse blastocyst. *Nature* *231*, 385–386.

Gayen, S., Maclary, E., Buttigieg, E., Hinten, M., and Kalantry, S. (2015). A Primary Role for the Tsix lncRNA in Maintaining Random X-Chromosome Inactivation. *Cell Rep* *11*, 1251–1265.

- Gayen, S., Maclary, E., Hinten, M., and Kalantry, S. (2016). Sex-specific silencing of X-linked genes by Xist RNA. *Proc. Natl. Acad. Sci. U.S.A.* *113*, E309–E318.
- Gieni, R.S., and Hendzel, M.J. (2009). Polycomb group protein gene silencing, non-coding RNA, stem cells, and cancer. *Biochem. Cell Biol.* *87*, 711–746.
- Gontan, C., Achame, E.M., Demmers, J., Barakat, T.S., Rentmeester, E., van IJcken, W., Grootegeod, J.A., and Gribnau, J. (2012). RNF12 initiates X-chromosome inactivation by targeting REX1 for degradation. *Nature* *485*, 386–390.
- Goto, Y., and Takagi, N. (2000). Maternally inherited X chromosome is not inactivated in mouse blastocysts due to parental imprinting. *Chromosome Res.* *8*, 101–109.
- Graves, J.A., and Schmidt, M.M. (1992). Mammalian sex chromosomes: design or accident? *Curr. Opin. Genet. Dev.* *2*, 890–901.
- Grumbach, M.M., Morishima, A., and Taylor, J.H. (1963). HUMAN SEX CHROMOSOME ABNORMALITIES IN RELATION TO DNA REPLICATION AND HETEROCHROMATINIZATION. *Proc. Natl. Acad. Sci. U.S.A.* *49*, 581–589.
- Guttman, M., Garber, M., Levin, J.Z., Donaghey, J., Robinson, J., Adiconis, X., Fan, L., Koziol, M.J., Gnirke, A., Nusbaum, C., et al. (2010). Ab initio reconstruction of cell type-specific transcriptomes in mouse reveals the conserved multi-exonic structure of lincRNAs. *Nat. Biotechnol.* *28*, 503–510.
- Hadjantonakis, A.K., Cox, L.L., Tam, P.P., and Nagy, A. (2001). An X-linked GFP transgene reveals unexpected paternal X-chromosome activity in trophoblastic giant cells of the mouse placenta. *Genesis* *29*, 133–140.
- Hall, L.L., and Lawrence, J.B. (2003). The cell biology of a novel chromosomal RNA: chromosome painting by XIST/Xist RNA initiates a remodeling cascade. *Semin Cell Dev Biol* *14*, 369–378.
- Han, D.W., Greber, B., Wu, G., Tapia, N., Araúzo-Bravo, M.J., Ko, K., Bernemann, C., Stehling, M., and Schöler, H.R. (2011). Direct reprogramming of fibroblasts into epiblast stem cells. *Nat. Cell Biol.* *13*, 66–71.
- Han, Z., Xing, X., Hu, M., Zhang, Y., Liu, P., and Chai, J. (2007). Structural basis of EZH2 recognition by EED. *Structure* *15*, 1306–1315.
- Hansen, K.H., Bracken, A.P., Pasini, D., Dietrich, N., Gehani, S.S., Monrad, A., Rappsilber, J., Lerdrup, M., and Helin, K. (2008). A model for transmission of the H3K27me3 epigenetic mark. *Nat. Cell Biol.* *10*, 1291–1300.
- Hasegawa, Y., Brockdorff, N., Kawano, S., Tsutui, K., Tsutui, K., and Nakagawa, S. (2010). The matrix protein hnRNP U is required for chromosomal localization of Xist RNA. *Dev. Cell* *19*, 469–476.

- Hayashi, K., Ohta, H., Kurimoto, K., Aramaki, S., and Saitou, M. (2011). Reconstitution of the mouse germ cell specification pathway in culture by pluripotent stem cells. *Cell* *146*, 519–532.
- Heard, E., Kress, C., Mongelard, F., Courtier, B., Rougeulle, C., Ashworth, A., Vourc'h, C., Babinet, C., and Avner, P. (1996). Transgenic mice carrying an Xist-containing YAC. *Hum. Mol. Genet.* *5*, 441–450.
- Heard, E., Mongelard, F., Arnaud, D., and Avner, P. (1999). Xist yeast artificial chromosome transgenes function as X-inactivation centers only in multicopy arrays and not as single copies. *Mol. Cell. Biol.* *19*, 3156–3166.
- Hill, P.W.S., Amouroux, R., and Hajkova, P. (2014). DNA demethylation, Tet proteins and 5-hydroxymethylcytosine in epigenetic reprogramming: an emerging complex story. *Genomics* *104*, 324–333.
- Hinten, M., Maclary, E., Gayen, S., Harris, C., and Kalantry, S. (2016). Visualizing Long Noncoding RNAs on Chromatin. *Methods Mol. Biol.* *1402*, 147–164.
- Hogan, B., Beddington, R., Costantini, F., and Lacy, E. (1999). *Manipulating the mouse embryo. 1994 (A Laboratory Manual.: Cold Spring ...)*.
- Hoki, Y., Kimura, N., Kanbayashi, M., Amakawa, Y., Ohhata, T., Sasaki, H., and Sado, T. (2009). A proximal conserved repeat in the Xist gene is essential as a genomic element for X-inactivation in mouse. *Development* *136*, 139–146.
- Hore, T.A., Koina, E., Wakefield, M.J., and Marshall Graves, J.A. (2007). The region homologous to the X-chromosome inactivation centre has been disrupted in marsupial and monotreme mammals. *Chromosome Res.* *15*, 147–161.
- Hung, T., and Chang, H.Y. (2010). Long noncoding RNA in genome regulation: prospects and mechanisms. *RNA Biol* *7*, 582–585.
- Jegalian, K., and Page, D.C. (1998). A proposed path by which genes common to mammalian X and Y chromosomes evolve to become X inactivated. *Nature* *394*, 776–780.
- Jiang, J., Jing, Y., Cost, G.J., Chiang, J.-C., Kolpa, H.J., Cotton, A.M., Carone, D.M., Carone, B.R., Shivak, D.A., Guschin, D.Y., et al. (2013). Translating dosage compensation to trisomy 21. *Nature* *500*, 296–300.
- Johnston, C.M., Newall, A.E.T., Brockdorff, N., and Nesterova, T.B. (2002). Enox, a novel gene that maps 10 kb upstream of Xist and partially escapes X inactivation. *Genomics* *80*, 236–244.
- Johnston, P.G., and Cattanach, B.M. (1981). Controlling elements in the mouse. IV. Evidence of non-random X-inactivation. *Genet. Res.* *37*, 151–160.
- Jonkers, I., Barakat, T.S., Achame, E.M., Monkhorst, K., Kenter, A., Rentmeester, E., Grosveld, F., Grootegoed, J.A., and Gribnau, J. (2009). RNF12 is an X-Encoded dose-dependent activator of X chromosome inactivation. *Cell* *139*, 999–1011.

- Jonkers, I., Monkhorst, K., Rentmeester, E., Grootegoed, J.A., Grosveld, F., and Gribnau, J. (2008). Xist RNA is confined to the nuclear territory of the silenced X chromosome throughout the cell cycle. *Mol. Cell. Biol.* 28, 5583–5594.
- Kalakonda, N., Fischle, W., Boccuni, P., Gurvich, N., Hoya-Arias, R., Zhao, X., Miyata, Y., Macgrogan, D., Zhang, J., Sims, J.K., et al. (2008). Histone H4 lysine 20 monomethylation promotes transcriptional repression by L3MBTL1. *Oncogene* 27, 4293–4304.
- Kalantry, S. (2011). Recent advances in X-chromosome inactivation. *J. Cell. Physiol.* 226, 1714–1718.
- Kalantry, S., and Magnuson, T. (2006). The Polycomb group protein EED is dispensable for the initiation of random X-chromosome inactivation. *PLoS Genet.* 2, e66.
- Kalantry, S., Mills, K.C., Yee, D., Otte, A.P., Panning, B., and Magnuson, T. (2006). The Polycomb group protein Eed protects the inactive X-chromosome from differentiation-induced reactivation. *Nat. Cell Biol.* 8, 195–202.
- Kalantry, S., Purushothaman, S., Bowen, R.B., Starmer, J., and Magnuson, T. (2009). Evidence of Xist RNA-independent initiation of mouse imprinted X-chromosome inactivation. *Nature* 460, 647–651.
- Karachentsev, D., Sarma, K., Reinberg, D., and Steward, R. (2005). PR-Set7-dependent methylation of histone H4 Lys 20 functions in repression of gene expression and is essential for mitosis. *Genes Dev.* 19, 431–435.
- Kattamis, C.A. (1967). Glucose-6-phosphate dehydrogenase deficiency in female heterozygotes and the X-inactivation hypothesis. *Acta Paediatr Scand Suppl* 172:103–.
- Kay, G.F., Barton, S.C., Surani, M.A., and Rastan, S. (1994). Imprinting and X chromosome counting mechanisms determine Xist expression in early mouse development. *Cell* 77, 639–650.
- Keane, T.M., Goodstadt, L., Danecek, P., White, M.A., Wong, K., Yalcin, B., Heger, A., Agam, A., Slater, G., Goodson, M., et al. (2011). Mouse genomic variation and its effect on phenotypes and gene regulation. *Nature* 477, 289–294.
- Keer, J.T., Hamvas, R.M., Brockdorff, N., Page, D., Rastan, S., and Brown, S.D. (1990). Genetic mapping in the region of the mouse X-inactivation center. *Genomics* 7, 566–572.
- Kohlmaier, A., Savarese, F., Lachner, M., Martens, J., Jenuwein, T., and Wutz, A. (2004). A chromosomal memory triggered by Xist regulates histone methylation in X inactivation. *PLoS Biol.* 2, E171.
- Kong, L., Zhang, Y., Ye, Z.-Q., Liu, X.-Q., Zhao, S.-Q., Wei, L., and Gao, G. (2007). CPC: assess the protein-coding potential of transcripts using sequence features and support vector machine. *Nucleic Acids Res.* 35, W345–W349.
- Kouzarides, T. (2007). Chromatin modifications and their function. *Cell* 128, 693–705.

- Kreutz, M., Schock, G., Kaiser, J., Hochstein, N., and Peist, R. (2015). PyroMark® Instruments, Chemistry, and Software for Pyrosequencing® Analysis. *Methods Mol. Biol.* *1315*, 17–27.
- Kunath, T., Arnaud, D., Uy, G.D., Okamoto, I., Chureau, C., Yamanaka, Y., Heard, E., Gardner, R.L., Avner, P., and Rossant, J. (2005). Imprinted X-inactivation in extra-embryonic endoderm cell lines from mouse blastocysts. *Development* *132*, 1649–1661.
- Kuzmichev, A., Nishioka, K., Erdjument-Bromage, H., Tempst, P., and Reinberg, D. (2002). Histone methyltransferase activity associated with a human multiprotein complex containing the Enhancer of Zeste protein. *Genes Dev.* *16*, 2893–2905.
- Lahn, B.T., and Page, D.C. (1999). Four evolutionary strata on the human X chromosome. *Science* *286*, 964–967.
- Laugesen, A., and Helin, K. (2014). Chromatin repressive complexes in stem cells, development, and cancer. *Cell Stem Cell* *14*, 735–751.
- Lee, J.T. (2000). Disruption of imprinted X inactivation by parent-of-origin effects at Tsix. *Cell* *103*, 17–27.
- Lee, J.T., and Jaenisch, R. (1997). Long-range cis effects of ectopic X-inactivation centres on a mouse autosome. *Nature* *386*, 275–279.
- Lee, J.T., and Lu, N. (1999). Targeted mutagenesis of Tsix leads to nonrandom X inactivation. *Cell* *99*, 47–57.
- Lee, J.T., Davidow, L.S., and Warshawsky, D. (1999a). Tsix, a gene antisense to Xist at the X-inactivation centre. *Nat. Genet.* *21*, 400–404.
- Lee, J.T., Lu, N., and Han, Y. (1999b). Genetic analysis of the mouse X inactivation center defines an 80-kb multifunction domain. *Proc. Natl. Acad. Sci. U.S.A.* *96*, 3836–3841.
- Lee, J.T., Strauss, W.M., Dausman, J.A., and Jaenisch, R. (1996). A 450 kb transgene displays properties of the mammalian X-inactivation center. *Cell* *86*, 83–94.
- Lee, J.T. (2005). Regulation of X-chromosome counting by Tsix and Xite sequences. *Science* *309*, 768–771.
- Lee, J.T. (2009). Lessons from X-chromosome inactivation: long ncRNA as guides and tethers to the epigenome. *Genes Dev.* *23*, 1831–1842.
- Lee, J.T. (2010). The X as model for RNA's niche in epigenomic regulation. *Cold Spring Harb Perspect Biol* *2*, a003749.
- Lee, J.T. (2011). Gracefully ageing at 50, X-chromosome inactivation becomes a paradigm for RNA and chromatin control. *Nat. Rev. Mol. Cell Biol.* *12*, 815–826.
- Leeb, M., and Wutz, A. (2007). Ring1B is crucial for the regulation of developmental control

- genes and PRC1 proteins but not X inactivation in embryonic cells. *J. Cell Biol.* *178*, 219–229.
- Levesque, M.J., Ginart, P., Wei, Y., and Raj, A. (2013). Visualizing SNVs to quantify allele-specific expression in single cells. *Nat. Methods* *10*, 865–867.
- Levin, J.Z., Yassour, M., Adiconis, X., Nusbaum, C., Thompson, D.A., Friedman, N., Gnirke, A., and Regev, A. (2010). Comprehensive comparative analysis of strand-specific RNA sequencing methods. *Nat. Methods* *7*, 709–715.
- Love, M.I., Huber, W., and Anders, S. (2014). Moderated estimation of fold change and dispersion for RNA-seq data with DESeq2. *Genome Biol.* *15*, 550.
- Luikenhuis, S., Wutz, A., and Jaenisch, R. (2001). Antisense transcription through the Xist locus mediates Tsix function in embryonic stem cells. *Mol. Cell. Biol.* *21*, 8512–8520.
- LYON, M.F. (1961). Gene action in the X-chromosome of the mouse (*Mus musculus* L.). *Nature* *190*, 372–373.
- LYON, M.F. (1962). Sex chromatin and gene action in the mammalian X-chromosome. *Am. J. Hum. Genet.* *14*, 135–148.
- LYON, M.F., and Rastan, S. (1984). Parental source of chromosome imprinting and its relevance for X chromosome inactivation. *Differentiation* *26*, 63–67.
- Maclary, E., Buttigieg, E., Hinten, M., Gayen, S., Harris, C., Sarkar, M.K., Purushothaman, S., and Kalantry, S. (2014). Differentiation-dependent requirement of Tsix long non-coding RNA in imprinted X-chromosome inactivation. *Nat Commun* *5*, 4209.
- Maclary, E., Hinten, M., Harris, C., and Kalantry, S. (2013). Long noncoding RNAs in the X-inactivation center. *Chromosome Res.* *21*, 601–614.
- Magnuson, T., Debrot, S., Dimpfl, J., Zweig, A., Zamora, T., and Epstein, C.J. (1985). The early lethality of autosomal monosomy in the mouse. *J. Exp. Zool.* *236*, 353–360.
- Mak, W., Baxter, J., Silva, J., Newall, A.E., Otte, A.P., and Brockdorff, N. (2002). Mitotically stable association of polycomb group proteins *eed* and *enx1* with the inactive x chromosome in trophoblast stem cells. *Curr. Biol.* *12*, 1016–1020.
- Mak, W., Nesterova, T.B., de Napoles, M., Appanah, R., Yamanaka, S., Otte, A.P., and Brockdorff, N. (2004). Reactivation of the paternal X chromosome in early mouse embryos. *Science* *303*, 666–669.
- Marahrens, Y., Loring, J., and Jaenisch, R. (1998). Role of the Xist gene in X chromosome choosing. *Cell* *92*, 657–664.
- Marahrens, Y., Panning, B., Dausman, J., Strauss, W., and Jaenisch, R. (1997). Xist-deficient mice are defective in dosage compensation but not spermatogenesis. *Genes Dev.* *11*, 156–166.

- Margueron, R., and Reinberg, D. (2010). Chromatin structure and the inheritance of epigenetic information. *Nat. Rev. Genet.* *11*, 285–296.
- Margueron, R., and Reinberg, D. (2011). The Polycomb complex PRC2 and its mark in life. *Nature* *469*, 343–349.
- Margueron, R., Justin, N., Ohno, K., Sharpe, M.L., Son, J., Drury, W.J., Voigt, P., Martin, S.R., Taylor, W.R., De Marco, V., et al. (2009). Role of the polycomb protein EED in the propagation of repressive histone marks. *Nature* *461*, 762–767.
- Marks, H., Kerstens, H.H.D., Barakat, T.S., Splinter, E., Dirks, R.A.M., van Mierlo, G., Joshi, O., Wang, S.-Y., Babak, T., Albers, C.A., et al. (2015). Dynamics of gene silencing during X inactivation using allele-specific RNA-seq. *Genome Biol.* *16*, 149.
- Masui, S., Ohtsuka, S., Yagi, R., Takahashi, K., Ko, M.S.H., and Niwa, H. (2008). Rex1/Zfp42 is dispensable for pluripotency in mouse ES cells. *BMC Dev. Biol.* *8*, 45.
- McHugh, C.A., Chen, C.-K., Chow, A., Surka, C.F., Tran, C., McDonel, P., Pandya-Jones, A., Blanco, M., Burghard, C., Moradian, A., et al. (2015). The Xist lncRNA interacts directly with SHARP to silence transcription through HDAC3. *Nature* *521*, 232–236.
- McMahon, A., Fosten, M., and Monk, M. (1983). X-chromosome inactivation mosaicism in the three germ layers and the germ line of the mouse embryo. *J Embryol Exp Morphol* *74*, 207–220.
- Minajigi, A., Froberg, J.E., Wei, C., Sunwoo, H., Kesner, B., Colognori, D., Lessing, D., Payer, B., Boukhali, M., Haas, W., et al. (2015). Chromosomes. A comprehensive Xist interactome reveals cohesin repulsion and an RNA-directed chromosome conformation. *Science* *349*.
- Minkovsky, A., Barakat, T.S., Sellami, N., Chin, M.H., Gunhanlar, N., Gribnau, J., and Plath, K. (2013). The pluripotency factor-bound intron 1 of Xist is dispensable for X chromosome inactivation and reactivation in vitro and in vivo. *Cell Rep* *3*, 905–918.
- Minkovsky, A., Patel, S., and Plath, K. (2012). Concise review: Pluripotency and the transcriptional inactivation of the female Mammalian X chromosome. *Stem Cells* *30*, 48–54.
- Minkovsky, A., Sahakyan, A., Bonora, G., Damoiseaux, R., Dimitrova, E., Rubbi, L., Pellegrini, M., Radu, C.G., and Plath, K. (2015). A high-throughput screen of inactive X chromosome reactivation identifies the enhancement of DNA demethylation by 5-aza-2'-dC upon inhibition of ribonucleotide reductase. *Epigenetics Chromatin* *8*, 42.
- Moindrot, B., Cerase, A., Coker, H., Masui, O., Grijzenhout, A., Pintacuda, G., Schermelleh, L., Nesterova, T.B., and Brockdorff, N. (2015). A Pooled shRNA Screen Identifies Rbm15, Spen, and Wtap as Factors Required for Xist RNA-Mediated Silencing. *Cell Rep* *12*, 562–572.
- Monfort, A., Di Minin, G., Postlmayr, A., Freimann, R., Arieti, F., Thore, S., and Wutz, A. (2015). Identification of Spen as a Crucial Factor for Xist Function through Forward Genetic Screening in Haploid Embryonic Stem Cells. *Cell Rep* *12*, 554–561.

- Monk, M., and Harper, M.I. (1979). Sequential X chromosome inactivation coupled with cellular differentiation in early mouse embryos. *Nature* *281*, 311–313.
- Monkhorst, K., Jonkers, I., Rentmeester, E., Grosveld, F., and Gribnau, J. (2008). X inactivation counting and choice is a stochastic process: evidence for involvement of an X-linked activator. *Cell* *132*, 410–421.
- Montgomery, N.D., Yee, D., Chen, A., Kalantry, S., Chamberlain, S.J., Otte, A.P., and Magnuson, T. (2005). The murine polycomb group protein Eed is required for global histone H3 lysine-27 methylation. *Curr. Biol.* *15*, 942–947.
- Morey, C., Arnaud, D., Avner, P., and Clerc, P. (2001). Tsix-mediated repression of Xist accumulation is not sufficient for normal random X inactivation. *Hum. Mol. Genet.* *10*, 1403–1411.
- Morey, C., and Avner, P. (2011). The demoiselle of X-inactivation: 50 years old and as trendy and mesmerising as ever. *PLoS Genet.* *7*, e1002212.
- Morey, C., Navarro, P., Debrand, E., Avner, P., Rougeulle, C., and Clerc, P. (2004). The region 3' to Xist mediates X chromosome counting and H3 Lys-4 dimethylation within the Xist gene. *Embo J.* *23*, 594–604.
- Müller, J., Hart, C.M., Francis, N.J., Vargas, M.L., Sengupta, A., Wild, B., Miller, E.L., O'Connor, M.B., Kingston, R.E., and Simon, J.A. (2002). Histone methyltransferase activity of a Drosophila Polycomb group repressor complex. *Cell* *111*, 197–208.
- Najm, F.J., Chenoweth, J.G., Anderson, P.D., Nadeau, J.H., Redline, R.W., McKay, R.D.G., and Tesar, P.J. (2011). Isolation of epiblast stem cells from preimplantation mouse embryos. *Cell Stem Cell* *8*, 318–325.
- Namekawa, S.H., Payer, B., Huynh, K.D., Jaenisch, R., and Lee, J.T. (2010). Two-step imprinted X inactivation: repeat versus genic silencing in the mouse. *Mol. Cell. Biol.* *30*, 3187–3205.
- Navarro, P., and Avner, P. (2010). An embryonic story: analysis of the gene regulative network controlling Xist expression in mouse embryonic stem cells. *Bioessays* *32*, 581–588.
- Navarro, P., Chambers, I., Karwacki-Neisius, V., Chureau, C., Morey, C., Rougeulle, C., and Avner, P. (2008). Molecular coupling of Xist regulation and pluripotency. *Science* *321*, 1693–1695.
- Navarro, P., Chantalat, S., Foglio, M., Chureau, C., Vigneau, S., Clerc, P., Avner, P., and Rougeulle, C. (2009). A role for non-coding Tsix transcription in partitioning chromatin domains within the mouse X-inactivation centre. *Epigenetics Chromatin* *2*, 8.
- Navarro, P., Oldfield, A., Legoupi, J., Festuccia, N., Dubois, A., Attia, M., Schoorlemmer, J., Rougeulle, C., Chambers, I., and Avner, P. (2010). Molecular coupling of Tsix regulation and pluripotency. *Nature* *468*, 457–460.

- Navarro, P., Page, D.R., Avner, P., and Rougeulle, C. (2006). Tsix-mediated epigenetic switch of a CTCF-flanked region of the Xist promoter determines the Xist transcription program. *Genes Dev.* *20*, 2787–2792.
- Navarro, P., Pichard, S., Ciaudo, C., Avner, P., and Rougeulle, C. (2005). Tsix transcription across the Xist gene alters chromatin conformation without affecting Xist transcription: implications for X-chromosome inactivation. *Genes Dev.* *19*, 1474–1484.
- Nesterova, T.B., Senner, C.E., Schneider, J., Alcayna-Stevens, T., Tattermusch, A., Hemberger, M., and Brockdorff, N. (2011). Pluripotency factor binding and Tsix expression act synergistically to repress Xist in undifferentiated embryonic stem cells. *Epigenetics Chromatin* *4*, 17.
- O'Neill, M.J. (2005). The influence of non-coding RNAs on allele-specific gene expression in mammals. *Hum. Mol. Genet.* *14 Spec No 1*, R113–R120.
- Oda, H., Okamoto, I., Murphy, N., Chu, J., Price, S.M., Shen, M.M., Torres-Padilla, M.E., Heard, E., and Reinberg, D. (2009). Monomethylation of histone H4-lysine 20 is involved in chromosome structure and stability and is essential for mouse development. *Mol. Cell. Biol.* *29*, 2278–2295.
- Ogawa, Y., and Lee, J.T. (2003a). Antisense regulation in X inactivation and autosomal imprinting. *Cytogenet. Genome Res.*
- Ogawa, Y., and Lee, J.T. (2003b). Xite, X-inactivation intergenic transcription elements that regulate the probability of choice. *Mol. Cell* *11*, 731–743.
- Ohhata, T., Hoki, Y., Sasaki, H., and Sado, T. (2006). Tsix-deficient X chromosome does not undergo inactivation in the embryonic lineage in males: implications for Tsix-independent silencing of Xist. *Cytogenet. Genome Res.* *113*, 345–349.
- Ohhata, T., Hoki, Y., Sasaki, H., and Sado, T. (2008). Crucial role of antisense transcription across the Xist promoter in Tsix-mediated Xist chromatin modification. *Development* *135*, 227–235.
- OHNO, S., KAPLAN, W.D., and KINOSITA, R. (1959). Formation of the sex chromatin by a single X-chromosome in liver cells of *Rattus norvegicus*. *Exp. Cell Res.* *18*, 415–418.
- Ohno, S. (1967). *Sex Chromosomes and Sex-Linked Genes* (Springer).
- Okamoto, I., Tan, S., and Takagi, N. (2000). X-chromosome inactivation in XX androgenetic mouse embryos surviving implantation. *Development* *127*, 4137–4145.
- Okamoto, I., Arnaud, D., Le Baccon, P., Otte, A.P., Distèche, C.M., Avner, P., and Heard, E. (2005). Evidence for de novo imprinted X-chromosome inactivation independent of meiotic inactivation in mice. *Nature* *438*, 369–373.
- Okamoto, I., Otte, A.P., Allis, C.D., Reinberg, D., and Heard, E. (2004). Epigenetic dynamics of

imprinted X inactivation during early mouse development. *Science* 303, 644–649.

Parkhomchuk, D., Borodina, T., Amstislavskiy, V., Banaru, M., Hallen, L., Krobisch, S., Lehrach, H., and Soldatov, A. (2009). Transcriptome analysis by strand-specific sequencing of complementary DNA. *Nucleic Acids Res.* 37, e123.

Pasque, V., and Plath, K. (2015). X chromosome reactivation in reprogramming and in development. *Curr. Opin. Cell Biol.* 37, 75–83.

Pasque, V., Gillich, A., Garrett, N., and Gurdon, J.B. (2011a). Histone variant macroH2A confers resistance to nuclear reprogramming. *Embo J.* 30, 2373–2387.

Pasque, V., Halley-Stott, R.P., Gillich, A., Garrett, N., and Gurdon, J.B. (2011b). Epigenetic stability of repressed states involving the histone variant macroH2A revealed by nuclear transfer to *Xenopus* oocytes. *Nucleus* 2, 533–539.

Pasque, V., Tchieu, J., Karnik, R., Uyeda, M., Sadhu Dimashkie, A., Case, D., Papp, B., Bonora, G., Patel, S., Ho, R., et al. (2014). X chromosome reactivation dynamics reveal stages of reprogramming to pluripotency. *Cell* 159, 1681–1697.

Patrat, C., Okamoto, I., Diabangouaya, P., Vialon, V., Le Baccon, P., Chow, J., and Heard, E. (2009). Dynamic changes in paternal X-chromosome activity during imprinted X-chromosome inactivation in mice. *Proc. Natl. Acad. Sci. U.S.A.* 106, 5198–5203.

Payer, B., and Lee, J.T. (2008). X chromosome dosage compensation: how mammals keep the balance. *Annu. Rev. Genet.* 42, 733–772.

Payer, B., Lee, J.T., and Namekawa, S.H. (2011). X-inactivation and X-reactivation: epigenetic hallmarks of mammalian reproduction and pluripotent stem cells. *Hum. Genet.* 130, 265–280.

Payer, B., Rosenberg, M., Yamaji, M., Yabuta, Y., Koyanagi-Aoi, M., Hayashi, K., Yamanaka, S., Saitou, M., and Lee, J.T. (2013). Tsix RNA and the germline factor, PRDM14, link X reactivation and stem cell reprogramming. *Mol. Cell* 52, 805–818.

Peeters, S.B., Cotton, A.M., and Brown, C.J. (2014). Variable escape from X-chromosome inactivation: identifying factors that tip the scales towards expression. *Bioessays* 36, 746–756.

Penny, G.D., Kay, G.F., Sheardown, S.A., Rastan, S., and Brockdorff, N. (1996). Requirement for Xist in X chromosome inactivation. *Nature* 379, 131–137.

Perche, P.Y., Vourc'h, C., Konecny, L., Souchier, C., Robert-Nicoud, M., Dimitrov, S., and Khochbin, S. (2000). Higher concentrations of histone macroH2A in the Barr body are correlated with higher nucleosome density. *Curr. Biol.* 10, 1531–1534.

Pfister, S., Steiner, K.A., and Tam, P.P.L. (2007). Gene expression pattern and progression of embryogenesis in the immediate post-implantation period of mouse development. *Gene Expr. Patterns* 7, 558–573.

- Plath, K., and Lowry, W.E. (2011). Progress in understanding reprogramming to the induced pluripotent state. *Nat. Rev. Genet.* *12*, 253–265.
- Plath, K., Fang, J., Mlynarczyk-Evans, S.K., Cao, R., Worringer, K.A., Wang, H., la Cruz, de, C.C., Otte, A.P., Panning, B., and Zhang, Y. (2003). Role of histone H3 lysine 27 methylation in X inactivation. *Science* *300*, 131–135.
- Plath, K., Mlynarczyk-Evans, S., Nusinow, D.A., and Panning, B. (2002). Xist RNA and the mechanism of X chromosome inactivation. *Annu. Rev. Genet.* *36*, 233–278.
- Plath, K., Talbot, D., Hamer, K.M., Otte, A.P., Yang, T.P., Jaenisch, R., and Panning, B. (2004). Developmentally regulated alterations in Polycomb repressive complex 1 proteins on the inactive X chromosome. *J. Cell Biol.* *167*, 1025–1035.
- Pontier, D.B., and Gribnau, J. (2011). Xist regulation and function explored. *Hum. Genet.* *130*, 223–236.
- Pruitt, K.D., Brown, G.R., Hiatt, S.M., Thibaud-Nissen, F., Astashyn, A., Ermolaeva, O., Farrell, C.M., Hart, J., Landrum, M.J., McGarvey, K.M., et al. (2014). RefSeq: an update on mammalian reference sequences. *Nucleic Acids Res.* *42*, D756–D763.
- Pullirsch, D., Härtel, R., Kishimoto, H., Leeb, M., Steiner, G., and Wutz, A. (2010). The Trithorax group protein Ash2l and Saf-A are recruited to the inactive X chromosome at the onset of stable X inactivation. *Development* *137*, 935–943.
- Quinlan, A.R., and Hall, I.M. (2010). BEDTools: a flexible suite of utilities for comparing genomic features. *Bioinformatics* *26*, 841–842.
- Ragunathan, K., Jih, G., and Moazed, D. (2015). Epigenetics. Epigenetic inheritance uncoupled from sequence-specific recruitment. *Science* *348*, 1258699.
- Rasmussen, T.P., Mastrangelo, M.A., Eden, A., Pehrson, J.R., and Jaenisch, R. (2000). Dynamic relocalization of histone MacroH2A1 from centrosomes to inactive X chromosomes during X inactivation. *J. Cell Biol.* *150*, 1189–1198.
- Rastan, S. (1982). Timing of X-chromosome inactivation in postimplantation mouse embryos. *J Embryol Exp Morphol* *71*, 11–24.
- Rastan, S. (1983). Non-random X-chromosome inactivation in mouse X-autosome translocation embryos--location of the inactivation centre. *J Embryol Exp Morphol* *78*, 1–22.
- Rastan, S., and Brown, S.D. (1990). The search for the mouse X-chromosome inactivation centre. *Genet. Res.* *56*, 99–106.
- Rastan, S., and Robertson, E.J. (1985). X-chromosome deletions in embryo-derived (EK) cell lines associated with lack of X-chromosome inactivation. *J Embryol Exp Morphol* *90*, 379–388.
- Rastan, S., Kaufman, M.H., Handyside, A.H., and LYON, M.F. (1980). X-chromosome

inactivation in extra-embryonic membranes of diploid parthenogenetic mouse embryos demonstrated by differential staining. *Nature* 288, 172–173.

Sado, T., Li, E., and Sasaki, H. (2002). Effect of TSIX disruption on XIST expression in male ES cells. *Cytogenet. Genome Res.* 99, 115–118.

Sado, T., Wang, Z., Sasaki, H., and Li, E. (2001). Regulation of imprinted X-chromosome inactivation in mice by Tsix. *Development* 128, 1275–1286.

Sado, T., and Ferguson-Smith, A.C. (2005). Imprinted X inactivation and reprogramming in the preimplantation mouse embryo. *Hum. Mol. Genet.* 14 Spec No 1, R59–R64.

Sado, T., Hoki, Y., and Sasaki, H. (2005). Tsix silences Xist through modification of chromatin structure. *Dev. Cell* 9, 159–165.

Sado, T., Okano, M., Li, E., and Sasaki, H. (2004). De novo DNA methylation is dispensable for the initiation and propagation of X chromosome inactivation. *Development* 131, 975–982.

Sandstedt, S.A., and Tucker, P.K. (2004). Evolutionary strata on the mouse X chromosome correspond to strata on the human X chromosome. *Genome Res.* 14, 267–272.

Sarkar, M.K., Gayen, S., Kumar, S., Maclary, E., Buttigieg, E., Hinten, M., Kumari, A., Harris, C., Sado, T., and Kalantry, S. (2015). An Xist-activating antisense RNA required for X-chromosome inactivation. *Nat Commun* 6, 8564.

Sauvageau, M., and Sauvageau, G. (2010). Polycomb group proteins: multi-faceted regulators of somatic stem cells and cancer. *Cell Stem Cell* 7, 299–313.

Savarese, F., Flahndorfer, K., Jaenisch, R., Busslinger, M., and Wutz, A. (2006). Hematopoietic precursor cells transiently reestablish permissiveness for X inactivation. *Mol. Cell. Biol.* 26, 7167–7177.

Schneider-Gädicke, A., Beer-Romero, P., Brown, L.G., Nussbaum, R., and Page, D.C. (1989). ZFX has a gene structure similar to ZFY, the putative human sex determinant, and escapes X inactivation. *Cell* 57, 1247–1258.

Schoeftner, S., Sengupta, A.K., Kubicek, S., Mechtler, K., Spahn, L., Koseki, H., Jenuwein, T., and Wutz, A. (2006). Recruitment of PRC1 function at the initiation of X inactivation independent of PRC2 and silencing. *Embo J.* 25, 3110–3122.

Schulz, E.G., and Heard, E. (2013). Role and control of X chromosome dosage in mammalian development. *Curr. Opin. Genet. Dev.* 23, 109–115.

Sheardown, S.A., Duthie, S.M., Johnston, C.M., Newall, A.E., Formstone, E.J., Arkell, R.M., Nesterova, T.B., Alghisi, G.C., Rastan, S., and Brockdorff, N. (1997). Stabilization of Xist RNA mediates initiation of X chromosome inactivation. *Cell* 91, 99–107.

Shen, X., Liu, Y., Hsu, Y.-J., Fujiwara, Y., Kim, J., Mao, X., Yuan, G.-C., and Orkin, S.H.

(2008). EZH1 mediates methylation on histone H3 lysine 27 and complements EZH2 in maintaining stem cell identity and executing pluripotency. *Mol. Cell* 32, 491–502.

Shevchenko, A.I., Zakharova, I.S., Elisaphenko, E.A., Kolesnikov, N.N., Whitehead, S., Bird, C., Ross, M., Weidman, J.R., Jirtle, R.L., Karamysheva, T.V., et al. (2007). Genes flanking Xist in mouse and human are separated on the X chromosome in American marsupials. *Chromosome Res.* 15, 127–136.

Shin, J., Bossenz, M., Chung, Y., Ma, H., Byron, M., Taniguchi-Ishigaki, N., Zhu, X., Jiao, B., Hall, L.L., Green, M.R., et al. (2010). Maternal Rnf12/RLIM is required for imprinted X-chromosome inactivation in mice. *Nature* 467, 977–981.

Shin, J., Wallingford, M.C., Gallant, J., Marcho, C., Jiao, B., Byron, M., Bossenz, M., Lawrence, J.B., Jones, S.N., Mager, J., et al. (2014). RLIM is dispensable for X-chromosome inactivation in the mouse embryonic epiblast. *Nature* 511, 86–89.

Silva, J., Mak, W., Zvetkova, I., Appanah, R., Nesterova, T.B., Webster, Z., Peters, A.H.F.M., Jenuwein, T., Otte, A.P., and Brockdorff, N. (2003). Establishment of histone h3 methylation on the inactive X chromosome requires transient recruitment of Eed-Enx1 polycomb group complexes. *Dev. Cell* 4, 481–495.

Simmler, M.C., Cunningham, D.B., Clerc, P., Vermat, T., Caudron, B., Cruaud, C., Pawlak, A., Szpirer, C., Weissenbach, J., Claverie, J.M., et al. (1996). A 94 kb genomic sequence 3' to the murine Xist gene reveals an AT rich region containing a new testis specific gene Tsx. *Hum. Mol. Genet.* 5, 1713–1726.

Simon, M.D., Pinter, S.F., Fang, R., Sarma, K., Rutenberg-Schoenberg, M., Bowman, S.K., Kesner, B.A., Maier, V.K., Kingston, R.E., and Lee, J.T. (2013). High-resolution Xist binding maps reveal two-step spreading during X-chromosome inactivation. *Nature*.

Song, L., Zhang, Z., Grasfeder, L.L., Boyle, A.P., Giresi, P.G., Lee, B.-K., Sheffield, N.C., Gräf, S., Huss, M., Keefe, D., et al. (2011). Open chromatin defined by DNaseI and FAIRE identifies regulatory elements that shape cell-type identity. *Genome Res.* 21, 1757–1767.

Stavropoulos, N., Rowntree, R.K., and Lee, J.T. (2005). Identification of developmentally specific enhancers for Tsix in the regulation of X chromosome inactivation. *Mol. Cell. Biol.* 25, 2757–2769.

Stevenson, K.R., Coolon, J.D., and Wittkopp, P.J. (2013). Sources of bias in measures of allele-specific expression derived from RNA-seq data aligned to a single reference genome. *BMC Genomics*.

Steward, M.M., Lee, J.-S., O'Donovan, A., Wyatt, M., Bernstein, B.E., and Shilatifard, A. (2006). Molecular regulation of H3K4 trimethylation by ASH2L, a shared subunit of MLL complexes. *Nat. Struct. Mol. Biol.* 13, 852–854.

Su, W.Y., Xiong, H., and Fang, J.Y. (2010). Natural antisense transcripts regulate gene expression in an epigenetic manner. *Biochemical and Biophysical Research ...*

- Sun, B.K., Deaton, A.M., and Lee, J.T. (2006). A transient heterochromatic state in Xist preempts X inactivation choice without RNA stabilization. *Mol. Cell* *21*, 617–628.
- Sun, S., Del Rosario, B.C., Szanto, A., Ogawa, Y., Jeon, Y., and Lee, J.T. (2013). Jpx RNA activates Xist by evicting CTCF. *Cell* *153*, 1537–1551.
- Sun, S., Payer, B., Namekawa, S., An, J.Y., Press, W., Catalan-Dibene, J., Sunwoo, H., and Lee, J.T. (2015). Xist imprinting is promoted by the hemizygous (unpaired) state in the male germ line. *Proc. Natl. Acad. Sci. U.S.A.* *112*, 14415–14422.
- Sunwoo, H., Wu, J.Y., and Lee, J.T. (2015). The Xist RNA-PRC2 complex at 20-nm resolution reveals a low Xist stoichiometry and suggests a hit-and-run mechanism in mouse cells. *Proceedings of the National Academy of Sciences* *112*, E4216–E4225.
- Surface, L.E., Thornton, S.R., and Boyer, L.A. (2010). Polycomb group proteins set the stage for early lineage commitment. *Cell Stem Cell* *7*, 288–298.
- Tada, T., Obata, Y., Tada, M., Goto, Y., Nakatsuji, N., Tan, S., Kono, T., and Takagi, N. (2000). Imprint switching for non-random X-chromosome inactivation during mouse oocyte growth. *Development* *127*, 3101–3105.
- Takada, T., Ebata, T., Noguchi, H., Keane, T.M., Adams, D.J., Narita, T., Shin-I, T., Fujisawa, H., Toyoda, A., Abe, K., et al. (2013). The ancestor of extant Japanese fancy mice contributed to the mosaic genomes of classical inbred strains. *Genome Res.*
- Takagi, N. (1978). Preferential inactivation of the paternally derived X chromosome in mice. *Basic Life Sci.* *12*, 341–360.
- Takagi, N. (1980). Primary and secondary nonrandom X chromosome inactivation in early female mouse embryos carrying Searle's translocation T(X; 16)16H. *Chromosoma* *81*, 439–459.
- Takagi, N., and Sasaki, M. (1975). Preferential inactivation of the paternally derived X chromosome in the extraembryonic membranes of the mouse. *Nature* *256*, 640–642.
- Takagi, N., Wake, N., and Sasaki, M. (1978). Cytologic evidence for preferential inactivation of the paternally derived X chromosome in XX mouse blastocysts. *Cytogenet. Cell Genet.* *20*, 240–248.
- Tanaka, S., Kunath, T., Hadjantonakis, A.K., Nagy, A., and Rossant, J. (1998). Promotion of trophoblast stem cell proliferation by FGF4. *Science* *282*, 2072–2075.
- Tanasijevic, B., and Rasmussen, T.P. (2011). X chromosome inactivation and differentiation occur readily in ES cells doubly-deficient for macroH2A1 and macroH2A2. *PLoS ONE* *6*, e21512.
- Tesar, P.J., Chenoweth, J.G., Brook, F.A., Davies, T.J., Evans, E.P., Mack, D.L., Gardner, R.L., and McKay, R.D.G. (2007). New cell lines from mouse epiblast share defining features with human embryonic stem cells. *Nature* *448*, 196–199.

- Thorvaldsen, J.L., Krapp, C., Willard, H.F., and Bartolomei, M.S. (2012). Nonrandom x chromosome inactivation is influenced by multiple regions on the murine x chromosome. *Genetics* *192*, 1095–1107.
- Tian, D., Sun, S., and Lee, J.T. (2010). The long noncoding RNA, Jpx, is a molecular switch for X chromosome inactivation. *Cell* *143*, 390–403.
- Tie, F., Furuyama, T., Prasad-Sinha, J., Jane, E., and Harte, P.J. (2001). The Drosophila Polycomb Group proteins ESC and E(Z) are present in a complex containing the histone-binding protein p55 and the histone deacetylase RPD3. *Development* *128*, 275–286.
- Trapnell, C., Roberts, A., Goff, L., Pertea, G., Kim, D., Kelley, D.R., Pimentel, H., Salzberg, S.L., Rinn, J.L., and Pachter, L. (2012). Differential gene and transcript expression analysis of RNA-seq experiments with TopHat and Cufflinks. *Nat Protoc* *7*, 562–578.
- Trapnell, C., Williams, B.A., Pertea, G., Mortazavi, A., Kwan, G., van Baren, M.J., Salzberg, S.L., Wold, B.J., and Pachter, L. (2010). Transcript assembly and quantification by RNA-Seq reveals unannotated transcripts and isoform switching during cell differentiation. *Nat. Biotechnol.* *28*, 511–515.
- Vakoc, C.R., Sachdeva, M.M., Wang, H., and Blobel, G.A. (2006). Profile of histone lysine methylation across transcribed mammalian chromatin. *Mol. Cell. Biol.* *26*, 9185–9195.
- Valk-Lingbeek, M.E., Bruggeman, S.W.M., and van Lohuizen, M. (2004). Stem cells and cancer; the polycomb connection. *Cell* *118*, 409–418.
- Vallot, C., Ouimette, J.-F., Makhlof, M., Féraud, O., Pontis, J., Côme, J., Martinat, C., Bennaceur-Griscelli, A., Lalande, M., and Rougeulle, C. (2015). Erosion of X Chromosome Inactivation in Human Pluripotent Cells Initiates with XACT Coating and Depends on a Specific Heterochromatin Landscape. *Cell Stem Cell* *16*, 533–546.
- Vigneau, S., Augui, S., Navarro, P., Avner, P., and Clerc, P. (2006). An essential role for the DXPas34 tandem repeat and Tsix transcription in the counting process of X chromosome inactivation. *Proc. Natl. Acad. Sci. U.S.A.* *103*, 7390–7395.
- Wang, J., Mager, J., Chen, Y., Schneider, E., Cross, J.C., Nagy, A., and Magnuson, T. (2001). Imprinted X inactivation maintained by a mouse Polycomb group gene. *Nat. Genet.* *28*, 371–375.
- Wang, Z., Zang, C., Rosenfeld, J.A., Schones, D.E., Barski, A., Cuddapah, S., Cui, K., Roh, T.-Y., Peng, W., Zhang, M.Q., et al. (2008). Combinatorial patterns of histone acetylations and methylations in the human genome. *Nat. Genet.* *40*, 897–903.
- Webb, S., de Vries, T.J., and Kaufman, M.H. (1992). The differential staining pattern of the X chromosome in the embryonic and extraembryonic tissues of postimplantation homozygous tetraploid mouse embryos. *Genet. Res.* *59*, 205–214.
- West, J.D., Frels, W.I., Chapman, V.M., and Papaioannou, V.E. (1977). Preferential expression of the maternally derived X chromosome in the mouse yolk sac. *Cell* *12*, 873–882.

West, J.D., Papaioannou, V.E., Frels, W.I., and Chapman, V.M. (1978). Preferential expression of the maternally derived X chromosome in extraembryonic tissues of the mouse. *Basic Life Sci.* *12*, 361–377.

Williams, A.G., Thomas, S., Wyman, S.K., and Holloway, A.K. (2014). RNA-seq Data: Challenges in and Recommendations for Experimental Design and Analysis. *Curr Protoc Hum Genet* *83*, 11.13.1–11.13.20.

Williams, L.H., Kalantry, S., Starmer, J., and Magnuson, T. (2011). Transcription precedes loss of Xist coating and depletion of H3K27me3 during X-chromosome reprogramming in the mouse inner cell mass. *Development* *138*, 2049–2057.

Wutz, A., and Jaenisch, R. (2000). A shift from reversible to irreversible X inactivation is triggered during ES cell differentiation. *Mol. Cell* *5*, 695–705.

Wutz, A., Rasmussen, T.P., and Jaenisch, R. (2002). Chromosomal silencing and localization are mediated by different domains of Xist RNA. *Nat. Genet.* *30*, 167–174.

Yalcin, B., Wong, K., Agam, A., Goodson, M., Keane, T.M., Gan, X., Nellåker, C., Goodstadt, L., Nicod, J., Bhomra, A., et al. (2011). Sequence-based characterization of structural variation in the mouse genome. *Nature* *477*, 326–329.

Yamaji, M., Seki, Y., Kurimoto, K., Yabuta, Y., Yuasa, M., Shigeta, M., Yamanaka, K., Ohinata, Y., and Saitou, M. (2008). Critical function of Prdm14 for the establishment of the germ cell lineage in mice. *Nat. Genet.* *40*, 1016–1022.

Yamaji, M., Ueda, J., Hayashi, K., Ohta, H., Yabuta, Y., Kurimoto, K., Nakato, R., Yamada, Y., Shirahige, K., and Saitou, M. (2013). PRDM14 ensures naive pluripotency through dual regulation of signaling and epigenetic pathways in mouse embryonic stem cells. *Cell Stem Cell* *12*, 368–382.

Yang, F., Babak, T., Shendure, J., and Disteche, C.M. (2010). Global survey of escape from X inactivation by RNA-sequencing in mouse. *Genome Res.* *20*, 614–622.

Zhang, T., Cooper, S., and Brockdorff, N. (2015). The interplay of histone modifications - writers that read. *EMBO Rep.*

Zhao, J., Sun, B.K., Erwin, J.A., Song, J.-J., and Lee, J.T. (2008). Polycomb proteins targeted by a short repeat RNA to the mouse X chromosome. *Science* *322*, 750–756.